Design and Synthesis of Multifunctional Leads for the Treatment of Neuropathic Pain

THESIS

Submitted in partial fulfillment
of the requirements for the degree of

DOCTOR OF PHILOSOPHY

by
Monika Sharma

Prof. P. Yogeeswari

BIRLA INSTITUTE OF TECHNOLOGY AND SCIENCE
PILANI (RAJASTHAN) INDIA
2012

BIRLA INSTITUTE OF TECHNOLOGY & SCIENCE
PILANI, RAJASTHAN

CERTIFICATE

This is to certify that the thesis entitled, "**Design and Synthesis of Multifunctional Leads for the Treatment of Neuropathic Pain**" submitted by **Monika Sharma**, ID.No. **2009PHXF415H** for award of Ph.D. degree of the Institute embodies the original work done by her under my supervision.

Signature in full of the Supervisor

_____

Name in capital block letters:
Prof. P. YOGEESWARI

Designation:
Associate Professor,
BITS, Pilani-Hyderabad Campus

Date:

ACKNOWLEDGEMENTS

Imagination is the beginning of creation. You imagine what you desire, you will what you imagine and at last you create what you will.

-George Bernard Shaw

An Irish playwright and political activist

Words are tools of expression, but they fail miserably when it comes to thanksgiving. I might not be able to do adequate justice in this task of acknowledging my indebtedness to all those who have directly as well as indirectly made it possible to complete my doctoral work.

First of all I acknowledge, all my family members, who brought me up to where I am today. I am in huge debt to them, which I will never to be able to ever repay.

It's a fact that every mission needs a spirit of hard work and dedication but it needs to be put on the right path to meet its destination and in my case this credit goes to my supervisor, **Prof. P. Yogeeswari**, Associate Professor and Head of Department, Department of Pharmacy, BITS, Pilani-Hyderabad Campus. Her encouragement, support and scientific guidance has always been available to me, which enabled this work to be carried through. Her affable nature, promptness and research acumen have all inculcated in me a tendency to perfect everything I do.

With immense pleasure and profound sense of gratitude, I express my heartfelt and sincere indebtedness to **Prof. D. Sriram**, my Doctoral Advisory Committee member, for his guidance, precious and erudite suggestions, propelling inspiration, informative and critical discussions and constant encouragement throughout the course of present study.

I would also like to thank another member of Doctoral Advisory Committee **Dr. Punna Rao Ravi**, who has been kind enough to help me in all possible ways at any time of need.

I derive immense pleasure in acknowledging **Prof. V.S Rao**, Director (BITS, Pilani-Hyderabad campus) and **Prof. B. N. Jain,** Vice-Chancellor (BITS, Pilani), for allowing me to carry out my doctoral research work in this premier Institute of India.

I extend my heartfelt gratitude and thanks to **Prof. Suman Kapur**, Dean, Research & Consultancy Division, BITS, Pilani-Hyderabad Campus and **Prof. A.K Das**, Dean, Research & Consultancy Division, BITS, Pilani for their co-operation and support during my research work.

I sincerely acknowledge the help rendered by faculty members of Department of Pharmacy, BITS, Pilani-Hyderabad Campus at various stages of my research work.

I extend my thanks to many graduate and undergraduate students, especially Yukti Singh, Deekshith Vanamala, Binita Kundu, Saumya Gargipati, Saketh M, Sriram Karthick and Shradda Suman Das for their help in my experimental work.

I express my thanks to our laboratory staff Ms. Sarita, Shalini, Mr. Venkat and Rekha Ji, for all their help in one way or the other.

Many thanks and to my friends and fellow PhD students Rukaiyya Khan, Priyanka Sharma, Ram Kumar Mishra, Gangadhar M., S. Mahibalan, Ms. J. T. Patrisha, Mahesh K., Ganesh S., Ganesh P., Srikant R., Madhu Babu B., Praveen K., C. Manoj, Jean Kumar, Mallika A., Vankat K, Renuka J., Reshma C., Poorna V., Shailender Joseph and Pritesh Bhat, who gave me moral support and made the whole degree more enjoyable in BITS.

Words are not enough to express thanks to my better half Dr. Arvind Semwal, who always inspired me, encouraged and helped me in one way or the other. I would like to thank my siblings Kalpana and Sujot for always being there for me.

I deeply acknowledge the Department of Biotechnology, Government of India for providing me with the project funding.

I would like to express my thankfulness and gratefulness to all others who made this dissertation possible, but forgot to mention their name.

I will remain forever indebted to all the animals, which were scarified for the purpose of widening the horizons of science.

I pay gratitude to the Almighty, with whose mercy; it has been made possible for me to reach so far.

Date: Monika Sharma

LIST OF FIGURES

LIST OF TABLES

LIST OF ABBREVIATIONS

5-HT	5-Hydroxy tryptophan
AIDS	Acquired immune deficiency syndrome
AMPA	α-Amino-3-hydroxy-5-methylisoxazole-4- propionic acid
ANOVA	Analysis of variance
ATP	Adenosine 5'-triphosphate
b.i.d.	bis in die (twice a day)
BDNF	Brain derived neurotropic factors
CB	Cannabinoid receptor
CCI	Chronic constriction injury
CCK	Chelocystokinine
CGRP	Calcitonin gene-related peptide
CMR1	Cold and menthol receptor 1
cNOS	Constitutive nitric oxide synthase
CNS	Central nervous system
COX	Cyclo-oxygenase
DCM	Dichloromethane
DEG	Degenerin
DMF	Dimethyl sulphoxide
DMSO	Dimethyl sulfoxide
DNP	Diabetic neuropathy
DPPH	1,1-Diphenyl-2-picrylhydrazyl
DRASIC	Dorsal root acid-sensing ion channel
DRG	Dorsal root ganglion
EC_{50}	Mean effective concentration
ED_{50}	Median effective dose
EDC	1-Ethyl-3-[3-(dimethylamino)propyl]carbodiimide hydrochloride
EDTA	Ethylene di amine tetra acetic acid
eNOS	endothelial nitric oxide synthase
GABA	γ -amino butyric acid

GBP	Gabapebtin
h	Hour/ Hours
HIV	Human immunodeficiency virus
HOBT	1-Hydroxybenzotriazole
i.p.	Intraperitoneal
i.v.	Intravenous
IAEC	Institutional animal ethics committee
IASP	International association for the study of pain
IC_{50}	Median inhibitory concentration
IL-1	Interleukin -1
IL-6	Interleukin -6
iNOS	Inducible nitric oxide synthase
Ki	Dissociation constant
K_2CO_3	Potassium carbonate
ION	Infraorbital nerve
L5	Fifth lumbar spinal nerve
L6	Sixth lumbar spinal nerve
LTP	Long term potentiation
MES	Maximal electroshock seizure
mGluR	Metabotrophic glutamate receptor
min	Minutes
mM	Micro mol
MNCV	Motor nerve conduction velocity
mRNA	Messenger ribonucleic acid
NGF	Nerve growth factor
NK-1	Neurokinin -1 receptor
NMDA	N-methyl-D-aspartate
NNT	Number needed to treat
NO	Nitric oxide
NOS	Nitric oxide synthase

NP	Neuropathic pain
NPY	Neuropeptide Y
NR_2B	NMDA receptor subunit 2 B
NS	Not significant
NSAID	Non steroidal anti-inflamamtory drugs
PEG	Polyethylene glycol
PGE_2	Prostaglandins E_2 subtype
PGI_2	Prostaglandins I_2 subtype
PHN	Postherpetic neuralgia
PKA	Protein kinase A
PKC	Protein kinase C
PSNL	Partial sciatic nerve ligation
PWD	Paw withdrawal duration
PWL	Paw withdrawal latency
RVM	Rostral ventromedial medulla
SCI	Spinal cord injury
scPIC	Subcutaneous pictrotoxin
scPTZ	Subcutaneous pentylenetetrazole
scSTY	Subcutaneous strychnine
SEM	Standard error of mean
SNL	Spinal nerve ligation
SSRIs	Selective serotonin reuptake inhibitors
STZ	Streptozotocin
TCAs	Tri-cyclic antidepressants
TFA	Trifluoromethane
TGN	Trigeminal neuralgia
THC	Δ9 -tetrahydrocannabinol
THF	Tetrahydrofuran
TNF-α	Tumor necrosis factor- α
TPE	Time to peak effect
TREK-1	TWIK-related K^+ channel -1

TRPV1	Transient receptor potential type vanilloid -1
TTX	Tetrodotoxin
VGCC	Voltage gated calcium channel
VGSC	Voltage gated sodium channel
VIP	Vasoactive intestinal peptide
VR1	Vanilloid receptor -1
WD	Wallerian degeneration
WDR	Wide dynamic range

ABSTRACT

A total of 81 compounds containing tetrahydropyrido-pyrazole (**16** compounds, series **MS1XX**), tetrahydropyrido-pyrimidines (**16** compounds, series **MS2XX**), 1,2,4-triazol-5-one (**24** compounds, series **MS3XX**) and [1,2,4]-triazolo-[3,4-b]-1,3,4-thiadiazole scaffolds (**25** compounds, series **MS4XX**) were synthesized and evaluated in various animal models of physiological and neuropathic pain. Following neurotoxicity studies, the acute antinociceptive efficacy of the compounds was assessed in acetic acid-induced writhing and formalin-induced flinching tests. Compounds were further evaluated in chronic constriction nerve injury (CCI) and partial sciatic nerve ligation (PSNL) models of neuropathic pain. The compounds exhibiting more than 90% reversal in one or more nociceptive parameters in the neuropathic animals were taken further for ED_{50} studies. To identify the underlying mechanism of action, some potential compounds were evaluated for reduction of carrageenan-induced paw edema, inhibition of TNF-α, cathepsin S enzyme and nitric oxide (NO) inhibition in sciatic nerve and brain, free radical scavenging activity, cannabinoids (CB_1 and CB_2) receptor affinity and effect on picrotoxin induced epilepsy (GABAergic pathways).

A total of 71 compounds were found to possess significant acute antinociceptive efficacy in acetic acid and formalin test. 49 compounds showed a significant efficacy in CCI, whereas 45 compounds were efficacious in PSNL model. Few of the compounds tested showed better efficacy than gabapentin (100 mg/kg). Among 11 promising compounds studied in ED_{50} and mechanistic studies, several compounds significantly reduced edema and TNF-α in the carrageenan injected paw indicating modulation of inflammatory pathways. The neuroprotection exhibited by the compounds was also found to be associated with their free radical scavenging abilities and subsequent attenuation of oxidative and nitrosative stress. **MS109** exhibited CB_1 affinity in nanomolar range (49.7 nM). Also, inhibition of cathepsin S and mediation of GABAergic pathways demonstrate the ability of compounds to modulate several systems. Since neuropathic pain syndromes are mediated by multiple mechanisms, above findings advocate the development of multifunctional compounds showing multiple mechanisms of actions for the treatment of neuropathic pain.

TABLE OF CONTENTS

CHAPTER 1
INTRODUCTION

"Pain is such an uncomfortable feeling that even a tiny amount of it is enough to ruin every enjoyment."

Will Rogers (American entertainer, 1879-1935)

1.1 Pain

According to the International Association for the Study of Pain (IASP); pain is defined as an unpleasant sensory and emotional experience associated with actual or potential tissue damage or described in terms of such damage [1]. It is very essential for the organism's survival and well-being as it prevents injury by generating a withdrawal reflex from the stimulus and gives a sensation of unpleasantness so that further contact with such stimuli can be avoided [2].

1.2 Physiology of Pain

Pain is a subjective result of nociception, which involves activation of nociceptors at free nerve endings of primary sensory neurons, generation of action potential, and transmission of the action potential to the dorsal horn, second-order neuron activation to transmit the signal to thalamus and parabrachial nucleus in the brainstem, third-order neuron transmission of the signal to the cerebral cortex via spinothalamic and spinoparabrachial ascending pathways, where the nociceptive stimulus is perceived as pain [3].

There are two major classes of nerve fibers involved in nociception: unmyelinated C fibers and thinly myelinated Aδ fibers, which are distinct from myelinated dynamic sensors (Aβ fibers) and proprioceptors. Aδ fibers are fast-conducting myelinated nerves activated by heat or high-threshold mechanical stimuli. In contrast, C fibres are non-myelinated, slow-conducting fibers and are polymodal in nature as they transduce all chemical, mechanical and thermal stimuli [4]. The nociceptors located at the terminal of Aδ or C fibers primary neurons transduce noxious chemical, mechanical or thermal stimuli into depolarizing current, which ultimately induces the generation of action potential by the opening of voltage-gated sodium channels (Na_v) (Table 1.1) [5].

Table 1.1 Sensory nerve fibers and their subtypes [4]

Sensory nerve fibers			
Class Axon	**Modality**	**Diameter (μm)**	**Conduction Velocity (m/s)**
	Myelinated		
Aα	Proprioceptors from muscles and tendons	20	120
Aβ	Low-threshold mechanoreceptors	10	80
Aδ	Cold, noxious, thermal	2.5	12
	Unmyelinated		
C-Pain	Noxious, heat, thermal	1	<1
C-Dynamic	Light stroking, gentle touch	1	<1
C-Autonomic	Autonomic, sweat glands, vasculature	1	<1

Nociceptors express a variety of ion channels and receptors such as transient receptor potential (TRP) ion channels: TRPV1(≥ 42°C), TRPV2 (≥ 52°C), TRPV3 (≥ 33°C) and TRPV4 (~ 27-42°C) for sensing heat; TRPM8 (≤ 25°C) and TRPA1 (≤ 17°C) for sensing cold; DEG (degenerin), DRASIC (dorsal root acid-sensing ion channel), and TREK-1 (TWIK-related K^+ channel-1) ion channels for perceiving noxious mechanical sensations; and chemical sensors, such as the purinoreceptor $P2X_3$ to detect adenosine triphosphate (ATP) and ASIC (acid sensing ion channel), DRASIC and TRPV1 to detect the change in H^+ (Figure 1.1) [6].

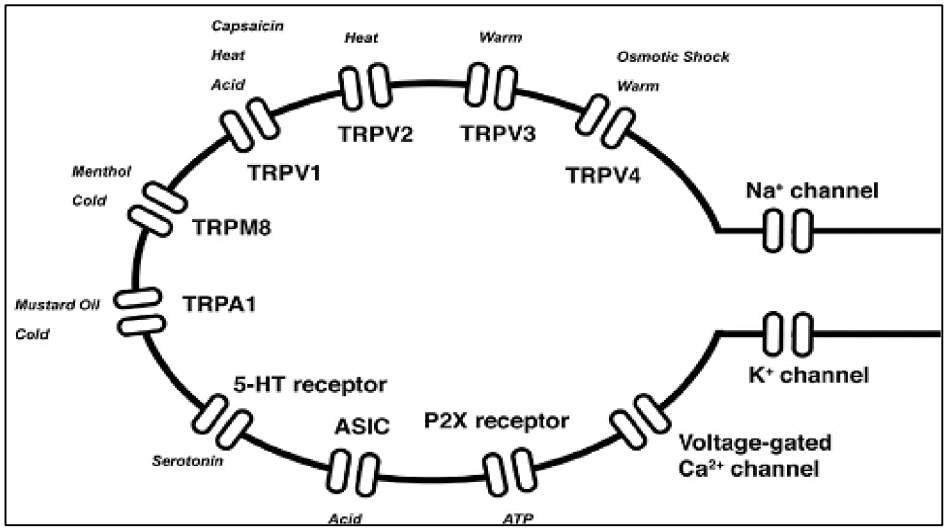

Figure 1.1 Ion channels / receptors expression in sensory nerve endings [6]

A variety of G-protein-coupled receptors (GPCR) are also expressed on sensory neurons and come into play in response to inflammatory mediators/cytokines released by tissue injury. These include opioid, cannabinoid, prostaglandin, endothelin, bradykinin, serotonin, adrenergic, chemokines and metabotropic glutamate receptors. Depending on the G-proteins to which these couple (Gs/Gq or Gi/o), they either activate or inhibit sensory nerve signaling [7].

Nociceptive specific (NS) Aδ and C fibers terminate superficially in laminae I–II of dorsal horn in spinal cord, whereas Aβ fibres predominantly terminate in laminae III–VI. Within the laminae of the dorsal horn, receiving second order neurons are specific to either Aδ or C fibre input, to Aβ input, or are wide dynamic range (WDR) neurons that recieve input from all three. Within these laminas, DRG neurons can be influenced by both excitatory glutamatergic and inhibitory GABAergic interneurons, which serve to modify intensity and quality of stimulus by receiving input from both ascending and descending pathways. In chronic pain conditions, astrocytes and microglia present in the dorsal horn also get involved in regulating pain transmission by virtue of the pro-inflammatory cytokines (Figure 1.2) [8].

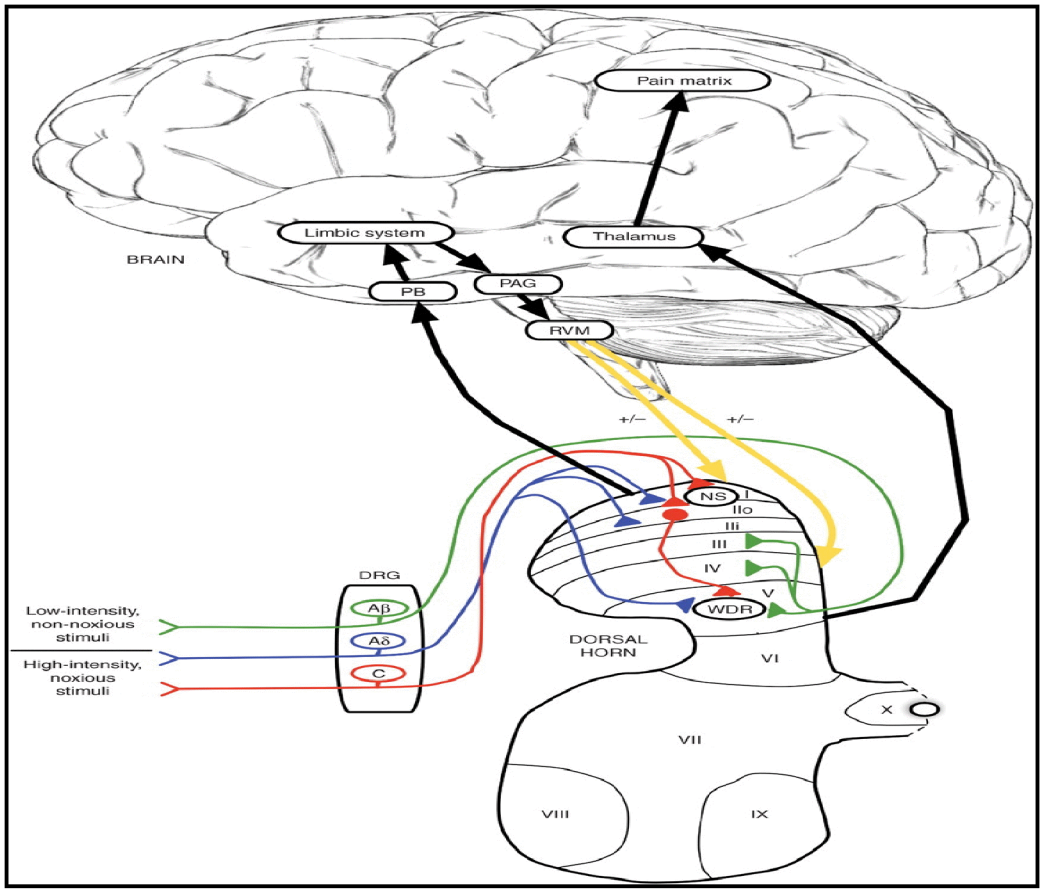

Figure 1.2 Pain pathways from periphery to brain [8]

Second order projection neurons originating from dorsal horn cross at the opposite side of spinal cord. A subset of these projection neurons transmits information to the somatosensory cortex via the thalamus (spinothalamic tract), providing information about the location and intensity of the painful stimulus. Other projection neurons engage the cingulate and insular cortices via connections in the brain stem (parabrachial nucleus) and amygdala, contributing to the affective component of the pain experience [3].

The central nervous system (CNS) can alter the afferent nociceptive information it receives; by a descending or modulatory system, which arises out of several regions of the CNS, including the somatosensory cortex, hypothalamus, rostral ventral medulla (RVM) and midbrain periaqueductal gray (PAG) and communicate with laminae in dorsal horn, to either inhibit or facilitate the pain transmission. Descending inhibition largely involves the release of norepinephrine in the dorsal horn to inhibit primary afferent terminals and suppress firing of projection neurons whereas descending facilitatory pathways, primarily involve a serotonergic mechanism. [4-6].

1.3 Neuropathic Pain

Neuropathic pain is a chronic pain disorder associated with damage or permanent alteration of the peripheral or central nervous system [9,10]. In contrast to acute nociceptive pain, the cascade of events that arise following peripheral nerve injury leads to a maintained abnormality in the sensory system, resulting in an abnormal pain phenomenon that can be grossly debilitating [10], leading to pain sensation which can be described as 'burning', 'stabbing', 'shooting', 'electric-like', or 'throbbing' along with two specific types of symptoms: allodynia (innocuous stimulation evokes intense pain sensation) and hyperalgesia (mildly noxious stimulation evokes abnormally intense, disproportionate and prolonged pain sensation (Table 1.2) [11]. It is a condition, when pain remains no protective mechanism but becomes a disease process [9].

Neuropathic pain represents a heterogeneous group of aetiologically different diseases or conditions including peripheral nerve trauma, surgery, limb crush or amputation or radiation damage (e.g., vertebral disk herniation, trigeminal neuralgia and phantom limb pain), drug regimens (e.g., chemotherapeutic or anti-HIV agents, e.g., vincristine

or cisplatin), metabolic disturbances (e.g., diabetic neuropathy), pressure due to growth (neoplasia), infection (e.g., postherpetic neuralgia, AIDS), and infarct (e.g., stroke) [11].

Table 1.2 Characteristics of Neuropathic Pain

Parameters	Characteristics
Quality	• Burning, lancinating, shooting, dull, aching, throbbing
Intensity	• From mild to excruciating
Temporal pattern	• Constant, lancinating or both
Negative sensory symptoms	• Loss of sensation: hypaesthesia, hypoalgesia, thermo-hypaesthesia, pallhypaesthesia
Positive sensory symptoms	• Spontaneous pain: paraesthesias, dysaesthesias 'pins and needles', burning pain, shock-like pain • Allodynia: pain at non-noxious stimuli • Hyperalgesia: exaggerated pain at noxious stimuli

1.3.1 Prevalence of Neuropathic Pain

The epidemiology of neuropathic pain is not well described, in part, due to the diversity of associated conditions. However, preliminary prevalence estimates of common conditions suggest that neuropathic pain affects 3-8% of the worldwide population [12]. Since the size of this population is increasing worldwide, it is inevitable that neuropathic pain will place a progressively demanding burden on health care resources.

Diabetic neuropathic pain (DNP) and postherpetic neuralgia (PHN) are two of the most common neuropathic pain syndromes. Diabetic neuropathy is experienced in approximately 20-24% of the diabetic patients [13]. PHN also is a very painful neuropathic condition that is still present between 1-6 months after the *Herpes zoster* (shingles) has cleared, representing roughly 10-15% of all *Herpes zoster*, or shingles, patients [14]. Occurrence of spinal cord injury (SCI) in the United States is approximately 11,000 people per year. 55% of people with SCIs experience neuropathic pain (i.e., sharp, stabbing, electric or burning pain) within the first 6 months post injury, and 75% have symptoms of neuropathic pain till 5 years post injury [15]. Trigeminal neuralgia (TGN) a unilateral neuropathic pain that occurs

along the distribution of one or more divisions of the trigeminal nerve in facial area, have incidence rate of 4.3 per 100,000 people per year [13]. Tumor-related pain which is generally associated with late-stage cancer; is also seen in approximately 50% of patients diagnosed with breast, ovarian, prostate and colon cancer [16].

1.3.2 Pathophysiological Mechanisms in Neuropathic Pain

After nerve injury, multiple physiological changes can be observed in the central and peripheral nervous systems leading to both positive (abnormal, spontaneous or evoked sensations) and negative symptoms (sensory deficits). A simplistic approach is to look at two main pathophysiological mechanisms: (1) Peripheral mechanisms and (2) Central mechanisms in both spinal and supraspinal level (Table 1.3, Figure 1.2) [17,18].

Table: 1.3 Peripheral and central mechanisms of neuropathic pain

Peripheral Mechanisms	Central Mechanisms
• Ectopic and spontaneous discharge	• Sprouting of Aβ afferent terminals (↑NGF)
• Changes in ion channel expression (↑Na^+, Ca^{2+}, TRP channels, $P2X_3$)	• Wind up (role of NMDA)
• Change in neuropeptide expression (↓ Substance P, CGRP, Somatostatin) (↑ NPY, CCK)	• Changes in descending inhibitory tone (↓GABA, Glycine) (↑Cholecystokinin, Dynorphin)
• Sympathetic sprouting (↑NGF)	• Micoglial cells activation, ↑cathepsin S
• Release of inflammatory mediators (Bradykinin, PGE_2, TNF-α, IL-6)	• Change in cannabinoid expression

1.3.3 Peripheral Mechanisms

Peripheral mechanism has been extensively studied using various animal models of neuropathic pain. The common changes after peripheral nerve injury include ectopic and spontaneous discharge, alteration in ion channel expression, collateral sprouting of primary afferent nerve discharge, sprouting of sympathetic nerves into dorsal root ganglion and nociceptor sensitization by pro-inflammatory mediators.

In normal peripheral afferent neurons, rarely any action potential reaches to firing threshold without any stimuli, however following nerve injury, a neuroma develops at

the proximal nerve stump, consisting of regenerative nerve sprouts growing into all directions and leads to large increase in spontaneous firing known as ectopic discharge [19].

Sodium channels are very critical for the neuronal excitability and contribute largely to the generation of ectopic activity. A variety of voltage gated sodium channels are expressed in DRG neurons, including the tetrodotoxin (TTX)-sensitive channels $Na_v1.1$, $Na_v1.6$ and $Na_v1.7$ and the TTX-resistant channels $Na_v1.8$ and $Na_v1.9$. After peripheral nerve injury, voltage gated sodium-channels (VGSCs) expression is significantly affected not only at the site of the nerve lesion, but also in intact dorsal root ganglion (DRG) and leads to spontaneous nociceptor activity, abnormal excitability, decreased threshold and an increased sensitivity to chemical, thermal and mechanical stimuli by the neuron of primary afferents [18,20]. Reduction in potassium currents is also observed afferent DRG neurons post neuronal injury [21].

Injury to the nerves lead to over-expression of voltage-gated calcium channels (VGCCs), particularly L-type calcium channel (Cav2.2) and $\alpha_2\delta_1$ subunits in DRG neurons. [22] This results in increase of intracellular Ca^{2+}, thereby affecting the release of neurotransmitters at synapse, altering membrane excitability and initiating the transcriptions of various proteins [23].

After nerve injury, increased expression of several transducers such as TRP receptors (TRPV1, TRPV4, TRPM8 etc.) results in increased sensitivity to noxious stimuli. Various models of neuropathic pain provide evidence that TRPV1 expression is decreased in the injured nerve fibers but increased in those proximal to the site of damage [24]. In models of inflammatory pain, there is increase in the transport of TRPV1 mRNA from neuronal cell bodies to central and peripheral axon terminals and an overall up-regulation of TRPV1 expression in unmyelinated axons [25].

Trauma, tumor, inflammation, vascular or visceral distension, or sympathetic activation following nerve injury may lead to accumulation of ATP in the extracellular space and activation of ionotropic P2X receptor family on sensory afferents [26]. Of the ionotropic P2X receptor family, the $P2X_3$ receptor have been reported to be more likely involved peripherally [27]. After peripheral axotomy, some neuropeptides viz. substance P, calcitonin gene-related peptides (CGRP) and somatostatin are down-regulated, while others such as vasoactive intestinal peptide

(VIP), galanin, neuropeptide Y (NPY) and cholecystokinin (CCK), present in sensory neurons are dramatically overexpressed [5,28]. These neuropeptides have broad range of activities within peripheral tissues and make a significant contribution in neuropathic pain.

Following a peripheral nerve injury (e.g. crush, stretch or axotomy), a neuroma develops at the proximal nerve stump as a result of unmyelinated sprouts (C fibers) growing out from the transected axons. Peripheral nerve injury also triggers the sprouting of noradrenergic sympathetic axon into the sensory dorsal root ganglion, rendering them sensitive to catecholamines and thus, providing an evidence of sympathetic component of neuropathic pain. In animal models of neuropathic pain, major symptoms of neuropathic pain have been relieved by sympathectomy [29]. Nerve growth factor (NGF) and brain-derived neurotropic factors (BDNF) have been implicated in the mechanism of sympathetic sprouting in DRG after the nerve injury [30].

After nerve lesion, activated macrophages infiltrate from endoneural blood vessels into the nerve and DRG, releasing chemical substances such as bradykinin, prostaglandins including PGE_2 and PGI_2, NGF and various pro-inflammatory cytokines (IL-6 and TNF-α) which sensitize the nociceptors [31,32]. These mediators induce ectopic activity in both injured and adjacent uninjured primary afferent nociceptors at the lesion site [33]. In patients with inflammatory neuropathies, such as vasculitic neuropathies or HIV neuropathy, COX-2 and pro-inflammatory cytokines (IL-6 and TNF-α) are found to be up-regulated in nerve biopsy specimens [34]. Stimulation of bradykinin and prostaglandin receptors have shown to stimulate protein kinase C (PKC) and protein kinase A (PKA), which further leads to phosphorylation of various ion channels like tetrodotoxin resistant Na^+ and vanilloid receptors [29].

There is increasing evidence that uninjured fibers that intermingle with degenerating fibers in a partially lesioned nerve might also participate in pain signaling. Products such as NGF that are associated with wallerian degeneration (WD) are released in the vicinity of spared fibers, triggering the release of TNF-α, as well as influencing the expression of various channels and receptors (sodium channels, TRPV1 receptors, adrenoreceptors), thereby altering the properties of uninjured afferents [35].

1.3.4 Central Mechanisms

Peripheral nerve injury causes anatomical and neuro-chemical changes not only in peripheral but also in spinal and supra-spinal level, which includes cyto-architectural reorganization [9], wind up phenomenon [36], glial cell activation and loss of inhibitory mechanisms [5].

In dorsal horn, Aδ fibers and C fibers terminate in laminae I and II respectively, while Aβ fibers terminate in laminae III and IV. Nerve injury results in withdrawal of C fibers axon terminals from laminae II along with sprouting of Aβ fibers at the site of C fibers to innervate the vacant synaptic site (Figure 1.3) [37]. Thus second order neurons, which generally receive high threshold input start receiving input from low threshold mechanoreceptors Aβ fibers, results in the phenomenon of allodynia [38]. The possible mechanism for this sprouting is mediated by nerve growth factor (NGF) [39].

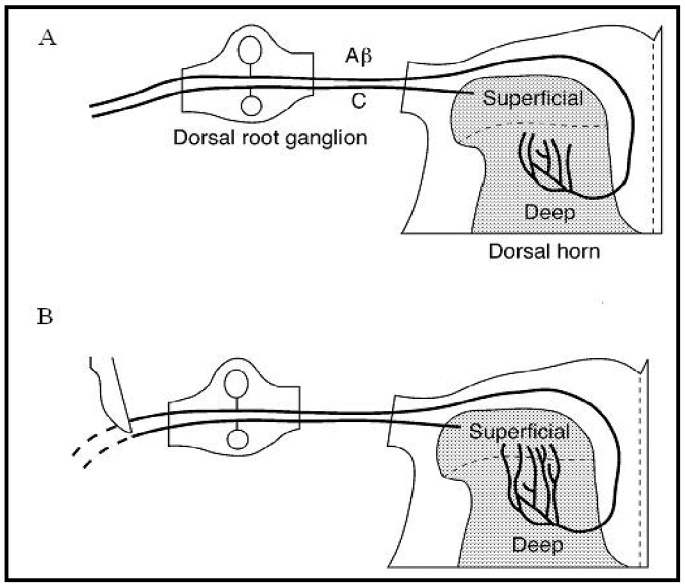

Figure 1.3 Anatomical reorganization after nerve injury [19]

Wind-up is a phenomenon where repeated stimulation of C nerve fibers results in generation of slow excitatory post-synaptic potential in wide dynamic range neurons that increase over the time. Under the normal physiological condition, depolarization of dorsal horn neurons occurs through activation of AMPA receptor by glutamate, while NMDA receptors remains blocked by Mg^{2+} plug inside the channel. After peripheral nerve injury, repeated fast and short-lived depolarization of C fibers causes removal of Mg^{2+} plug followed by enhanced NMDA gating. By increasing glutamate

sensitivity, there is a progressively increased action potential in response to each repeated stimuli [40].

NMDA receptor activation further lead to a subsequent Ca^{2+} influx into the cell cytoplasm from both extracellular and intracellular sources, which activates several enzyme cascades including protein kinase A (PKA), protein kinase C (PKC), phosphatidylinositol 3-kinase (PI3K), mitogen-activated protein kinase (MAPK), protein phospholipase A_2 and nitric oxide synthase (NOS), each of which promotes further responses (Figure 1.4)[38,41].

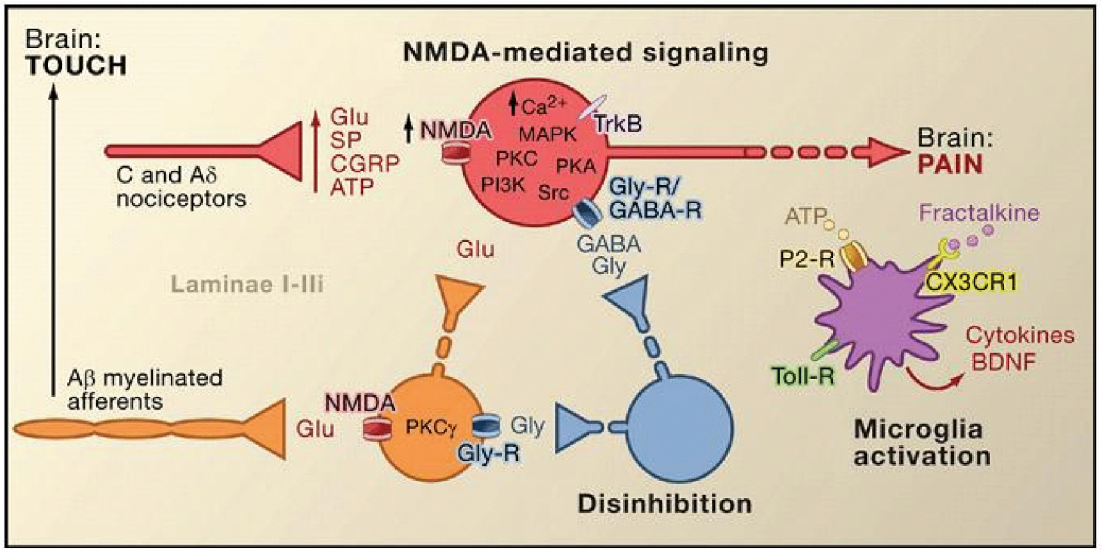

Figure 1.4: Major central mechanisms of neuropathic pain [42]

Peripheral nerve injuries have also been shown to activate spinal cord microglial cells, which play a vital role in initiating and maintaining central sensitization. In animal models of pain, microglial cells are activated within 4 hours, increase 2- 4 fold by day 2 and remains active for several months. Microglial cells are activated by ATP/purinergic receptors, CX3CL1 (Fractalkine)/ CX3CR-1 receptor and TLR (toll-like receptor) and release BDNF, which through activation of TrkB receptors in lamina I output neurons, promotes hyperexcitability [43]. Activated microglial cells also releases cathepsin S that cleaves neuronal fractalkine, which binds to CX3CR1 and stimulates phosphorylation of p38 MAPK in microglia and leads to stimulation of various pro-nocciceptive cytokines particulary TNF-α, IL1 β and IL6 [44].

Up-regulation of the spinal CB_1 cannabinoid receptor after nerve injury is also reported [45]. Although normally not expressed in the CNS, cannabinoid receptor

CB_2 is up-regulated in spinal microglia under conditions of neuropathic pain [46]. This up-regulation may explain the preserved antinociceptive effect of exogenous cannabinoid compounds under neuropathic pain conditions.

Reduction of inhibitory tone on nociceptive transmission plays an important role in pathophysiology of neuropathic pain. After peripheral nerve injury, the ongoing activity from primary afferents may cause a degeneration of dorsal horn neurons including GABA and interneurons, leading to decreased synthesis of GABA. This loss of inhibitory interneurons and GABA results in a marked decrease in inhibitory postsynaptic currents, contributing to hypersensitivity and pain [47].

Dorsal horn neurons receive a powerful descending modulating control from supra-spinal brain-stem centers. It is hypothesized that a loss of function in descending inhibitory serotonergic and noradrenergic pathways contributes to central sensitization and pain chronification. Decreased efficacy of spinal opioids [48] and upregulation of anti-opioids such as cholicystokinin and dynorphin also contributes to the mechanism of neuropathic pain [49].

Over all, neuropathic pain is a series of complex processes and need to be explored further. Better understanding of underlying molecular mechanisms, together with discovery of new therapeutic targets will strengthen the future treatment strategy.

CHAPTER 2
STRATEGIES FOR THE TREATMENT OF NEUROPATHIC PAIN: A LITERATURE REVIEW

"Science is a wonderful thing, but it has not yet succeeded in maximizing pleasure and minimizing pain, and that's all we asked of it"

-Anonymous

Neuropathic pain, a persistent chronic pain resulting from damage to the central or peripheral pain signaling pathway, has become an area of intense research activity largely because it represents a disorder with high unmet medical need. Clinically neuropathic pain is not adequately managed, as there are very few truly effective, well-tolerated therapies for neuropathic pain. Till date, treatment of neuropathic pain is dependent primarily on handful of medications, including old-fashioned anticonvulsants, tricyclic antidepressants (TCAs), opiates, topical lidocaine and capsaicin patches.

2.1 Existing Treatments

2.1.1 Anticonvulsant Drugs

Cellular and molecular similarities between the pathophysiologic phenomena observed in epilepsy and in neuropathic pain justify the use of anticonvulsants in the symptomatic management of neuropathic pain [50]. The wind-up phenomenon caused by nerve injury and the kindling of hippocampal neurons in epilepsy are remarkably similar and results in part, from activation of NMDA receptors [51]. The susceptibility of primary afferents and transmission neurons to the effect of sodium channel blockers in neuropathic pain models has been well recognized, which are found to be similar to the models of epilepsy.

The exact mechanism of action of the anticonvulsant agents in pain syndromes remains uncertain, but is thought to limit neuronal excitation and enhance inhibition. Relevant sites of action include voltage gated ion channels (i.e., Na^+ and Ca^{2+} channels), ligand-gated ion channels, the excitatory receptors for glutamate and the inhibitory receptors for GABA and glycine (Table 2.1).

Table.2.1 Mechanisms of action for antiepileptic drugs used in Neuropathic pain

Drugs	Mechanism of action	Limitations / Side effects
Phenytoin	Voltage-dependent Na^+ channel blocker	Dizziness, ataxia, in coordination, gum hyperplasia, metabolism saturation
Carbamazepine	Blockade of sodium channel and enhancement of GABA	Ataxia, sedation, aplastic anemia, hepatotoxicity, hyponatremia
Lamotrigine	Voltage-gated Na^+ and Ca^{2+} channel blocker	Sedation, ataxia, headache, skin rash, Stevens-Johnson syndrome
Gabapentin	Blockade of Ca^{2+} channel	Sedation, ataxia and gastric irritation
Pregabalin	Blockade of Ca^{2+} channel	Dizziness, skin rash, weight gain and loss of coordination

Many anticonvulsants like phenytoin, carbamazepine, lamotrigine, gabapentin and pregabalin are used as initial approaches to the treatment of sharp, shooting "electric-like" (lancinating) neuropathic pain. The first report of analgesia with an anticonvulsant in neuropathic pain was reported with phenytoin in 1942, [52] which was confirmed by subsequent randomized clinical trials (RCTs) for diabetic neuropathy and for various other neuropathies [53-55].

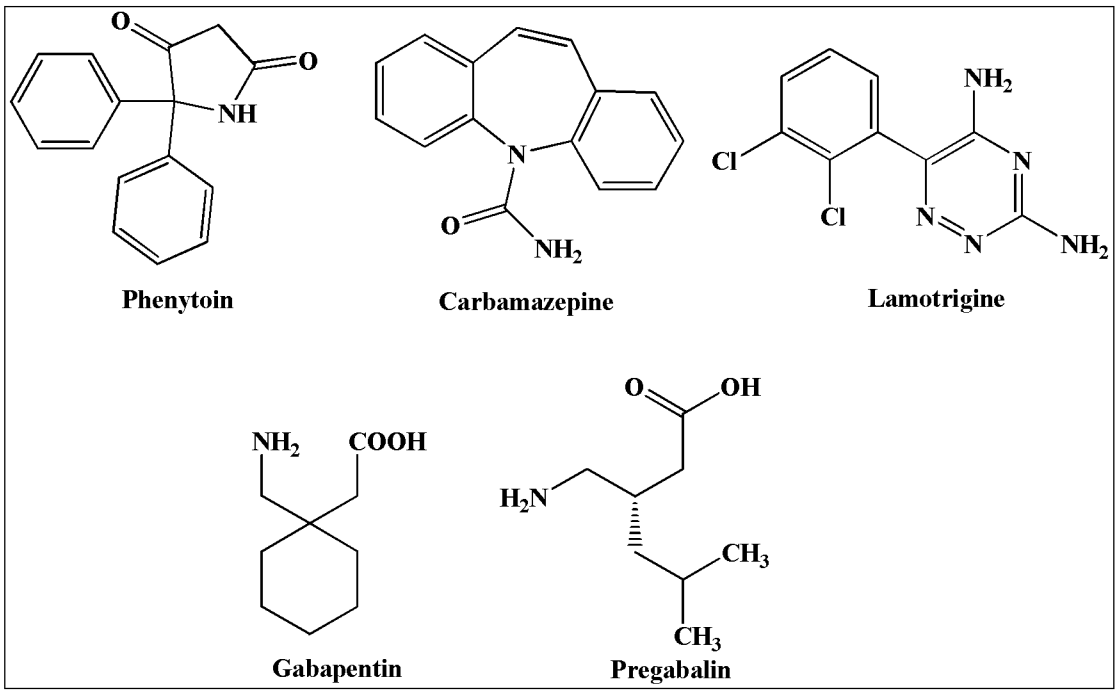

Figure-2.1 Anticonvulsants used for the treatment of neuropathic pain

The analgesic effect of carbamazepine on patients with trigeminal neuralgia was first reported in 1962 and till date, 12 RCTs evaluating the efficacy of carbamazepine in neuropathic pain have been published [51]. Lamotrigine, one of the newer antiepileptic agents has demonstrated efficacy in relieving pain in patients with trigeminal neuralgia, HIV-associated neuropathy and central post-stroke pain [56,57]. Gabapentin and pregabalin, which are structural analogues of the inhibitory neurotransmitter GABA, have been demonstrated to reduce post herpetic neuralgia [58] and painful diabetic neuropathy (Table 2.1; Figure 2.1) [59,60].

2.1.2 Antidepressants

Three basic reasons are considered for the use of antidepressants in neuropathic pain. First, psychiatric disorders are common in patients with severe or disabling chronic pain. Second, sleep disturbance is common in both the disorders. Third, there are several evidences that certain classes of antidepressants produce pain relief regardless of their use in depression [61].

Table: 2.2 Antidepressant drugs for the treatment of neuropathic pain

Drugs	Mechanism of action	Limitations / Side effects
Tricyclic Antidepressants		
Amitriptyline Nortryptyline Imipramine	Inhibition of norepinephrine reuptake	Dry mouth, blurred vision, drowsiness, dizziness, tremors, sexual dysfunctions, skin rash, and weight gain or loss
SNRIs		
Venlafaxine	Inhibition of serotonin and norepinephrine reuptake	Dry mouth, blurred vision, drowsiness, dizziness,tremors, sexual dysfunctions, skin rash, and weight gain or loss
SSRIs		
Paroxetine Citalopram	Selective inhibition of serotonin reuptake	Headache, agitation, nausea

The use of tricyclic antidepressants (TCAs) in the treatment of neuropathic pain can be dated back to a report by Woodforde *et al.,* for treatment of postherpetic neuralgia in 1965 [62]. Later in 1982, Watson *et al.,* reported the effect of amitriptyline in reducing postherpetic neuralgia in a randomized, double-blind, placebo-controlled, crossover trials [63]. Imipramine, another tricyclyclic antidepressant has been shown

to be efficacious in painful diabetic neuropathy where the drug regimen was 50 mg/day during the first week and 100 mg/day from second to the fifth week [64]. TCAs are thought to exert their analgesic effects mainly through central modulation of both serotonergic and noradrenergic activities (Table 2.2). Selective serotonin reuptake inhibitors (SSRIs) like paroxetine and citalopram, and serotonin norepinephrine reuptake inhibitors (SNRIs) like venlafaxine have shown efficacy in neuropathic pain. One study demonstrated that paroxetine (40 mg/day) was effective for painful diabetic neuropathy [65]. In a double-blind, placebo-controlled, crossover study, citalopram 40 mg/day was shown to provide slight relief from the symptoms of chronic diabetic neuropathy [66]. In an open study by Taylor and Rowbotham, involving 12 patients with chronic pain, all 7 with neuropathic pain responded to venlafaxine, with mild to moderate relief (Figure 2.2) [67].

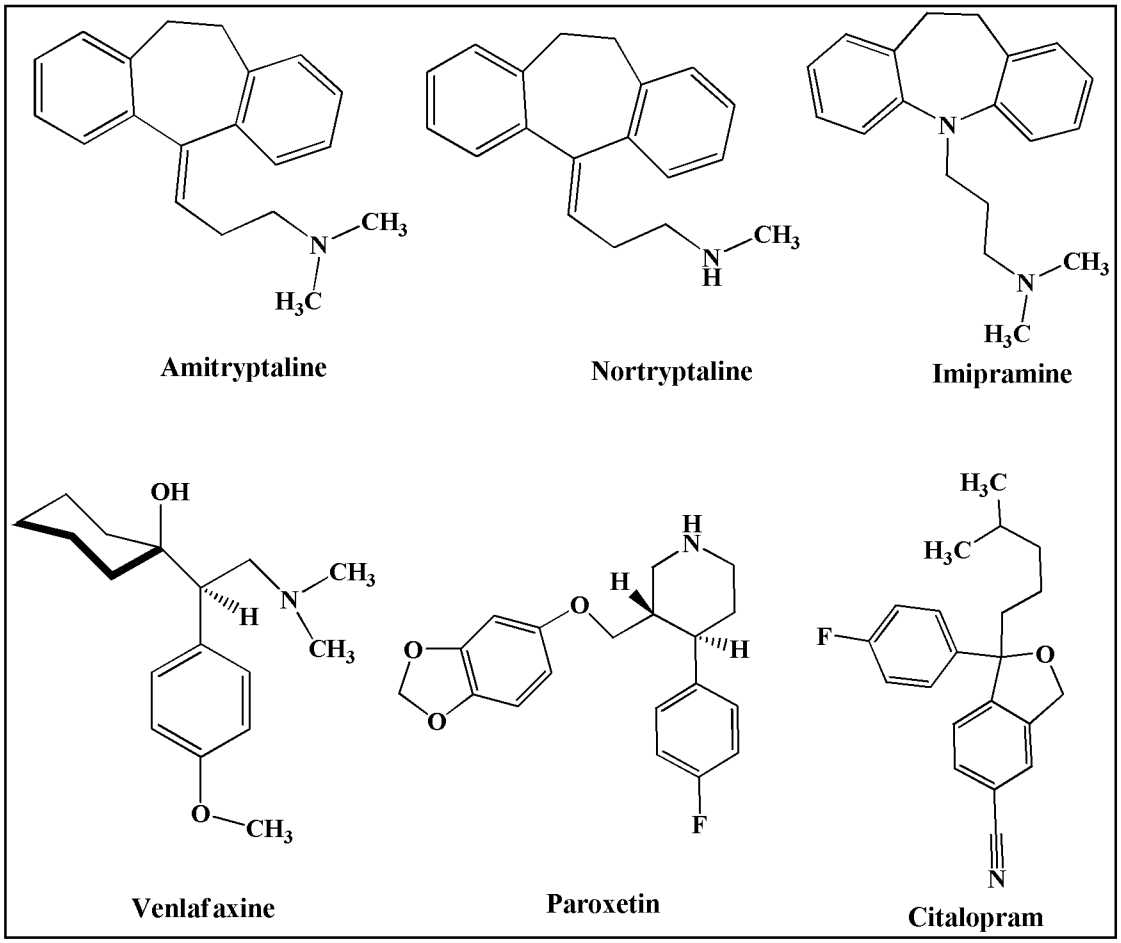

Figure 2.2 Antidepressant drugs used for the treatment of neuropathic pain

2.1.3 Opioids

Opioids are the most potent analgesics available and are well established for the treatment of severe acute, surgical and cancer pain, however their efficicay in neuropathic pain is still controversial. Since the report of Portenoy was published [68], the use of opioids in certain types of neuropathic pain, e.g. oxycodone for postherpetic pain [69] and tramadol for diabetic polyneuropathy [70] has been advocated.

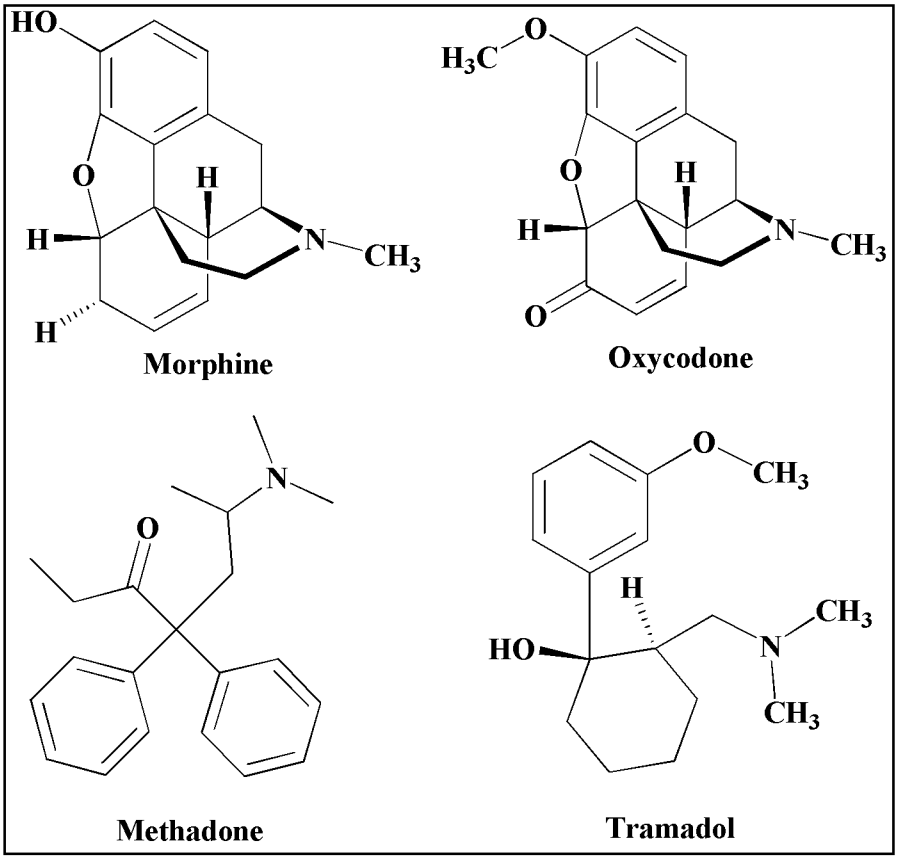

Figure-2.3 Opioids used for the treatment of neuropathic pain

A clinical study with evaluation of intrathecal morphine in chronic mixed neuropathic pain patients confirmed pain reduction (moderate) in half of the patients studied, although morphine was often combined with other treatment modalities [71]. Results from clinical trials have demonstrated the effectiveness of tramadol (an agent that combines opioid receptor antagonist activity with norepinephrine reuptake inhibition) in patients with polyneuropathy (Table2.3; Figure 2.3) [70].

Table 2.3 Opiates for the treatment of neuropathic pain

Drugs	Mechanism of action	Limitations / Side effects
Morphine	μ, κ and δ receptor agonist	Constipation, addiction, withdrawal symptoms, respiratory depression
Methadone	μ receptor agonist	Constipation, increased sweating, heat intolerance, constricted pupils, hallucination, headache, vomiting, cardiac arrhythmia, dry mouth, blurred vision
Oxycodone	μ receptor agonist	Euphoria, constipation, fatigue, dizziness, nausea, lightheadedness, headache, dry mouth, anxiety, pruritus, and diaphoresis
Tramadol	μ receptor agonist	Nausea, vomiting, memory loss, sweating, constipation and respiratory depression

2.1.4 Topical Agents

Topical agents such as lidocaine and capsaicin are also used for various neuropathic pain conditions. Topical lidocaine patches (5%) have been effacious in reducing the pain of postherpetic neuralgia in double blind, randomized and vehicle controlled clinical trials [72]. Capsaicin that is extracted from hot chilli peppers has shown significant effects in several studies involving diabetic neuropathy and postherpetic neuralgia at the dose of 0.025% to 0.075%.[73].

2.1.5 Limitation of Current Neuropathic Treatments

Most of the medications presently available for the treatment of neuropathic pain are not specifically indicated for neuropathic pain, and exhibit inadequate efficacy and adverse events profile. Anticonvulsants have been traditionally used for the management of neuropathic pain, as most of these either stabilize the membrane hyper-excitability or enhance inhibitory GABA and/or glycine neurotransmission but their efficacy has not been unequivocally established and moreover they are associated with numerous side effects such as impaired motor and mental functions [74]. Gabapentin, a structural analogue of GABA has been approved for the treatment of neuropathic pain but still in many patients it does not provide adequate pain relief [75].

Comparison trials between TCAs and SSRIs have shown that SSRIs are inferior to TCAs in treating neuropathic pain. TCAs causes variuos side effects like dry mouth,

blurred vision, drowsiness, dizziness, tremors, sexual dysfunctions, skin rash, and weight gain or loss which impede their use in chronic administration [76].

The use of opioids to treat neuropathic pain is controversial owing to concerns about addiction, high rates of adverse effects including constipation, sedation, nausea and the beliefs that neuropathic pain does not always respond well to opioids [71].

The adverse effect of lidocaine patch like erythema, edema and abnormal sensation and with capsaicin cream like transient burning and erythema followed by anesthesia are major confronts in the treatment. Since the capsaicin cream needs to be applied 3 to 5 times daily, the increased risk of poor compliance makes it less prefered option for treatment of neuropathic pain [73].

2.2 Emerging Drugs (Under Preclinical/Clinical Development Stage)

Developing well tolerated novel analgesics to be effective in mild to severe, acute to chronic pain is the focus of current research in neuropathic pain worldwide. Various new approaches targeting neuropathic pain include sodium channel blockade, calcium channel blockade, TRP channels blockade, purinergic receptor antagonism, drugs acting on glutamatergic system, cannabinergic agonism, cytokine inhibitors, cathepsin S inhibition, nitric oxide (NO) inhibition and enhancement of GABAergic neurotransmission.

2.2.1 Sodium Channel Blockade

Voltage gated sodium ion channels (VGSCs, Na_v) are the key players in electrical conduction along the axons, including those of primary sensory neurons. Starting in 1960s, a parallel line of research led to the serendipitous observation that certain known anticonvulsants and antiarrythmics were highly efficacious in certain painful conditions in man including neuropathic pain. Since then, it has been hypothesized that voltage gated sodium channels might play specialized roles in the development and the maintenance of hyperexcitability observed in primary afferent neurons as a result of nerve or tissue injury [77]. Carbamazepine is one such drug which still remains today as one of the drugs of choice for treating pain associated with trigeminal neuralgia [78].

Table 2.4 Subtypes of voltage sensitive Na^+ channels and some key properties

Na_V type	Location	TTX-sensitive	Abundance in Adult DRG
1.1	CNS, DRG	Yes	Moderate
1.2	CNS, DRG	Yes	Moderate
1.3	CNS	Yes	Very Low
1.4	Skeletal Muscle	Yes	Absent
1.5	Cardiac	No	Absent
1.6	CNS, DRG	Yes	High
1.7	DRG, Glia	Yes	High
1.8	DRG (small neurons)	No	High
1.9	DRG (small neurons)	No	High
Na_X	DRG, Cardiac, Glia, Skeletal muscle	No	Moderate

DRG: Dorsal root ganglion; TTX: Tetrodotoxin.

VGSCs are a family of nine structurally related α subunits (Na_v 1.1 to Na_v 1.9) which show distinct expression patterns and are associated with one or more accessory β subunits (β_1 to β_3) [79]. The expression of the subunit isoforms is developmentally regulated and tissue specific (Table 2.4). VGSCs are classified into two groups according to their sensitivity to tetrodotoxin (TTX): TTX-sensitive and TTX-resistant channels [77]. Na_v 1.5, 1.8 and 1.9 are TTX-resistant while others are TTX sensitive. With the exception of Na_v 1.4 and 1.5, it seems that all VGSCs are expressed to some extent in sensory neurons [80]. Among these Na_v1.7, Na_v1.8 and Na_v1.9 have got special attention for neuropathic pain since they have exclusive expression in DRG neurons.

Various anticonvulsant drugs like lamotrigine, carbamazepine, topiramate, oxcarbazepine and local anaesthetics like lidocaine, used clinically for neuropathic pain have shown their activity through voltage gated sodium channels. Several clinical trials have showed efficacy of sodium channel blockers in neuropathic disorders like diabetic neuropathy and postherpetic neuralgia [81].

Raflinamide (NW-1029), a preferencial $Na_v1.7$ channel blocker, currently undergoing clinical trial for neuropathic low back pain has previously shown to reverse mechanical allodynia in animal models of inflammatory pain and neuropathic pain (SNL and CCI) [82]. Tectin™ (Wex Pharmaceuticals) is a TTX derivative that has proven to be promising for the treatment of cancer-induced neuropathic pain in phase-III clinical trials. Tectin works by acting as a tonic blocker of TTX-sensitive voltage-gated Na^+ channels as opposed to acting as a state-dependent blocker [81]. Tetrodin™ (Wex Pharmaceuticals) is a purified form of TTX that is in phase-I trials for pain management working similarly as Tectin.

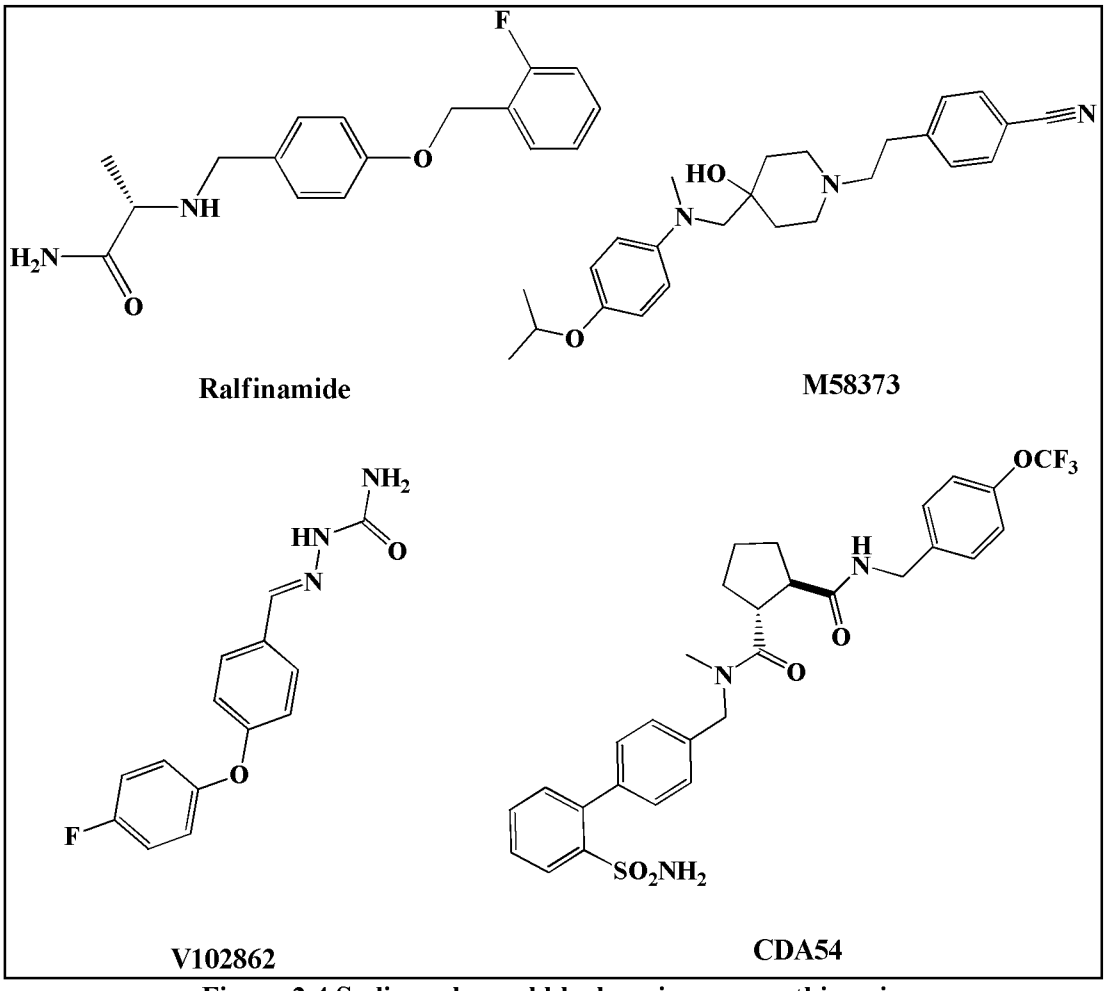

Figure 2.4 Sodium channel blockers in neuropathic pain

Various other molecules have shown their efficacy in animal models of pain. Brochu *et al.*, (2006) described the functional properties of *trans-N*-{[2'-(aminosulfonyl)biphenyl-4-yl]methyl}-*N*-methyl-*N*'-[4-(trifluoromethoxy)benzyl] cyclopentane-1,2-dicarboxamide (CDA54), a peripherally acting sodium channel

blocker in alleviating behavioral signs of neuropathic pain in two nerve injury models (Figure 2.4) [83].

In 2006 Patel *et al.,* reported the reversal of neuropathic pain by α-hydroxyphenylamide, a novel sodium channel blocker. In the CCI rat model of neuropathic pain, intraperitoneal administration of α-hydroxyphenylamide attenuated the hyperalgesic response by 53% at 100 mg/kg, without affecting motor coordination in the roto-rod test [84]. The analgesic Effect of a putative sodium channel blocker M58373,(4-[2-(4-hydroxy-4[*N*-(4-isopropoxyphenyl)-*N*-methylamino]methyl}piperidin--1-yl)ethyl]benzonitrile mono hydrochloride, on formalin-induced and neuropathic pain in rats were studied by Akada *et al.,* (2006) wherein, it attenuated mechanical allodynia and thermal hyperalgesia in the nerve-injured paw without affecting normal responses in the uninjured paw at the dose of 1-10 mg/kg (*p.o.*) [85].

In 2007, Ilyin *et al.,* studied the efficacy of 2-[4-(4-Chloro-2-fluorophenoxy) phenyl]-pyrimidine-4-carboxamide, a novel and potent structural analog of the state-dependent Na^+ channel blocker [4-(4-fluorophenoxy)benzaldehyde semicarbazone] (V102862) in partial sciatic nerve ligation, Freund's complete adjuvant induced pain, and postincisional pain when tested in rat pain models [86].

Unfortunately the sodium channel blockers currently available are not considered selective for specific subtype of Na_v involved in pain and have relatively narrow therapeutic windows, which can limit their usefulness. Isoform selective pharmacological blockers or gene therapy approaches targeted at downregulating specific isoforms could show increased therapeutic efficacy for treating pain, being an important area of sodium channel research.

2.2.2 Voltage Gated Calcium Channel (VGCC) Blockade

Voltage-gated calcium channels (VGCC) that transduce electrical activity into intracellular biochemical signals play an important role in various physiological functions. Activation of VGCCs allows rapid calcium influx into cells, which, in turn, regulates numerous physiological processes such as neurotransmitter release, neuronal excitability, plasticity and calcium-dependent intracellular signaling events like gene induction and development as well as cell survival and death [87]. Since some of these phenomena are also involved in nociception, hyperalgesia and allodynia, a

major emerging concept is that VGCCs may be selectively targeted in pain therapy [23].

Table 2.5 Summary of calcium channel classification

Type	Subtype	Location
L	Cav1.1	Skeletal muscle
	Cav1.2	Cardiac, smooth muscle, neuronal
	Cav1.3	Sinoatrial node, cochlear hair cells, neuronal (dendritic)
	Cav1.4	Retina
P/Q	Cav2.1	Neuronal (presynaptic)
N	Cav2.2	Neuronal (presynaptic)
R	Cav2.3	Neuronal
T	Cav3.1	Neuronal, cardiac
	Cav3.2	Neuronal, (+ many other tissues)
	Cav3.3	Neuronal

VGCCs mainly comprises of a pore-forming α1 subunit as the center piece, surrounded by auxiliary α2δ, β and γ subunits. They are classified into 4 types; L (Cav 1.1-1.4), P/Q (Cav 2.1), N (Cav 2.2), R (Cav 2.3) and T (Cav 3.1-3.3) type Ca^{2+} channels based on the type of α1 subunit. L,P/Q and R type Ca^{2+} channels require strong depolarization for activation, whereas T-type Ca^{2+} channels is triggered by much milder depolarization [88].

Among all the VGCCs, L-, N-, P/Q- and T-type Ca^{2+} channels as well as the auxiliary α2δ subunit that has been most extensively studied in nociception [89]. N-type calcium channel (Cav 2.2) blocker have been found to block both phase-I (acute, fast, glutamate activated) and phase-II (delayed, persistant. NMDA activated) nocciceptive responses [90], where as L-type of calcium channel (Cav 1.1-1.4) blockers have been found to block only phase-II nociceptive response of the formalin test (Table 2.5). [91].

Studies have shown the effectiveness of Cav blockers in various animal models of neuropathic pain. Bowersox *et al.,* (1996) reported a selective N-type calcium channel blocker SNX-111 (Prialt; ziconotide, a synthetic form of a ω-conotoxin peptide) to be effective in producing spinal antinociception in rat models of acute, persistent and neuropathic pain [92]. Clinical trials of intrathecal application of SNX-111 resulted in significant pain relief for patients with severe chronic pain including neuropathic pain

and pain secondary to cancer or AIDS [93]. The usage of this drug is limited by the route of administration and undesirable side effects including sedation, dizziness, nausea, and emesis and memory impairment. AM336 (omega-conotoxin, CVID), another N-type calcium channel blocker was shown to be efficacious in a small phase-IIa clinical trial for patients with severe cancer pain, but unfortunately, the side effects were undesirable and dose limiting [94].

Evidence from clinical studies showed that L-type VGCC blockers such as topiramate, are efficacious for neuropathic pain management. Topiramate has been shown to cause statistically significant reduction in pain intensity compared to a placebo, for up to 12 weeks in diabetic peripheral neuropathy patients [95]. However, topiramate has been reported to show other pharmacologic actions including blockade of VGCCs in a dose-dependent manner, potentiation of GABA inhibition, and AMPA receptor blockade [94].

Many recent findings have suggested that the $\alpha_2\delta$ subunit of Ca^{2+} channel may play an important role in neuropathic pain. The prototype drugs currently used in the drug therapy of neuropathic pain namely gabapentin and pregabalin have infact been reported to act at the α2δ subunit of voltage-gated calcium channels [88]. Studies show that α2δ subunit have marked effects on the properties of Cav channels, providing a potential target in pain research (Figure 2.5).

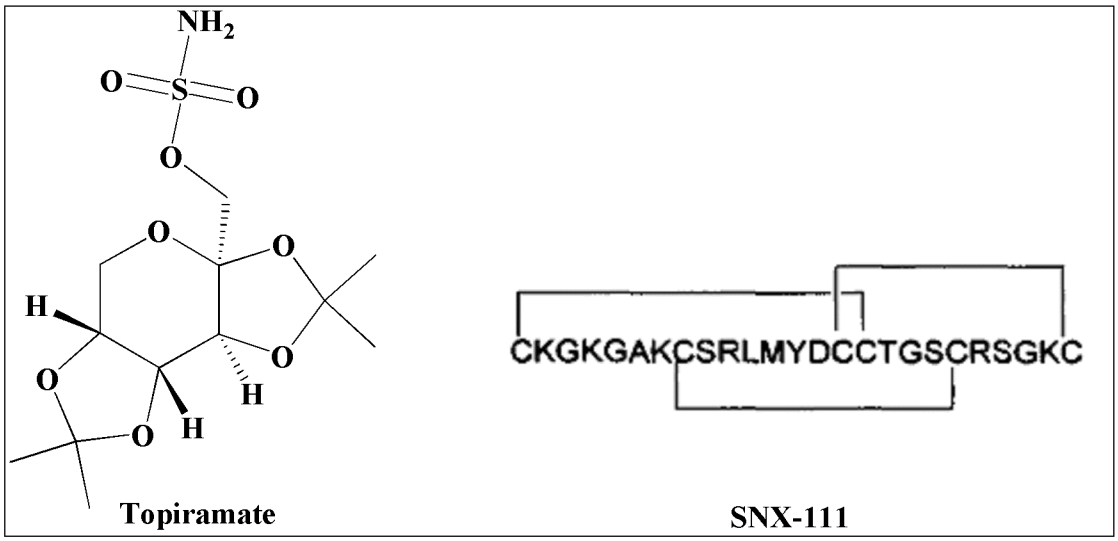

Figure 2.5 Calcium channel blockers in neuropathic pain

For the past several decades, preclinical and clinical research in developing VGCC blockers or modulators for chronic pain management has been fruitful. However, their

efficacy in pain relief is limited in some patients, and their long-term use is limited by their side-effect profiles.

2.2.3 Transient Receptor Potential (TRP) Channels Antagonists

Recent studies indicate that several members of the transient receptor potential (TRP) family, namely TRPV1 and TRPA1 function as either sensory transducers for noxious mechanical stimuli or play an essential role in the development of mechanical hypersensitivity under various pain conditions.

Over recent years several publications have appeared describing the Effect of TRPV1 antagonists in animal models of pain. In 2003, Walker *et al.,* reported the antihyperalgesic properties of capsazepine, a competitive TRPV1 antagonist in models of inflammatory and neuropathic pain [96]. In the guinea pig, capsazepine (1-30 mg/kg, *s.c.*) produced 44% reversal of mechanical hyperalgesia induced by Freund's complete adjuvant and an even more profound (80%) reversal of neuropathic pain following partial sciatic nerve ligation (PSNL). In the clinic, treatment with topical capsaicin has been shown to be of some benefit in a number of painful conditions such as diabetic neuropathy [97] and postherpetic neuralgia [98].

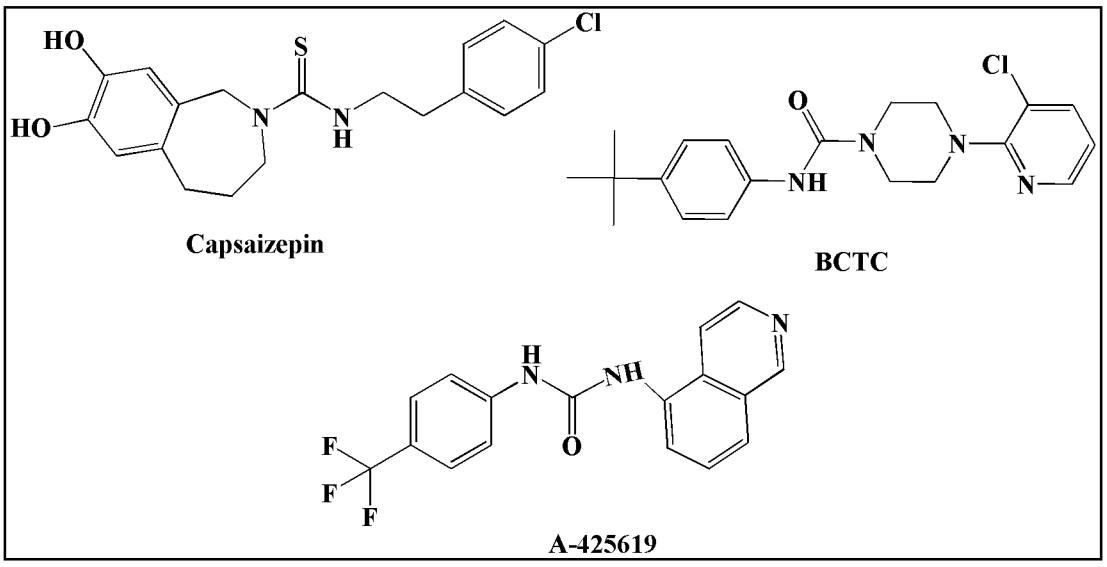

Figure 2.6 Transient Receptor Potential (TRP) Channels antagonists

An inhibitor of capsaicin and acid-mediated currents at rat TRPV1 receptor, *N*-(4-tertiarybutylphenyl)-4-(3-cholorphyridin-2-yl)tetrahydropyrazine-1(2*H*)-carboxamide (BCTC) was reported to reduce mechanical hyperalgesia and dynamic allodynia 2 weeks after PSNL [96]. Later in 2005, Honore *et al.,* reported the analgesic profile of

1-isoquinolin-5-yl-3-(4-trifluoromethyl-benzyl)-urea (A-425619) possessing efficacy in models of inflammatory, postoperative and neuropathic pain (Figure 2.6) [99].

2.2.4 Purinergic Antagonism

The ability of endogenous ATP to evoke pain has been known for nearly 40 years [100-102] but pharmacological and biochemical evidence on the mechanisms of action of ATP and the role of purinergic receptors in nociceptive signaling was highlighted by Burnstock (1996), who hypothesized that ATP released from different cells is implicated in the initiation of pain by acting on purinoceptors on sensory nerve terminals [103].

The development of a competitive $P2X_3$ antagonist A-317491 underpinned the significance of $P2X_3$ receptor signaling in neuropathic pain conditions [104]. At doses of upto 100 μmol/kg compound 5-([(3-phenoxybenzyl)[1S)-1,2,3,4-tetrahydro-1-naphthalenyl]amino]carbonyl)-1,2,4 -benzenetricarboxylic acid (A-317491) abolished both mechanical allodynia and thermal hyperalgesia in CCI rats. A-317491 was also effective against dynamic allodynia induced by L5-L6 SNL injury in rat. Honore *et al.*, (2006) have reported a novel and selective $P2X_7$ receptor antagonist, N-(1-{[(cyanoimino) (5-quinolinylamino) methyl]amino}-2,2-dimethylpropyl)-2-(3,4-dimethoxyphenyl)acetamide (A-740003), which reversed SNL-induced mechanical allodynia in a dose-related manner (ED_{50} of 19 mg/kg, *i.p.*). A-740003 also attenuated CCI-induced mechanical allodynia in a dose dependent manner (Figure 2.7) [105].

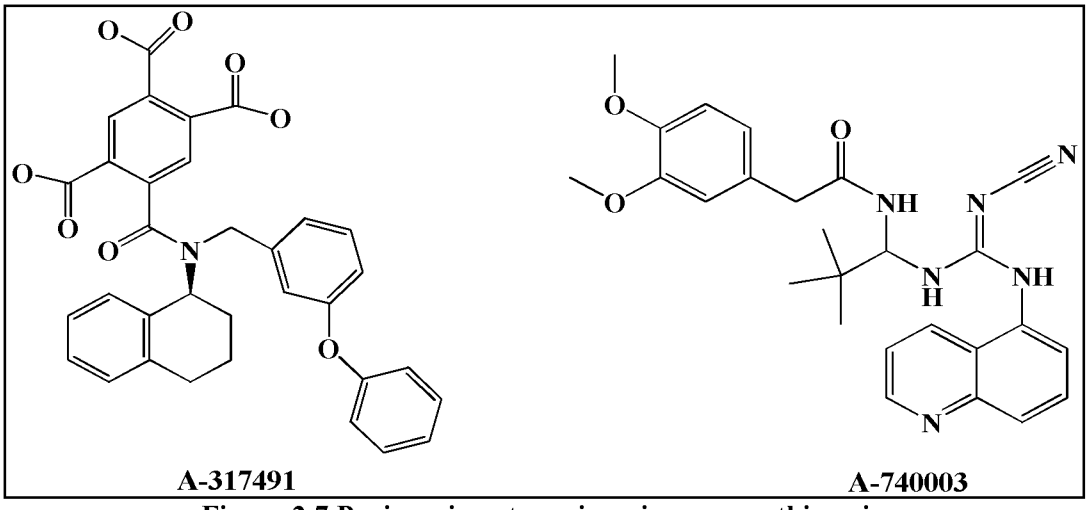

Figure 2.7 Purinergic antagonisms in neuropathic pain

2.2.5 Cytokine Inhibitors

After tissue injury, cytokines such as TNF-α, IL-1β, IL-6 and IL-8 released from immune cells are pro-inflammatory and hyperalgesic. The activity of cytokines at their receptors activate intracellular p38 MAPK and extracellular signal-regulated protein kinase [106]. The inhibitors of these kinases also reduce allodynia in neuropathic rats [107]. Application of TNF-α to the nerve, nerve roots, or administered to the ganglia results in mechanical hyperalgesia [108,109] and systemic or intrathecal admistration of Etanercept, a recombinant TNF-α, (p75-)Fc fusion protein, reduces pain in neuropathic animals [110,111].

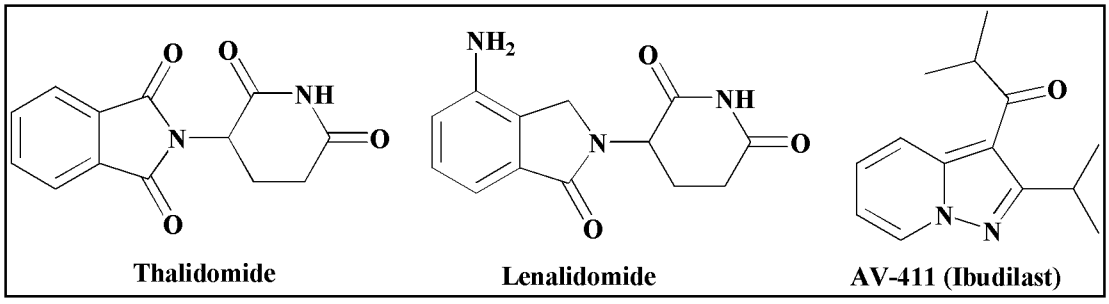

Figure 2.8 Cytokine inhibitors in neuropathic pain

Thalidomide, which blocks the production of TNF-α by activated macrophages, has shown to diminish mechanical allodynia and thermal hyperalgesia in CCI but only when pretreatment is given [112]. Thalidomide and its derivative Lenalidomide (CC-5013) are in phase-II clinical trial for complex regional pain syndrome. AV-411 (Ibudilast) a cytokine inhibitor, glial attenuator, IL-1β and IL-6 inhibitor is currently being investigated for diabetic neuropathy in clinical phase-II by Medicinova (formerly known as Avigen) (Figure 2.8) [113].

2.2.6 Nitric Oxide Inhibition

There is strong evidence that nitric oxide (NO) is an important mediator of hyperalgesia. It is generated via the oxidation of the terminal guanidino nitrogen atom of L-arginine by inducible and neuronal nitric oxide synthases (iNOS and nNOS). Nitric oxide may directly influence injured axons in the periphery and indirectly influence pain by its role in the process of wallerian degeneration or may influence local inflammatory process [114,115]. Besides its pronociceptive properties, NO is known to affect apoptotic pathways. High concentrations of NO or peroxynitrite induce apoptotic cell death in several cell types, including neurons through the activation of caspase signalling and ceramide generation [116,117].

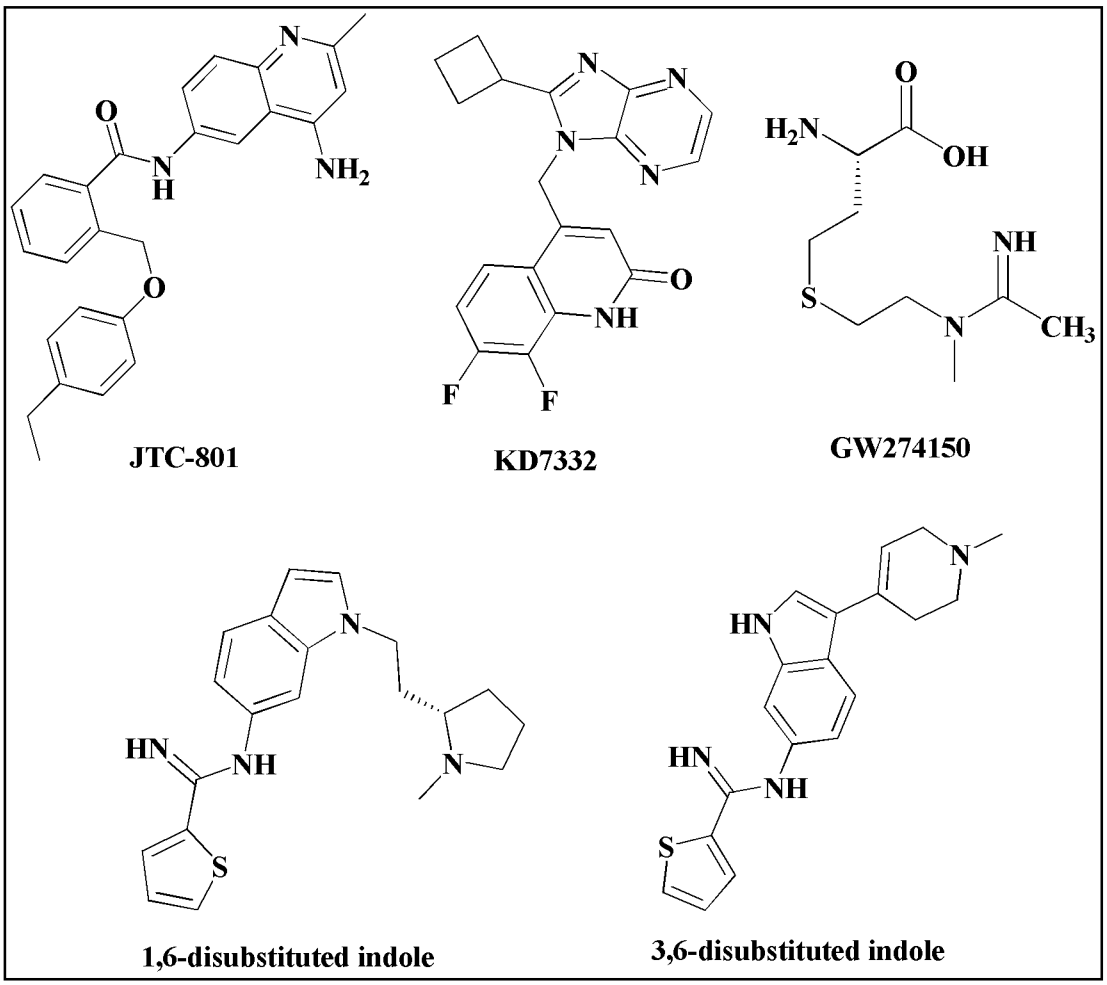

Figure 2.9 NO/ NOS inhibitors in neuropathic pain

Following nerve injury in animals, NOS is found to be overexpressed in dorsal root ganglion (DRG) and in the sciatic nerve [118]. Compounds which selectively inhibit NO or iNOS have shown to reduce hyperalgesia in various animal models. Pretreatment of oral JTC-801 an opiod analgesic has shown to decrease NOS activity and NO production in dorsal horn of mice following L-5 nerve transaction [119]. GW274150, a novel and highly selective inhibitor of the iNOS, shows analgesic effects in CFA induced inflammatory pain and CCI induced neuropathic pain in rat at the dose of 3-30 mg/kg [120]. KD7332 (KLYP961), a dual iNOS/ nNOS inhibitor inhibitor has been efficacious in the mouse formalin model of nociception and Chung model of neuropathic pain, without showing any tolerance after repeat dosing [121]. NeurAxon Inc., Canada has recently published selective nNOS inhibitors; 3,6-di-substituted indole derivatives and 1,6-di-substituted indole derivatives to be efficacious in SNL model and in a model of migraine pain respectively (Figure 2.9) [122,123].

2.2.7 Drugs Acting on Glutamatergic System

Glutamate is a widely distributed excitatory neurotransmitter in the mammalian nervous system. It is released at synapses when a nerve impulse is triggered and mediates its actions through both ionotropic and metabotropic receptor families. NMDA, AMPA and kainate receptors are ionotropic receptors, while the eight receptors of mGlu-family (mGlu1 to mGluR8) are together classified as metabotropic receptors [124].

The possibilities of using glutamate receptor antagonists for reducing neuropathic pain was widely investigated in the second half of the 1990s, as these receptors appear to be the key site for the transmission of pain from periphery to the central nervous system. There is substantial evidence indicating the presence of and a potential role of NMDA, AMPA, kainate and mGluR receptors in periphery, spinal cord and brain level which induces and maintains central sensitization [125]. Zhou *et al.,* reported the induction of pain behaviors in rats after peripheral administration of AMPA or kainate [126]. Similarly intrathecal injection of NMDA resulted in an enhanced neuropathic pain behavior in a chronic constriction nerve injury (CCI) model of neuropathic pain [127]. Some of the non-selective NMDA antagonists including ketamine, dextromethorphan, amantadine and memantine hydrochloride are in clinical use for a variety of indications including chronic pain, but suffer from undesirable side effects like psychomimetic effects, ataxia, motor incoordination and vacuolizations [128,129].

There are many preclinical reports on competitive and noncompetitive antagonist of NMDA. A study by Wei *et al.,* in 1999, reported MK-801 (Dizocipline), a high-affinity, non-competitive antagonist of the NMDA receptor to be active in attenuating the development of neuropathic symptoms in the rat [130]. Later in 2000, Wilcox *et al.,* reported that agmatine, NMDA antagonist when exogenously administered to rodents, decreased hyperalgesia accompanying inflammation, normalized the mechanical hypersensitivity produced by chemical or mechanical nerve injury, and reduced autotomy-like behavior after excitotoxic spinal cord injury (SCI) [131]. The antinociceptive effect of a low-affinity, non-competitive NMDA antagonist, N-(2-indanyl)-glycinamide (CHF3381) was studied in rats with a sciatic nerve injury and found to relieve both cold and mechanical allodynia (100 mg/kg, *p.o.*) [132].

Other than primary transmitter site (competitive), strychnine-insensitive glycine site (glycine B), polyamine site (NR_2B selective) and phencyclidine site located inside the cationic channel have also been evaluated [124]. CP101606 (Traxoprodil), a NR_2B antagonist has shown a reduction of allodynia and hyperalgesia in various models of inflammatory and neuropathic pain. Compound {(aR,bS)-a-(4-hydroxyphenyl)-b-methyl-4-(phenylmethyl)-1-piperidinepropanol} (Ro25-6981), another NR_2B antagonist has been reported to attenuate carrageenan-induced mechanical hyperalgesia in rats [133]. RGH-896 (Radiprodil), EVT101, EVT102 and EVT103 are other selective NR_2B antagonists in various stages of drug discovery [124]. The Effect of NMDA antagonists at the $glycine_B$ site namely 7-chloro-4-hydroxy-3-(3-phenoxy)phenyl-2(1H)-quinolinone (L-701,324) and 5,7-dichlorokynurenic acid were tested after systemic administration in rats in formalin test and in two models of neuropathic pain. Both L-701,324 (2.15-21.5 mg/kg, *i.p.*) and 5,7-dichlorokynurenic acid (10-46.4 mg/kg, *i.v.)* dose-dependently inhibited phase-II of formalin-evoked behavior. Likewise, both compounds reversed cold allodynia in the CCI model and dynamic allodynia in the spinal nerve injury (SNL) model. However, only L-701,324 was able to inhibit neuronal responses to NMDA in the antihyperalgesic dose range [134]. Similarly, Quartaroli *et al.,* in 1999 reported the antihyperalgesic activity produced by GV196771A, yet another glycine site antagonist of the NMDA receptor [135].

Munger *et al.,* reported the antiallodynic and antihyperalgesic properties of the kainate receptor antagonist (2*S*,4*R*)-4-methylglutamate (SYM-2081) (100 mg/kg, *i.p.*) in a rat model of nerve injury [136]. Later in 2000, SYM-2081 (100 mg/kg, *i.p.*) was reported to be active against mechanical allodynia and thermal hyperalgesia in a freeze injury model of neuropathic pain [137]. The Effect of systemic administration of the novel AMPA/GluR5 selective receptor antagonist NS1209 in animal models of experimental pain have been tested and compared with the AMPA receptor antagonist 2,3-dioxo-6-nitro-1,2,3,4-tetrahydrobenzo[f]quinoxaline-7-sulfonamide (NBQX) and the opiate morphine [138]. In the CCI model of neuropathic pain, NS1209 (3 and 6 mg/kg, *i.p.*), NBQX (10 and 20 mg/kg, *i.p.*) and morphine (3 and 6 mg/kg, *s.c.*) reduced mechanical allodynia and hyperalgesia responses to von frey hair and pin-prick stimulation of the injured hind paw. To date, there is no clinical proof of

concept, though there are few AMPA/kainate receptor antagonists available in early phase-I of clinical trials.

MGluRs have been shown to process role in central sensitization and various recent drug discovery programs are aimed at identifying antagonists of group I (mGluR1 and mGluR5) receptors, agonists of group II (mGluR2) and group III (mGluR4) receptors for treating neuropathic pain [139]. In particular mGluR1 and mGluR5 antagonists have shown good efficacy in both inflammatory and neuropathic pain states. Compound 6-amino-N-cyclohexyl-N,3-dimethylthiazolo[3,2-a]benzimidazole-2-carboxamide (YM298198), a mGluR1 antagonist was found to be efficacious in streptozotocin-induced hyperalgesia models with no sedation or impairment of locomotor activity [140]. Currently AZD9272 and AZD2066, the mGluR1 antagonists are being studied in phase-I clinical trials. Since the group II and group III mGluRs work as autoreceptors to reduce glutamatergic effect, several potent and selective agonists have been developed. Among the drugs acting on group II mGlu receptor, a mGluR2/3 agonist {1R,4R,5S,6R)-4-Amino-2-oxabicyclo[3.1.0]hexane-4,6-dic arboxylic acid} (LY379268) and mGluR7 agonist N,N'-bis(diphenylmethyl)-1,2-ethanediamine (AMN082) have been shown to attenuate allodynia and hyperalgesia on day seven after CCI in swiss albino mice [141].

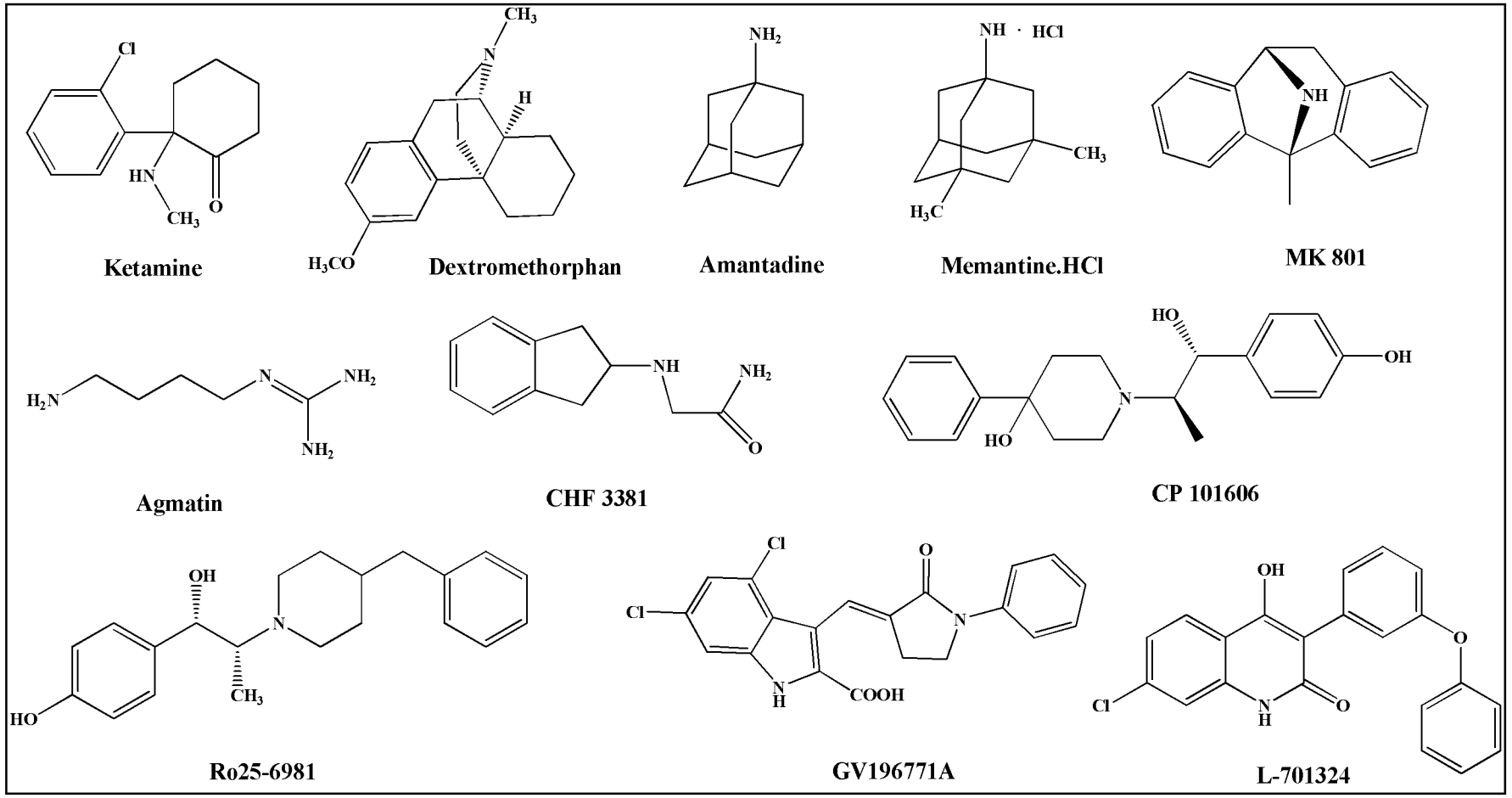

Figure 2.10 Glutamatergic compounds for neuropathic pain

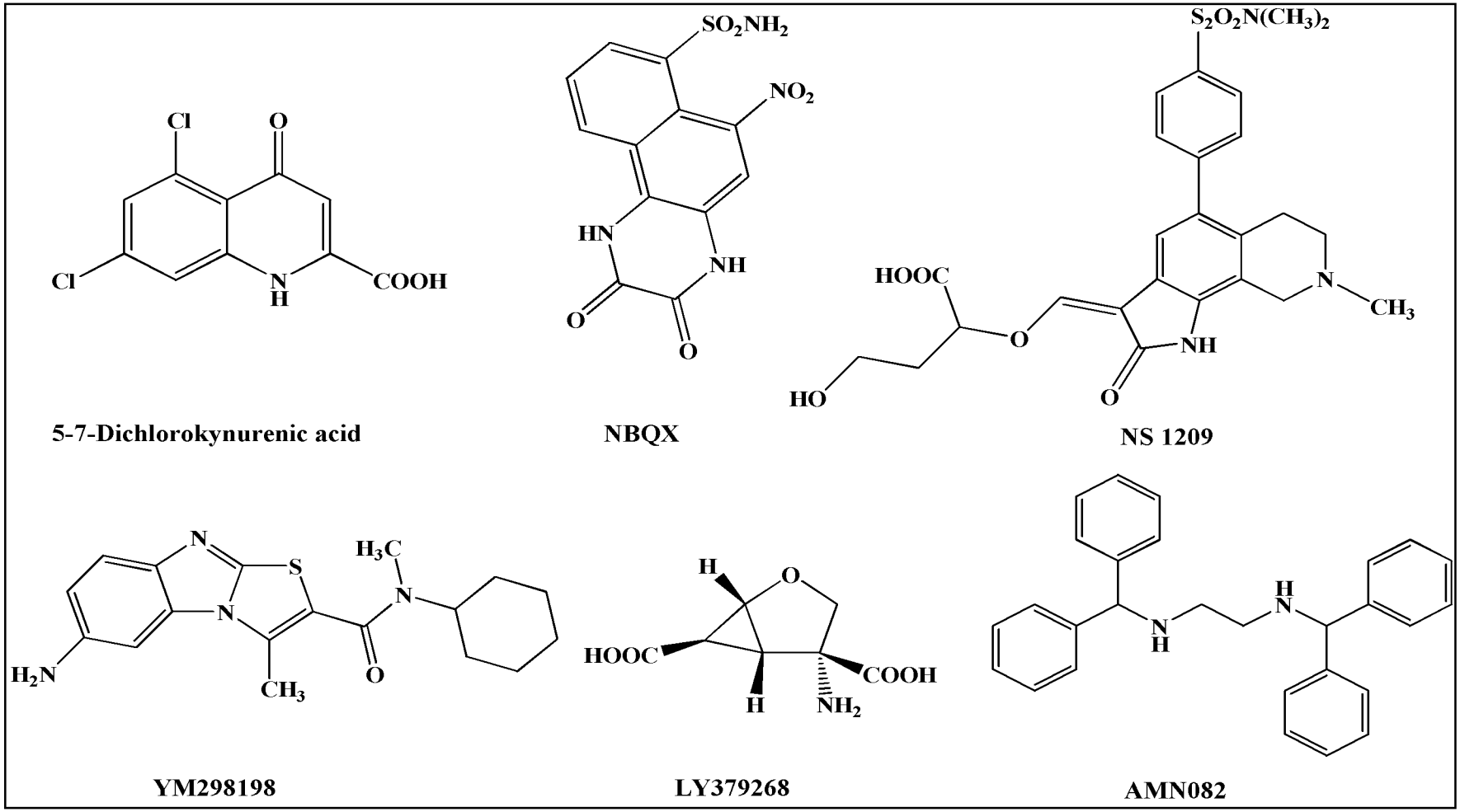

Fig 2.11 Glutamatergic compounds for neuropathic pain

2.2.8 Cathepsin S Inhibition

Cathepsin S is primarily a single chain, non-glycosylated lysosomal cysteine proteinase, belonging to the papain superfamily. It has a structure similar to several other members of the family with approximately 30% identity to cathepsin B and 57% sequence identity to cathepsins L and K [142]. Cathepsin S has received recent attention as a target for therapeutic intervention for neuropathic pain [143]. It has been demonstrated that cathepsin S is secreted from spinal microglial cells and induces nociception by cleaving fractalkine (CX3CL1) from the surface of sensory neurons. Free fractalkine subsequently binds to its receptor CX3C chemokine receptor-1 (CX3CR1) which activates microglial cells and induces pro-inflammatory cytokine production, thus contributing to the maintenance of neuropathic pain [144].

The initial development of cathepsin S inhibitors was targeted as irreversible, covalent inhibitors. But more recently the focus has been on reversible inhibitors, representing both covalent modifiers of the enzyme and, of late, noncovalent inhibitors [145]. Within the realm of covalent inhibitors, which form a chemical bond between an electrophilic site on the inhibitor and the Cys25 residue of cathepsin S, Ward *et al.*, reported nitrile-based amide compounds as cathepsin S inhibitors. Pharmacokinetic limitations, later led to the synthesis of succinyl nitrile-based covalent inhibitors (Figure 2.12) [146].

Using cathepsin K as a starting point in the development of cathepsin S inhibitors, non-peptidic pyrrolopyrimidine cathepsin K inhibitors [147] have been adapted into cathepsin S inhibitors [148]. The various inhibitors exhibited pronounced potency and selectivity for cathepsin S, as well as reasonable pharmacokinetic profiles. Peptidic cyanopyrazolidines was identified as potent cathepsin S inhibitors in the course of studies directed at identifying potent cathepsin B inhibitors. These compounds possess an electrophilic nitrile functional group, akin to other covalent modifiers to achieve marginal selectivity for cathepsin S over cathepsin K [149].

A series of peptidic amidofuranone analogs moved away from the nitrile-based electrophilic covalent binding element in favor of an electrophilic furanone moiety [150]. A substrate activity screening (SAS) protocol was previously used by Wood *et al.*, to identify non-peptidic, triazole-based cathepsin S inhibitors such as which operated via

covalent linkage of the aldehyde functional group to the cysteine residue of cathepsin S [151]. More recent studies used the SAS protocol to identify inhibitors in which the aldehyde moiety is replaced with a nitrile group [152].

Further details and SAR with regard to noncovalent, non-peptidic pyrazole-based cathepsin S inhibitors exhibited increased potency in a cellular assay. Selectivity over other cathepsins was identified, though no information relating to the binding mode of these inhibitors to cathepsin S has been reported (Figure 2.12) [153].

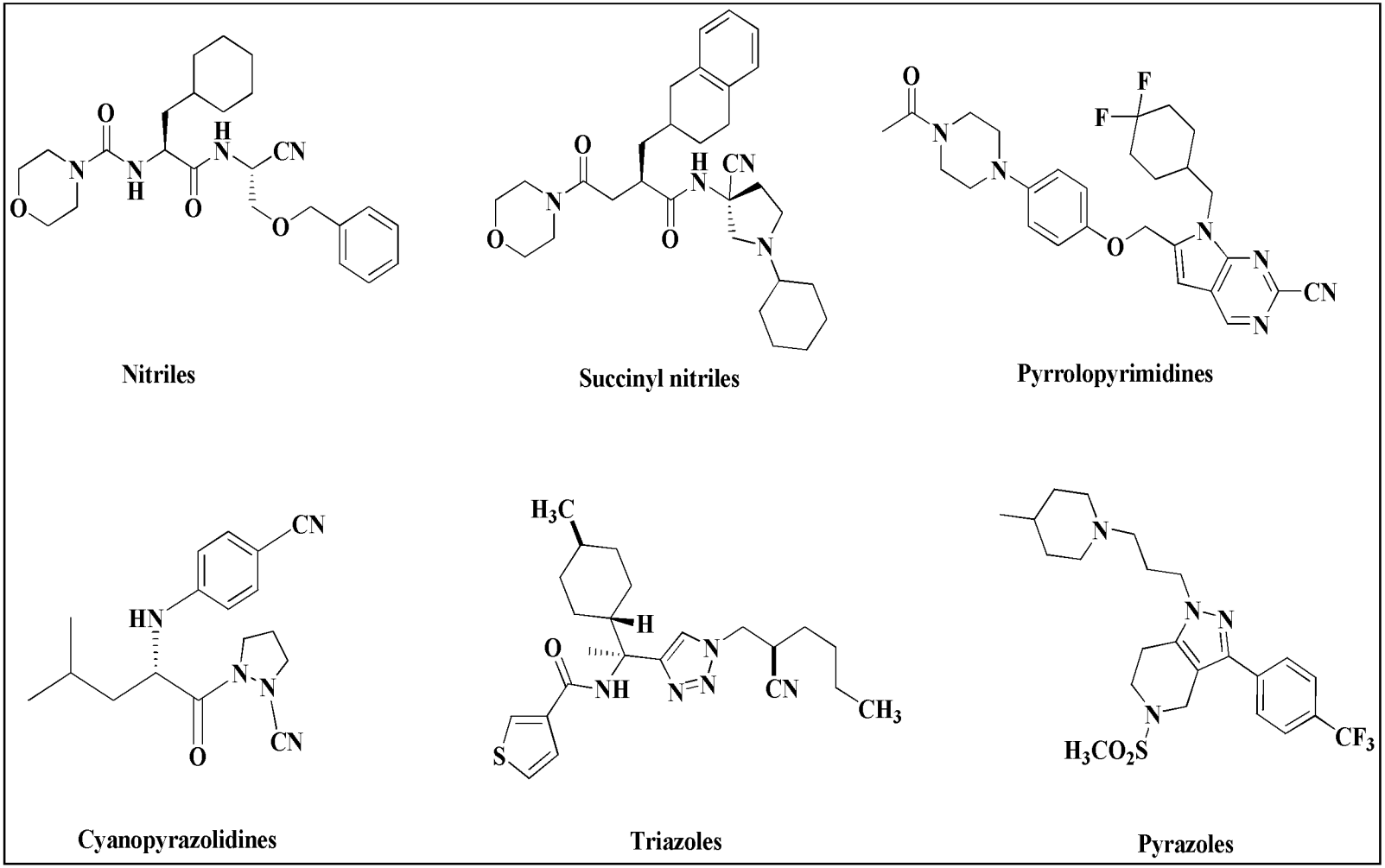

Figure 2.12 Cathepsin S inhibitors for neuropathic pain

2.2.9 Cannabinergic Agonism

The mechanism of action of cannabinoids on neuropathic pain may depend on presynaptic modulation of transmitter release, inhibition of calcium transients, reduction in adenylyl cyclase or modulation of immune cell function [154].

Evidence for the use of Marijuana (*Cannabis sativa*) as a treatment for pain can be traced back to the beginnings of recorded history [155]. The discovery of Δ^9 -tetrahydrocannabinol (Δ^9 -THC), the primary psychoactive ingredient in cannabis by Gaoni and Mechoulam (1964), set the stage for the identification of an endogenous cannabinoid (endocannabinoid) transmitter system in the brain [156]. The endocannabinoid signaling system includes cannabinoid receptors (e.g., CB_1 and CB_2), their endogenous ligands (e.g., anandamide and 2-arachido-noylglycerol), and the synthetic and hydrolytic enzymes that control the bioavailability of the endocannabinoids.

Modulation of the endocannabinoid system offers promising therapeutic opportunities for the treatment of pain conditions. Scott *et al.,* (2004) elucidated the roles of the two cannabinoid receptor subtypes, CB_1 and CB_2 in cannabinoid-mediated analgesia. CB_1 receptors have a widespread distribution in the central and peripheral nervous systems, whereas CB_2 receptors are restricted largely to cells of the immune system [157]. Activation of CB_1 receptors suppresses calcium conductance and inhibits inward rectifying potassium conductance, thereby suppressing neuronal excitability and transmitter release [158]. CB_2 receptor activation stimulates MAPK activity but does not modulate calcium or potassium conductance and thought to have anti-inflammatory effect [159].

Cannabinoids have long been known to be analgesic in various animal models of pain. Bridges *et al.,* (2001) investigated the efficacy of the non-selective cannabinoid agonist, (R)-(+)-[2,3-dihydro-5-methyl-3-(4-morpholinylmethyl)pyrrolo [1,2,3)-1,4-benzoxazin-6-yl]-1-napthalenylmethanone (WIN55,212-2) in the L5 SNL model of neuropathic pain. Administration of WIN55,212-2 reversed cold allodynia produced by SNL at a dose of 2.5 mg/kg over 90 minutes and also reversed thermal hyperalgesia dose and time-dependently [160,161]. Another study by Costa *et al.,* (2004) investigated the effect of repeated treatments with WIN55,212-2 on both hyperalgesia and production of pronociceptive mediators in a rat model of

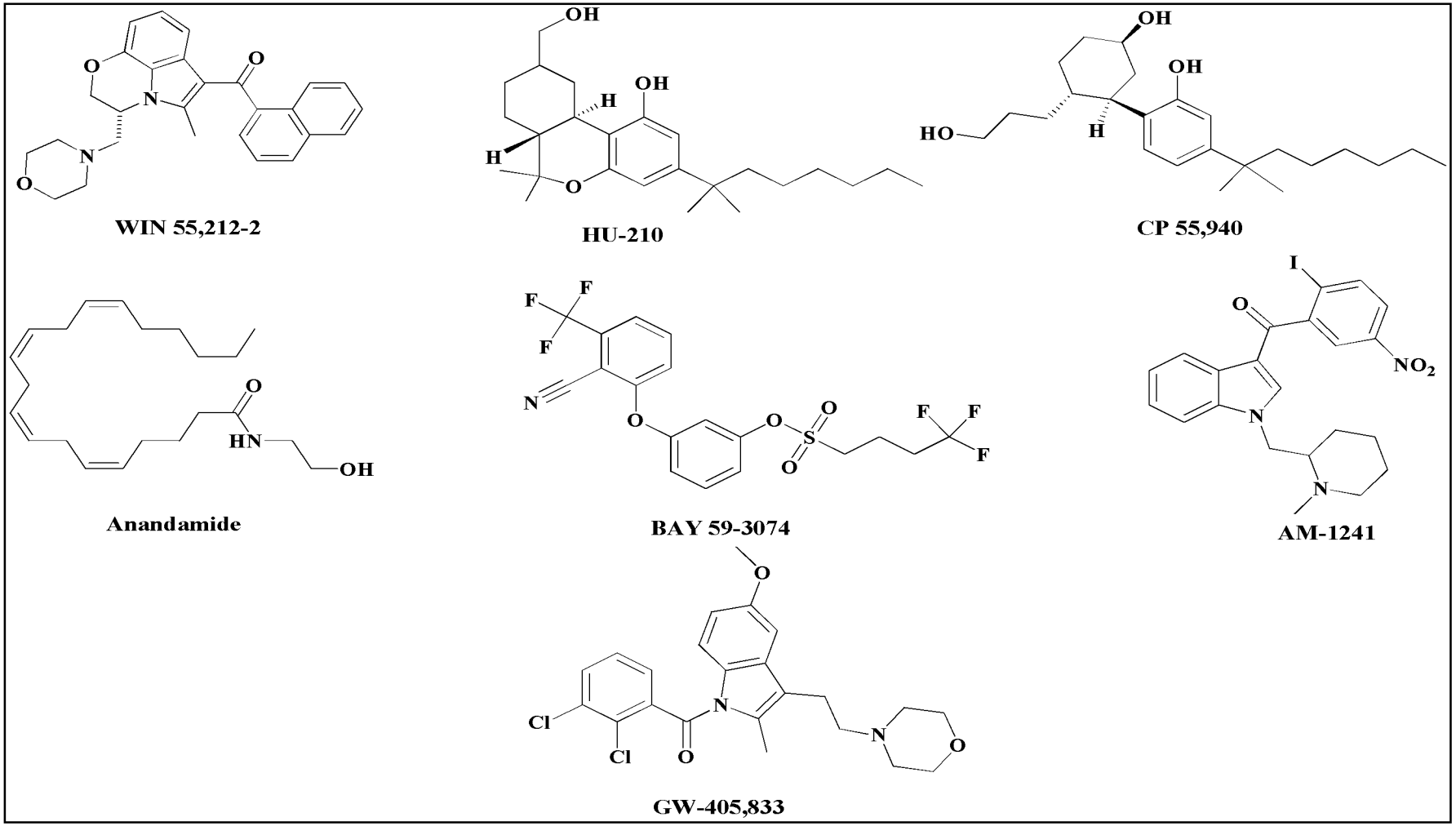

Figure 2.13 Cannabinoid agonists for neuropathic pain

neuropathic pain [162,163]. Electrophysiologic studies have shown that WIN-55,212-2, is a non-selective cannabinoid agonist that inhibited calcium currents in dissociated DRG neurons, and mechanically induced firing of single sensory fibers in an isolated skin-nerve preparation [158].

Also, apart from WIN55,212-2, another synthetic cannabinoid, CP-55940 as well as the endogenous cannabinoid agonist anandamide were proved to be effective in animal models of chronic neuropathic and inflammatory pain, reversing mechanical or thermal hyperalgesia and dynamic allodynia [162]. Moreover, De *et al.*, (2004) reported the antihyperalgesic and antiallodynic effect of BAY 59-3074 (3-[2-cyano-3-(trifluoromethyl)phenoxy]phenyl-4,4,4-trifluoro-1-butanesulfonate), a novel cannabinoid CB_1/CB_2 receptor partial agonist which (0.3-3.0 mg/kg, *p.o.*) was effective against thermal or mechanical stimuli in rat models of chronic neuropathic and inflammatory pain [163].

Studies conducted on multiple animal models of pain have shown that the CB_2-selective agonist {(1-(methylpiperidin-2-ylmethyl)-3-(2-iodo-5-nitrobenzoyl)indole} (AM1241), an aminoalkylindole showed robust analgesic effects and was very potent in neuropathic pain models [164]. In 1999, Mechoulam *et al.*, reported the synthesis and antinociceptive properties of [(1R,2R,5R)-2-[2,6-dimethoxy-4-(2-methyloctan-2-yl)phenyl]-7,7-dimethyl-4-bicyclo[3.1.1]hept-3-enyl] methanol (HU-308), yet another specific agonist for the CB_2 receptor subtype [165]. Another compound {(2,3-dichloro-phenyl)-[5-methoxy-2-methyl-3-(2-morpholin-4-yl-ethyl)-indol-1-yl] methanone} (GW405833) of the same class elicited robust antihyperalgesic effects in mouse models of inflammatory (Freund's complete adjuvant) and neuropathic (SNL) pain (Figure 2.13) [166].

Taken together, these studies in animals show that cannabinoid receptor agonists have considerable potential utility in the treatment of neuropathic pain. However, it is clear that if they are to be used routinely in the clinic then they must have analgesic efficacy without CB_1 mediated CNS side effects such as catalepsy, hypothermia and motor dysfunction. An approach to develop peripherally restricted CB_1 receptor or selective CB_2 agonists would be of a great potential for the treatment for neuropathic pain.

2.2.10 GABAergic agonism

γ- Amino butyric acid (GABA) pathways form a major inhibitory neurotransmitter system in CNS. GABA receptors are commonly thought to be divided into two groups: chloride channel-coupled (ionotropic) $GABA_A$ receptors which belong to the superfamily of ligand-gated ion channels and G-protein-coupled (metabotropic) $GABA_B$ receptors. GABA acts at GABA/benzodiazepine ($GABA_A$) receptor to increase the membrane chloride ion conductance and thereby stabilizing or hyperpolarizing the resting membrane potential. Pentameric $GABA_A$ receptors mediate the majority of fast synaptic inhibition in the brain and are composed of combinations of α(1-6), β(1-3), and γ(1-3) subunits [167].

Dorsal horn neuronal activity is determined by a balance between excitatory and inhibitory signals from peripheral, spinal, and descending sites. Under healthy conditions, GABAergic interneurons serve as gate-keepers controlling the relay of nociceptive signals from the periphery through the spinal cord to higher CNS areas and preventing the excitation of normally 'pain-specific' projection neurons by innocuous stimuli (gate theory). Studies show loss of spinal GABAergic interneurons in inflammatory and neuropathic pain, which leads to diminished inhibitory control of pain [168,169].

Plenty of evidence indicates that increasing $GABA_A$ receptor-mediated inhibition in the CNS alleviates pain both in rodents and in humans. Intrathecal injection of GABA has shown to permanently reverse pain after nerve injury [170]. NS11394, a novel subtype-selective $GABA_A$ receptor-positive allosteric modulator has been shown to produce antinociceptive effect in rat models of inflammatory and neuropathic pain [171] (Figure 2.14).

Giardina *et al.*, (1998) evaluated the GABA-reuptake blocker tiagabine in animal models of neuropathic and nociceptive pain [172]. The antiallodynic effect of tiagabine was dose-dependent, with significant increases in response threshold to dynamic stimulation occurring at 72.8 μM/kg *i.p.* The spinal injection of the $GABA_B$ agonist baclofen (0.03-0.3 μg) and $GABA_A$ agonist muscimol (0.1-1.0 μg) resulted in a dose-dependent antagonism of dynamic allodynia at doses which had no detectable effect upon motor function [173]. Later in 1999, Alves *et al.*, reported the analgesic effect of vigabatrin, an irreversible GABA transaminase inhibitor in two animal

models of neuropathic pain (CCI and PSNL). The results showed a possible dose-dependent analgesic effect of vigabatrin, which was evident by the significant decrease in scratching behavior and by its significant increasing effect on the latency of the hind paw withdrawal to noxious thermal stimulus [174].

Franek *et al.*, in 2004 reported the antinociceptive effect of baclofen, a specific agonist of the metabotropic $GABA_B$ receptor, in the CCI model of neuropathic pain [175]. The effect of baclofen in increasing the pain threshold for thermal stimulation was dose-dependent and the maximum response without motor deficits was observed at a dose of 15 mg/kg, *s.c.* Similar results have also been reported for mechanical stimulation [176].

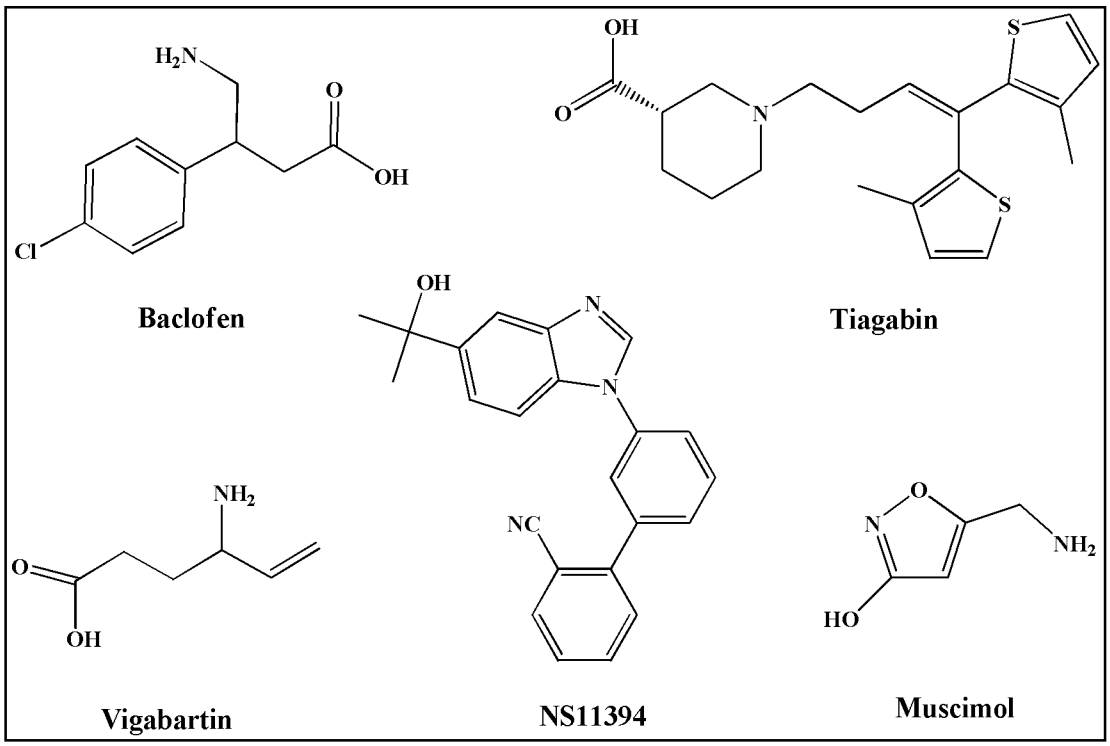

Figure 2.14 Compounds acting through GABAergic mechanisms

Owing to the widespread expression of $GABA_A$ receptors in the CNS, however, unrestricted activation of all $GABA_A$ receptors in the CNS leads to strong sedation and various other side effects like impairment of learning and liability to addiction and dependence. However to avoid these side effects subtype-selective agents directed towards only a subset of $GABA_A$ receptors might provide a potential solution to this dilemma. Studies have shown that α2- and/or α3-containing $GABA_A$ receptors in the spinal dorsal horn serve a key role in nociception, while α1- containing $GABA_A$ receptors are responsible for benzodiazepine like side effects. Novel compounds activating α2- and/or α3-containing $GABA_A$ receptors and sparing α1-containing

$GABA_A$ receptors are recommended for further development of molecules for pain [177].

The development of animal models and constant progress in understanding the anatomical, cellular and molecular basis of neuropathic pain, has led to multifarious drug targets and treatment options. Drugs of different class have been screened in a variety of models of neuropathic pain and promising research holds out the possibility of alternative future treatments.

CHAPTER 3

OBJECTIVE & PLAN OF WORK

3.1 Rationale for the Design of Proposed Compounds

Neuropathic pain has multiple etiologies including metabolic disease, infectious disease, mechanical trauma, central nervous system disorders, toxic agents, compression injuries, and malignant conditions. At present there are very few effective and well-tolerated therapies for neuropathic pain. The current pharmacotherapy of neuropathic pain includes the use of unconventional agents like topical capsaicin, tricyclic antidepressants, anticonvulsants and in some cases the opioids [1, 2, 5, 9-11]

Opiates (which work well for acute pain) are not particularly effective and the tricyclic antidepressants (which act by blocking the uptake of the neurotransmitters noradrenaline or serotonin or both) have been claimed to be effective, but they suffer from undesirable side effects [10]. Anticonvulsants have been traditionally used for the management of neuropathic pain, as most of these either stabilize the membrane hyper-excitability or enhance inhibitory GABA and/or glycine neurotransmission but their efficacy has not been unequivocally established and moreover they are associated with numerous side effects [74]. Gabapentin, a structural analogue of γ-aminobutyric acid (GABA) has been approved for the treatment of neuropathic pain but still in many patients it does not provide adequate pain relief. Thus there is an immediate need to develop drugs for sole indication of alleviating neuropathic pain [75,178].

In recent years, numerous heterocycles with tetrahydropyridine framework have gained considerable attention in the treatment of neuropathic pain. Various tetrahydropyrido-pyrazoles [153,179,180], tetrahydropyrido-pyrimidines [181], tetrahydropyrido-indoles [182], tetrahydropyrido-quinazolines [183] have been found to embark antinociceptive efficacies mediating cannabinergic, GABAergic, purinergic and histaminergic pathways. Various N-Methyl-D-Aspartate (NMDA) and cathepsin S inhibitors [153,179,180,181] possessing this fused ring systems have also been reported.

Likewise, the privileged structured triazole heterocyclic compounds have been paid special attention representing molecular frameworks capable of binding to several diverse biological receptors with high affinity. Triazole ring is a quite important five-membered heterocycle with three nitrogen atoms, possesses aromaticity and is an electron rich system [182]. This type of unique structure endows triazole derivatives to readily bind with a variety of enzymes and receptors in biological system via weak interactions such as coordination bonds, hydrogen bonds, ion-dipole, cation-stacking, hydrophobic effect, van der waals force and so on, and thus display a broad spectrum of biological activities. Furthermore, triazole ring can be used as an attractive linker to combine different pharmacophore fragments to produce innovative bifunctional drug molecules, providing a convenient and efficient pathway to develop various bioactive and functional molecules [183-195].

In the present scenario, lack of effective and well-tolerated therapy for neuropathic pain has resulted in a need for development of the multi-faceted treatment strategy, shifting the paradigm from the well established concept of biological activity at single receptor (magic bullets) to designed multi-targeted ligands (DMLs) [196,197].

The advantages of combining two (or more) pharmacophores in a single molecule (combination drug/ conjugate/ hybrid drug) can be stated as: (1) they offer both palliative and disease modifying actions, (2) act on targets that produce additive or synergistic therapeutic responses, (3) simultaneously evoke a therapeutic response at the desired target and prevent an undesired response mediated by an alternate target, (4) allow one component to promote the drugable characteristics (e.g., brain penetration) of the therapeutic component, and (5) prolong the duration of effectiveness of one compound by contributing the pharmacodynamic actions of another [198].

These benefits are already utilized in cancer therapy e.g., Sutent, which is one of four DMLs in this medical field. Additionally, Cymbalta, a drug presenting both serotonin and norepinephrine reuptake inhibition properties, is employed in depression and neuropathic pain [199]. Extensive research aimed at the introduction of novel multifunctional drugs is recently carried out in areas including Alzheimer's [200], Parkinson's diseases [201], malaria and tuberculosis [202].

3.2 Objective

In view of the above reports, the objective of the present research work was to design and identify multifunctional leads utilizing pharmacophore hybridization approach for the treatment of neuropathic pain.

3.3 Plan of Work

The plan of work is briefly outlined as follows,

I. DESIGN AND SYNTHESIS

A) 4,5,6,7-tetrahydro-1H-pyrazolo[4,3-c]pyridine-1-carboxamides

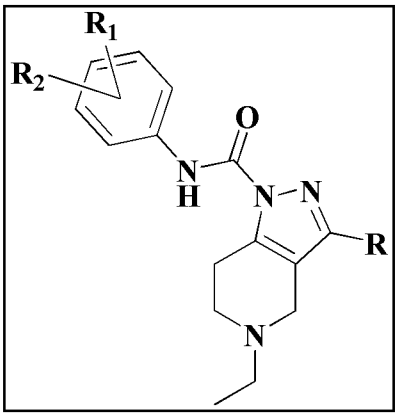

R = $-CH_3$, $-C(CH_3)_3$; R_1, R_2 = H/Alkyl/Halo

MS101-MS116

B) 5,6,7,8-tetrahydropyrido[4,3-d]pyrimidines

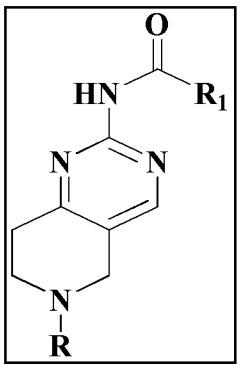

R, R_1 = Alkyl/Substituted phenyl

MS201-MS216

C) 1,2,4-triazol-5(4H)-ones

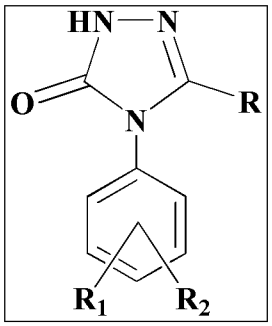

R = Various aliphatic, aryl and heteroaryl acids, R_1, R_2 = H/Alkyl/Halo

MS301-MS324

D) [1,2,4]triazolo[1,3,4]thiadiazoles

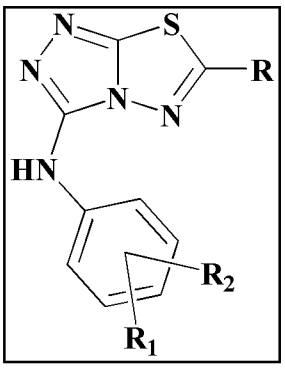

R = Various aliphatic, aryl and heteroaryl acids, R_1, R_2 = H/Alkyl/Halo

MS401-MS425

II. Pharmacology

The profile of anti-neuralgic activity of the synthesized compounds was established using animal models of physiological and neuropathic pain. The various pharmacological interventions are outlined as follows

1. **Efficacy in acute pain models**
    a. Acetic acid-induced writhing test
    b. Formalin-induced flinching test
2. **Efficacy in neuropathic pain models**
    a. Chronic constriction injury (CCI) model
    b. Partial sciatic nerve ligation (PSNL) model
    c. Estimation of median effective dose (ED_{50}) of potential compounds in CCI and PSNL model

3. Mechanistic studies of selected compounds

a. Effect of potential compounds on carrageenan induced paw edema
b. Effect of potential compounds on TNF-α
c. Effect of potential compounds on nitric oxide (NO) level
d. Effect of potential compounds on free radical assay
e. Effect of potential compounds on cannabinoid (CB_1 and CB_2) receptors
f. Effect of potential compounds on cathepsin S enzyme
g. Effect of potential compounds on picrotoxin induced epilepsy (GABAergic pathways)

CHAPTER 4

MATERIALS & METHODS

4.1 Chemistry

Melting points were determined in one end open capillary tubes on a Büchi 530 melting point apparatus and are uncorrected. Proton nuclear magnetic resonance (^{1}H-NMR) spectra were recorded for the compounds on Brucker Avance (300 MHz) spectrophotometers, respectively. Chemical shifts were reported in parts per million (ppm) using tetramethyl silane (TMS) as an internal standard. All exchangeable protons were confirmed by the addition of deuterated water (D_2O). Mass spectra were recorded with Shimadzu GC-MS-QP5000 spectrophotometer. Elemental analyses (C, H, N) were undertaken with Perkin-Elmer model 240C analyzer. The homogeneity of the compounds was monitored by ascending thin layer chromatography (TLC) on silica gel-G (Merck) coated aluminum plates and visualized under UV irradiation or by using iodine vapor. The solvent system used was DCM:CH_3OH (9.5:0.5).

(A) Synthesis of substituted tetrahydropyrido-pyrazoles

The tetrahydropyrido-pyrazoles were synthesized as follows,

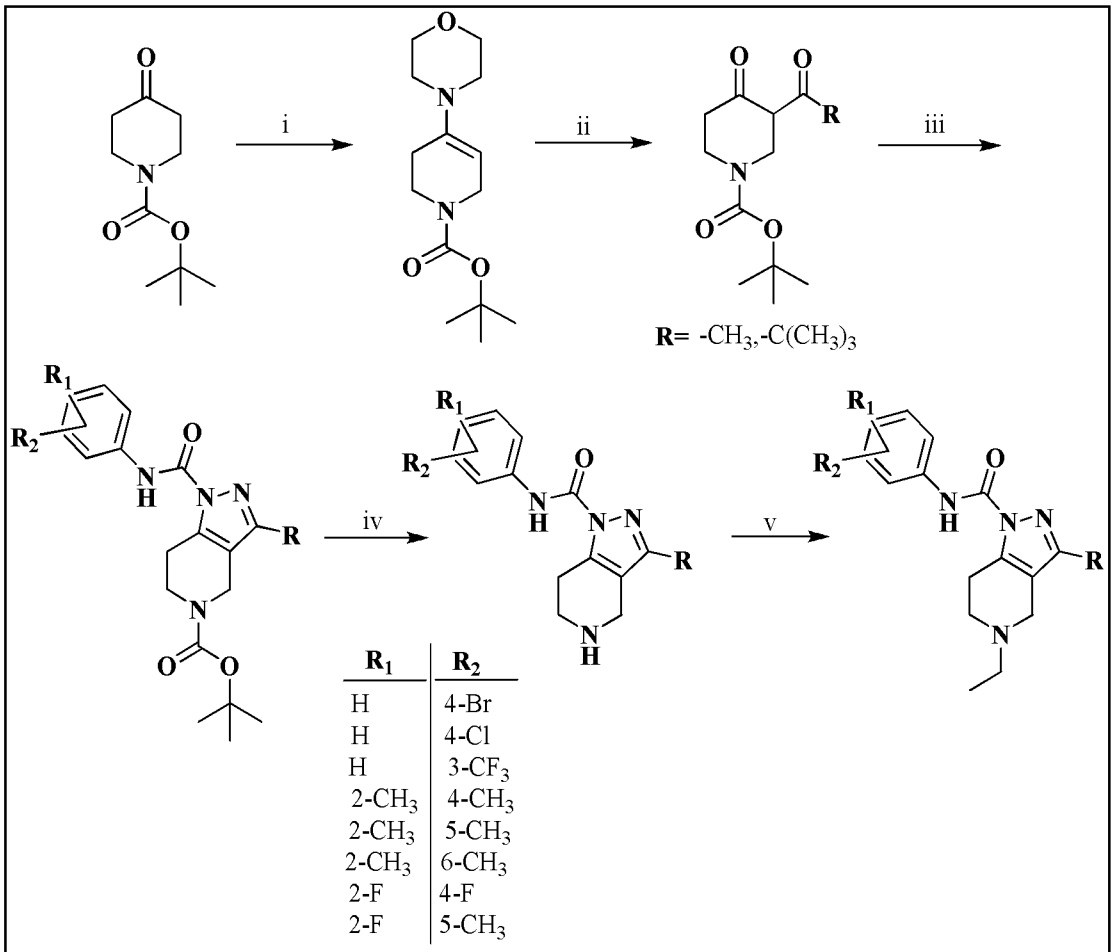

R_1	R_2
H	4-Br
H	4-Cl
H	3-CF_3
2-CH_3	4-CH_3
2-CH_3	5-CH_3
2-CH_3	6-CH_3
2-F	4-F
2-F	5-CH_3

Reagents and conditions: **i.** morpholine,*p*-TSA, toluene, reflux, 16 h; **ii.** RCOCl, Et_3N, CH_2Cl_2,0°C-rt, 5 h; **iii.** substituted phenyl semicarbazides, K_2CO_3, C_2H_5OH, reflux, 18 h; **iv.** TFA, CH_2Cl_2, rt, 24 h; **v.** C_2H_5I, K_2CO_3, rt, 4 h

Enamine formation of N-Boc-piperidone was carried out with morpholine and catalytic amounts of p-toluenesulphonyl chloride with concomitant removal of water. Reaction of the enamine with various acid chlorides and subsequent hydrolysis resulted in the formation of 1,3-diketone [153,179]. Base catalysed cyclisation of various substituted aryl semicarbazide with the 1,3-diketone resulted in the formation of substituted tetrahydropyido-pyrazoles. Deprotection was then carried out with trifluoroacetic acid followed by N-alkylation with ethyl iodide.

B) Synthesis of substituted tetrahydropyrido-pyrimidines

The tetrahydropyrido-pyrimidines were synthesized as follows,

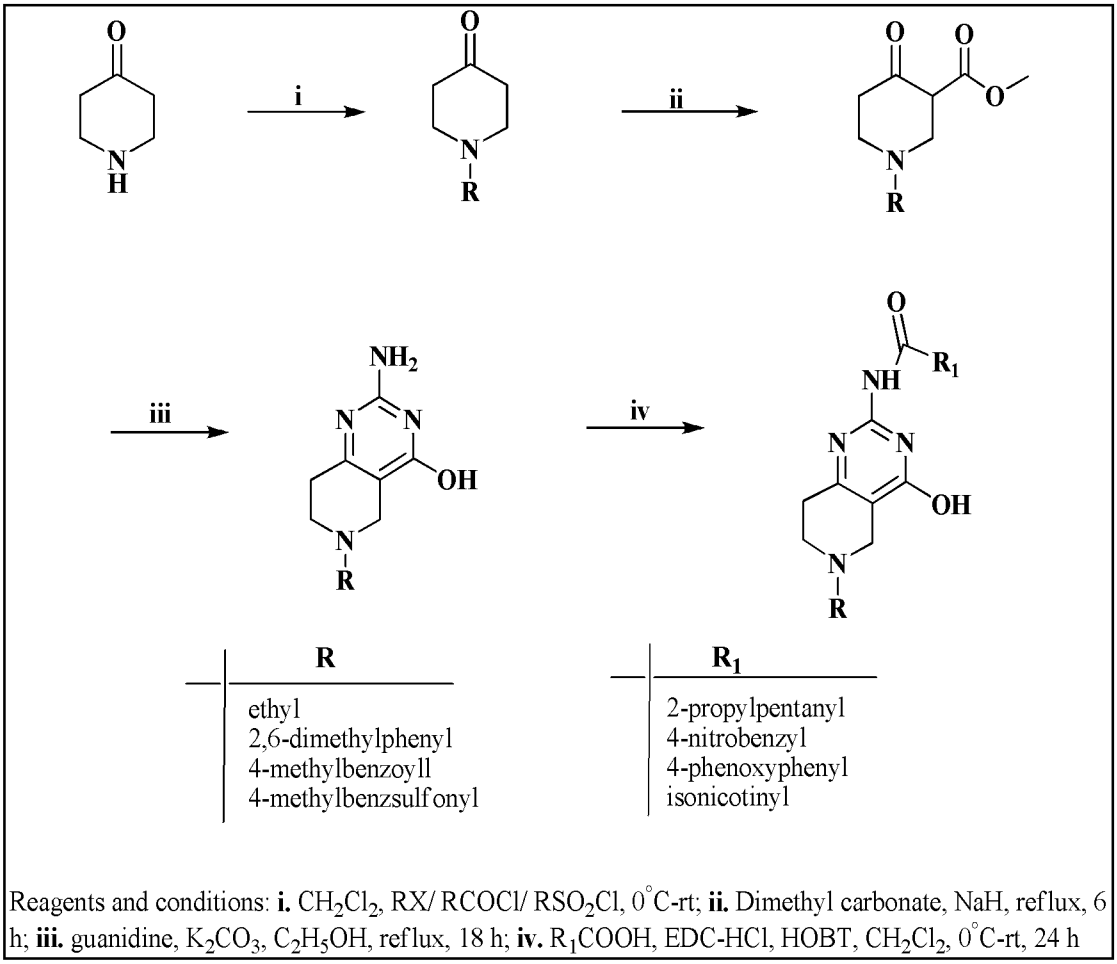

Reagents and conditions: **i.** CH_2Cl_2, RX/ RCOCl/ RSO_2Cl, 0°C-rt; **ii.** Dimethyl carbonate, NaH, reflux, 6 h; **iii.** guanidine, K_2CO_3, C_2H_5OH, reflux, 18 h; **iv.** R_1COOH, EDC-HCl, HOBT, CH_2Cl_2, 0°C-rt, 24 h

Various alkyl, acid and sulphonyl halides were reacted with 4-piperidone to form N-substituted piperidin-4-one. Methoxycarbonylation of the same in the presence of sodium hydride afforded the ketoester which underwent base catalysed reaction with guanidine to form substituted tetrahydropyrido-pyrimidine scaffold [181]. Utilizing various alkyl, aryl and hetroaryl acids, the acid amine coupling was then carried out with the aid of 1-ethyl-3-[3-(dimethylamino)propyl]carbodiimide hydrochloride (EDC) and 1-hydroxy benzotriazole (HOBT) to form the titled compounds.

C) Synthesis of substituted 1,2,4-triazol-5-ones

The substituted 1,2,4-triazol-5-ones were synthesized as follows,

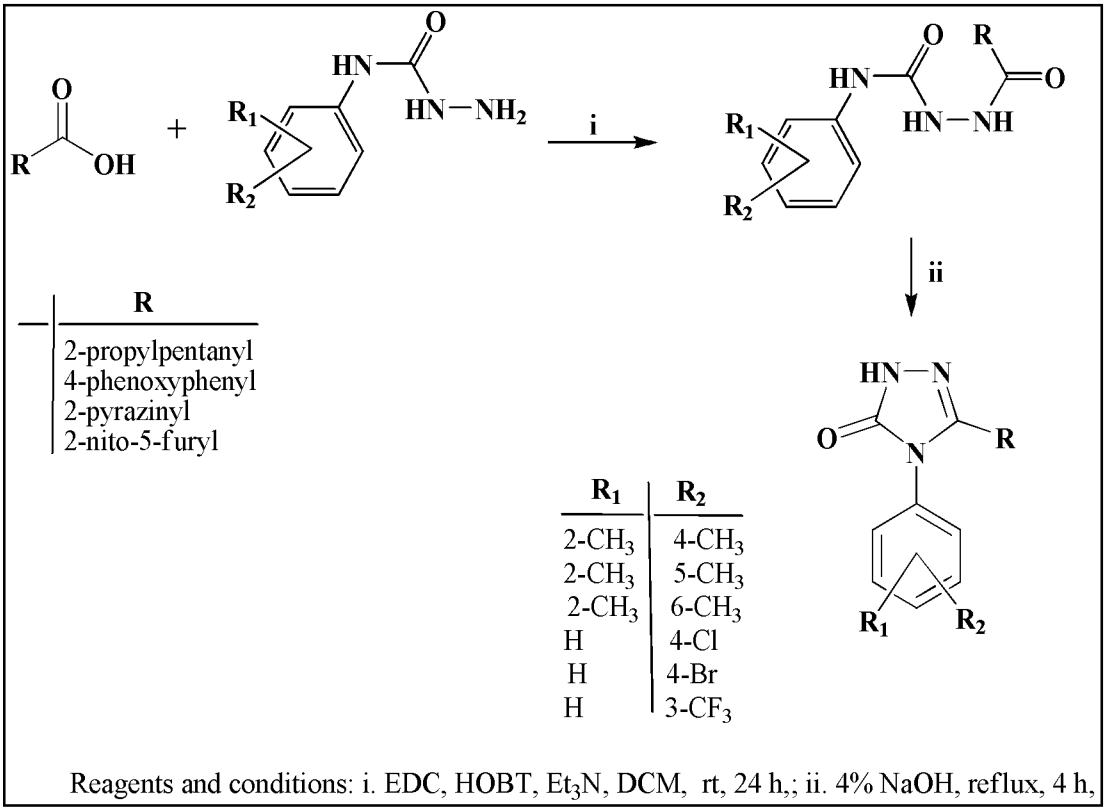

Reagents and conditions: i. EDC, HOBT, Et_3N, DCM, rt, 24 h,; ii. 4% NaOH, reflux, 4 h,

Coupling of the substituted N^4-(substituted phenyl) semicarbazides with various aliphatic, aryl and heteroaryl acids with the aid of 1-ethyl-3-[3-(dimethylamino)propyl]carbodiimide hydrochloride (EDC) and 1-hydroxybenzotriazole (HOBT) resulted in the synthesis of N^1-(substituted)-N^4-(substituted phenyl) hydrazine-carboxamides. Cyclodehydration of the same in alkaline medium resulted in N^1-(substituted)-N^4-(substituted phenyl)-1H-1,2,4-triazol-5(4H)-ones [203].

D) Synthesis of substituted triazolo-thiadiazoles

Various substituted triazolo-thiadiazoles were prepared as follows,

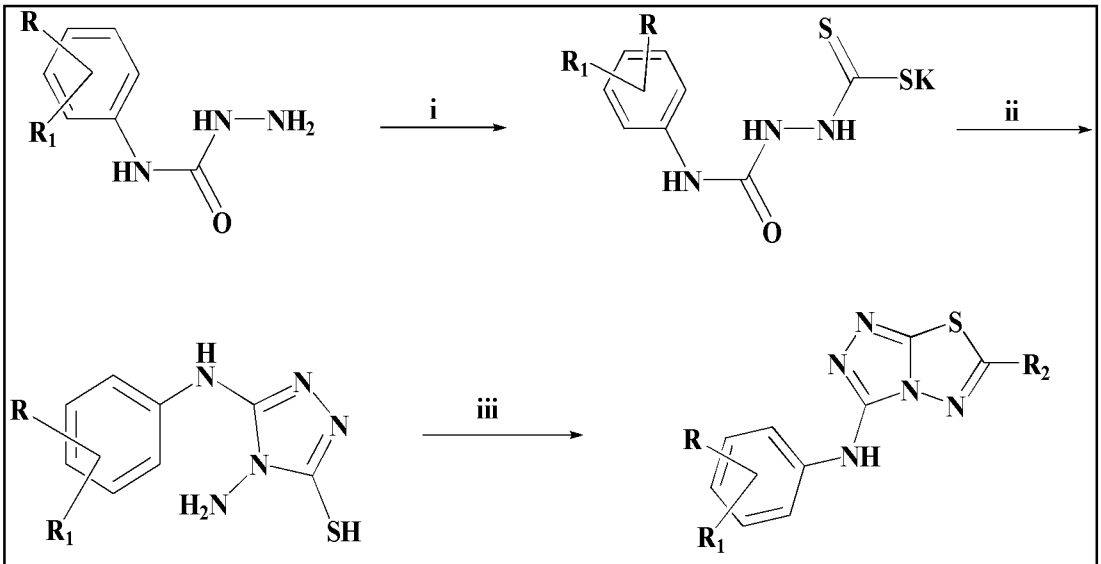

R_1	R_2
H	4-Br
H	4-Cl
2-CH_3	4-CH_3
2-CH_3	5-CH_3
2-CH_3	6-CH_3

R
4-aminobutanyl
2-propylpentanyl
4-nitro benzyl
isoniconityl
4-(2,4-dioxo-3-azaspiro[5.5]-undecan-3-yl)butanyl

Reagents and conditions: **i.** CS_2, KOH, 0°C-rt, 18 h; **ii.** $NH_2NH_2.H_2O$, reflux, 12 h; **iii.** R_2COOH, $POCl_3$, reflux, 6 h

Substituted phenyl semicarbazides on treatment with carbon disulphide in the presence of potassium hydroxide in ethanol gave the potassium salt of the corresponding 4-dithiocarbamate derivatives, which underwent ring closure with an excess of hydrazine hydrate to give 4-amino-3-substituted-5-mercapto-(4H)-1,2,4-triazoles. Resultant triazoles were further converted to 1,2,4-triazolo-[3,4-b]-1,3,4-thiadiazoles through one-pot reaction by condensation with various acids in the presence of phosphorous oxychloride [204].

4.2 Pharmacology

4.2.1 Animals

Swiss albino mice (either sex) with weight ranging from 20-25 g were used for the assessment of neurotoxicity, acetic acid-induced writhing, formalin-induced flinching models. Wistar rats of either sex (200-250 g) were used for the inflammatory and neuropathic pain models. All experiments were approved by the Institutional Animal Ethics Committee of BITS-Pilani, Hyderabad campus with the protocol number IAEC/RES/6/2. Animals were housed six (mice) and four (rats) per cage at a constant temperature under a 12 h light/dark cycle (lights on at 7:00 AM), with food and water *ad libitum*. All of the animals were acclimatized to the housing conditions for a period of one week before the start of experiments.

The various pharmacological tests performed are as follows,

4.3 Acute Nociceptive Models

4.3.1 Motor Impairment

Minimal motor impairment was measured in mice by the rotarod test. The mice were trained to stay on a rotarod that rotates at 10 revolutions per minute. The rod diameter was 3.2 cm. Neurotoxicity was indicated by the inability of the animal to maintain equilibrium on the rod for at least 1 min in each of the three trials [205]. Test compounds at the dose of 30, 100 and 300 mg/kg (*i.p.)* were administered 30 min before the experiment.

4.3.2 Acetic Acid-Induced Writhing Test

Writhing was induced in a group of mice by an intraperitoneal injection of 0.1 mL of 2% v/v acetic acid. Test group mice received acetic acid half an hour after the administration of test compounds (100 mg/kg, *i.p.*). The number of writhings occurring for a period of 30 min was recorded. For scoring purposes, a writhe was indicated by stretching of the abdomen with simultaneous stretching of at least one hind limb. The percentage inhibition of the writhing response was calculated as follows [206].

$$\% \text{ inhibition of writhing response} = \frac{(\text{No. of writhes}_{\text{Drug}} - \text{No. of writhes}_{\text{Control}}) \times 100}{\text{No. of writhes}_{\text{Control}}}$$

4.3.3 Formalin-Induced Flinchings Test

The test involved intra plantar injection of 25 μL of 1% formalin into the hind paw of mice, which resulted in flinches in the paw in the early phase (0-5 min) and the late phase (10-30 min). Time spent in paw licking and biting was monitored in each 5 min and calculated for both the phases. Test compounds were administered 30 min before the experiment [207].

4.4 Neuropathic Pain Models

4.4.1 Chronic Constriction Nerve Injury Model

Unilateral mononeuropathy was produced in rats using the CCI model performed essentially as described by Bennett & Xie [208]. The rats were anesthetized with an intraperitoneal dose of ketamine (55 mg/kg) and xylazine (5 mg/kg) with additional doses of the anesthetic given as needed. Under aseptic conditions, a 3-cm incision was made on the lateral aspect of the left hindlimb at the mid-thigh level. The left paraspinal muscles were then separated from the spinous processes and the common left sciatic nerve was exposed just above the trifurcation point. Four loose ligatures were made with a 4-0 braided silk suture around the sciatic nerve with about 1-mm spacing. The wound was then closed by suturing the muscle using chromic catgut with a continuous suture pattern. Finally, the skin was closed using silk thread with horizontal-mattress suture pattern.

4.4.2 Partial Sciatic Nerve Ligation Model

As described by Seltzer [29], in anaesthetized rats, left sciatic nerve was exposed at mid thigh level through small incision, cleared of adhering muscle tissue, and one-half of the nerve thickness was tightly ligated using 7.0 silk suture. The wound was closed and dusted with neomycin powder. The animals were then transferred to their home-cages and left for recovery.

4.4.3 Sensory Testing Using Nociceptive Assays

Four nociceptive assays aimed at determining the severity of behavioral neuropathic responses namely spontaneous pain, allodynia and hyperalgesia were performed on 9^{th} day post CCI/PSNL surgery. The assays involved pre-drug measurement of the degree of spontaneous (ongoing) pain and tests of hind limb withdrawal to cold and mechanical stimuli (dynamic allodynia, cold allodynia and mechanical hyperalgesia).

Testing was re-performed at 30 min, 60 min and 120 min post drug administration. A minimum of 10 min separated the testing procedures to reduce the influence of prior nociceptive testing. The order of testing was as follows: spontaneous pain, dynamic allodynia, cold allodynia and lastly mechanical hyperalgesia.

Compounds (100 mg/kg, *i.p.*) were administered at t=0, in 30% v/v PEG 400. The control group of rats received only the vehicle. Gabapentin (100 mg/kg, *i.p.*) was used as positive control. Paw withdrawal duration (PWD) was observed in spontaneous pain and cold allodynia while paw withdrawal threshold (PWT) was assessed in dynamic allodynia and mechanical hyperalgesia. Percentage reversal in spontaneous pain, allodynia or hyperalgesia was calculated for each animal as defined below [209],

$$\% \text{ Reversal} = \frac{(\text{post dose value} - \text{pre dose value})}{(\text{contralateral paw value} - \text{pre dose value})} \times 100$$

4.4.3.1 Spontaneous Pain

Spontaneous pain was assessed for a total time period of 5 min as described previously by Choi *et. al.* [210]. The operated rat was placed inside an observation cage that was kept 5 cm from the ground level. An initial acclimatization period of 10 min was given to each of the rats. A total number of four rats (n=4) were assigned to each treatment group. The test consisted of noting the cumulative duration for which the rat holds its ipsilateral paw off the floor. The paw lifts associated with locomotion or body repositioning was not counted. It has been suggested that those paw lifts in the absence of any overt external stimuli are associated with spontaneous pain, and are correlative of ongoing pain.

4.4.3.2 Dynamic Allodynia

Dynamic allodynia was assessed for the examination of neuropathic pain state in rats, as previously described [211]. Paw withdrawal in response to mechanical stimuli was measured using Von Frey filaments (Touch-Test Sensory Evaluator, North Coast Medical, Morgan Hill, CA). Each rat was placed on a metallic mesh floor covered with a plastic box. A set of von frey monofilaments (0.4-15 g), with intensities of mechanical stimulation increasing in graded manner with successively greater diameter filaments, were applied to the plantar surface of the hind paw five times at intervals of 1-2 seconds. The weakest force (g) inducing withdrawal of the stimulated

paw at least three times was taken as the paw withdrawal threshold with cut off value at 15 g.

4.4.3.3 Cold Allodynia

The rats demonstrating unilateral mononeuropathy were assessed for acute cold allodynia using the acetone drop application technique [212]. The operated rat was placed inside the observation cage, kept 5 cm from the ground level and was allowed to acclimatize for 10 min or until exploratory behaviour ceased. A total number of four rats (n=4) were assigned to each group. 100 µL of freshly dispensed acetone was squirted as a fine mist onto the midplantar region of the affected paw. A cold allodynic response was assessed by noting down the duration of paw-withdrawal response. For each measurement, the paw was sampled three times and mean was calculated. At least 3 min elapsed between each test.

4.4.3.4 Mechanical Hyperalgesia

Mechanical paw withdrawal thresholds were assessed with Randall–Selitto [213] analgesymeter (UGO Basile, Italy). The instrument exerts a force that increases at a constant rate. This force was applied to the hind paw of the rat, which was placed on a small plinth under a cone-shaped pusher with a rounded tip (1.5 mm in diameter) until the animal withdrew its paw. A cut off of 250 g was used to avoid injury. Mechanical paw withdrawal thresholds were calculated as the average of two consecutive measurements.

4.5 Determination of Median Effective Dose (ED_{50})

To determine ED_{50} as an estimate of the compounds' potency, a dose–response curve for various sensory tests was plotted. ED_{50} was the dose that yielded 50% reversal of the sensory response [214]. This value was linearly interpolated between the dose just above and just below the ED_{50} value.

4.6 Carrageenan-Induced Paw Edema and Quantification of TNF-α

Paw edema was induced in wistar rats by intra-plantar injection of 50 µL of 2% carrageenan (λ-carrageenan, type IV, Sigma) diluted in saline, atleast one week before the experiment. The volume of the paw edema (mL) was determined at 0, 60, 120 and 180 min using a plethysmometer (Ugo Basile, Italy). Indomethacin (10 mg/kg, *i.p.*)

was used as positive control [215]. The percentage protection against inflammation was calculated as:

$$\% \text{ Protection} = \frac{\{V_c - V_d\}}{V_c} \times 100$$

where V_c is the increase in paw volume after carrageenan in the vehicle control group and V_d is the increase in paw volume after carrageenan in test compound treated group. For the measurement of TNF-α, the whole right hind paws were harvested at the third hour after carrageenan injection. After rinsing with ice-cold normal saline, it was homogenized at 4°C and the homogenate was centrifuged at 12,000 rpm for 5 min. The supernatant obtained was assayed using TNF-α ELISA kit (R & D System, USA) [216].

4.7 Estimation of Total Nitrite/Nitrate

On the 9th day post-chronic constriction nerve injury, the test compounds were administerd and the total nitrate/nitrite in brain and sciatic nerve was estimated after 2 h according to the reported procedure [217]. The method involved reduction of nitrate to nitrite followed by calorimetric estimation using Griess reagent. The concentration of nitrite in the supernatant was calculated using standard curve and expressed as percentage of control.

4.8 DPPH Assay

A solution of DPPH was prepared by dissolving 5 mg of DPPH in 2 mL of methanol, and was kept in the dark at 4°C. Varying concentrations of test compounds (200 µL) were taken in 96-well microplate. Then, 5 µL of methanolic DPPH solution (final concentration 300 µM) was added to each well. After 20 min of incubation, absorbance of the solution was read using an ELISA Reader (EL340 Biokinetic reader, Bio-Tek Instrumentation, USA) at a wavelength of 517 nm. A methanolic solution of DPPH served as a control. A dose response curve was plotted to determine the IC_{50} values. All tests and analyses were run in triplicate and averaged curcumin was used as a standard [218].

Percentage scavenging was calculated according to the following equation.

$$\% \text{ scavenging} = \frac{\{\text{Absorbance (DPPH)} - \text{Absorbance (DPPH + compound)}\}}{\text{Absorbance (DPPH)}} \times 100$$

4.9 Radioligand Binding Assay for Cannabinoid (CB_1 and CB_2) Receptors

Packard Top Count NXTv2.50 instrument was used for the assays. CP55940 [^{3}H] was used as hot ligand. Rat whole-brain membrane was used as a protein at the concentration of 100 µg/well (1 mg/mL) for radioligand binding of CB_1 and rat spleen membrane was used as protein in the concentration of 100 µg/well (1mg/mL) for radioligand binding assay of CB_2.

For the preparation of rat brain and spleen membranes, rats were sacrificed by decapitation and then brain and spleen tissues were removed and rapidly homogenized in ice-cold tris buffer (50 mM tris, 100 mM NaCl, 10 mM $MgCl_2$, pH 7.4) with a glass/teflon homogenizer. The homogenates were centrifuged at 20000 xg at 41°C for 10 min and the pellet re-suspended in tris buffer. Homogenization and centrifugation were repeated twice and the final pellet was re-suspended in storage buffer (50 mM tris, 1 mM EDTA, pH 7.4) to make a protein concentration of 1mg/mL [219].

Radioligand assays were done as reported by Leggett *et al.,* (2004) [220]. Briefly 96 well plates were prepared in triplicate to a final volume of 1 mL containing 0.5 nM [^{3}H] CP55940 (Perkin-Elmer Life Sciences Inc., U.S.A.) and 250 mg of protein diluted in tris buffer (50 mM Tris. hydrochloric acid, 2 mM EDTA, 5 mM magnesium chloride also containing 0.2 mg/mL bovine serum albumin (BSA), pH 7.4). Stock drugs were diluted in the same buffer containing 5mg/mL BSA. Plates were incubated for 90 min at 19.1°C. Specific binding was calculated by subtracting nonspecific binding (NSB), determined in the presence of 1 µM of WIN (Ambersham, UK) for CB_1 and 1 µM of SR144528 (Amersham, U.K.) for CB_2.

4.10 Cathepsin S Assay

A microplate-based screening procedure was applied to identify potential cathepsin S inhibitors using fluorescent peptide substrates and recombinant human cathepsin S. The activity of human recombinant cathepsin S was measured using benzyloxycarbonyl-valine-valine-arginine-7-amido-4-methylcoumarin (Z-VVR-AMC) as the substrate. All the test compounds were dissolved in DMSO to a final concentration of 50 µM and incubated with recombinant activated enzyme at 37°C for 10 min in the assay buffer containing 0.1M sodium acetate (pH 7.0), 1 mM EDTA, 0.01% Triton X-100, 1 mM DDT before initiating the reaction with the addition of substrate Z-Val-Val-Arg-AMC (K_m = 1.7 M). After 30 min, the reaction was stopped

by addition of E-64 and the fluorescence generated by release of methylcoumarin (nMec) from the substrate was read in Perkin Elmer LS50B luminescence spectrophotometer (Perkin Elmer, Shelton, CT, USA) with excitation and emission wavelengths of 354 nm and 442 nm, respectively [221].

4.11 Subcutaneous Picrotoxin-Induced Seizure Threshold Test (scPIC)

The test compounds were evaluated for their ability to antagonize scPIC-induced convulsions in mice after *i.p.* administration. After 30 min of drug administration, the in-house validated convulsive dose of picrotoxin (3.15 mg/kg) was injected subcutaneously in a volume of 10 ml/kg body weight into each of the mice. The mice were placed in isolated cages and observed for the next 45 min for the presence or absence of threshold convulsion. Absence of a threshold convulsion was taken as the end point, which indicates that the test substance has the ability to elevate the picrotoxin seizure threshold [222].

4.12 Statistical Analysis

All data are expressed as means ± standard error of mean (S.E.M.). The data were analyzed using Student's *t* test only when two means were compared (acute pain assay). In the case of neuropathic pain studies, statistical significance was determined for drug effects by one-way ANOVA, and Bonferroni's post hoc test was used for individual comparisons with vehicle values. Significance was assigned to a P value of less than 0.05. The statistical software package PRISM (Graphpad Software Inc., San Diego, CA) was used for the analysis.

CHAPTER 5

SERIES I: TETRAHYDROPYRIDO-PYRAZOLES

5.1 Chemistry

5.1.1 Rationale of Design

In recent years, fused ring system of pyrido-pyrazole has gained considerable attention in the treatment of neuropathic pain acting through various targets. Molecules with pyrido-pyrazole ring system have been reported as cannabinoid modulators and TNF-α inhibitors for the treatment of neuropathic pain [223]. Also, literature reveals various pyrazole based derivatives mediating GABAergic pathways useful for the treatment of neuropathic pain [224]. Literature also reveals the development of several molecules with tetrahydropyido-pyrazole scaffold acting as non-peptidic, non-covalent and selective inhibitors of cathepsin S [179,180].

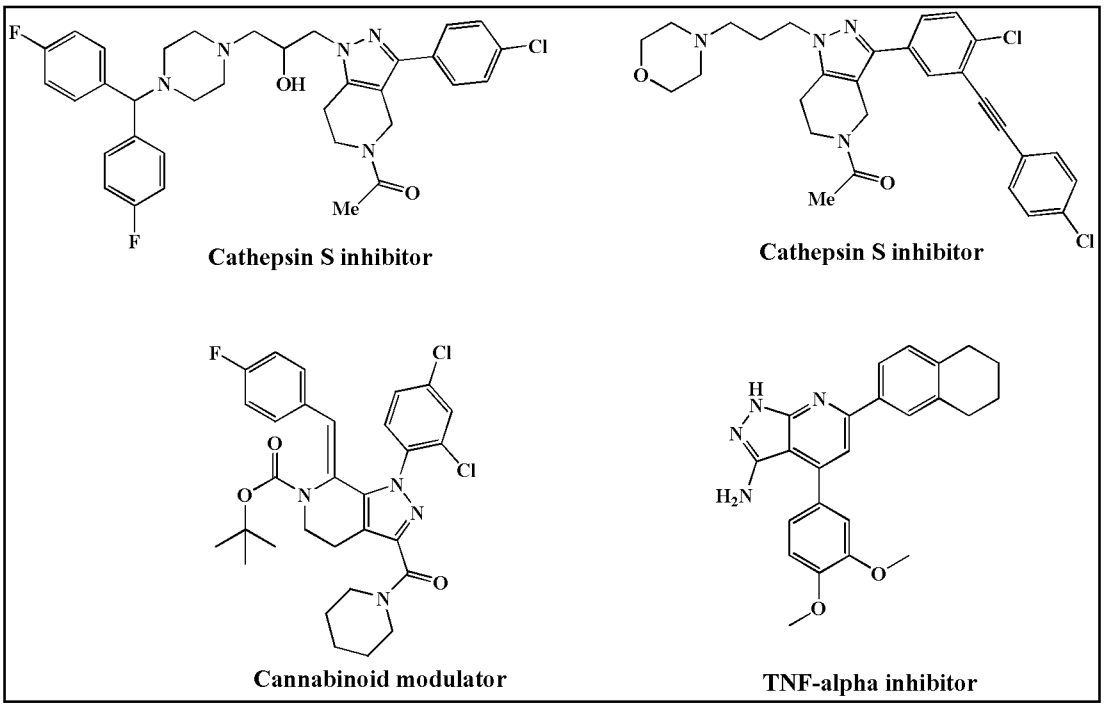

Due to the similar pathophysiology between epilepsy and neuropathic pain, several antiepileptic drugs are used to manage neuropathic pain [117]. Also, various aryl semicarbazones have been established as a novel class of anticonvulsants attenuating various neuropathic pain conditions [153-157]. In order to develop newer heterocyclic scaffolds for neuropathic pain, integration of aryl semicarbazide template into the tetrahydropyrido-pyrazoles pharmacophore was proposed.

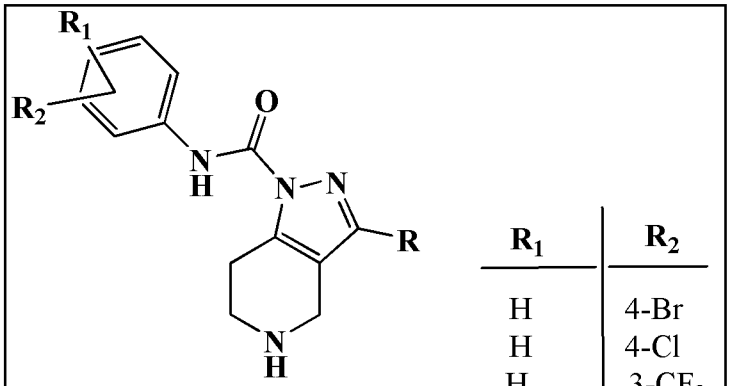

MS101-MS116

R= $-CH_3$ (MS101-MS108)
$-C(CH_3)_3$ (MS109-MS116)

R_1	R_2
H	4-Br
H	4-Cl
H	3-CF_3
2-CH_3	4-CH_3
2-CH_3	5-CH_3
2-CH_3	6-CH_3
2-F	4-F
2-F	5-CH_3

5.1.2 Synthesis

Step-1: Synthesis of *tert*-butyl-4-morpholino-5,6-dihydropyridine-1(2H)-carboxylate

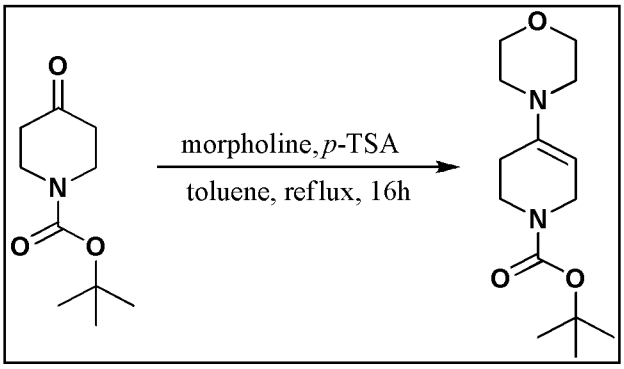

In a round-bottom flask equipped with a dean-stark trap, a reflux condenser, and an internal thermocouple, morpholine (1.05 equiv.), and *p*-toluenesulfonic acid (0.5%) were added to N-Boc-piperidone (1.0 equiv.) in toluene. The reaction mixture was refluxed overnight under N_2 atmosphere. The solvent was evaporated *in vacuo* to afford 4-*tert*-butyl-4-morpholino-5,6-dihydropyridine-1(2H)-carboxylate, which was used directly for the next step. (Colorless oil, 100%).

Step-2: Synthesis of *tert*-butyl-3-alkanoyl-4-oxopiperidine-1-carboxylate

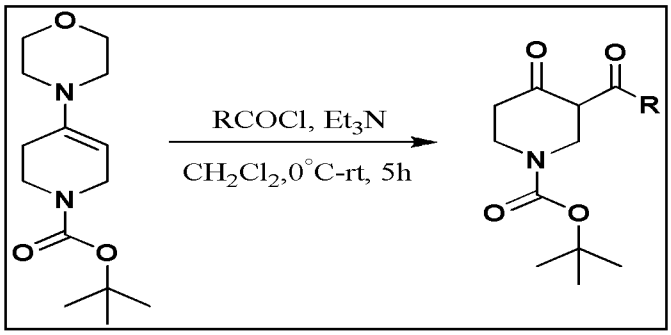

The enamine prepared in step-1 was taken in DCM. To this, triethylamine (1.2 equiv.) was added, followed by slow addition of acid chlorides [acetyl chloride (**MS101-MS108**), pivaloyl chloride (**MS109-MS116**)] at 0°C under nitrogen. The reaction mixture was stirred for 3 h followed by addition of water and stirring was further continued for 1 h. The organic layer was washed with 0.1N hydrochloric acid and brine, dried over sodium sulphate, filtered and concentrated.

Step-3: Synthesis of *tert*-butyl-3-alkyl-1-(substituted phenyl carbamoyl)-6,7-dihydro-1H-pyrazolo[4,3-c]pyridine-5(4H)-carboxylate

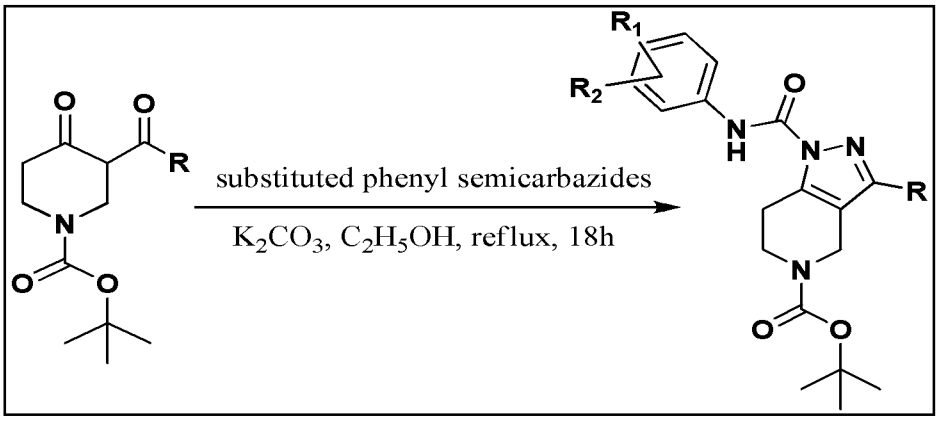

Equimolar quantites of *tert*-butyl-3-alkanoyl-4-oxopiperidine-1-carboxylate and substituted phenyl semicarbazides were added to ethanol containing potassium carbonate (1.3 equiv.). The reaction mixture was refluxed overnight, and then concentrated. The residue was diluted with ethyl acetate, then washed with 1N hydrochloric acid and brine. The organic layer was dried over sodium sulphate, filtered and concentrated to give a crude product which was purified on silica gel column.

Step-4: Deprotection of amino group of 3-alkyl-N-substitued phenyl-4,5,6,7-tetrahydro-1H-pyrazolo[4,3-c]pyridine-1-carboxamide

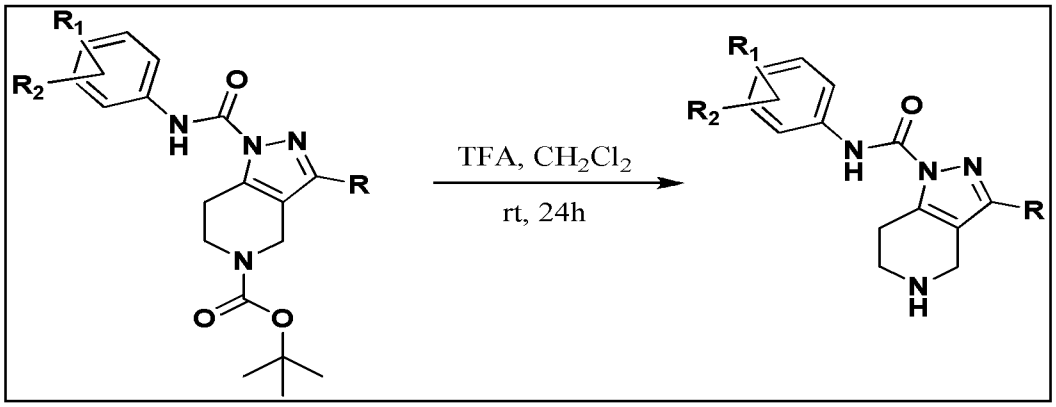

The compound obtained from step-3 was dissolved in 10 mL DCM followed by slow addition of 10 mL of trifluoroacetic acid. The mixture was stirred overnight at room temperature, concentrated, partitioned between DCM and saturated aqueous sodium bicarbonate solution. The organic layer was dried over sodium sulphate, filtered and concentrated *in vacuo.* The residue was purified by column chromatography on silica gel eluting with DCM:CH_3OH to yield the desired compound.

Step-5: Synthesis of 5-ethyl-3-alkyl-N-substituted phenyl-4,5,6,7-tetrahydro-1H-pyrazolo[4,3-c]pyridine-1-carboxamide

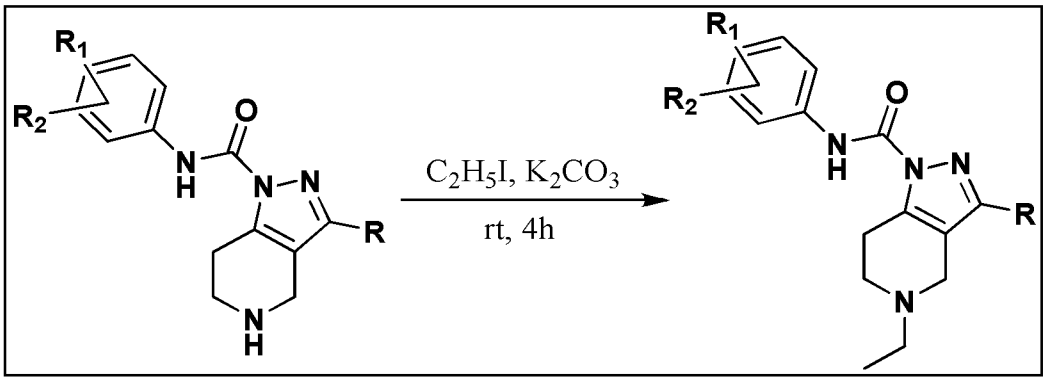

The compound was taken in acetonitrile. To it potassium carbonate (1.5 equiv.) was added followed by slow addition of ethyl iodide (1.3 equiv.) in ice cold condition. The reaction mixture was stirred at room temperature for 3-4 h, filtered, dried *in vacuo* and column purified.

Table 5.1 Physical data of 5-ethyl-3-alkyl-N-substituted-phenyl-4,5,6,7-tetra hydro-1H-pyrazolo[4,3-c]pyridine-1-carboxamides

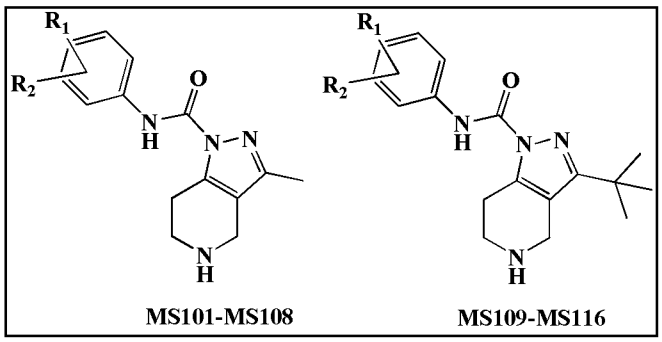

Compound	R_1	R_2	Molecular formula	M.W.	Yield (%)	M.P. (°C)
MS101	H	4-Br	$C_{16}H_{19}BrN_4O$	363.25	62	232
MS102	H	4-Cl	$C_{16}H_{19}ClN_4O$	318.80	72	241
MS103	H	3-CF_3	$C_{17}H_{19}F_3N_4O$	352.35	71	228
MS104	2-CH_3	4-CH_3	$C_{18}H_{24}N_4O$	312.41	66	213
MS105	2-CH_3	5-CH_3	$C_{18}H_{24}N_4O$	312.41	70	242[b]
MS106	2-CH_3	6-CH_3	$C_{18}H_{24}N_4O$	312.41	67	231
MS107	2-F	4-F	$C_{17}H_{19}F_3N_4O$	320.34	65	174
MS108	2-F	5-CH_3	$C_{17}H_{21}FN_4O$	316.37	69	209
MS109	H	4-Br	$C_{19}H_{25}BrN_4O$	405.33	67	187
MS110	H	4-Cl	$C_{19}H_{25}ClN_4O$	360.88	63	210
MS111	H	3-CF_3	$C_{20}H_{25}F_3N_4O$	394.43	73	214
MS112	2-CH_3	4-CH_3	$C_{21}H_{30}N_4O$	354.49	67	237
MS113	2-CH_3	5-CH_3	$C_{21}H_{30}N_4O$	354.49	64	251
MS114	2-CH_3	6-CH_3	$C_{21}H_{30}N_4O$	354.49	78	235
MS115	2-F	4-F	$C_{19}H_{24}F_2N_4O$	363.20	65	192
MS116	2-F	5-CH_3	$C_{20}H_{27}FN_4O$	358.45	69	190

Table 5.2 Spectral and elemental analyses data of 5-ethyl-3-alkyl-N-substituted phenyl-4,5,6,7-tetrahydro-1H-pyrazolo[4,3-c]pyridine-1-carboxamide

Compound	^{1}H-NMR (δ ppm, DMSO-d_6)	Elemental Analyses (Calculated/Found)			Mass Spectroscopy (m/z)
		C (%)	H (%)	N (%)	
MS101	δ 1.34 (t, 3H), 2.52 (s, 3H), 2.91-3.21 (m, 4H), 3.81 (t, 2H), 4.91 (s, 2H), 7.56 (d, 2H), 7.81 (d, 2H), 8.52 (s, 1H, D_2O exchangeable)	52.90 52.91	5.27 5.29	15.42 15.43	364.07
MS102	δ 1.33 (t, 3H), 2.53 (s, 3H), 2.65 (s, 6H), 2.91-3.22 (m, 4H), 3.82 (t, 2H), 4.92(s, 2H), 7.08 (t, 1H), 7.22 (d, 2H), 8.44 (s, 1H, D_2O exchangeable)	60.28 60.29	6.01 6.03	17.57 17.59	320.12
MS103	1.33 (t, 3H), 2.53 (s, 3H), 2.92-3.22 (m, 4H), 3.82 (t, 2H), 4.91 (s, 2H), 7.38-7.42 (m, 2H), 7.69 (d, 1H), 8.12 (s, 1H), 8.74 (s, 1H, D_2O exchangeable)	57.95 57.96	5.44 5.43	15.90 15.91	353.15
MS104	δ 1.33 (t, 3H), 2.53 (s, 3H), 2.67 (s, 6H), 2.92-3.21 (m, 4H), 3.81 (t, 2H), 4.89 (s, 2H), 7.11(s, 1H), 7.24 (d, 1H), 7.36 (d, 1H), 8.52 (s, 1H, D_2O exchangeable)	69.20 69.22	7.74 7.72	17.93 17.94	313.20
MS105	δ 1.34 (t, 3H), 2.52 (s, 3H), 2.67 (s, 6H), 2.92-3.22 (m, 4H), 3.81 (t, 2H), 4.92 (s, 2H), 7.12 (d, 1H), 7.43 (d, 1H), 7.51 (s, 1H), 8.41 (s, 1H, D_2O exchangeable)	69.20 69.20	7.74 7.70	17.93 17.92	313.20
MS106	δ 1.33 (t, 3H), 2.53 (s, 3H), 2.65 (s, 6H), 2.91-3.22 (m, 4H), 3.82 (t, 2H), 4.92(s, 2H), 7.08 (t, 1H), 7.22 (d, 2H), 8.41 (s, 1H, D_2O exchangeable)	69.20 69.21	7.74 7.71	17.93 17.94	313.20
MS107	δ 1.34 (t, 3H), 2.52 (s, 3H), 2.91-3.23 (m, 4H), 3.81 (t, 2H), 4.91 (s, 2H), 6.83-7.06 (m, 2H), 7.17-7.21 (m, 1H), 8.91 (s, 1H, D_2O exchangeable)	59.99 59.98	5.66 5.65	17.49 17.46	321.15
MS108	δ 1.33 (t, 3H), 2.52 (s, 3H), 2.91-3.21 (m, 4H), 3.82 (t, 2H), 4.92 (s, 2H), 7.01(d, 1H), 7.24-7.32 (m, 1H), 7.61 (s, 1H), 8.64 (s, 1H D_2O exchangeable)	64.54 64.52	6.69 6.67	17.71 17.70	317.17

MS109	δ 1.33 (t, 3H), 1.89 (s, 6H), 2.53 (s, 3H), 2.92-3.21 (m, 4H), 3.82 (t, 2H), 4.91 (s, 2H), 7.56 (d, 2H), 7.81 (d, 2H), 8.52 (s, 1H, D_2O exchangeable)	56.30 56.31	6.22 6.20	13.82 13.84	406.12
MS110	δ 1.33 (t, 3H), 2.52 (s, 3H), 2.92-3.22 (m, 4H), 3.81 (t, 2H), 4.91 (s, 2H), 7.44 (d, 2H), 7.61(d, 2H), 8.67 (s, 1H D_2O exchangeable)	63.24 63.22	6.98 6.97	15.53 15.51	362.17
MS111	1.34 (t, 3H), 1.89 (s, 6H), 2.53 (s, 3H), 2.71 (s, 6H), 2.92-3.23 (m, 4H), 3.82 (t, 2H), 4.91 (s, 2H), 7.12 (d, 1H), 7.43 (d, 1H), 7.51(s, 1H), 8.41 (s, 1H, D_2O exchangeable)	60.90 60.92	6.39 6.41	14.20 14.22	395.20
MS112	δ 1.33 (t, 3H), 1.88 (s, 6H), 2.52 (s, 3H), 2.74 (s, 6H), 2.92-3.22 (m, 4H), 3.81 (t, 2H), 4.91 (s, 2H), 7.11(s, 1H), 7.24 (d, 1H), 7.36 (d, 1H), 8.52 (s, 1H, D_2O exchangeable)	71.15 71.16	8.53 8.54	15.80 15.81	355.24
MS113	δ 1.34 (t, 3H), 1.89 (s, 6H), 2.53 (s, 3H), 2.71 (s, 6H), 2.92-3.23 (m, 4H), 3.82 (t, 2H), 4.91 (s, 2H), 7.12 (d, 1H), 7.43 (d, 1H), 7.51(s, 1H), 8.41 (s, 1H, D_2O exchangeable)	71.15 71.16	8.53 8.54	15.80 15.82	355.24
MS114	δ 1.33 (t, 3H), 1.87 (s, 6H), 2.53 (s, 3H), 2.65 (s, 6H), 2.91-3.22 (m, 4H), 3.81 (t, 2H), 4.93 (s, 2H), 7.08 (t, 1H), 7.22 (d, 2H), 8.41 (s, 1H, D_2O exchangeable)	71.15 71.16	8.53 8.54	15.80 15.81	355.24
MS115	δ 1.33 (t, 3H), 1.89 (s, 6H), 2.53 (s, 3H), 2.91-3.32 (m, 4H), 3.83 (t, 2H), 4.92 (s, 2H), 6.83-7.06 (m, 2H), 7.17-7.21 (m, 1H), 8.91 (s, 1H, D_2O exchangeable)	62.97 62.98	6.67 6.69	15.46 15.47	394.20
MS116	1.33 (t, 3H), 1.88 (s, 6H), 2.52 (s, 3H), 2.91-3.33 (m, 4H), 3.82 (t, 2H), 4.91 (s, 2H), 7.01 (d,1H), 7.24-7.32 (m, 1H), 7.61 (s, 1H), 8.64 (s, 1H, D_2O exchangeable)	67.01 67.02	7.59 7.60	15.63 15.64	359.22

Elemental analyses for C, H, N were within ± 0.4 % of the theoretical value

5.2 Pharmacology

Initial biological evaluation was carried out at a single intraperitoneal dose of 100 mg/kg of the synthesized tetrahydropyrido-pyrazoles (**MS101-MS116**), in both acute and chronic pain models. To examine the potential therapeutic value of these newer derivatives for the treatment of pain, the first part of the study examined the ability of the derivatives to inhibit writhing and flinching responses in the acetic acid-induced writhing test and formalin-induced flinching test respectively. In the next part,

antiallodynic and antihyperalgesic activities of the synthesized compounds were evaluated in CCI and PSNL models of neuropathic pain followed by assessment of underlying mechanism of action of most potent compounds.

5.2.1 Acetic Acid Induced Writhing

Table 5.3 Neurotoxicity and effect of [MS(101-116)] on writhing induced by acetic acid in mice

Treatment	Neurotoxicity[a]		Acetic Acid Induced Writhing[b]	
	0.5 h	4 h	Number of writhes (30 min)	% Inhibition
Vehicle	-	-	53.0 ± 3.5	-
MS101	-	-	21.3 ± 3.1	59.7*
MS102	-	-	21.1 ± 2.2	60.5*
MS103	300	300	19.9 ± 2.1	62.2*
MS104	300	300	23.3 ± 3.4	56.1*
MS105	-	-	12.6 ± 2.5	76.3*
MS106	-	-	47.5 ± 3.9	10.5
MS107	-	-	23.3 ± 2.7	56.1*
MS108	-	-	23.7 ± 4.8	55.2*
MS109	-	-	14.4 ± 5.2	72.8*
MS110	-	-	13.9 ± 2.9	73.7*
MS111	-	-	19.5 ± 2.8	63.1*
MS112	-	-	15.3 ± 3.9	71.1*
MS113	100	100	14.9 ± 7.3	71.9*
MS114	-	-	43.7 ± 8.4	17.5
MS115	-	-	20.5 ± 5.8	61.4*
MS116	-	-	44.6 ± 3.1	15.8
Indomethacin[c]			2.1 ± 0.1	96.1*

[a]Doses of 30, 100 and 300 mg/kg were administered. The figures in the table indicate the minimum dose whereby bioactivity was demonstrated in half or more of the mice (three in each group). The animals were examined at 0.5 h and 4 h. The line (-) indicates an absence of neurotoxicity at the maximum dose tested.
[b]A single dose of test compounds (100 mg/kg, *i.p.)* was administered to each of the mice.
*denotes values are significantly different from the vehicle control at $p<0.05$. [c]Indomethacin was tested at the dose of 10 mg/kg *i.p.*

5.2.2 Formalin Test

Table 5.4 Effect of [MS(101-116)] on formalin induced pain in mice

Treatment	Formalin Induced Flinching			
	Phase-I (0-5 min)	% Inhibition	Phase-II (10-30 min)	% Inhibition
Vehicle	57.5 ± 4.8	-	73.5 ± 0.8	-
MS101	56.5 ± 5.1	1.7	13.3 ± 2.1	81.6*
MS102	50.5 ± 4.6	12.2	16.0 ± 4.1	78.9*
MS103	56.0 ± 3.1	2.6	25.5 ± 3.1	55.8*
MS104	53.5 ± 1.1	7.0	48.5 ± 3.9	16.3
MS105	53.0 ± 7.4	7.8	49.5 ± 2.8	14.3
MS106	54.5 ± 1.1	5.2	48.6 ± 4.6	15.0
MS107	55.0 ± 2.3	4.4	44.2 ± 4.1	23.1
MS108	56.5 ± 7.1	1.7	53.6 ± 6.2	7.5
MS109	57.5 ± 3.2	0.0	20.0 ± 1.5	72.1*
MS110	48.5 ± 3.7	15.7	23.0 ± 7.8	68.0*
MS111	57.5 ± 4.1	0.0	48.5 ± 3.1	15.7
MS112	48.5 ± 5.1	15.7	23.5 ± 5.1	59.9*
MS113	55.0 ± 4.2	4.4	19.5 ± 5.1	73.2*
MS114	53.5 ± 3.0	7.0	22.6 ± 2.7	60.5*
MS115	56.0 ± 4.2	2.6	33.0 ± 3.1	55.1*
MS116	54.9 ± 2.7	3.5	18.0 ± 2.8	68.3*
Indomethacin[a]	54.8 ± 7.4	4.7	20.5 ± 3.1	72.1*

*denotes significance at $p<0.05$ (One-way ANOVA, followed by post-hoc Dunnett's test).
[a]Indomethacin was tested at the dose of 10 mg/kg *i.p.*

5.2.3 Peripheral Nerve Injury-CCI

Table 5.5 Effect of [MS(101-116)] on spontaneous pain in CCI model

Treatment	Spontaneous Pain		
	% Reversal in CCI (Mean ± S.E.M.)		
	30 min	60 min	120 min
Vehicle	8.9 ± 1.2	4.6 ± 1.6	4.5 ± 0.2
MS101	73.9 ± 0.2*	65.1 ± 0.2*	63.6 ± 1.2*
MS102	77.3 ± 7.3*	68.3 ± 6.7*	53.7 ± 0.4*
MS103	23.6 ± 4.2	33.3 ± 1.6	27.7 ± 2.1
MS104	72.9 ± 0.8*	67.5 ± 1.3*	64.4 ± 5.6*
MS105	69.3 ± 5.5*	63.6 ± 1.1*	72.8 ± 5.6*
MS106	15.0 ± 3.3	11.0 ± 5.6	51.8 ± 0.2*
MS107	13.3 ± 8.5	15.2 ± 3.0	12.5 ± 0.3
MS108	16.9 ± 4.2	15.0 ± 0.4	27.4 ± 1.7
MS109	90.6 ± 2.1*	85.9 ± 1.3*	83.2 ± 1.4*
MS110	95.0 ± 0.7*	90.7 ± 2.1*	88.5 ± 1.5*
MS111	21.1 ± 2.4	19.8 ± 2.2	12.4 ± 4.6
MS112	85.4 ± 0.8*	90.9 ± 0.5*	89.5 ± 0.6*
MS113	81.6 ± 3.9*	85.9 ± 2.5*	91.6 ± 4.7*
MS114	14.4 ± 2.1	20.5 ± 1.8	53.9 ± 1.4*
MS115	89.5 ± 4.5*	65.6 ± 10.6*	75.2 ± 6.9*
MS116	18.3 ± 6.3	22.3 ± 8.5	12.5 ± 2.9
GBP	71.2 ± 0.2*	91.2 ± 0.7*	88.8 ± 4.7*

Each value represents the % reversal of allodynia (mean ± S.E.M.) of four rats; * denotes the values (≥ 50%), significantly different from their respective vehicle control at $p < 0.05$ (One-way ANOVA, followed by post-hoc Dunnett's test)

Table 5.6 Antiallodynic effect of [MS(101-116)] against dynamic allodynia in CCI model

Treatment	Dynamic Allodynia		
	% Reversal in CCI (Mean ± S.E.M.)		
	30 min	60 min	120 min
Vehicle	3.4 ± 0.8	2.3 ± 0.3	0.0 ± 0.0
MS101	57.7 ± 9.0*	70.5 ± 3.8*	57.7 ± 9.0*
MS102	55.0 ± 1.5*	58.0 ± 5.0*	65.1 ± 3.4*
MS103	17.3 ± 1.9	9.9 ± 5.5	2.2 ± 0.2
MS104	17.2 ± 4.0	56.6 ± 9.2*	66.1 ± 8.9*
MS105	31.3 ± 2.3	69.6 ± 1.2*	67.0 ± 2.2*
MS106	6.6 ± 2.2	9.9 ± 5.5	13.7 ± 9.3
MS107	4.4 ± 0.1	11.8 ± 7.4	11.8 ± 7.4
MS108	13.2 ± 1.6	8.0 ± 1.1	19.7 ± 1.6
MS109	66.7± 3.3*	58.2 ± 5.3*	50.5 ± 5.0*
MS110	90.1± 1.5*	54.5 ± 1.5*	69.7 ± 3.3*
MS111	4.5 ± 0.5	19.7 ± 1.9	44.7 ± 5.3
MS112	69.7± 7.3*	54.5 ± 5.5*	58.0 ± 8.6*
MS113	61.2± 5.2*	58.3 ± 8.3*	51.7 ± 8.3*
MS114	19.7 ± 1.9	12.2 ± 3.1	4.5 ± 0.5
MS115	6.7 ± 2.7	13.7± 9.3	9.9 ± 5.5
MS116	13.8 ± 1.6	13.8 ± 1.6	12.8 ± 1.2
GBP	35.4 ± 3.0	59.4 ± 1.7*	50.7 ± 1.4*

Each value represents the % reversal of allodynia (mean ± S.E.M.) of four rats; * denotes the values (≥ 50%), significantly different from their respective vehicle control at $p < 0.05$ (One-way ANOVA, followed by post-hoc Dunnett's test)

Table 5.7 Antiallodynic effect of [MS(101-116)] against cold allodynia in CCI model

Treatment	Cold Allodynia		
	% Reversal in CCI (Mean ± S.E.M.)		
	30 min	60 min	120 min
Vehicle	3.6 ± 0.7	4.3 ± 1.9	5.4 ± 2.1
MS101	67.4 ± 1.7*	38.1 ± 1.0	32.6 ± 7.2
MS102	63.4 ± 1.6*	52.6 ± 8.8*	13.4 ± 4.6
MS103	18.4 ± 4.9	18.7 ± 1.2	14.1 ± 9.4
MS104	54.4 ± 5.6*	37.3 ± 3.7	41.8 ± 0.8
MS105	72.7 ± 7.4*	53.1 ± 5.4*	40.6 ± 2.3
MS106	15.0 ± 0.3	21.2 ± 8.3	2.8 ± 0.3
MS107	12.1 ± 2.3	13.7 ± 0.7	7.0 ± 3.8
MS108	15.9 ± 2.5	23.0 ± 3.8	9.5 ± 2.8
MS109	73.0 ± 1.0*	65.0 ± 0.5*	56.9 ± 3.5*
MS110	61.4 ± 3.8*	61.2 ± 7.2*	18.8 ± 0.8
MS111	17.9 ± 1.0	10.1 ± 1.0	40.5 ± 8.2
MS112	53.9 ± 1.6*	50.4 ± 1.8*	40.4 ± 4.4
MS113	64.3 ± 1.6*	64.4 ± 1.9*	40.0 ± 7.1
MS114	3.4 ± 0.3	7.1 ± 0.4	12.0 ± 8.2
MS115	55.6 ± 1.8*	35.0 ± 2.1	9.3 ± 2.6
MS116	17.8 ± 1.0	10.8 ± 4.1	10.5 ± 3.0
GBP	58.0 ± 6.4*	42.9 ± 7.4	35.6 ± 1.7

Each value represents the % reversal of allodynia (mean ± S.E.M.) of four rats; * denotes the values (≥ 50%), significantly different from their respective vehicle control at $p < 0.05$ (One-way ANOVA, followed by post-hoc Dunnett's test)

Table 5.8 Antihyperalgesic effect of [MS(101-116)] in CCI model

Treatment	Mechanical Hyperalgesia		
	% Reversal in CCI (Mean ± S.E.M.)		
	30 min	60 min	120 min
Vehicle	4.7 ± 2.1	4.9 ± 1.0	5.3 ± 0.5
MS101	83.3 ± 1.7*	66.7 ± 0.8*	61.1 ± 5.1*
MS102	67.0 ± 4.5*	73.2 ± 1.8*	26.1 ± 1.8
MS103	3.8 ± 1.0	20.7 ± 2.4	16.8 ± 1.4
MS104	70.8 ± 4.6*	57.5 ± 1.2*	65.0 ± 1.2*
MS105	62.1 ± 1.7*	58.9 ± 1.9*	63.3 ± 1.3*
MS106	35.7 ± 1.8	42.9 ± 1.3	14.3 ± 1.2
MS107	13.4 ± 0.9	20.5 ± 8.0	21.8 ± 6.4
MS108	14.6 ± 2.1	14.6 ± 2.1	8.3 ± 0.8
MS109	81.9 ± 6.9*	66.0 ± 2.1*	65.3 ± 9.7*
MS110	69.4 ± 1.4*	84.4 ± 4.4*	78.9 ± 1.1*
MS111	18.2 ± 9.1	18.2 ± 9.1	9.1 ± 2.0
MS112	93.8 ± 6.3*	80.0 ± 5.8*	67.5 ± 5.5*
MS113	70.8 ± 4.2*	72.9 ± 1.4*	11.2 ± 2.4
MS114	13.8 ± 6.2	12.7 ± 2.7	8.8 ± 1.2
MS115	3.6 ± 1.6	12.2 ± 2.2	12.1 ± 0.4
MS116	20.0 ± 1.3	11.7 ± 5.0*	2.2 ± 0.9
GBP	92.9 ± 7.1*	78.6 ± 7.1*	75.7 ± 3.1*

Each value represents the % reversal of allodynia (mean ± S.E.M.) of four rats; * denotes the values (≥ 50%), significantly different from their respective vehicle control at $p < 0.05$ (One-way ANOVA, followed by post-hoc Dunnett's test

2.4 Peripheral Nerve Injury-PSNL

Table 5.9 Effect of [MS(101-116)] on spontaneous pain in PSNL model

Treatment	Spontaneous Pain		
	% Reversal in PSNL (Mean ± S.E.M.)		
	30 min	60 min	120 min
Vehicle	3.2 ± 0.3	2.9 ± 0.3	1.2 ± 0.1
MS101	56.7 ± 3.3*	60.8 ± 4.2*	41.3 ± 1.7
MS102	70.3 ± 2.2*	66.1 ± 4.5*	58.4 ± 2.2*
MS103	7.5 ± 2.0	15.1 ± 4.0	4.8 ± 0.4
MS104	40.7 ± 5.9	34.4 ± 5.6	5.9 ± 0.3
MS105	59.2 ± 9.2*	28.2 ± 1.4	14.7 ± 6.4
MS106	57.6 ± 1.3*	26.6 ± 1.5	17.3 ± 7.7
MS107	20.7 ± 0.7	10.2 ± 3.1	13.8 ± 0.5
MS108	13.6 ± 3.1	12.7 ± 3.1	11.0 ±5.7
MS109	90.4 ± 3.7*	55.7 ± 9.4*	43.1 ± 9.8
MS110	93.9 ± 0.6*	78.3 ± 5.0*	57.8 ± 2.2*
MS111	4.9 ± 0.4	14.4 ± 3.8	13.6 ± 3.6
MS112	89.9 ± 5.7*	67.3 ± 5.4*	64.2 ± 8.4*
MS113	89.3 ± 2.7*	65.0 ± 8.0*	56.9 ± 0.6*
MS114	15.5 ± 1.2	9.9 ± 4.4	7.5 ± 3.2
MS115	87.3 ± 3.1*	42.2 ± 5.4	19.8 ± 4.0
MS116	20.9 ± 2.2	13.9 ± 1.4	6.3 ± 1.3
GBP	92.9 ± 1.9*	94.2 ± 2.1*	82.4 ± 5.1*

Each value represents the % reversal of allodynia (mean ± S.E.M.) of four rats; * denotes the values (≥ 50%), significantly different from their respective vehicle control at $p < 0.05$ (One-way ANOVA, followed by post-hoc Dunnett's test).

Table 5.10 Effect of [MS(101-116)] against dynamic allodynia in PSNL model

Treatment	Dynamic Allodynia		
	% Reversal in PSNL (Mean ± S.E.M.)		
	30 min	60 min	120 min
Vehicle	4.7 ± 0.7	2.5 ± 1.2	0.8 ± 0.1
MS101	58.3 ± 8.3*	58.3 ± 8.0*	29.2 ± 4.2
MS102	18.4 ± 1.6	46.4 ± 7.0	38.3 ± 3.1
MS103	27.6 ± 2.6	16.0 ± 9.0	3.5 ± 0.3
MS104	53.3 ± 2.1*	41.9 ± 1.1	30.2 ± 2.3
MS105	58.3 ± 8.3*	41.7 ± 8.3	39.2 ± 4.2
MS106	20.2 ± 1.3	15.1 ± 1.5	3.5 ± 0.3
MS107	69.7 ± 3.3*	11.1 ± 2.0	11.1 ± 2.0
MS108	18.1 ± 5.0	8.2 ± 1.1	14.2 ± 1.2
MS109	61.6 ± 5.1*	44.9 ± 1.6	44.9 ± 1.6
MS110	89.4 ± 3.5*	61.6 ± 8.1*	46.6 ± 7.0
MS111	36.4 ± 3.0	16.7 ± 1.6	4.5 ± 0.5
MS112	61.6 ± 8.4*	50.4 ± 1.9*	88.4 ± 9.6*
MS113	66.7 ± 3.3*	51.7 ± 8.3*	38.3 ± 8.3
MS114	12.2 ± 3.1	12.2 ± 3.1	4.5 ± 0.5
MS115	24.7 ± 5.6	13.0 ± 6.1	13.0 ± 6.1
MS116	15.1 ± 1.5	3.5 ± 0.4	28.5 ± 2.8
GBP	43.1 ± 2.5	56.1 ± 2.3*	58.5 ± 6.1*

Each value represents the % reversal of allodynia (mean ± S.E.M.) of four rats; * denotes the values (≥ 50%), significantly different from their respective vehicle control at $p < 0.05$ (One-way ANOVA, followed by post-hoc Dunnett's test)

Table 5.11 Antiallodynic effect of [MS(101-116)] against cold allodynia in PSNL model

Treatment	Cold Allodynia		
	% Reversal in PSNL (Mean ± S.E.M.)		
	30 min	60 min	120 min
Vehicle	4.1 ± 1.0	2.5 ± 0.3	1.9 ± 0.5
MS101	59.7 ± 1.1*	43.7 ± 2.0	41.5 ± 1.0
MS102	61.3 ± 6.2*	41.6 ± 4.9	37.2 ± 5.0
MS103	17.1 ± 5.9	14.8 ± 3.6	12.0 ± 6.4
MS104	60.4 ± 4.2*	14.3 ± 4.1	38.7 ± 2.0
MS105	58.7 ± 5.8*	35.4 ± 3.1	40.0 ± 1.5
MS106	13.0 ± 7.3	16.0 ± 0.8	7.9 ± 2.3
MS107	30.2 ± 1.3	15.7 ± 1.2	20.9 ± 1.6
MS108	13.2 ± 1.9	7.9 ± 2.2	11.0 ± 5.9
MS109	55.4 ± 7.4*	50.6 ± 7.1*	48.2 ± 0.1
MS110	58.3 ± 9.9*	56.0 ± 0.9*	10.4 ± 4.8
MS111	12.0 ± 3.2	12.7 ± 1.2	9.5 ± 0.7
MS112	62.1 ± 0.7*	52.7 ± 4.4*	38.2 ± 1.8
MS113	64.3 ± 1.6*	64.4 ± 1.9*	40.0 ± 1.2
MS114	19.3 ± 0.9	16.4 ± 1.1	19.3 ± 0.9
MS115	52.7 ± 9.3*	19.4 ± 9.0	15.0 ± 0.5
MS116	18.2 ± 9.5	17.2 ± 8.1	10.6 ± 7.1
GBP	54.1 ± 4.3*	58.2 ± 5.1*	32.1 ± 1.4

Each value represents the % reversal of allodynia (mean ± S.E.M.) of four rats; * denotes the values (≥ 50%), significantly different from their respective vehicle control at $p < 0.05$ (One-way ANOVA, followed by post-hoc Dunnett's test)

Table 5.12 Antihyperalgesic effect of [MS(101-116)] in PSNL model

Treatment	Mechanical Hyperalgesia		
	% Reversal in PSNL (Mean ± S.E.M.)		
	30 min	60 min	120 min
Vehicle	2.9 ± 0.3	2.8 ± 0.3	5.1 ± 1.0
MS101	50.0 ± 1.0*	70.0 ± 1.0*	40.0 ± 1.0
MS102	57.8 ± 2.2*	69.4 ± 1.9*	44.4 ± 1.8
MS103	39.6 ± 2.7	20.8 ± 4.2	14.6 ± 2.1
MS104	63.3 ± 1.3*	50.5 ± 0.8*	18.7 ± 1.3
MS105	62.1 ± 1.7*	58.9 ± 1.9*	63.3 ± 1.3*
MS106	44.8 ± 1.8	40.2 ± 1.3	18.2 ± 1.8
MS107	15.6 ± 4.4	11.1 ± 1.1	10.6 ± 0.6
MS108	17.5 ± 7.5	5.0 ± 0.5	11.3 ± 1.1
MS109	59.8 ± 2.7*	53.6 ± 3.6*	41.1 ± 16.1
MS110	95.5 ± 1.1*	57.7 ± 2.3*	50.0 ± 1.0*
MS111	14.3 ± 7.1	7.1 ± 1.7	14.3 ± 7.1
MS112	62.3 ± 1.2*	56.3 ± 1.2*	46.3 ± 1.6
MS113	60.0 ± 6.1*	60.2 ± 1.4*	43.9 ± 1.0
MS114	12.1 ± 2.1	12.1 ± 2.1	8.8 ± 1.2
MS115	52.8 ± 2.8*	59.5 ± 3.5*	45.8 ± 2.8
MS116	11.1 ± 1.0	16.7 ± 5.6	11.1 ± 1.0
GBP	86.2 ± 2.1*	91.3 ± 5.2*	55.8 ± 3.8*

Each value represents the % reversal of allodynia (mean ± S.E.M.) of four rats; * denotes the values (≥ 50%), significantly different from their respective vehicle control at $p < 0.05$ (One-way ANOVA, followed by post-hoc Dunnett's test)

Table 5.13 Median effective dose (ED_{50}) of selected MS1XX compounds in CCI Model

Treatment	ED_{50} Values (mg/kg) in CCI Model (TPE in min)			
	Spontaneous pain	Dynamic allodynia	Cold allodynia	Mechanical hyperalgesia
MS109	27.3 (30)	23.8 (60)	41.4 (30)	31.0 (30)
MS110	10.4 (60)	21.7 (30)	37.4 (60)	38.3 (60)
MS112	15.5 (60)	21.4 (30)	29.8 (60)	25.7 (60)

Table shows the ED_{50} values (mg/kg) in CCI model calculated at time of peak effect (TPE in min)

Table 5.14 Median effective dose (ED_{50}) of selected MS1XX compounds in PSNL model

Treatment	ED_{50} Values (mg/kg) in PSNL Model (TPE in min)			
	Spontaneous pain	Dynamic allodynia	Cold allodynia	Mechanical hyperalgesia
MS109	29.0 (60)	37.5 (60)	68.0 (30)	29.0 (30)
MS110	8.1 (30)	24.9 (30)	65.8 (60)	23.6 (30)
MS112	7.4 (30)	36.1 (120)	44.4 (60)	31.8 (30)

Table shows the ED_{50} values (mg/kg) in PSNL model calculated at time of peak effect (TPE in min)

5.2.5 Efficacy in Carrageenan Induced Paw Edema and TNF-α Quantification

Table 5.15 Effect of MS1XX compounds on carrageenan induced paw edema

Treatment	Change in paw volume (mL), Mean ± S.E.M.			(%) Protection		
	60 Min	120 min	180 min	60 min	120 min	180 min
Vehicle	0.23 ± 0.12	0.43 ± 0.12	0.67 ± 0.12	-	-	-
MS109	0.13 ± 0.14	0.05 ± 0.06	0.09 ± 0.11	43.5*	87.1*	85.7*
MS110	0.06 ± 0.10	0.05 ± 0.01	0.18 ± 0.01	76.1*	89.4*	72.9*
MS112	0.25 ± 0.01	0.53 ± 0.84	0.86 ± 1.1	-	-	-
Indomethacin[a]	0.12 ± 0.05	0.17 ± 0.12	0.22 ± 0.11	52.2*	61.2*	66.9*

A single dose of test compounds (100 mg/kg, *i.p.*) was administered to the animals. Table shows the change in paw volume (mL) after 1% carrageenan. * represents significance at $p<0.05$ compared to vehicle (One way ANOVA followed by Dunnett's Test, n=6). [a]Indomethacin was tested at the dose of 10 mg/kg *i.p.*

Table 5.16 Effect of Compounds on TNF-α level

Treatment	TNF-α (pg/ml)	% inhibition of TNF-α production
Vehicle	3175.5 ± 161.6	-
MS109	452.4 ± 25.0	86.4*
MS110	415.0 ± 12.5	77.6*
MS112	705.4 ± 22.6	58.9*

Table shows the concentration of TNF-α in the paw of carrageenan treated animals. * represents the significance at $p<0.05$, compared to vehicle control (One way ANOVA followed by Dunnett's test, n=4). All the compounds were tested at the dose of 100 mg/kg *i.p.*

5.2.6 Nitric Oxide Estimation in Brain and Sciatic Nerve

Table 5.17 Effect of MS1XX compounds on nitric oxide in brain and sciatic nerve

Total Nitrate/Nitrite (% of SHAM control)				
Treatment	**Brain**	**Sciatic Nerve**	**% Inhibition of Nitrosative stress (nitrite)[a]**	
			Brain	**Sciatic nerve**
SHAM	100.0 ± 7.8	100.0 ± 3.9	-	-
Vehicle	194.3 ± 15.3	193.7 ± 8.4	-	-
MS109	178.8 ± 1.5	149.1 ± 1.2	16.4	47.8*
MS110	180.8 ± 0.3	129.0 ± 1.4	15.3	68.7*
MS112	182.5 ± 0.7	132.4 ± 1.9	12.5	65.4*

Table shows the concentration of nitric oxide in brain and sciatic nerve after CCI in rats. * represents the significance at $p<0.05$, compared to vehicle control (One way ANOVA followed by Dunnett's test, n=4). All the compounds were tested at the dose of 100 mg/kg *i.p.*

5.2.7 DPPH Scavenging Assay

Table 5.18 DPPH scavenging activity of MS1XX compounds

Trestment	IC_{50} (μM)
MS109	81
MS110	102
MS112	134
Curcumin	135

DPPH radical scavenging activity of test compounds. Values are represented as % scavenging compared to vehicle, calculated from the average of triplicate experiments

5.2.8 Effect of Compounds on Cannabinoid Receptors

Table 5.19 Effect of MS1XX compounds on cannabinoid receptors

% Replacement of Specific Bound ^{3}H [CP 55,940] on CB_1 receptor by test compounds	
Treatment	**IC_{50}**
MS109	49.6 nM
MS110	>1 μM
MS112	>1 μM
% Replacement of Specific Bound ^{3}H [CP 55,940] on CB_2 receptor by test compounds	
Treatment	**IC_{50}**
MS109	>1 μM
MS110	>1 μM
MS112	>1 μM

Equilibrium-competition binding of compounds vs. [^{3}H] CP55940 using either rat brain (CB_1) or rat spleen homogenates (CB_2). The data shown are average of triplicates

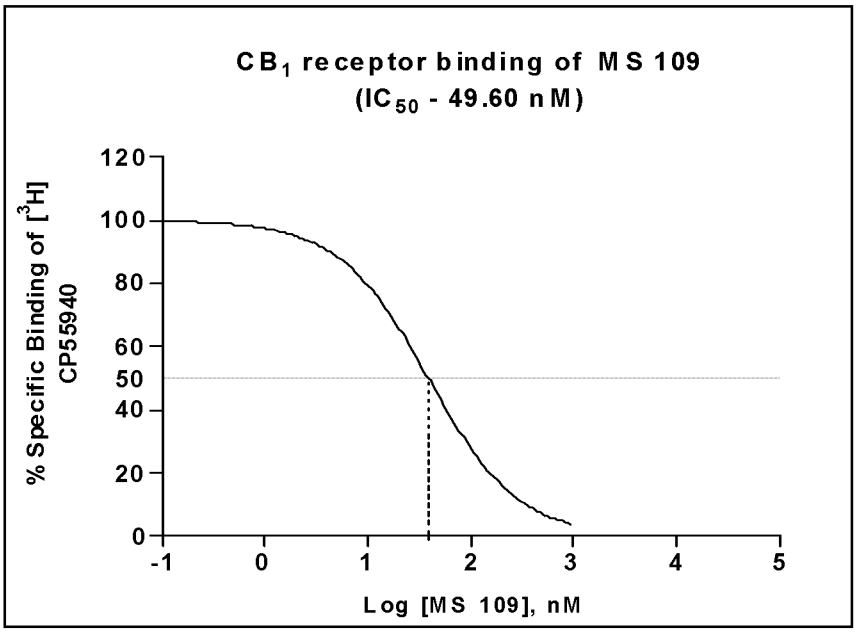

Figure 5.1 Effect of MS109 on cannabinoid (CB1) receptors
Specific binding of [^{3}H] CP55940 in presence of **MS109**. The curves shown are average of three replicates

5.2.9 Effect of Compounds on Cathepsin S Enzyme

Table 5.20 Effect of compounds on cathepsin S enzyme

Treatment	% inhibition
Vehicle	-
MS109	39.8 ± 2.1
MS110	34.1 ± 1.2

Inhibition of recombinant human cathepsin S by test compounds (50 μM), in a fluorescence assay, employing Z-Leu-Leu-Arg-MCA as synthetic substrates. Data represents means of two experiments performed in triplicate

5.2.10 Effect on GABAergic Pathway

Table 5.21 Picrotoxin induced epilepsy (scPIC) model

Treatment	Antiepileptic Activity (scPIC)	
	30 min	240 min
Vehicle	-	-
MS109	100	100
MS110	100	100
MS112	300	-
Diazepam	10	10

The figures in the table indicate the minimum dose (mg) whereby bioactivity was demonstrated in half or more of the mice (n=3). The animals were examined at 30 min and 240 min. The line (-) indicates an absence of anticonvulsant activity at the maximum dose tested

5.3 Results and Discussion

The synthesis of tetrahydropyrido-pyrazoles was achieved by a five-step process. The anilines employed for the synthesis of substituted phenyl semicarbazides were randomly selected that included 4-bromo, 4-chloro, 3-trifluoromethyl, 2,4-dimethyl, 2,5-dimethyl, 2,6-dimethyl, 2,4-difluoro and 2-fluoro-5-chloro anilines. The compounds were obtained in yields ranging between 62% to 78% (Table 5.1). The homogeneity of the compounds was monitored by performing TLC. The eluant system for all the compounds was DCM:CH_3OH (9.5:0.5). The assignments of structures were based on elemental and spectroscopic methods and the chemical shifts obtained from ^{1}H-NMR spectra supported the proposed structures. In general, the hydrogens of tetrahydro-pyridine scaffold resonated from δ~1.31-2.53 ppm in the NMR spectrum. The CO-NH proton resonated at δ~8.41-8.91 ppm for the compounds. The singlet of the CO-NH proton was D_2O exchangeable. The percentage

composition of C, H, N of all the compounds found from elemental analyses were within ± 0.4 % of the theoretical values (Table-5.2).

5.3.2 Efficacy in Acute Pain Models

Intraperitoneal administration of acetic acid causes irritation of serous membranes provoking stereotyped behavior, characterized by abdominal contractions [225,226]. This model represents a very sensitive procedure to establish peripherally acting analgesics. All of the tested compounds, except **MS106**, **MS114** and **MS116** suppressed the acetic acid-induced writhing response significantly ($p<0.05$) in comparison to the vehicle control. Compounds **MS105**, **MS109**, **MS110**, **MS112** and **MS113** exhibited more than 70.0% inhibition. Among these, **MS105** was found to be the most active compound with 76.3% inhibition of writhing response (Table 5.3). Standard compound indomethacin (10 mg/kg, *i.p.*) showed 96.1% inhibition in acetic acid-induced writhing test (Table-5.3).

The formalin test is considered a valid model for clinical pain [227-228]. In this test, the first phase or acute phase (0-5 min) has been thought to result from direct activation of nociceptive afferent fibers while the second or tonic phase (10-30 min) is peripheral inflammatory process [229-231], due to activation of NMDA and non-NMDA receptors [231] and nitric oxide production in the spinal cord [232]. Among the 16 compounds tested in this assay, none of the compounds showed significant inhibition in phase-I, whereas 10 compounds showed significant inhibition in phase-II (Table 5.4). Four compounds namely **MS101**, **MS102**, **MS109** and **MS113** showed more than 70.0% inhibition in phase-II and better efficacy than indomethacin. Compound **MS101** was the most active compound in formalin test showing 81.6 % inhibition in phase-II. Standard drug indomethacin reversed flinching in the phase-II with an inhibition of 72.1%.

5.3.3 Efficacy in Neuropathic Pain Models (CCI and PSNL)

In the CCI model, 9 compounds out of 16 completely reversed the spontaneous pain response throughout the time period of testing (30 min-120 min.) i.e. **MS101**, **MS102**, **MS104**, **MS105**, **MS109**, **MS110**, **MS112**, **MS113** and **MS115**. Gabapentin (GBP) was also found to be effective throughout the 120 min period of the experiment. Compounds **MS106** and **MS114** showed reversal of spontaneous pain only at 120 min (Table-5.5).

Eight compounds (**MS101**, **MS102**, **MS104**, **MS105**, **MS109**, **MS110**, **MS112** and **MS113**) were active in attenuating the dynamic allodynic response. Compounds **MS101**, **MS102**, **MS109**, **MS110**, **MS112** and **MS113** were effective throughout the 120 min time period, while compounds **MS104**, **MS105** and gabapentin were effective only at two time points (60-120 min). All other compounds were found to be ineffective (Table-5.6).

In the cold allodynia produced in CCI rats, the percentage reversal was significantly reduced by the administration of compounds **MS101**, **MS102**, **MS104**, **MS105**, **MS109**, **MS110**, **MS112**, **MS113** and **MS115**. Compound **MS109** was found to be effective throughout the 120 min. The duration of action for compounds **MS101**, **MS104** and **MS115** were found to be 30 min whereas compounds **MS102**, **MS105** **MS110**, **MS112** and **MS113** were effective for 60 min. All other compounds were found to be ineffective in this test (Table-5.7).

Mechanical hyperalgesia was effectively attenuated at all the time-points (30-120 min) of study by compounds **MS101**, **MS104**, **MS105**, **MS109**, **MS110** and **MS112**. Gabapentin was also found to be effective at all timepoints. The compounds **MS102** and **MS113** were found to be effective for 60 min. All other compounds were ineffective in this test (Table-5.8).

Overall, it appears that in the CCI model of neuropathic pain, compounds that showed promising results include **MS101**, **MS102**, **MS104**, **MS105**, **MS109**, **MS110**, **MS112**, and **MS113** effective in all the four tests whereas compound **MS115** was effective in two tests.

In the PSNL model, the paw withdrawal durations due to spontaneous ongoing pain were significantly reduced by compounds **MS102**, **MS110**, **MS112** and **MS113** throughout the time period (30-120 min) similar to gabapentin, while compounds **MS101** and **MS109** showed activity up to 60 min duration and compounds **MS105** , **MS106** and **MS115** showed activity only for a shorter duration (30 min). All other compounds were ineffective in this test (Table-5.9).

The dynamic allodynia produced by PSNL was effectively reversed by compound **MS112** throughout the 120 min duration while compounds **MS101**, **MS110** and **MS113** were effective till 60 min. Compounds **MS104**, **MS105**, **MS107** and **MS109**

showed activity for 30 min. Gabapentin reversed the dynamic allodynia from 60 to 120 min duration (Table-5.10).

Cold allodynia produced by PSNL model was reversed till 60 min duration by compounds **MS109**, **MS110**, **MS112** and **MS113** as observed with gabapentin. Administration of compounds **MS101**, **MS102**, **MS104**, **MS105** and **MS115** to animals with an allodynic response to cold stimuli resulted in antiallodynic activity at 30 min period. All other compounds were ineffective in this test (Table-5.11).

Mechanical hyperalgesia produced by PSNL was reversed significantly at all time-points by compounds **MS105** and **MS110** similar to gabapentin (Table-5.12). The duration of action of compounds **MS101**, **MS102**, **MS104**, **MS109**, **MS112**, **MS113** and **MS115** was up to 60 min of the experiment. Overall, it appears that in the PSNL model, compounds that showed promising results include **MS101**, **MS105**, **MS109**, **MS110**, **MS112** and **MS113** effective in all the four tests, **MS102**, **MS104** and **MS115** in three out of four tests and **MS106** and **MS107** in one test.

5.3.4 Structure-Activity Relationship Studies

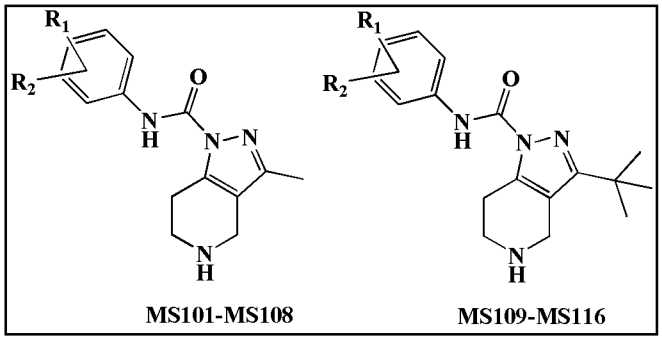

Analysis of the structure and activity revealed that in general compounds with pivaloyl group (**MS109-MS116**) at the pyrazole nucleus were more active than those with methyl function (**MS101-MS108**) as these molecules significantly alleviated one or more nociceptive responses in CCI and PSNL rats. Mono-substitution of phenyl ring at C-4 position with chloro or bromo (**MS101**, **MS102**, **MS109** and **MS112**) resulted in compounds with pronounced activity against nociceptive parameters in neuropathic animals. Substitution of C-4 of phenyl with trifluoromethyl (**MS103** and **MS111**) proved to be detrimental for the activity. Compound **MS103** was also neurotoxic. Hence trifluoromethyl was found to be unfavorable for bioactivity. The order of bioactivity in neuropathic pain models, when the phenyl ring was disubstituted with methyl functions was 2,4-dimethyl (**MS104** and **MS112**) > 2,5-

dimethyl (**MS105** and **MS113**) > 2,6-dimethyl (**MS106** and **MS114**). When C-2 of phenyl ring was substituted with fluoro group in combination with C-4 fluoro (**MS107** and **MS115**) or C-5 methyl (**MS108** and **MS116**), it was found to be detrimental to bioactivity.

5.3.5 ED_{50} Studies

Three compounds (**MS109**, **MS110** and **MS112**), exhibiting more than 90% reversal in one or more nociceptive assays in both CCI and PSNL animals were taken further for dose quantification and mechanistic studies. In the CCI model, compound **MS110** reversed spontaneous pain and dynamic allodynia with an ED_{50} value of 10.4 mg/kg and 21.7 mg/kg with time to peak effect (TPE) at 60 min and 30 min respectively, emerging as the most potent compound in CCI model (Table-5.13). In the PSNL model, compound **MS112** reversed spontaneous pain with an ED_{50} value of 7.4 mg/kg, at 30 min and cold allodynia with an ED_{50} value of 44.4 mg/kg, at 60 min (Table-5.14).

5.3.6 Mechanistic Studies

Following nerve injury, the development of inflammatory micro-environment at the site of nerve injury and the release of inflammatory mediators with their coupled signaling pathways contribute to the generation and maintenance of neuropathic pain [35,36]. Inflammatory mediators have been widely implicated in both the establishment and the perpetuation of the inflammatory process and neuropathic pain-related behavior in rodents [233]. The efficacy of the synthesized compounds in the second phase of the formalin test led us to investigate their anti-inflammatory activity against λ-carrageenan-induced rat paw edema.

Subcutaneous injection of carrageenan into rat hind paw produces inflammation with three characteristic phases [234]. The first phase (first 90 min) is attributed to histamine and serotonin release from perivenular mast cells and activation of plasmatic proteins. The second phase (90–150 min) is characterized by kinin system activation and bradykinin release. After 150 min, when the third phase is installed, cyclooxygenase (COX) metabolites are released, presenting mainly high amounts of prostaglandin E_2 (PGE_2) [235]. Cytokines like TNF-α, IL-1β, IL-6 and CINC-1 have also been found to be elevated in carrageenan induced paw edema, where TNF-α peaks at 3 h whereas IL-1β, IL-6 CINC-1 at 6 h [236]. Among the three compounds

(**MS109**, **MS110** and **MS112**) tested for carrageenan induced paw edema, 2 compounds (**MS109** and **MS110**) were found to significantly reduce paw edema throughout the period of 180 min, indicating a possible modulation of inflammatory pathways in the analgesic activity through blockade of peripheral mediators (Table-5.15). The carrageenan injected paws of the animals were harvested and the TNF-α levels were quantified using TNF-α ELISA kit (R&D Systems, USA). All the compounds were found to significantly inhibit TNF-α at 100 mg/kg. (Table- 5.16).

Peripheral nerve injuries have been shown to induce an increase in nitric oxide synthase (NOS) expression in dorsal root ganglion [156] as well as in the sciatic nerve [102]. Nine days after the lesion, the nitrite/nitrate content in brain and sciatic nerve has been found to be increased by about two to four fold, as compared to sham animals. In the present study, **MS109**, **MS110** and **MS112** were tested for their effect on nitric oxide after CCI nerve injury. All the tested compounds exhibited significant reduction ($p<0.05$) of nitric oxide in sciatic nerve. However, none of the compounds significantly attenuated nitrosative stress in the brain (Table 5.17).

In past few years, there has been growing interest in the involvement of reactive oxygen species (ROS) in several pathological conditions including nerve injury [237]. ROS produced *in vivo* include superoxide radical (O_2•-), hydrogen peroxide (H_2O_2) and hypochlorous acid (HOCl). H_2O_2 and O_2•-can interact in the presence of certain transition metal ions to yield a highly-reactive oxidizing species, the hydroxyl radical (•OH). Compounds acting as scavengers of singlet oxygen and free radicals could serve as an option for treating these pathological conditions. DPPH assay is one of the protocols for antioxidant testings, which is based on the ability of 1,1-diphenyl-2-picryl-hydrazyl (DPPH), a stable free radical, to decolorize in the presence of antioxidants. The DPPH radical contains an odd electron, which is responsible for the absorbance at 515 nm and also for a visible deep purple color. When DPPH accepts an electron donated by an antioxidant compound, the DPPH is decolorized, which can be quantitatively measured from the changes in absorbance. Selected compounds (**MS109**, **MS110** and **MS112**) were studied for their free radical scavenging activity using DPPH method. The compounds were found to possess free radical scavenging activity showing IC_{50} values between 81-134 μM being more potent than curcumin (IC_{50} 135μM) (Table-5.18).

Several studies have reported that cannabinoid agonists reduce thermal and mechanical allodynia as well as hyperalgesia in neuropathic animals [154,160,163,164]. While CB_1 receptors are known to modulate transmission in neuronal pain pathways in CNS, CB_2 receptor present in immune cells, during inflammation, prevent the release of inflammatory mediators (e.g., nerve growth factor, cytokines, and ATP) that result in nociceptor sensitization [238]. Activation of CB_2 receptor also reduces substance P-induced plasma extravasation [239] and arachidonic acid–induced ear edema [163]. Various cannabinoid agonists like 2-hydroxyethyl-hexadecanamide, WIN 55,212-2 and AM1241 have shown their efficacy in both carrageenan induced paw edema and neuropathic pain models through their action on CB_2 receptors [165,238]. Moreover, WIN 55,212-2, a non selective cananbinoid receptor agonist, has shown to modulate the levels of nitric oxide by activating CB_2 receptors [239]. However there are also evidences of CB_1 receptors mediated inhibition of nitric oxide production by rat microglial cells [240]. Compounds **MS109**, **MS110** and **MS112**, were studied for their affinity for cannabinoid receptors (Table-5.19; Figure-5.1). Only ompound **MS109** exhibited CB_1 receptor activity in nanomolar range (49.7 nm).

The compounds were also tested for inhibition of cathepsin S, a promising target for the treatment of neuropathic pain. **MS109** and **MS110** showed inhibition of 39.8% and 34.1% inhibition respectively at a dose of 50 μM (Table-5.20). The possible mediation of GABAergic pathway was also explored by assessing the anticonvulsant potential of the test compounds in picrotoxin-induced seizure. Picrotoxin acts as a noncompetitive antagonist for the $GABA_A$ receptor chloride channels. Since GABA is an inhibitory neurotransmitter, its antagonist picrotoxin shows stimulant and convulsant effects. The compounds **MS109**, **MS110** and **MS112** exhibited protection in the scPIC screen ($\geq$100 mg/kg) indicating the role of the compounds in the enhancement of GABAergic neurotransmission (Table-5.21).

To summarize, a series of 16 structurally novel tetrahydropyrido-pyrazoles were synthesized and evaluated for acute antinociceptive, antiallodynic and antihyperalgesic potential. In acute models of pain, significant inhibition of acetic acid-induced writhing by 13 compounds established their role as peripherally acting analgesics. Also, significant suppression of phase-II of the formalin test by 11 compounds suggested the modulation of anti-inflammatory pathways. Two

compounds (**MS109** and **MS110**) significantly reduced edema in carrageenan-induced paw edema model. **MS109**, **MS110** and **MS112** were found to attenuate levels of TNF-α, a pro-inflammatory cytokine, in the carrageenan injected paw.

Following nerve injury, subsequent generation of free radicals leads to oxidative and nitrosative stress which exaggerates pain states. The neuro-protection exhibited by the compounds was found to be associated with their free radical scavenging abilities (81-134 μM) resulting in attenuation of oxidative and nitrosative stress. Also, the CB_1 receptor affinity for compound **MS109** in nanomolar range (49.6 nM) and enhancement of peripheral GABAergic neurotransmission by **MS109**, **MS110** and **MS112** demonstrate the ability of compounds to modulate several systems for the alleviation of neuropathic pain.

CHAPTER 6

SERIES II - TETRAHYDROPYRIDO-PYRIMIDINES

6.1 Chemistry

6.1.1 Rationale of Design

In recent years, several amino and alkoxy tetrahydropyrido-pyrimidines have been reported as leads for the treatment of neuropathic pain modulating various targets viz. phosphodiesterase 10 (PDE10), metabotropic glutamate receptor 5 (mGLuR5) and Batrachotoxin receptor regulation [241]. Literature also reveals $P2X_7$ antagonists possessing the above mentioned template [187]. Several pyrido-pyrimidines mediating histaminergic pathways have also been reported for the alleviation of neuropathic pain. In view of the above reports, synthesis of several substituted pyridopyrimidines was accomplished [183].

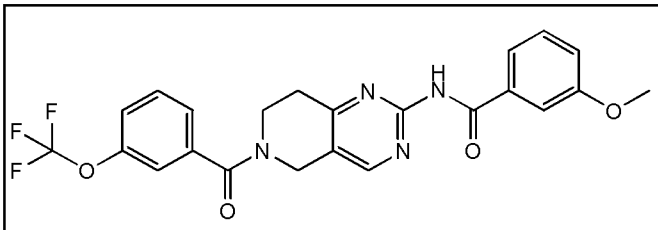

mGLuR5 receptor regulation

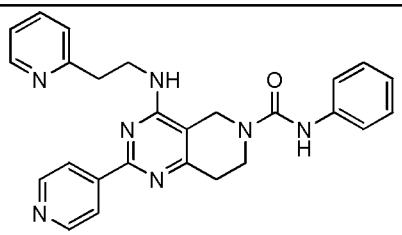

Phosphodiesterase PDE(10) inhibitor

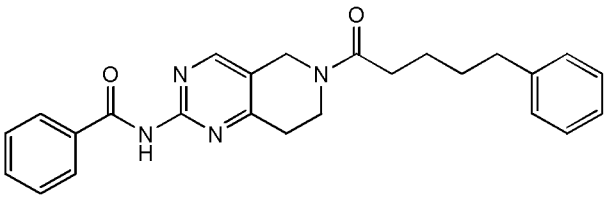

Batrachotoxin (BTX) receptor regulation

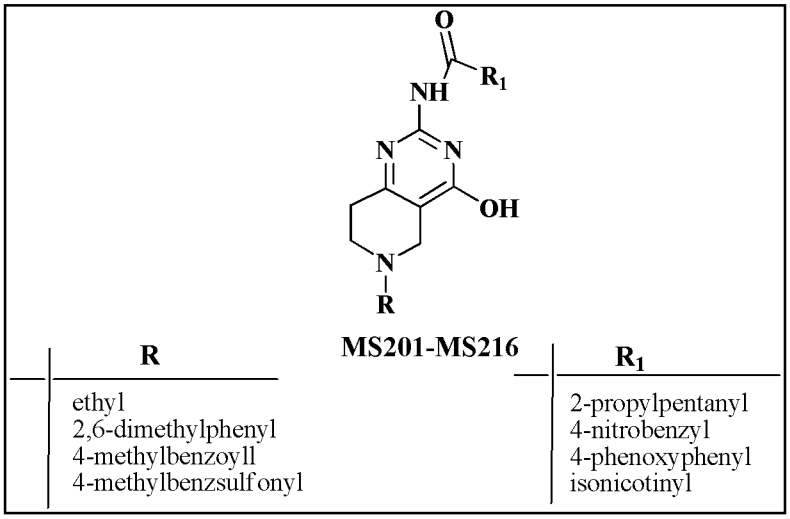

6.1.2 Synthesis

Step-1: Synthesis of N-substituted piperidin-4-one

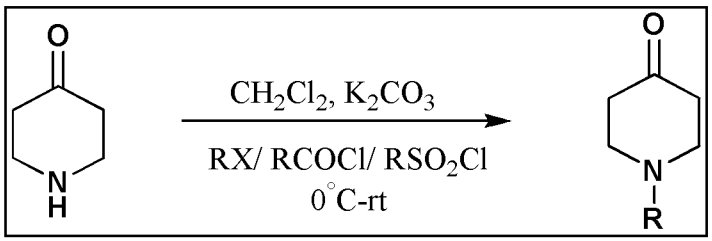

4-Piperidone (1.0 equiv.) was taken in DCM. To it potassium carbonate (2.0 equiv.) was added followed by the addition of various alkyl, acid and sulphonyl halides (1.0 equiv.) at 0°C. The reaction was stirred at room temperature overnight, diluted with water (40 mL), and neutralized to pH 6 with acetic acid. The solid was collected by filtration, washed with water, and dried under vacuum to provide the title compound.

Step-2: Synthesis of methyl N-substituted-4-oxo-piperidine-3-carboxylate

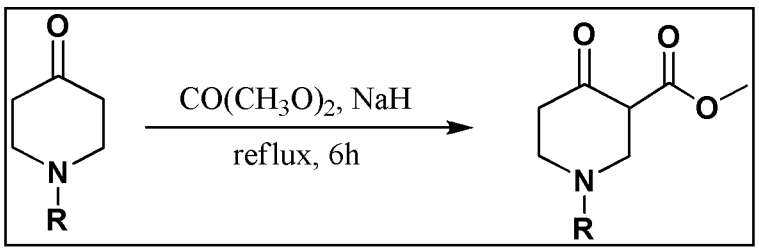

A 500-mL, three-necked, round-bottomed flask was equipped with a mechanical stirrer, a reflux condenser, and a pressure-equalizing dropping funnel bearing a nitrogen inlet. The flask was flushed with nitrogen and charged with dimethyl carbonate (8.0 equiv.), 50 mL of anhydrous THF, and sodium hydride (2.2 equiv.). The suspension was stirred and heated to reflux temperature, when the slow, dropwise

addition of various N-substituted piperidin-4-ones in 20 mL of dry THF begun. The addition of N-substituted piperidin-4-ones was continued over a 1 h period. The mixture was stirred and heated at reflux for 6 h, cooled in an ice bath for 15–20 min, and hydrolyzed by slowly adding 75 mL of 3M aqueous acetic acid. The contents of the flask were poured into 100 mL of aqueous sodium chloride, and the aqueous mixture was extracted with (4 × 150) mL portions of DCM. The organic layers were combined, dried with anhydrous sodium sulphate, and concentrated at room temperature with a rotary evaporator. Distillation of the residual liquid under reduced pressure resulted in N-substituted-4-oxo-piperidine-3-carboxylate (79–87%) as a yellow liquid.

Step-3: Synthesis of 2-amino-6-substituted-5,6,7,8-tetrahydropyrido pyrimidin-4-ol

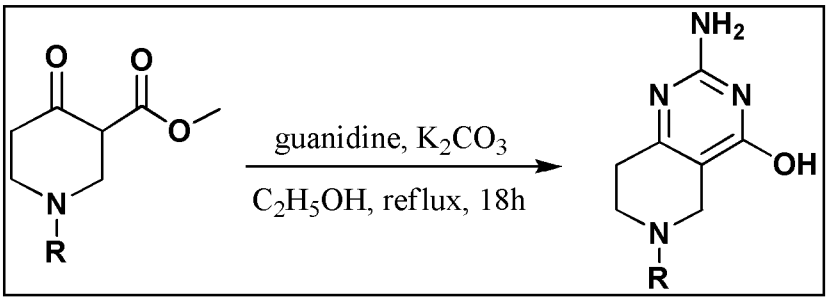

A solution of N-substituted-4-oxo-piperidine-3-carboxylate (1.0 equiv.) in DMF (5 mL) was treated with guanidine hydrochloride (2 equiv.) followed by the addition of potassium carbonate (2.0 equiv.), and the mixture was stirred at 110°C for 16 h. The mixture was cooled to ambient temperature, diluted with water (40 mL), and neutralized to pH 6 with acetic acid. The solid was collected by filtration, washed with water, and dried under vacuum to provide the title compound.

Step-4: Synthesis of 2-amino-6-substituted-5,6,7,8-tetrahydropyrido-pyrimidine compounds

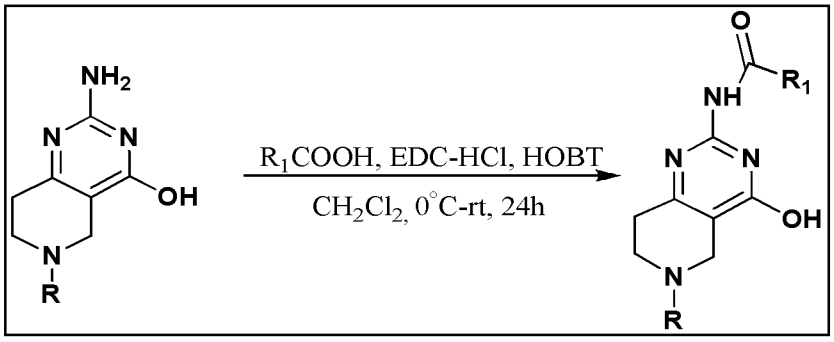

Substituted acids (1.0 equiv.) and 2-amino-6-substituted-5,6,7,8-tetrahydropyrido pyrimidin-4-ols (1.0 equiv.) were taken in DCM followed by addition of triethylamine (1.1 equiv.), 1-ethyl-3-[3-(dimethylamino)propyl]carbodiimide hydrochloride (EDC) (1.1 equiv.) and 1-hydroxybenzotriazole (HOBT) (1.1 equiv.) at 0°C. The reaction mixture was stirred at room temperature overnight. Following completion, the reaction mixture was washed with saturated aqueous sodium bicarbonate and brine. The organic layer was collected, dried over anhydrous sodium sulphate, filtered, and evaporated *in vacuo* to give the product in 59-82% yield.

Table 6.1 Physical data of Tetrahydropyrido-pyrimidines

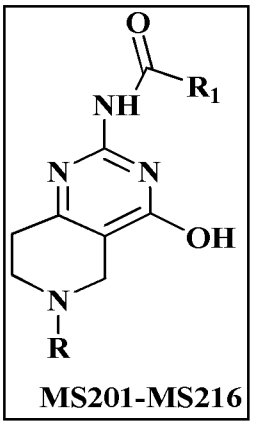

MS201-MS216

Compound	R	R_1	Molecular Formula	M.W.	Yield (%)	M.P. (°C)
MS201	Ethyl	2-propylpentanyl	$C_{17}H_{28}N_4O_2$	320.43	78	192
MS202	Ethyl	4-nitrobenzyl	$C_{16}H_{17}N_5O_4$	343.34	67	201
MS203	Ethyl	4-phenoxyphenyl	$C_{22}H_{22}N_4O_3$	390.44	71	169
MS204	Ethyl	Isonicotinyl	$C_{15}H_{17}N_5O_2$	299.33	72	193
MS205	2,6-dimethylphenyl	2-propylpentanyl	$C_{23}H_{32}N_4O_2$	396.53	63	231
MS206	2,6-dimethylphenyl	4-nitrobenzyl	$C_{22}H_{21}N_5O_4$	419.43	65	201
MS207	2,6-dimethylphenyl	4-phenoxyphenyl	$C_{28}H_{26}N_4O_3$	466.53	61	190
MS208	2,6-dimethylphenyl	Isonicotinyl	$C_{21}H_{21}N_5O_2$	375.42	77	198
MS209	4-methyl benzoyl	2-propylpentanyl	$C_{23}H_{30}N_4O_3$	410.51	78	189
MS210	4-methyl benzoyl	4-nitrobenzyl	$C_{22}H_{19}N_5O_5$	433.42	71	209
MS211	4-methyl benzoyl	4-phenoxyphenyl	$C_{28}H_{24}N_4O_4$	480.51	60	231
MS212	4-methyl benzoyl	Isonicotinyl	$C_{21}H_{19}N_5O_3$	389.41	70	163
MS213	4-methylbenzsulfonyl	2-propylpentanyl	$C_{22}H_{30}N_4O_4S$	446.56	61	180
MS214	4-methylbenzsulfonyl	4-nitrobenzyl	$C_{21}H_{19}N_5O_6S$	469.47	59	195
MS215	4-methylbenzsulfonyl	4-phenoxyphenyl	$C_{27}H_{24}N_4O_5S$	516.57	81	198
MS216	4-methylbenzsulfonyl	Isonicotinyl	$C_{20}H_{19}N_5O_4S$	425.46	82	205

Table 6.2 Spectral and elemental analyses data of Tetrahydropyrido-pyrimidines

Compound	^{1}H-NMR (δ ppm, DMSO-d_6)	Elemental Analyses (Calculated/Found)[a]			Mass Spectroscopy (m/z)
		C (%)	H (%)	N (%)	
MS201	δ 0.96-1.11 (t, 6H), 1.23 (t, 3H), 1.37-1.41 (m, 4H), 1.54-1.59 (q, 4H), 2.65-2.67 (t, 1H), 2.92-3.23 (m, 4H), 3.73 (t, 2H), 4.41 (s, 2H), 9.32 (br s, 1H, D_2O exchangeable)	63.72 63.71	8.81 8.82	17.48 17.49	321.22
MS202	δ 1.23 (t, 3H), 2.92-3.23 (m, 4H), 3.73 (t, 2H), 4.41 (s, 2H), 8.11 (d, 2H), 8.44 (d, 2H), 9.11 (br s, 1H, D_2O exchangeable)	55.97 55.96	4.99 4.98	20.40 20.41	344.13
MS203	δ 1.24 (t, 3H), 2.91-3.21 (m, 4H), 3.71 (t, 2H), 4.42 (s, 2H), 7.14-7.17 (m, 3H), 7.32-7.41 (m, 4H), 8.01 (d, 2H), 9.41 (br s, 1H, D_2O exchangeable)	67.68 67.65	5.68 5.69	14.35 14.26	391.17
MS204	δ 1.23 (t, 3H), 2.92-3.23 (m, 4H), 3.73 (t, 2H), 4.41 (s, 2H), 7.81 (d, 2H), 8.89 (d, 2H), 9.51 (br s, 1H, D_2O exchangeable)	60.19 60.09	5.72 5.73	23.40 23.36	300.14
MS205	δ 0.96-1.11 (t, 6H), 1.23 (t, 3H), 1.37-1.41 (m, 4H), 1.54-1.59 (q, 4H), 2.14 (s, 6H), 2.65-2.67 (t, 1H), 2.92-3.23 (m, 4H), 3.73 (t, 2H), 4.41 (s, 2H), 6.76 (t, 1H), 7.03 (d, 2H), 9.11 (br s, 1H, D_2O exchangeable)	69.67 69.69	8.13 8.14	14.13 14.15	397.26
MS206	δ 2.13 (s, 6H), 2.91 (t, 2H), 3.71 (t, 2H), 4.52 (s, 2H), 6.76 (t, 1H), 7.03 (d, 2H), 7.14-7.17 (m, 3H), 7.32-7.41 (m, 4H), 8.01 (d, 2H), 9.41 (br s, 1H, D_2O exchangeable)	63.00 63.03	5.05 5.07	16.70 16.72	420.26
MS207	δ 2.13 (s, 6H), 2.91 (t, 2H), 3.71 (t, 2H), 4.52 (s, 2H), 6.76 (t, 1H), 7.03 (d, 2H), 8.11 (d, 2H), 8.44 (d, 2H), 9.11 (br s, 1H, D_2O exchangeable)	72.09 72.11	5.62 5.64	12.01 12.03	467.20
MS208	δ 2.13 (s, 6H), 2.91 (t, 2H), 3.71 (t, 2H), 4.52 (s, 2H), 6.76 (t, 1H), 7.03 (d, 2H), 7.81 (d, 2H), 8.89 (d, 2H), 9.11 (br s, 1H, D_2O exchangeable)	67.18 67.21	5.64 5.67	18.65 18.66	376.17

MS209	δ 0.96-1.11 (t, 6H), 1.37-1.41 (m, 4H), 1.54-1.59 (q, 4H), 2.34 (s, 3H), 2.53 (q, 1H), 2.98 (t, 2H), 3.79 (t, 2H), 4.62 (s, 2H), 7.41 (d, 2H), 7.93 (d, 2H), 9.61 (br s, 1H, D_2O exchangeable)	67.29 67.33	7.37 7.38	13.65 13.67	411.24
MS210	δ 2.35 (s, 3H), 2.98 (t, 2H), 3.79 (t, 2H), 4.62 (s, 2H), 7.41 (d, 2H), 7.91 (d, 2H), 8.11 (d. 2H), 8.44 (d, 4H), 9.54 (br s, 1H, D_2O exchangeable)	60.97 60.99	4.42 4.44	16.16 16.18	434.14
MS211	δ 2.35 (s, 3H), 2.98 (t, 2H), 3.79 (t, 2H), 4.62 (s, 2H), 7.14-7.17 (m, 3H), 7.32-741 (m, 6H), 7.98 (d, 2H), 8.01 (d, 2H), 9.44 (br s, 1H, D_2O exchangeable)	69.99 69.99	5.03 5.05	11.66 11.67	481.18
MS212	δ 2.35 (s, 3H), 2.98 (t, 2H), 3.79 (t, 2H), 4.62 (s, 2H), 7.41 (d, 2H), 7.91 (d, 2H), 7.81 (d. 2H), 8.89 (d, 4H), 9.54 (br s, 1H, D_2O exchangeable)	64.77 64.79	4.92 4.94	17.98 18.01	390.15
MS213	δ 0.96-1.11 (t, 6H), 1.37-1.41 (m, 4H), 1.54-1.59 (q, 4H), 2.44 (s, 6H), 2.53-2.57 (t, 1H),), 2.78 (t, 2H), 3.63 (t, 2H), 4.42 (s, 2H), 7.40 (d, 2H), 7.74 (d, 2H), 9.11 (br s, 1H, D_2O exchangeable)	59.17 59.19	6.77 6.79	12.55 12.57	447.20
MS214	δ 2.35 (s, 3H), 2.78 (t, 2H), 3.63 (t, 2H), 4.42 (s, 2H), 7.41 (d, 2H), 7.75 (d, 2H), 8.11 (d. 2H), 8.44 (d, 4H), 9.54 (br s, 1H, D_2O exchangeable)	53.73 53.76	4.08 4.10	14.92 14.92	470.11
MS215	δ 2.35 (s, 3H), 2.78 (t, 2H), 3.69 (t, 2H), 4.42 (s, 2H), 7.14-7.17 (m, 3H), 7.32-741 (m, 6H), 7.74 (d, 2H), 8.01 (d, 2H), 9.44 (br s, 1H, D_2O, exchangeable)	62.78 67.79	4.68 4.70	10.85 10.88	517.15
MS216	δ 2.35 (s, 3H), 2.78 (t, 2H), 3.69 (t, 2H), 4.42 (s, 2H), 7.41 (d, 2H), 7.81-7.85 (m, 4H), 8.89 (d, 4H), 9.54 (br s, 1H, D_2O exchangeable)	56.46 56.48	4.50 4.52	16.46 16.48	426.12

Elemental analyses for C, H, N were within ± 0.4 % of the theoretical values

6.2 Pharmacology

6.2.1 Acetic Acid Induced Writhing

Table 6.3 Neurotoxicity and effect of [MS(201-216)] on writhing induced by acetic acid in mice

Treatment	Neurotoxicity[a]		Acetic Acid Induced Writhing	
	0.5 h	4 h	Number of writhes (30 min)	% Inhibition[b]
Vehicle	-	-	53.0 ± 3.5	-
MS201	-	-	31.5 ± 0.7	40.5*
MS202	-	-	21.5 ± 0.4	59.4*
MS203	-	-	20.5 ± 1.0	61.3*
MS204	-	-	28.5 ± 2.1	46.2*
MS205	-	-	28.5 ± 3.1	46.3*
MS206	-	-	43.5 ± 6.3	17.9
MS207	-	-	47.0 ± 3.1	11.3
MS208	-	-	28.5 ± 3.2	46.2*
MS209	-	-	18.5 ± 4.2	65.0*
MS210	-	-	20.5 ± 4.6	61.3*
MS211	-	-	28.5 ± 7.3	46.2*
MS212	-	-	17.5 ± 4.2	61.8*
MS213	300	300	41.5 ± 5.4	21.7
MS214	-	-	13.0 ± 5.3	75.4*
MS215	-	-	28.5 ± 2.5	46.2*
MS216	-	-	13.5 ± 5.2	74.5*
Indomethacin[c]			2.0 ± 4.6	96.1*

[a]Doses of 30, 100 and 300 mg/kg were administered. The figures in the table indicate the minimum dose whereby bioactivity was demonstrated in half or more of the mice (three in each group). The animals were examined at 0.5 h and 4 h. The line (-) indicates an absence of neurotoxicity at the maximum dose tested.

[b]A single dose of test compounds (100 mg/kg, *i.p.*) was administered to each of the mice. Data are expressed as mean ± S.E.M. number of writhing reactions. * denotes a value significantly different from the vehicle control at $p<0.05$. [c]Indomethacin was tested at the dose of 10 mg/kg *i.p.*

6.2.2 Formalin Test

Table 6.4 Effect of [MS(201-216)] on formalin induced pain in mice

Treatment	Formalin Induced Flinching			
	Phase-I (0-5 min)	% Inhibition	Phase-II (10-30 min)	% Inhibition
Vehicle	57.5 ± 4.8	-	73.5 ± 0.8	-
MS201	43.0 ± 2.1	25.2	36.5 ± 2.1	50.3*
MS202	40.0 ± 4.3	30.4	58.0 ± 4.1	21.0
MS203	47.5 ± 0.4	17.4	57.0 ± 3.1	22.4
MS204	45.5 ± 1.1	20.9	41.5 ± 3.9	43.5*
MS205	42.9 ± 3.5	25.3	62.5 ± 2.8	15.6
MS206	27.0 ± 0.4	53.0*	32.5 ± 4.6	55.7*
MS207	55.0 ± 1.1	4.3	55.5 ± 4.1	24.5
MS208	47.0 ± 2.3	18.3	32.0 ± 1.2	54.7*
MS209	48.5 ± 3.4	15.7	43.5 ± 1.5	40.8*
MS210	49.0 ± 3.7	14.8	22.0 ± 7.8	70.1*
MS211	49.5 ± 3.1	13.9	32.0 ± 3.1	56.5*
MS212	46.5 ± 5.1	19.1	26.0 ± 2.9	64.6*
MS213	32.7 ± 3.1	43.4*	51.5 ± 5.1	29.9
MS214	48.5 ± 3.0	15.7	22.0 ± 5.1	70.1*
MS215	36.0 ± 6.1	37.4	41.9 ± 3.1	43.0*
MS216	41.9 ± 4.2	28.7	14.5 ± 2.8	80.2*
Indomethacin	54.8 ± 7.4	4.7	20.5 ± 3.1	72.1*

Each value represents the mean ± S.E.M. of six mice.* denotes significant at $p<0.05$ (One-way ANOVA, followed by post-hoc Dunnett's test). Indomethacin was tested at the dose of 10 mg/kg *i.p.*

6.2.3 Peripheral Nerve Injury - CCI

Table 6.5 Effect of [MS(201-216)] on spontaneous pain in CCI model

Treatment	Spontaneous Pain		
	% Reversal in CCI (Mean ± S.E.M.)		
	30 min	60 min	120 min
Vehicle	8.9 ± 1.2	4.6 ± 1.6	4.5 ± 0.2
MS201	16.8 ± 6.9	53.5 ± 7.5*	63.5 ± 4.4*
MS202	15.1 ± 5.7	55.8 ± 9.2*	57.2 ± 4.2*
MS203	64.4 ± 3.5*	61.5 ± 4.0*	68.0 ± 5.5*
MS204	52.6 ± 2.7*	68.6 ± 1.7*	81.2 ± 2.2*
MS205	35.4 ± 4.2	55.6 ± 5.8*	64.3 ± 5.2*
MS206	29.2 ± 6.2	56.7 ± 3.3*	63.8 ±1.1*
MS207	14.1 ± 6.7	12.0 ± 5.9	10.4 ± 6.7
MS208	26.0 ± 0.8	10.2 ± 4.7	67.1 ± 1.4*
MS209	22.7 ± 3.4	27.8 ± 0.8	28.5 ± 2.0
MS210	1.7 ± 4.7	22.4 ± 3.8	20.8 ± 1.0
MS211	12.1 ± 6.3	12.2± 1.7	24.1 ±7.1
MS212	5.9 ± 7.1	60.4 ± 4.7*	57.2 ± 6.6*
MS213	51.3 ± 1.2*	59.5 ± 3.3*	54.6 ± 3.1*
MS214	71.3 ± 1.2*	92.8 ± 4.6*	84.6 ± 6.3*
MS215	11.3 ± 1.2	19.5 ± 1.6	14.6 ±1.5
MS216	91.8 ± 2.8*	93.2 ± 0.7*	87.0 ± 1.8*
GBP	71.2 ± 0.2*	91.2 ± 0.7*	88.8 ± 3.9*

Each value represents the % reversal of allodynia (mean ± S.E.M.) of four rats; * denotes the values (≥ 50%), significantly different from their respective vehicle control at $p < 0.05$ (One-way ANOVA, followed by post-hoc Dunnett's test)

Table 6.6 Antiallodynic effect of [MS(201-216)] against dynamic allodynia in CCI model

Treatment	Dynamic Allodynia		
	% Reversal in CCI (Mean ± S.E.M.)		
	30 min	60 min	120 min
Vehicle	3.4 ± 0.8	2.3 ± 0.3	0.0 ± 0.0
MS201	12.1 ± 0.7	9.8 ± 0.8	16.1 ± 9.7
MS202	21.9 ± 2.3	16.1 ± 9.7	22.3 ± 8.2
MS203	59.9 ± 4.8*	25.7 ± 8.8	9.9 ± 4.9
MS204	17.1 ± 2.1	58.4 ± 2.1*	61.3 ± 5.8*
MS205	4.0 ± 2.4	17.4 ± 10.2	29.6 ± 10.2
MS206	14.1 ± 3.1	60.5 ± 2.0*	53.4 ± 8.7*
MS207	21.7 ± 6.8	19.2 ± 7.8	39.1 ± 4.8
MS208	10.1 ± 1.9	13.8 ± 8.0	17.6 ± 2.6
MS209	4.5 ± 1.6	14.9 ± 3.5	24.2 ± 1.7
MS210	3.5 ± 2.0	15.1 ± 1.7	31.8 ± 0.9
MS211	12.1 ± 5.8	21.7 ± 2.1	18.4 ± 6.1
MS212	0.0 ± 0.0	53.0 ± 0.0*	63.0 ± 4.3*
MS213	62.1 ± 3.1*	55.6 ± 2.1*	25.0 ± 0.0
MS214	60.0 ± 6.8*	72.9 ± 10.4*	94.5 ± 7.2*
MS215	56.7 ± 2.7*	13.7 ± 9.3	9.9 ± 5.5
MS216	73.8 ± 1.6*	63.8 ± 1.6*	52.8 ± 1.2*
GBP	35.4 ± 3.0	59.4 ± 1.7*	50.7 ± 1.4*

Each value represents the % reversal of allodynia (mean ± S.E.M.) of four rats; * denotes the values (≥ 50%), significantly different from their respective vehicle control at $p < 0.05$ (One-way ANOVA, followed by post-hoc Dunnett's test)

Table 6.7 Antiallodynic effect of [MS(201-216)] against cold allodynia in CCI model

Treatment	Cold Allodynia		
	% Reversal in CCI (Mean ± S.E.M.)		
	30 min	60 min	120 min
Vehicle	3.6 ± 0.7	4.3 ± 1.9	5.4 ± 2.1
MS201	7.4 ± 1.8	20.1 ± 1.7	25.4 ± 4.3
MS202	1.4 ± 0.9	23.7 ± 1.3	22.5 ± 7.9
MS203	56.4 ± 7.9*	56.1 ± 7.2*	68.7 ± 7.3*
MS204	60.5 ± 1.0*	54.6 ± 2.4*	58.2 ± 2.8 *
MS205	51.6 ± 4.2*	58.5 ± 3.5*	69.1 ± 1.6 *
MS206	16.5 ± 2.8	59.9 ± 1.2*	59.7 ± 2.2 *
MS207	19.6 ± 3.9	20.9 ± 7.5	10.3 ± 8.4
MS208	21.4 ± 3.4	10.3 ± 1.8	15.7 ± 2.0
MS209	22.4 ± 6.6	27.6 ± 7.6	13.6 ± 4.2
MS210	34.7 ± 3.1	14.4 ± 5.8	14.2 ± 0.6
MS211	21.4 ± 7.1	9.1 ± 3.1	33.6 ± 6.1
MS212	11.4 ± 2.1	55.4 ± 5.1*	54.3 ± 3.1 *
MS213	59.5 ± 4.8*	70.8 ± 5.4*	60.0 ± 8.0 *
MS214	68.9 ± 2.5*	92.7 ± 5.3*	63.4 ± 5.5 *
MS215	15.6 ± 1.8	15.0 ± 2.1	9.3 ± 2.6
MS216	77.8 ± 1.0*	80.8 ± 4.1*	70.5 ± 3.0 *
GBP	58.0 ± 6.4*	42.9 ±7 .4	35.6 ± 1.7

Each value represents the % reversal of allodynia (mean ± S.E.M.) of four rats; * denotes the values (≥ 50%), significantly different from their respective vehicle control at $p < 0.05$ (One-way ANOVA, followed by post-hoc Dunnett's test)

Table 6.8 Antihyperalgesic effect of [MS(201-216)] in CCI model

Treatment	Mechanical Hyperalgesia		
	% Reversal in CCI (Mean ± S.E.M.)		
	30 min	60 min	120 min
Vehicle	2.9 ± 0.3	2.8 ± 0.3	5.1 ± 1.0
MS201	5.9 ± 3.4	11.5 ± 4.5	14.6 ± 2.6
MS202	12.9 ± 0.4	16.5 ± 6.5	19.6 ± 6.6
MS203	16.9 ± 8.4	56.1 ± 8.6*	64.7 ± 9.7*
MS204	59.2 ± 5.4*	15.8 ± 2.8	9.1 ± 3.2
MS205	54.5 ± 4.5*	22.8 ± 3.5	2.1 ± 3.2
MS206	9.4 ± 3.1	51.9 ± 3.1*	52.3 ± 3.6*
MS207	15.5 ± 0.7	27.4 ± 4.5	12.9 ± 5.1
MS208	17.5 ± 5.3	21.1 ± 5.8	24.7 ± 8.0
MS209	59.0 ± 2.0*	12.0 ± 4.5	19.0 ± 12.3
MS210	21.4 ± 5.4	14.6 ± 1.2	14.6 ± 1.2
MS211	31.3 ± 6.4	32.1 ± 6.3	5.3 ± 1.5
MS212	32.1 ± 5.2	19.1 ± 4.2	24.1 ± 5.3
MS213	17.3 ± 4.5	8.1 ± 1.1	23.7 ± 6.3
MS214	53.6 ± 1.6*	52.2 ± 2.2*	55.0 ± 8.7*
MS215	17.2 ± 1.1	23.4 ± 1.1	22.1± 0.4
MS216	70.0 ± 1.3*	61.7 ± 5.0*	81.2 ± 0.8*
GBP	92.9 ± 7.1*	78.6 ± 7.1*	75.7 ± 3.1*

Each value represents the % reversal of allodynia (mean ± S.E.M.) of four rats; * denotes the values (≥ 50%), significantly different from their respective vehicle control at $p < 0.05$ (One-way ANOVA, followed by post-hoc Dunnett's test)

6.2.4 Peripheral Nerve Injury - PSNL

Table 6.9 Effect of [MS(201-216)] on spontaneous pain in PSNL model

Treatment	Spontaneous Pain		
	% Reversal in PSNL (Mean ± S.E.M.)		
	30 min	60 min	120 min
Vehicle	3.2 ± 0.3	2.9 ± 0.3	1.2 ± 0.1
MS201	21.1 ± 5.1	54.1 ± 4.1*	21.1 ± 3.5
MS202	10.6 ± 6.1	62.1 ± 6.1*	55.1 ± 3.9*
MS203	55.1 ± 6.8*	67.1 ± 5.6*	65.1 ± 9.3*
MS204	23.1 ± 4.5	76.2 ± 3.1*	78.1 ± 7.3*
MS205	51.4 ± 6.2*	59.1 ± 3.1*	56.7 ± 7.2*
MS206	28.9 ± 8.3	76.1 ± 7.2*	54.1 ± 5.4*
MS207	26.1 ± 5.3	20.2 ± 3.5	25.6 ± 5.2
MS208	30.2 ± 7.8	56.3 ± 5.1*	51.3 ± 4.1*
MS209	28.6 ± 4.1	31.2 ± 6.2	14.2 ± 5.2
MS210	12.2 ± 3.2	15.6 ± 1.3	15.1 ± 5.2
MS210	2.1 ± 0.2	23.1 ± 1.1	6.1 ± 1.0
MS212	21.2 ± 4.2	54.9 ± 3.1*	14.1 ± 5.4
MS213	21.1 ± 3.2	65.5 ± 6.2*	63.5 ± 3.2*
MS214	83.2 ± 1.1*	91.5 ± 1.2*	76.1 ± 1.2*
MS215	21.1 ± 1.2	24.1 ± 2.1	31.1 ± 2.1
MS216	91.1 ± 3.4*	88.3 ± 4.1*	56.7 ± 3.7*
GBP	92.9 ± 1.9*	94.2 ± 2.1*	82.4 ± 5.1*

Each value represents the % reversal of allodynia (mean ± S.E.M.) of four rats; * denotes the values (≥ 50%), significantly different from their respective vehicle control at $p < 0.05$ (One-way ANOVA, followed by post-hoc Dunnett's test)

Table 6.10 Antiallodynic effect of [MS(201-216)] against dynamic allodynia in PSNL model

Treatment	Dynamic Allodynia		
	% Reversal in PSNL (Mean ± S.E.M.)		
	30 min	60 min	120 min
Vehicle	4.7 ± 0.7	2.5 ± 1.2	0.8 ± 0.1
MS201	21.3 ± 3.1	16.5 ± 4.3	22.4 ± 3.4
MS202	9.1 ± 1.1	29.1 ± 4.3	2.4 ± 1.4
MS203	62.9 ± 8.3*	28.3 ± 4.3	26.2 ± 3.2
MS204	27.1± 4.1	59.2 ± 4.2*	55.2 ± 6.2*
MS205	24.1± 6.4	56.7 ± 2.1*	64.1 ± 5.8*
MS206	4.0 ± 2.4	57.4 ± 10.2*	51.1± 6.2*
MS207	26.1± 1.7	53.1± 2.0*	52.4 ± 8.7*
MS208	24.9 ± 6.8	56.1± 7.8*	22.1 ± 7.8
MS209	18.5 ± 4.1	21.3 ± 2.3	24.9 ± 4.5
MS210	14.4 ± 3.6	16.1 ± 3.2	4.4 ± 3.6
MS211	23.1 ± 4.1	32.1± 2.1	13.1 ± 3.2
MS212	23.4 ± 4.1	21.2 ± 6.1	14.2 ± 2.1
MS213	29.2 ± 3.1	53.2 ± 4.3*	63.8 ± 3.1*
MS214	55.1 ± 6.5*	79.9 ± 3.2 *	63.5 ± 3.2*
MS215	23.0 ± 4.3	12.1± 4.1	13.1 ± 2.1
MS216	71.1 ± 4.1*	56.4 ± 8.2*	55.1 ± 4.3*
GBP	43.1 ± 2.5	56.1 ± 2.3*	58.5 ± 6.1*

Each value represents the % reversal of allodynia (mean ± S.E.M.) of four rats; * denotes the values (≥ 50%), significantly different from their respective vehicle control at $p < 0.05$ (One-way ANOVA, followed by post-hoc Dunnett's test)

Table 6.11 Antiallodynic effect of [MS(201-216)] against cold allodynia in PSNL model

Treatment	Cold Allodynia		
	% Reversal in PSNL (Mean ± S.E.M.)		
	30 min	60 min	120 min
Vehicle	4.1 ± 1.0	2.5 ± 0.3	1.9 ± 0.5
MS201	13.2 ± 2.1	16.2 ± 2.1	13.1± 1.1
MS202	9.2 ± 4.3	14.1 ± 6.2	12.5 ± 2.1
MS203	16.2 ± 1.9	55.1 ± 4.1*	53.1 ± 6.3*
MS204	51.1 ± 7.0*	77.2 ± 9.0*	55.1 ± 1.2*
MS205	21.3 ± 5.1	71.2 ± 3.2*	75.3 ± 6.7 *
MS206	55.2 ± 8.2*	52.3 ± 4.5*	55.1 ± 5.1*
MS207	3.1 ± 1.2	28.9 ± 5.1	25.1 ± 8.3
MS208	4.8 ± 2.1	26.1 ± 4.1	23.1 ± 2.1
MS209	11.2 ± 1.1	21.9 ± 3.2	15.3 ± 2.1
MS210	51.8 ± 4.3*	14.3 ± 3.1	11.2 ± 4.1
MS211	21.8 ± 4.4	12.7 ± 5.1	7.7 ± 1.0
MS212	51.4 ± 2.1*	15.4 ± 5.1	14.3 ± 3.1
MS213	21.1 ± 9.2	62.6 ± 4.2*	55.1 ± 4.1*
MS214	75.2 ± 6.1*	87.7 ± 5.3*	63.4 ± 5.5*
MS215	2.1 ± 1.2	12.7 ± 1.2	21.3 ± 2.2
MS216	75.1 ± 8.2*	91.1 ± 2.1*	70.5 ± 3.1*
GBP	54.1 ± 4.3*	58.2 ± 5.1*	32.1 ± 1.4

Each value represents the % reversal of allodynia (mean ± S.E.M.) of four rats; * denotes the values (≥ 50%), significantly different from their respective vehicle control at $p < 0.05$ (One-way ANOVA, followed by post-hoc Dunnett's test)

Table 6.12 Antihyperalgesic effect of [MS(201-216)] in PSNL model

Treatment	Mechanical Hyperalgesia		
	% Reversal in PSNL (Mean ± S.E.M.)		
	30 min	60 min	120 min
Vehicle	2.9 ± 0.3	2.8 ± 0.3	2.9 ± 0.3
MS201	21.1 ± 2.9	28.9 ± 4.1	23.1 ± 3.1
MS202	24.8 ± 1.2	12.1 ± 2.1	10.9 ± 2.1
MS203	12.6 ± 4.1	64.2 ± 7.2*	71.2 ± 5.1*
MS204	24.7 ± 4.2	65.4 ± 3.1*	53.1 ± 8.2*
MS205	28.1 ± 3.1	53.2 ± 4.5*	43.9 ± 5.1
MS206	53.1 ± 3.7*	71.3 ± 6.2*	51.2 ± 4.1*
MS207	21.1 ± 7.3	22.9 ± 6.1	9.8 ± 2.1
MS208	11.2 ± 2.1	27.1 ± 2.1	3.1 ± 8.0
MS209	54.1 ± 7.1*	11.2 ± 5.1	19.1 ± 2.2
MS210	12.1 ± 4.1	16.1 ± 5.3	21.3 ± 4.2
MS211	31.9 ± 6.1	13.1 ± 5.2	26.2 ± 6.1
MS212	61.1 ± 4.2*	12.5 ± 8.3	2.3 ± 6.2
MS213	12.1 ± 5.4	11.1± 7.2	9.2 ± 5.4
MS214	64.1 ± 2.3*	75.2 ± 4.2*	81.0 ± 5.2*
MS215	21.6 ± 3.1	29.6 ± 6.9	15.1 ± 4.1
MS216	67.1 ± 6.1*	51.7 ± 9.6	79.0 ± 5.8 *
GBP	86.2 ± 2.1*	91.3 ± 5.2*	55.8 ± 3.8*

Each value represents the % reversal of allodynia (mean ± S.E.M.) of four rats; * denotes the values (≥ 50%), significantly different from their respective vehicle control at $p < 0.05$ (One-way ANOVA, followed by post-hoc Dunnett's test)

Table 6.13 Median effective dose (ED_{50}) of selected MS2XX compounds in CCI model

Treatment	ED_{50} values (mg/kg) in CCI model (TPE in min)			
	Spontaneous pain	Dynamic allodynia	Cold allodynia	Mechanical hyperalgesia
MS214	34.1 (60)	18.2 (120)	42.7 (60)	26.3 (60)
MS216	21.8 (60)	24.2 (30)	54.3 (60)	41.3 (120)

Table shows the ED_{50} values (mg/kg) in CCI model calculated at time of peak effect (TPE in min)

Table 6.14 Median effective dose (ED_{50}) of selected MS2XX compounds in PSNL model

Treatment	ED_{50} values (mg/kg) in PSNL model (TPE in min)			
	Spontaneous pain	Dynamic allodynia	Cold allodynia	Mechanical hyperalgesia
MS214	15.1 (60)	41.1 (60)	57.1 (60)	65.1 (60)
MS216	21.6 (30)	43.2 (30)	38.2 (60)	55.5 (120)

Table shows the ED_{50} values (mg/kg) in PSNL model calculated at time of peak effect (TPE in min)

6.2.5 Efficacy in Carrageenan Induced Paw Edema and TNF-α Quantification

Table 6.15 Effect of MS2XX compounds on carrageenan induced paw edema

Treatment	Change in paw volume (mL) Mean ± S.E.M.			(%) Protection		
	60 min	120 min	180 min	60 min	120 min	180 min
Vehicle	0.23 ± 0.12	0.43 ± 0.12	0.67 ± 0.12	-	-	-
MS214	0.19 ± 0.05	0.38 ± 0.21	0.36 ± 0.09	17.4	11.8	46.7*
MS216	0.08 ± 0.04	0.07 ± 0.03	0.11 ± 0.01	67.4*	83.5*	84.2*
Indomethacin	0.12 ± 0.05	0.17 ± 0.12	0.22 ± 0.11	52.2*	61.2*	66.9*

Table shows the change in paw volume (mL) after 1% carrageenan. * represents significance at $p<0.05$ compared to vehicle (One way ANOVA followed by Dunnett's Test, n=6). Indomethacin was tested at the dose of 10 mg/kg *i.p.*

Table 6.16 Effect of compounds on TNF-α level

Treatment	TNF-α (pg/ml)	% inhibition of TNF-α production
Vehicle	3175.5 ± 161.6	-
MS214	2867.0 ± 137.4	14.1 ± 4.1
MS216	2845.4 ± 139.1	14.7 ± 4.2

Table shows the concentration of TNF-α in the paw of carrageenan treated animals. * represents the significance at $p<0.05$, compared to vehicle control (One way ANOVA followed by Dunnett's test, n=4). All the compounds were tested at the dose of 100 mg/kg *i.p.*

Table 6.17 Effect of MS2XX compounds on nitric oxide in brain and sciatic nerve

Total Nitrate/Nitrite (% of SHAM control)				
Treatment	**Brain**	**Sciatic Nerve**	**% Inhibition of Nitrosative stress (nitrite)[a]**	
			Brain	**Sciatic nerve**
SHAM	100.0 ± 7.8	100.0 ± 3.9	-	-
Vehicle	194.3 ± 15.3	193.7 ± 8.4	-	-
MS214	179.9 ± 3.8	175.8 ± 4.7	15.2	19.0
MS216	176.5 ± 3.98	156.1 ± 5.8	18.9	50.1*

Table shows the concentration of nitric oxide in brain and sciatic nerve after CCI in rats. * represents the significance at $p<0.05$, compared to vehicle control (One way ANOVA followed by Dunnett's test, n=4). All the compounds were tested at the dose of 100 mg/kg *i.p.*

6.2.7 DPPH Scavenging Assay

Table 6.18 DPPH scavenging activity of MS2XX compounds

Compound	IC_{50} (μM)
MS214	254
MS216	213
Curcumin	135

DPPH radical scavenging activity of test compounds. Values are represented as % scavenging comparedto vehicle, calculated from the average of triplicate experiments

6.2.8 Effect of Compounds on Cannabinoid Receptors

Table 6.19 Effect of MS2XX compounds on cannabinoid receptors

% Replacement of Specific Bound ^{3}H [CP 55,940] on CB_1 receptor by test compounds	
Treatment	**IC_{50}**
MS214	>1 μM
MS216	>1 μM
% Replacement of Specific Bound ^{3}H [CP 55,940] on CB_2 receptor by test compounds	
Treatment	**IC_{50}**
MS214	>1 μM
MS216	>1 μM

Equilibrium-competition binding of compounds vs. [^{3}H] CP55940 using either rat brain (CB_1) or rat spleen homogenates (CB_2). The data shown are average of triplicates

6.2.9 Effect of Compounds on Cathepsin S Enzyme

Table 6.20 Effect of compounds on cathepsin S enzyme

Treatment	% inhibition
Vehicle	-
MS214	38.5 ± 4.1
MS216	12.1 ± 1.2

Inhibition of recombinant human Cathepsin S by test compounds (50 μM) in a fluorescence assay, employing Z-Leu-Leu-Arg-MCA as synthetic substrates. Data represent means of two experiments performed in triplicate

6.2.10 Effect on GABAergic Pathway

Table 6.21 Picrotoxin induced epilepsy (scPIC) model

Treatment	Antiepileptic activity (scPIC)	
	30 min	**240 min**
Vehicle	-	-
MS214	-	-
MS216	-	-
Diazepam	10	10

The figures in the table indicate the minimum dose whereby bioactivity was demonstrated in half or more of the mice (n=3). The animals were examined 30 min and 240 min. The line (-) indicates an absence of anticonvulsant activity at the maximum dose tested

6.3 Results and Discussion

6.3.1 Chemistry

A four-step process was carried out to synthesize tetrahydropyrido-pyrimidines in yields ranging between 61% to 82% (Table-6.1). The homogeneity of the compounds was monitored by performing TLC. The eluant system for all the compounds was DCM:CH_3OH (9.5:0.5). The assignments of structures were based on elemental and spectroscopic methods and the chemical shifts obtained from ^{1}H-NMR spectra supported the proposed structures. In general, the hydrogens of tetrahydro-pyridine scaffold resonated from δ~2.35-4.62 ppm in the NMR spectrum. The CO-NH proton resonated at δ~9.11-9.61 ppm. The singlet of the CO-NH proton was D_2O exchangeable. The percentage composition of C, H, N of all the compounds found from elemental analyses were within ± 0.4 % of the theoretical values (Table-6.2).

6.3.2 Efficacy in Acute Pain Models

In acetic acid test, all of the compounds except **MS206**, **MS207** and **MS213** suppressed the acetic acid-induced writhing response significantly ($p<0.05$) in comparison to vehicle control (Table-6.3). Compounds **MS214** and **MS216** exhibited inhibition of 70.0% or above. **MS214** was the most active compound with 75.4% inhibition.

Formalin-induced pain in phase-I was reduced by compounds **MS206** and **MS213** with 53% and 43.4% inhibition respectively (Table-6.4). In Phase-II, all the tested compounds except **MS202**, **MS203**, **MS205**, **MS207** and **MS213** showed efficacy. More than 70.0% inhibition was exhibited by compounds **MS210**, **MS214** and **MS216**. Maximum of 80.2% reduction was found with compound **MS216**, which was more efficacious than Indomethacin (72.1% at the dose of 10 mg/kg).

6.3.3 Efficacy in Neuropathic Pain Models (CCI and PSNL)

In the CCI model, compounds **MS203**, **MS204**, **MS213**, **MS214** and **MS216** completely reversed the spontaneous pain response throughout the time period of testing (30-120 min) similar to gabapentin. Compounds **MS201**, **MS202**, **MS205**, **MS206** and **MS212** exhibited activity between 60-120 min. The onset of action of compound **MS208** was at 120 min of the experiment. Other compounds were ineffective in this test (Table 6.5).

Two compounds **MS214** and **MS216** were active in attenuating the dynamic allodynia throughout the 120 min of experiment. The onset of action of compounds **MS204**, **MS206** and **MS212** was at 60 min like gabapentin. The duration of action of **MS203** and **MS215** was only up to 30 min, whereas for **MS213** was up to 60 min. All other compounds were ineffective in this test (Table 6.6).

In the cold allodynia produced in CCI rats, significant reversal of paw withdrawal durations was observed at all time points after the administration of compounds **MS203**, **MS204**, **MS205**, **MS213**, **MS214** and **MS216**. The onset of action for compounds **MS206** and **MS212** was at 60 min. Other compounds were found to be ineffective in the nociceptive assay. Gabapentin was effective only at 30 min (Table 6.7).

Mechanical hyperalgesia was significantly attenuated at all the time points by **MS214** and **MS216** similar to gabapentin. The onset of action of compounds **MS203** and **MS206** was at 60 min. The compounds **MS204**, **MS205** and **MS209** were active only at first 30 min. Overall, it appears that, in the CCI model of neuropathic pain, compounds that showed promising results include **MS203**, **MS204**, **MS206**, **MS214** and **MS216** effective in four tests, **MS205**, **MS212** and **MS213** in three tests and **MS201**, **MS202**, **MS108**, **MS109** and **MS115** active in two tests (Table 6.8).

In the PSNL model, the paw withdrawal durations due to spontaneous ongoing pain were significantly reduced by compounds **MS203**, **MS205**, **MS214** and **MS216** throughout the experiment similar to gabapentin. The onset of action for compounds **MS202**, **MS204**, **MS206**, **MS208** and **MS213** was at 60 min. **MS201** and **MS212** exhibited efficacy only at 60 min (Table 6.9).

The dynamic allodynia produced in PSNL model was effectively reversed by compounds **MS214** and **MS216** at all the time points. Compounds **MS204**, **MS205**, **MS206**, **MS207** and **MS213** showed efficacy between 60-120 min like gabapentin. Compound **MS203** was only effective at 30 min. **MS208** exhibited irregular activity pattern, being effective at only one time point (60 min) (Table 6.10).

Cold allodynia produced in PSNL model was completely reversed by the compounds **MS204**, **MS206**, **MS214** and **MS216**. Compounds **MS210** and **MS212** were effective only at 30 min of the experiment. The onset of action for compounds **MS203**, **MS205** and **MS213** was at 60 min (Table 6.11).

Compounds **MS206**, **MS214** and **MS216** significantly reversed mechanical hyperalgesia at all the time points like gabapentin. Compounds **MS209** and **MS212** were effective in the first 30 min of the experiment whereas compounds **MS203** and **MS204** were effective from 60 to 120 min (Table 6.12).

Overall, it appears that in PSNL model, compounds that exhibited promising results were **MS203**, **MS204**, **MS205**, **MS206**, **MS214** and **MS216** effective in four tests, **MS212** and **MS213** effective in three tests and **MS208** effective in two tests.

6.3.4 Structure-Activity Relationships

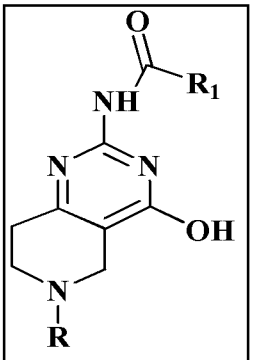

MS201-MS216

A closer look of the structure-activity relationships revealed that in general, isonicotinyl substitution (**MS204**, **MS208**, **MS212** and **MS216)** resulted in attenuation of one or more nociceptive assays in both CCI and PSNL animals. 4-nitrophenyl substitution also proved to be additive to the antinociceptive efficacies (**MS202**, **MS206**, **MS210** and **MS214)** in both CCI and PSNL animals. Aliphatic substituent (2-propylpentanyl) in **MS201**, **MS205**, **MS209** and **MS213** resulted in comparatively moderate attenuation of nociceptive parameters in neuropathic animals. However, 4-phenoxyphenyl substitution (**MS203**, **MS207**, **MS211** and **MS215)** proved to be detrimental for the efficacy. The general trend of antinociceptive efficacy followed by the tetrahydropyrido-pyrimidine derivatives in terms of the R_1 substitution was: isonicotinyl > 4-nitrophenyl > 2-propylpentanyl > 4-phenoxyphenyl substitution.

N-alkyaltion of the tetrahydropyrimidine moiety resulted in compounds with varied antinociceptive efficacy. The order of bioactivity of the N-substituted tetrahydropyrido-pyrimidine derivatives in terms of the R substitution was 4-methylbenzsulfonyl > 4-methyl benzoyl > 2,6-dimethylphenyl > ethyl.

6.3.5 ED_{50} Studies

Compounds exhibiting more than 90% reversal in one or more of the nociceptive assays (**MS214** and **MS216**) were taken further for ED_{50} studies. In the CCI model, compound **MS216** reversed spontaneous pain with an ED_{50} value of 21.8 mg/kg with the TPE at 60 min. Compound **MS214** reversed dynamic and cold allodynia with an ED_{50} value of 18.2 mg/kg and 42.7 mg/kg and TPE at 120 min and 60 min respectively. Compound **MS214** reversed mechanical hyperalgesia with an ED_{50} value of 26.3 mg/kg, TPE being at 60 min (Table-6.13). In the PSNL model, compound **MS214** reversed spontaneous pain and dynamic allodynia with an ED_{50} value of 15.1 mg/kg and 41.1 mg/kg both exhibiting TPE at 60 min respectively. In cold allodynia and mechanical hyperalgesia, compound **MS216** emerged as the most effective compound with an ED_{50} value of 38.2 mg/kg and 55.5 mg/kg with TPE at 60 and 120 min respectively (Table-6.14).

6.3.6 Mechanistic Studies

The anti-inflammatory profile of the selected compounds (**MS214** and **MS216**) as evidenced in formalin-induced flinching test was investigated in the carrageenan induced paw edema model. **MS216** showed a significant reduction in paw edema throughout the period of 180 min, whereas compound **MS214** showed 46.7% inhibition at 180 min (Table-6.15). However, none of the two compounds exhibited TNF-α inhibition in this model (Table-6.16).

Following nerve injury, subsequent generation of free radicals leads to oxidative and nitrosative stress which exaggerates pain states. The putative role of nitric oxide (NO) in the pathophysiology of chronic nerve ligation as evident by significant increase in nitrite and nitrate levels in both brain and sciatic nerve led us to estimate the levels of nitrite, a metabolite of NO in brain and sciatic nerve of CCI rats. **MS216** exhibited significant reduction ($p<0.05$) of nitric oxide in sciatic nerve. None of the compounds significantly attenuated nitrosative stress in the brain suggesting the specific inhibition of peripheral nitric oxide (Table-6.17). The free radical scavenging abilities of the compounds (**MS214** and **MS216**) were assessed using DPPH method. **MS214** exhibited IC_{50} value of 254 μM whereas IC_{50} value of 213 μM was observed with **MS216** (Table 6.18).

Compounds **MS214** and **MS216** were studied for their affinity for cannabinoid receptors However, the compounds exhibited no efficacy at 1 μM for both CB_1 and CB_2 receptors (Table-6.19). The compounds were also tested for any inhibition of cathepsin S, a promising target in the treatment of neuropathic pain. **MS214** was found to exhibit inhibition of cathepsin S (38.5%) (Table-6.20). The possible mediation of GABAergic pathway was explored by assessing the anticonvulsant potential of the test compounds in picrotoxin-induced seizure. However, none of the compounds exhibited significant protection in the picrotoxin induced epilepsy indicating no mediation of GABAergic pathways (Table-6.20).

To conclude, in the present series, 16 novel tetrahydropyrido-pyrimidine derivatives were synthesized and assessed for acute antinociceptive, antiallodynic and antihyperalgesic potential. In acute models of pain, significant inhibition of acetic acid-induced writhings by 13 compounds established their role as peripherally acting analgesics. Also, significant suppression of phase-I by 2 compounds and phase-II of the formalin test by 11 compounds suggested possible modulation of anti-inflammatory pathways. **MS216** significantly reduced edema in carrageenan induced paw edema model at all the time points. Additionally, **MS216** was found to significantly attenuate nitric oxide locally in the sciatic nerve. None of the two compounds inhibited TNF-α. There was no evidence for the mediation of cannabinergic and GABAergic pathways by the compounds.

CHAPTER 7

SERIES III - 1,2,4-TRIAZOL-5-ONES

7.1 Chemistry

7.1.1 Rationale of Design

Triazole nucleus has been well documented to possess wide spectrum of biological activities including anti-microbial [242], anticonvulsant [203], anti-inflammatory [243] and analgesic [244] activities. In recent years, triazole motif has gained a considerable attention against neuropathic pain acting through various targets. Many triazole based P_2X_7 antagonists [188], opioid agonist [189] and sodium channel blockers [190] and sigma receptor inhibitors [185] have been reported.

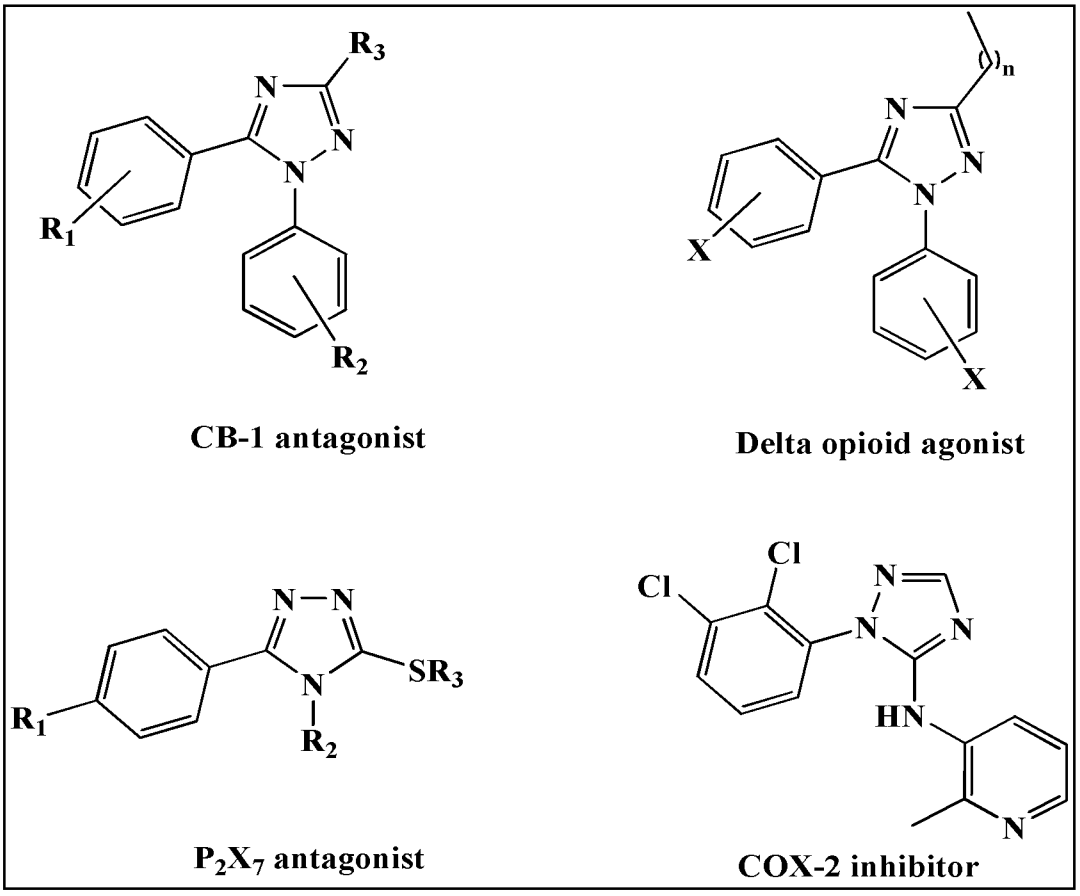

Literature also reveals many 1,2,4-triazole based cannabinoid modulators [245] possessing anti-nociceptive efficacies. In view of the above reports several 1,2,4-triazol-5-ones were synthesized employing hybrid pharmacopohore based design. The triazole ring is also an important isostere of imidazole, oxazole, pyrazole, thiazole, amide moiety in designing various types of new drug molecules. More and more

triazole derivatives, with strong pharmacological activity, low toxicity, less adverse effects, fewer multi-drug resistances, high bioavailability, good pharmacokinetic property and drug-targeting, diversity of drug administration, broad spectrum, better curative effect etc., have been frequently becoming clinical drugs or candidates for the treatment of various types of diseases [184-195].

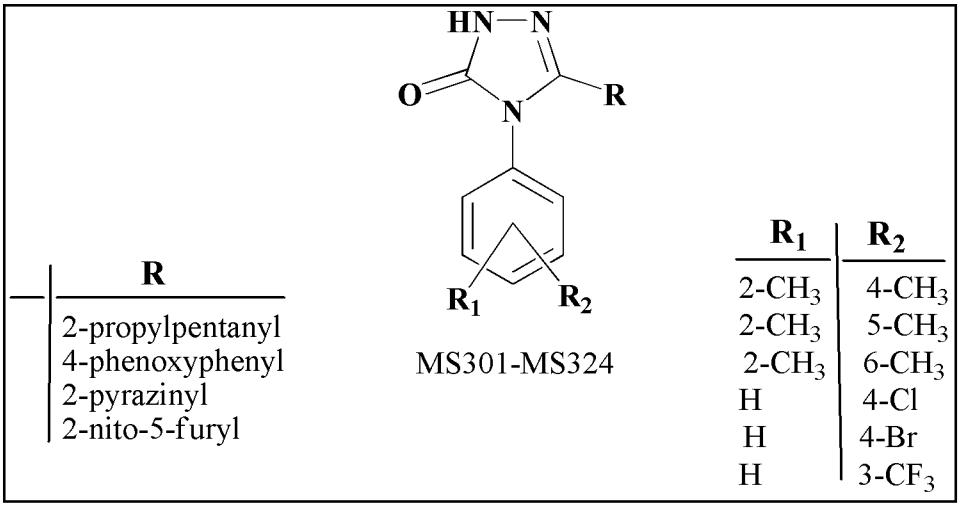

R
2-propylpentanyl
4-phenoxyphenyl
2-pyrazinyl
2-nito-5-furyl

R_1	R_2
2-CH_3	4-CH_3
2-CH_3	5-CH_3
2-CH_3	6-CH_3
H	4-Cl
H	4-Br
H	3-CF_3

7.1.2 Synthesis

Step-1: Synthesis of substituted N-phenylhydrazine-carboxamides

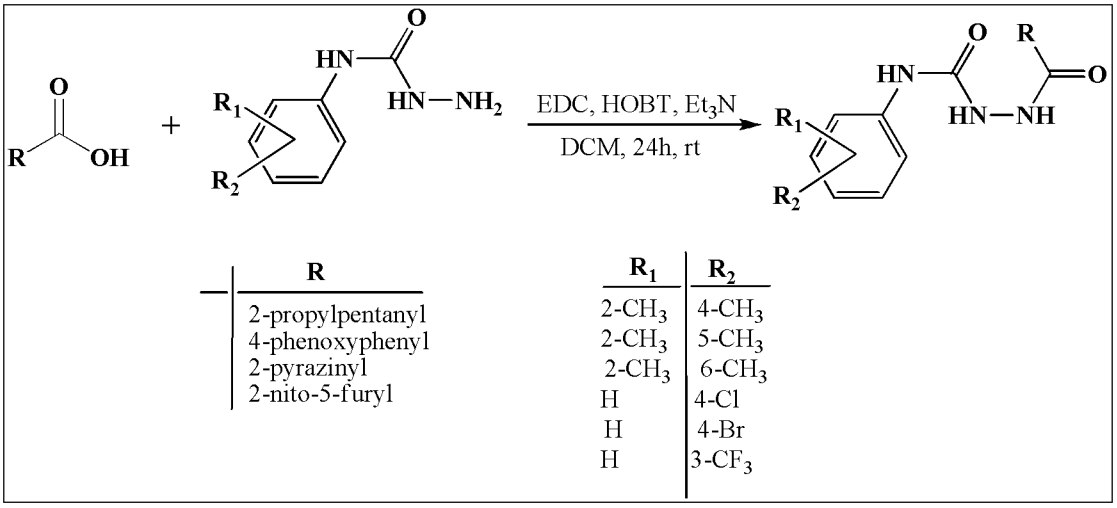

R
2-propylpentanyl
4-phenoxyphenyl
2-pyrazinyl
2-nito-5-furyl

R_1	R_2
2-CH_3	4-CH_3
2-CH_3	5-CH_3
2-CH_3	6-CH_3
H	4-Cl
H	4-Br
H	3-CF_3

Various substituted acids (1.0 equiv.) and substituted phenyl semicarbazides (1.0 equiv.) were taken in DCM followed by addition of triethylamine (1.1 equiv.), 1-ethyl-3-[3-(dimethylamino)propyl]carbodiimide hydrochloride (EDC) (1.1 equiv.) and 1-hydroxybenzotriazole (HOBT) (1.1 equiv.) at 0°C. The reaction mixture was stirred at room temperature overnight. Following completion, the reaction mixture was washed with saturated aqueous sodium bicarbonate and brine. The organic layer

was collected, dried over anhydrous sodium sulphate, filtered, and evaporated *in vacuo* to give the product in 78-85% yield.

Step-2: Synthesis of substituted 1,2,4-triazol-5-ones

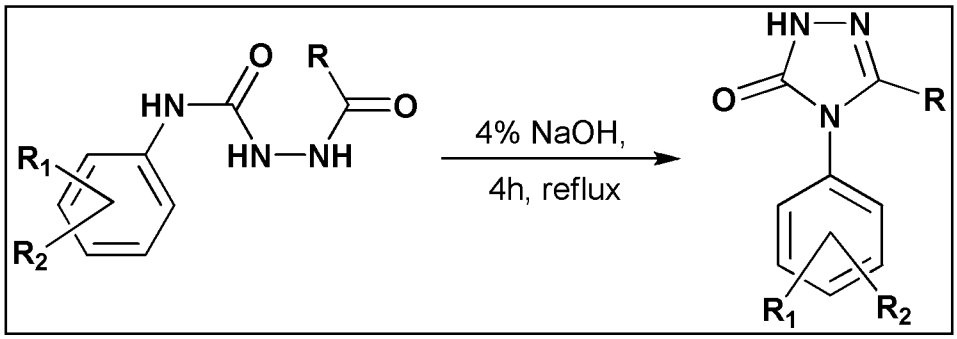

0.05M of the synthesized hydrazine-carboxamide from step-1 was taken in 4% w/v aqueous sodium hydroxide and heated on water bath for 3-4 h. After the completion of the reaction, the mixture was allowed to cool and then filtered. The filtrate was acidied with 2.0M hydrochloric acid. The precipitated solid was filtered, washed thoroughly with water, dried and recrystallized from ethanol/water.

Table 7.1 Physical data of 1,2,4-triazol-5-ones

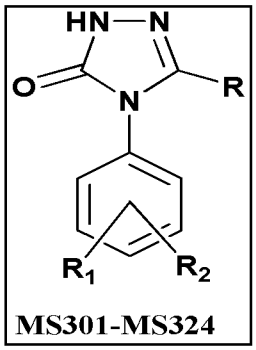

MS301-MS324

Compound	R	R_1	R_2	M.F.	M.W.	Yield (%)	M.P. (°C)
MS301	2-propylpentanyl	2-CH_3	4-CH_3	$C_{17}H_{25}N_3O$	287.40	78	112
MS302	2-propylpentanyl	2-CH_3	5-CH_3	$C_{17}H_{25}N_3O$	287.40	79	131
MS303	2-propylpentanyl	2-CH_3	6-CH_3	$C_{17}H_{25}N_3O$	287.40	78	129
MS304	2-propylpentanyl	H	4-Cl	$C_{15}H_{20}ClN_3O$	293.79	81	132
MS305	2-propylpentanyl	H	4-Br	$C_{15}H_{20}BrN_3O$	338.24	85	160
MS306	2-propylpentanyl	H	3-CF_3	$C_{16}H_{20}F_3N_3O$	327.34	88	128
MS307	4-phenoxyphenyl	2-CH_3	4-CH_3	$C_{22}H_{19}N_3O_2$	357.41	87	188
MS308	4-phenoxyphenyl	2-CH_3	5-CH_3	$C_{22}H_{19}N_3O_2$	357.41	84	173
MS309	4-phenoxyphenyl	2-CH_3	6-CH_3	$C_{22}H_{19}N_3O_2$	357.41	79	179
MS310	4-phenoxyphenyl	H	4-Cl	$C_{20}H_{14}ClN_3O_2$	363.80	78	191
MS311	4-phenoxyphenyl	H	4-Br	$C_{20}H_{14}BrN_3O_2$	408.25	85	213
MS312	4-phenoxyphenyl	H	3-CF_3	$C_{21}H_{14}F_3N_3O_2$	397.35	85	195
MS313	2-pyrazinyl	2-CH_3	4-CH_3	$C_{14}H_{13}N_5O$	267.29	82	167
MS314	2-pyrazinyl	2-CH_3	5-CH_3	$C_{14}H_{13}N_5O$	267.29	71	172
MS315	2-pyrazinyl	2-CH_3	6-CH_3	$C_{14}H_{13}N_5O$	267.29	72	165
MS316	2-pyrazinyl	H	4-Cl	$C_{12}H_8ClN_5O$	273.68	78	187
MS317	2-pyrazinyl	H	4-Br	$C_{12}H_8BrN_5O$	318.13	81	201
MS318	2-pyrazinyl	H	3-CF_3	$C_{13}H_8F_3N_5O$	307.23	76	176
MS319	2-nito-5-furyl	2-CH_3	4-CH_3	$C_{14}H_{12}N_4O_4$	300.27	71	173
MS320	2-nito-5-furyl	2-CH_3	5-CH_3	$C_{14}H_{12}N_4O_4$	300.27	81	178
MS321	2-nito-5-furyl	2-CH_3	6-CH_3	$C_{14}H_{12}N_4O_4$	300.27	76	174
MS322	2-nito-5-furyl	H	4-Cl	$C_{12}H_7ClN_4O_4$	306.66	86	181
MS323	2-nito-5-furyl	H	4-Br	$C_{12}H_7BrN_4O_4$	351.11	82	209
MS324	2-nito-5-furyl	H	3-CF_3	$C_{13}H_7F_3N_4O_4$	354.49	87	192

Table 7.2 Spectral and elemental analyses data of 1,2,4-triazol-5-ones

Compound	^{1}H-NMR (δ ppm, DMSO-d_6)	Elemental Analyses (Calculated/Found)[a]			Mass Spectroscopy (m/z)
		C (%)	H (%)	N (%)	
MS301	δ 0.84-0.92 (m, 6H), 1.43-1.55 (m, 9H), 2.21 (s, 3H), 2.43 (s, 3H), 7.12-7.27 (m, 2H), 7.69 (d, 1H), 8.01 (s, 1H, D_2O exchangeable)	71.04 71.06	8.77 8.78	14.62 14.64	288.20
MS302	δ 0.83-0.98 (m, 6H), 1.34-1.47 (m, 9H), 2.21 (s, 3H), 2.44 (s, 3H), 7.18-7.21 (m, 2H), 7.73 (s, 1H), 8.13 (s, 1H, D_2O exchangeable)	71.04 71.06	8.77 8.79	14.62 14.64	288.20
MS303	δ 0.82-0.98 (m, 6H), 1.44-1.55 (m, 5H), 2.45 (s, 6H), 7.16-7.21 (m, 3H), 7.98 (s, 1H, D_2O exchangeable)	71.04 71.06	8.77 8.79	14.62 14.64	288.20
MS304	δ 0.82-0.98 (m, 6H), 1.34-1.46 (m, 9H), 7.50-7.59 (m, 4H), 8.05 (s, 1H, D_2O exchangeable)	61.32 61.34	6.86 6.88	14.30 14.32	295.13
MS305	δ 0.81-0.96 (m, 6H), 1.32-1.51(m, 9H), 7.63 (d, 2H), 8.42 (s, 1H, D_2O exchangeable), 8.55 (d, 2H)	53.26 53.23	5.96 5.96	12.42 12.40	339.08
MS306	δ 0.82-0.96 (m, 6H), 1.33-1.47(m, 9H), 7.46-7.59 (m, 3H), 8.17 (s, 1H), 8.02 (s, 1H, D_2O exchangeable)	58.71 58.70	6.16 6.17	12.84 12.85	328.16
MS307	δ 2.13 (s, 3H), 2.43 (s, 3H), 7.12-7.28 (m, 7H), 7.53-7.57 (m, 2H), 7.62-7.71 (m, 3H), 8.11 (s, 1H, D_2O exchangeable)	73.93 73.95	5.36 5.37	11.76 11.77	358.15
MS308	δ 2.14 (s, 3H), 2.45 (s, 3H), 6.91 (d, 1H), 7.09-7.18 (m, 6H), 7.41-7.49 (m, 2H), 7.54-7.59 (m, 2H), 7.78 (s, 1H), 8.13 (s, 1H, D_2O exchangeable)	73.93 73.94	5.36 5.37	11.76 11.77	358.15
MS309	δ 2.13 (s, 6H), 7.21-7.28 (m, 8H), 7.42-7.49 (m, 2H), 7.52-7.59 (m, 2H), 8.01 (s, 1H, D_2O exchangeable)	73.93 73.95	5.36 5.34	11.76 11.78	358.15
MS310	δ 7.19-7.32 (m, 5H), 7.44-7.73 (m, 8H), 8.11 (s, 1H, D_2O exchangeable)	66.03 66.04	3.88 3.89	11.55 11.56	365.07
MS311	δ 7.18-7.29 (m, 5H), 7.42-7.68 (m, 6H), 8.13 (s, 1H, D_2O exchangeable), 8.76 (d, 2H)	58.84 58.85	3.46 3.46	10.29 10.23	409.02
MS312	δ 7.12-7.28 (m, 5H), 7.41-7.62 (m, 7H), 8.12 (s, 1H), 8.23 (s, 1H, D_2O exchangeable)	63.48 63.49	3.55 3.56	10.58 10.59	398.11

MS313	δ 2.21 (s, 3H), 2.43 (s, 3H), 7.10-7.23 (m, 2H), 7.54 (d, 1H), 8.08 (s, 1H, D_2O exchangeable), 8.71 (s, 2H), 8.93 (s, 1H)	62.91 62.92	4.90 4.92	26.20 26.22	268.12
MS314	δ 2.23 (s, 3H), 2.42 (s, 3H), 6.94-7.16 (m, 2H), 7.62 (d, 1H), 8.34 (s, 1H, D_2O exchangeable), 8.72 (s, 2H), 8.92 (s, 1H)	62.91 62.92	4.90 4.91	26.20 26.22	268.12
MS315	δ 2.44 (s, 6H), 7.16-7.19 (m, 3H), 8.11 (s, 1H, D_2O exchangeable), 8.76 (s, 2H), 8.93 (s, 1H)	62.91 62.92	4.90 4.91	26.20 26.22	268.12
MS316	δ 7.51-7.59 (m, 4H), 8.21 (s, 1H, D_2O exchangeable), 8.73 (s, 2H), 8.95 (s, 1H)	52.66 52.66	2.95 2.94	25.59 25.58	275.04
MS317	δ 7.62 (d, 2H), 8.11 (s, 1H, D_2O exchangeable), 8.73-8.82 (m, 4H), 8.96 (s, 1H)	45.31 45.32	2.53 2.54	22.01 22.03	318.99
MS318	δ 7.38-7.44 (m, 3H), 8.14 (s, 1H), 8.42 (s, 1H, D_2O exchangeable), 8.73 (s, 2H), 8.94 (s, 1H)	50.82 50.80	2.62 2.63	22.80 22.82	308.07
MS319	δ 2.21 (s, 3H), 2.43 (s, 3H), 7.12-7.21 (m, 3H), 7.64-7.72 (m, 2H), 7.92 (s, 1H, D_2O exchangeable)	56.00 56.02	4.03 4.05	18.66 18.66	301.09
MS320	δ 2.21 (s, 3H), 2.41 (s, 3H), 7.14 (d, 1H), 7.21-7.28 (m, 2H), 7.71-7.82 (m, 2H), 8.12 (s, 1H, D_2O exchangeable)	56.00 56.01	4.03 4.04	18.66 18.67	301.09
MS321	δ : 2.14 (s, 6H), 7.16-7.21 (m, 3H), 7.63-7.74 (m, 2H), 8.22 (s, 1H, D_2O exchangeable)	56.00 56.01	4.03 4.04	18.66 18.68	301.09
MS322	δ 7.17 (d, 1H), 7.51-7.58 (m, 4H), 7.65 (d, 1H), 7.73 (s, 1H, D_2O exchangeable)	47.00 47.05	2.30 2.32	18.27 18.26	308.01
MS323	δ 7.15 (d, 1H), 7.63-7.71 (m, 3H), 8.01 (s, 1H, D_2O exchangeable), 8.75 (m, 2H)	41.05 41.06	2.01 2.03	15.96 15.94	351.96
MS324	δ 7.14 (d, 1H), 7.34-7.51 (m, 3H), 7.62 (d, 1H), 7.92 (s, 1H, D_2O exchangeable), 8.11 (s, 1H)	45.89 45.90	2.07 2.08	16.47 16.44	341.05

Elemental analyses for C, H, N were within ± 0.4 % of the theoretical values

7.2 Pharmacology

7.2.1 Acetic Acid Induced Writhing

Table 7.3 Neurotoxicity and Effect of [MS(301-324)] on writhing induced by acetic acid in mice

Treatment	Neurotoxicity[a]		Acetic Acid Induced Writhing[b]	
	0.5 h	4 h	Number of writhes (30 min)	% Inhibition
Vehicle	-	-	53.0 ± 3.5	-
MS301	-	-	44.2 ± 1.2	16.8
MS302	-	-	12.1 ± 4.2	77.4*
MS303	-	-	4.3 ± 1.7	91.9*
MS304	-	-	11.0 ± 4.2	92.3*
MS305	-	-	27.4 ± 3.1	48.2*
MS306	-	-	39.9 ± 6.3	24.6
MS307	-	-	17.7 ± 3.8	66.9*
MS308	-	-	32.5 ± 8.1	38.7*
MS309	-	-	15.0 ± 3.5	71.7*
MS310	-	-	4.8 ± 1.7	90.2*
MS311	-	-	38.5 ± 3.1	27.4
MS312	-	-	32.0 ± 0.7	39.6
MS313	-	-	25.0 ± 4.2	52.8*
MS314	-	-	21.5 ± 3.1	59.4*
MS315	-	-	4.2 ± 2.4	91.8*
MS316	-	-	3.7 ± 0.3	92.1*
MS317	-	-	20.5 ± 4.6	61.3*
MS318	-	-	13.5 ± 2.4	74.5*
MS319	-	-	3.2 ± 0.1	93.8*
MS320	-	-	26.5 ± 6.0	50.0*
MS321	-	-	20.0 ± 4.2	62.3*
MS322	-	-	27.3 ± 5.1	48.2*
MS323	-	-	23.5 ± 2.4	55.7*
MS324	-	-	22.0 ± 3.8	58.1*
Indomethacin[c]			2.0 ± 4.6	96.1*

[a]Doses of 30, 100, and 300 mg/kg were administered. The figures in the table indicate the minimum dose whereby bioactivity was demonstrated in half or more of the mice (three in each group). The animals were examined at 0.5 and 4 h. The line (-) indicates an absence of neurotoxicity at the maximum dose tested. [b]A single dose of test compounds (100 mg/kg, *i.p.*) was administered to each of the mice. * denotes significantly different from the vehicle control at $p<0.05$. [c] Indomethacin was tested at the dose of 10 mg/kg *i.p.*

7.2.2 Formalin Test

Table 7.4 Effect of [MS(301-324)] on formalin induced pain in mice

Treatment	Formalin Induced Flinching			% Inhibition
	Phase-I (0-5 min)	% Inhibition	Phase-II (10-30 min)	
Vehicle	57.5 ± 4.8	-	73.5 ± 0.8	-
MS301	32.1 ± 3.5	44.1*	18.5 ± 0.4	74.7*
MS302	27.4 ± 1.4	52.4*	42.0 ± 3.5	42.9*
MS303	32.6 ± 1.4	43.5*	3.5 ± 0.4	95.5*
MS304	19.5 ± 1.8	66.5*	10.9 ± 2.8	87.1*
MS305	47.1 ± 14.1	18.2	14.3 ± 8.5	80.6*
MS306	45.1 ± 4.2	21.5	17.0 ± 4.2	76.7*
MS307	30.0 ± 4.2	47.9*	9.1 ± 3.2	87.7*
MS308	30.2 ± 3.9	47.2*	10.1 ± 3.9	86.4*
MS309	46.9 ± 2.1	18.6	4.5 ± 0.1	93.5*
MS310	28.5 ± 1.8	50.2*	10.5 ± 0.7	85.8*
MS311	32.5 ± 5.7	43.5*	65.4 ± 2.1	11.0
MS312	15.5 ± 5.1	73.2*	35.2 ± 4.9	52.1*
MS313	19.9 ± 9.5	65.0*	31.0 ± 1.8	57.9*
MS314	48.7 ± 2.5	15.3	15.5 ± 3.9	78.6*
MS315	51.5 ± 14.1	10.9	15.0 ± 4.6	79.9*
MS316	34.0 ± 0.7	40.5*	8.0 ± 2.1	89.9*
MS317	30.9 ± 2.8	46.0*	43.1 ± 10.6	41.7*
MS318	44.5 ± 2.8	22.6	41.6 ± 7.4	43.7*
MS319	30.0 ± 2.1	47.9*	6.5 ± 1.1	91.6*
MS320	33.1 ± 4.6	42.3*	5.0 ± 0.7	93.5*
MS321	50.0 ± 10.6	13.3	29.0 ± 3.2	60.5*
MS322	22.5 ± 4.6	60.6*	5.5 ± 2.8	92.2*
MS323	33.9 ± 5.7	41.5*	5.5 ± 0.4	92.8*
MS324	25.1 ± 10.6	56.1*	11.0 ± 2.8	85.8*
Indomethacin	26.5 ± 4.6	4.7	20.5 ± 3.1	72.1*

Effect of [**MS(301-324)**] on formalin-induced pain in mice. * represents the mean ± S.E.M. of a significantly different value from control at $p < 0.05$

7.2.3 Peripheral Nerve Injury–CCI Model

Table 7.5 Effect of [MS(301-324)] on spontaneous pain in CCI model

Treatment	Spontaneous Pain		
	% Reversal in CCI (Mean ± S.E.M.)		
	30 min	60 min	120 min
Vehicle	8.9 ± 1.2	4.6 ± 1.6	4.5 ± 0.2
MS301	17.6 ± 0.6	13.9 ± 7.9	15.3 ± 1.7
MS302	16.7 ± 8.3	33.7 ± 2.4	18.5 ± 3.1
MS303	73.4 ± 6.6*	87.1 ± 0.3*	92.7 ± 0.3*
MS304	10.8 ± 0.8	10.1 ± 0.9	12.0 ± 1.1
MS305	14.9 ± 1.8	11.4 ± 2.0	17.2 ± 1.2
MS306	18.3 ± 3.5	15.3 ± 1.7	13.8 ± 0.9
MS307	10.4 ± 4.9	26.6 ± 1.6	10.0 ± 0.7
MS308	17.5 ± 3.2	12.6 ± 2.6	12.5 ± 6.1
MS309	22.2 ± 9.2	50.0 ± 4.7*	71.1 ± 8.3*
MS310	25.6 ± 2.9	28.9 ± 7.0	10.2 ± 1.6
MS311	21.0 ± 3.4	21.1 ± 8.1	17.8 ± 0.2
MS312	16.4 ± 5.8	12.6 ± 1.6	22.4 ± 2.9
MS313	27.6 ± 4.7	13.9 ± 4.8	21.1 ± 2.9
MS314	16.9 ± 1.3	12.9 ± 9.1	24.2 ± 3.3
MS315	61.1 ± 1.2*	94.7 ± 3.4*	89.6 ± 5.1*
MS316	50.8 ± 2.8*	70.1 ± 7.2*	72.0 ± 1.8*
MS317	8.3 ± 1.5	7.5 ± 8.3	4.7 ± 8.2
MS318	17.0 ± 7.6	12.5 ± 1.8	22.5 ± 2.5
MS319	17.5 ± 1.2	82.6 ± 1.0*	72.5 ± 1.5*
MS320	18.8 ± 5.2	4.7 ± 2.7	17.1 ± 1.1
MS321	53.3 ± 1.8*	72.4 ± 0.0*	73.0 ± 6.9*
MS322	75.6 ± 7.4*	78.9 ± 5.5*	80.2 ± 1.7*
MS323	71.0 ± 1.5*	61.0 ± 1.3*	17.8 ± 0.6
MS324	21.1 ± 1.8	26.8 ± 1.2	29.8 ± 3.2
GBP	67.1 ± 3.2*	72.1 ± 5.1*	62.0 ± 2.4*

Each value represents the % reversal of allodynia (mean ± S.E.M.) of four rats; * denotes the values (≥ 50%), significantly different from their respective vehicle control at $p < 0.05$ (One-way ANOVA, followed by post-hoc Dunnett's test)

Table 7.6 Antiallodynic effect of [MS(301-324)] against dynamic allodynia in CCI model

Treatment	Dynamic Allodynia		
	% Reversal in CCI (Mean ± S.E.M.)		
	30 min	60 min	120 min
Vehicle	3.4 ± 0.8	2.3 ± 0.3	0.0 ± 0.0
MS301	31.0 ± 3.2	5.0 ± 3.1	7.2 ± 5.2
MS302	11.7 ± 1.7	15.1 ± 1.5	16.0 ± 9.1
MS303	81.0 ± 2.2*	82.7 ± 1.0*	17.2 ± 1.1
MS304	19.2 ± 1.4	13.4 ± 1.3	3.5 ± 0.4
MS305	5.2 ± 1.1	18.6 ± 1.1	7.0 ± 0.0
MS306	19.7 ± 2.0	53.0 ± 1.4*	11.5 ± 8.1
MS307	25.0 ± 2.5	15.0 ± 2.5	20.0 ± 0.1
MS308	12.9 ± 0.3	26.7 ± 3.3	22.4 ± 1.9
MS309	22.6 ± 2.4	21.7 ± 1.7	19.2 ± 1.4
MS310	19.2 ± 4.2	16.6 ± 1.7	12.5 ± 1.3
MS311	21.1 ± 1.2	19.7 ± 2.0	11.2 ± 1.2
MS312	3.5 ± 0.4	15.1 ± 1.5	20.2 ± 1.3
MS313	55.6 ± 2.5*	77.8 ± 1.4*	54.0 ± 1.2*
MS314	8.0 ± 1.1	9.4 ± 1.1	19.7 ± 2.0
MS315	82.4 ± 0.0*	85.0 ± 2.6*	60.0 ± 0.0*
MS316	16.0 ± 9.2	3.5 ± 0.4	15.1 ± 1.5
MS317	7.9 ± 0.9	14.2 ± 1.0	13.4 ± 1.3
MS318	6.5 ± 0.7	23.2 ± 2.0	6.5 ± 0.7
MS319	75.0 ± 1.7*	81.7 ± 5.5*	65.5 ± 1.7*
MS320	75.0 ± 0.0*	68.6 ± 1.9*	51.6 ± 1.9*
MS321	9.0 ± 2.1	20.7 ± 9.6	17.3 ± 0.5
MS322	56.1 ± 1.5*	68.0± 9.0*	52.5 ± 0.4*
MS323	16.0 ± 9.0	10.1 ± 9.9	28.5 ± 2.1
MS324	13.5 ± 0.0	15.1 ± 1.6	11.6 ± 1.6
GBP	19.7 ± 2.8	53.0 ± 2.8*	51.5 ± 3.2*

Each value represents the % reversal of allodynia (mean ± S.E.M.) of four rats; * denotes the values (≥ 50%), significantly different from their respective vehicle control at $p < 0.05$ (One-way ANOVA, followed by post-hoc Dunnett's test)

Table 7.7 Antiallodynic effect of [MS(301-324)] against cold allodynia in CCI model

Treatment	Cold Allodynia		
	% Reversal in CCI (Mean ± S.E.M.)		
	30 min	60 min	120 min
Vehicle	3.6 ± 0.7	4.3 ± 1.9	5.4 ± 2.1
MS301	7.9 ± 4.5	14.1 ± 8.1	18.7 ± 3.5
MS302	15.6 ± 0.6	16.7 ± 1.7	16.2 ± 1.2
MS303	22.8 ± 6.3	70.4 ± 2.0*	61.8 ± 1.2*
MS304	15.6 ± 1.2	8.7 ± 3.9	4.3 ± 0.4
MS305	16.0 ± 7.8	18.4 ± 5.9	14.8 ± 6.3
MS306	12.2 ± 1.7	14.9 ± 1.8	19.1 ± 3.5
MS307	4.2 ± 2.8	2.7 ± 9.6	15.0 ± 1.6
MS308	14.5 ± 1.5	18.8 ± 1.5	16.8 ± 6.7
MS309	50.7 ± 1.2*	70.4 ± 1.8*	72.4 ± 9.8*
MS310	15.4 ± 3.3	15.5 ± 0.9	18.8 ± 1.6
MS311	2.8 ± 1.2	19.9 ± 1.3	23.5 ± 3.6
MS312	5.5± 1.2	19.3 ± 0.3	8.0 ± 1.3
MS313	15.0 ± 2.9	20.4 ± 7.0	8.8 ± 5.6
MS314	15.9 ± 2.9	18.9 ± 2.6	16.0 ± 1.6
MS315	17.6 ± 1.1	82.4 ± 6.2*	62.6 ± 7.8*
MS316	16.5 ± 2.5	18.9 ± 4.5	12.6 ± 3.0
MS317	9.2 ± 1.1	17.6 ± 7.3	17.7 ± 1.9
MS318	53.3 ± 1.8*	72.4 ± 3.3*	73.0 ± 9.9*
MS319	87.5 ± 0.3*	85.9 ± 5.5*	80.2 ± 2.9*
MS320	26.2 ± 4.8	15.6 ± 8.5	14.1 ± 3.8
MS321	11.8 ± 3.4	15.5 ± 0.1	13.0 ± 0.8
MS322	71.0 ± 5.8*	61.1 ± 2.6*	17.8 ± 2.8
MS323	66.4 ± 2.1*	62.6 ± 1.3*	22.4± 1.5
MS324	67.1± 5.0*	72.1 ± 3.0*	63.0 ± 1.5*
GBP	43.4 ± 2.4	58.5 ± 3.1*	54.3 ± 4.1*

Each value represents the % reversal of allodynia (mean ± S.E.M.) of four rats; * denotes the values (≥ 50%), significantly different from their respective vehicle control at $p < 0.05$ (One-way ANOVA, followed by post-hoc Dunnett's test)

Table 7.8 Antihyperalgesic effect of [MS(301-324)] in CCI model

Treatment	Mechanical Hyperalgesia		
	% Reversal in CCI (Mean ± S.E.M.)		
	30 min	60 min	120 min
Vehicle	4.7 ± 2.1	4.9 ± 1.0	5.3 ± 0.5
MS301	13.5 ± 3.5	11.2 ± 1.2	6.9 ± 1.2
MS302	13.3 ± 4.9	13.6 ± 1.3	8.7 ± 0.4
MS303	93.3 ± 0.3*	70.0 ± 1.0*	19.1 ± 6.9
MS304	12.9 ± 3.8	21.1 ± 1.2	25.8 ± 7.6
MS305	6.1 ± 9.6	10.1 ± 9.0	9.1 ± 1.0
MS306	14.3 ± 1.4	18.8 ± 9.7	20.5 ± 12.3
MS307	13.8 ± 6.3	15.5 ± 5.0	12.5 ± 1.3
MS308	7.5 ± 2.5	10.0 ± 1.0	3.8 ± 1.6
MS309	25.4 ± 3.8	15.4 ± 7.7	11.5 ± 3.8
MS310	15.5 ± 5.0	10.0 ± 1.0	15.5 ± 5.0
MS311	19.3± 9.3	12.1 ± 2.1	7.1 ± 0.7
MS312	14.6 ± 2.1	10.4 ± 2.1	18.3 ± 0.8
MS313	73.5 ± 4.0*	11.2 ± 1.0	6.9 ± 5.0
MS314	13.3 ± 3.3	26.7 ± 6.7	14.2 ± 5.8
MS315	77.0 ± 1.0*	66.0 ± 1.7*	60.0 ± 1.3*
MS316	33.3 ± 3.0	12.5 ± 1.3	4.2 ± 0.4
MS317	18.3 ± 6.3	14.6 ± 2.1	25.5 ± 0.3
MS318	5.0 ± 0.5	15.1 ± 5.0	18.8 ± 2.1
MS319	93.0 ± 0.8*	65.6 ± 2.1*	13.6 ± 2.8
MS320	15.7 ± 6.6	10.0 ± 1.0	13.6 ± 1.4
MS321	65.3 ± 1.1*	15.0 ± 1.4	14.3 ± 1.3
MS322	16.2 ± 7.7	19.2 ± 3.8	23.1 ± 3.2
MS323	6.3 ± 0.6	29.2 ± 3.2	28.1 ± 3.1
MS324	15.5 ± 5.0	11.1 ± 1.7	18.3± 1.7
GBP	51.0 ± 2.1*	53.3 ± 3.1*	58.1 ± 3.2*

Each value represents the % reversal of allodynia (mean ± S.E.M.) of four rats; * denotes the values (≥ 50%), significantly different from their respective vehicle control at $p < 0.05$ (One-way ANOVA, followed by post-hoc Dunnett's test)

7.2.4 Peripheral Nerve Injury-PSNL

Table 7.9 Effect of [MS(301-324)] on spontaneous pain in PSNL model

Treatment	Spontaneous Pain		
	% Reversal in PSNL (Mean ± S.E.M.)		
	30 min	60 min	120 min
Vehicle	3.2 ± 0.3	2.9 ± 0.3	1.2 ± 0.1
MS301	27.4 ± 8.8	15.1 ± 8.1	7.4 ± 0.3
MS302	21.8 ± 0.4	14.7 ± 7.5	7.1 ± 0.7
MS303	82.2 ± 1.2 *	68.2 ± 4.2 *	13.6 ± 1.1
MS304	2.6 ± 0.3	6.5 ± 1.2	9.1 ± 1.4
MS305	18.2 ± 1.2	29.1 ± 1.9	10.0 ± 1.0
MS306	14.3 ± 1.4	8.6 ± 1.4	7.1 ± 0.7
MS307	33.6 ± 3.6	26.1 ± 1.1	33.4 ± 2.8
MS308	28.1 ± 4.8	20.7 ± 1.7	7.1 ± 0.7
MS309	61.7 ± 1.8*	14.3 ± 1.7	11.0 ± 1.0
MS310	15.0 ± 5.0	10.0 ± 1.0	15.0 ± 5.0
MS311	19.3 ± 9.3	12.2 ± 2.1	7.1 ± 0.7
MS312	32.1 ± 3.2	23.8 ± 3.0	28.6± 2.8
MS313	13.7 ± 2.0	11.8 ± 1.0	6.8 ± 0.9
MS314	8.8 ± 1.2	19.2 ± 1.9	10.0 ± 1.0
MS315	81.3 ± 5.2*	95.6 ± 2.8*	78.1 ± 0.9 *
MS316	12.2 ± 1.2	18.2 ± 6.6	13.6 ± 1.1
MS317	29.2 ± 1.2	16.7 ± 8.3	20.8 ± 4.2
MS318	13.8 ± 1.3	15.3 ± 9.7	19.4 ± 2.8
MS319	83.8 ± 1.3*	65.3 ± 9.7*	13.3 ± 8.2
MS320	18.2 ± 2.2	15.6 ± 0.3	3.8 ± 0.4
MS321	60.5 ± 6.5*	51.3 ± 2.4*	10.8 ± 3.8
MS322	54.8 ± 0.5*	55.7 ± 4.4*	3.6 ± 0.4
MS323	59.0 ± 1.5*	23.4 ± 5.2	17.9 ± 1.8
MS324	6.3 ± 0.6	15.6 ± 3.1	6.3 ± 1.6
GBP	92.0 ± 2.6*	92.0 ± 4.1*	81.0 ± 3.2*

Each value represents the % reversal of allodynia (mean ± S.E.M.) of four rats; * denotes the values (≥ 50%), significantly different from their respective vehicle control at $p < 0.05$ (One-way ANOVA, followed by post-hoc Dunnett's test)

Table 7.10 Antiallodynic effect of [MS(301-324)] against dynamic allodynia in PSNL model

Treatment	Dynamic Allodynia		
	% Reversal in PSNL (Mean ± S.E.M.)		
	30 min	60 min	120 min
Vehicle	4.7 ± 0.7	2.5 ± 1.2	0.8 ± 0.1
MS301	23.8 ± 9.5	14.8 ± 1.1	23.8 ± 9.5
MS302	13.7 ± 0.6	13.7 ± 0.6	28.0 ± 1.4
MS303	52.7 ± 6.2*	87.7 ± 4.2*	66.7 ± 6.8*
MS304	29.2 ± 4.2	28.3 ± 8.3	16.7 ± 1.7
MS305	4.5 ± 0.5	19.7 ± 1.9	18.3 ± 2.3
MS306	10.6 ± 3.5	36.5 ± 6.3	18.0 ± 2.3
MS307	25.4 ± 6.0	26.3 ± 1.9	7.1 ± 0.7
MS308	14.5 ± 0.5	29.5 ± 2.3	4.5 ± 0.5
MS309	34.1 ± 1.0	27.2 ± 1.0	12.10 ± 1.0
MS310	8.5± 0.5	19.7 ± 9.7	14.5 ± 5.5
MS311	23.3 ± 3.3	6.5 ± 0.7	25.0 ± 0.3
MS312	9.6 ± 0.9	2.2 ± 0.2	2.2 ± 0.2
MS313	59.5 ± 2.9*	54.7 ± 1.9*	51.0 ± 0.3*
MS314	6.5 ± 0.7	28.3 ± 0.3	19.0 ± 6.0
MS315	79.2 ± 7.4*	71.0 ± 2.2*	56.7 ± 1.3*
MS316	69.2 ± 7.8*	58.6 ± 4.4*	10.0 ± 1.0
MS317	30.6 ± 1.9	21.7 ± 8.3	22.8 ± 2.8
MS318	41.7 ± 1.7	11.7 ± 2.6	11.7 ± 2.6
MS319	75.3 ± 1.4*	94.1 ± 1.0*	7.1 ± 1.0
MS320	11.7 ± 2.6	21.4 ± 2.1	7.1 ± 0.7
MS321	51.0 ± 3.7*	67.9 ± 1.9*	10.8 ± 2.0
MS322	26.8 ± 1.3	11.7± 2.6	2.3 ± 1.4
MS323	3.5 ± 0.4	15.1 ± 1.5	20.2 ± 1.3
MS324	6.5 ± 0.7	6.5 ± 0.7	13.7 ± 0.6
GBP	51.2 ± 2.8*	56.0 ± 4.7*	58.0 ± 4.3*

Each value represents the % reversal of allodynia (mean ± S.E.M.) of four rats; * denotes the values (≥ 50%), significantly different from their respective vehicle control at $p < 0.05$ (One-way ANOVA, followed by post-hoc Dunnett's test)

Table 7.11 Antiallodynic effect of [MS(301-324)] against cold allodynia in PSNL model

Treatment	Cold Allodynia		
	% Reversal in PSNL (Mean ± S.E.M.)		
	30 min	60 min	120 min
Vehicle	4.1 ± 1.0	2.5 ± 0.3	1.9 ± 0.5
MS301	15.9 ± 6.3	26.2 ± 7.1	17.5 ± 6.3
MS302	17.0 ± 2.1	24.1 ± 0.6	14.2 ± 2.9
MS303	8.1 ± 0.4	75.3± 5.8*	64.7 ± 6.1*
MS304	19.4 ± 0.8	19.1 ± 9.0	16.9 ± 1.8
MS305	17.6 ± 4.8	14.4 ± 8.1	3.2 ± 0.3
MS306	10.0 ± 2.7	9.5 ± 0.9	6.8 ± 0.5
MS307	16.0 ± 2.4	19.1 ± 0.9	4.5 ± 0.5
MS308	11.4 ± 2.8	4.2 ± 0.3	3.4 ± 0.3
MS309	9.6 ± 1.3	61.1 ± 0.5*	53.6 ± 1.2*
MS310	29.5 ± 0.3	11.9 ± 1.2	3.6 ± 0.4
MS311	23.0 ± 5.1	14.2 ± 8.1	11.4 ± 5.4
MS312	9.9 ± 2.0	12.5 ± 5.0	6.9 ± 1.0
MS313	16.9 ± 3.1	6.7 ± 0.7	8.5 ± 1.8
MS314	14.9 ± 5.4	12.2 ± 2.1	7.5 ± 2.7
MS315	68.1 ± 3.2*	75.0 ± 7.0*	54.2 ± 1.0*
MS316	10.0 ± 5.0	15.1 ± 5.0	2.5 ± 0.3
MS317	9.3 ± 2.0	9.3 ± 2.0	2.8 ± 2.8
MS318	3.2 ± 4.3	16.4 ± 4.2	26.1 ± 8.0
MS319	89.4 ± 4.3*	86.2 ± 2.9*	51.0 ± 2.1*
MS320	9.4 ± 1.7	17.1 ± 6.0	5.6 ± 0.6
MS321	9.6 ± 2.4	11.3± 1.6	29.1 ± 2.8
MS322	69.0 ± 0.3*	14.8 ± 2.1	5.6 ± 0.6
MS323	14.2 ± 3.8	13.6 ± 1.6	5.5 ± 0.5
MS324	10.9 ± 1.0	11.2 ± 3.3	12.0 ± 1.1
GBP	54.0 ± 2.8*	58.0 ± 3.9*	68.0 ± 3.2*

Each value represents the % reversal of allodynia (mean ± S.E.M.) of four rats; * denotes the values (≥ 50%), significantly different from their respective vehicle control at $p < 0.05$ (One-way ANOVA, followed by post-hoc Dunnett's test)

Table 7.12 Antihyperalgesic effect of [MS(301-324)] in PSNL model

Treatment	Mechanical Hyperalgesia		
	% Reversal in PSNL (Mean ± S.E.M.)		
	30 min	60 min	120 min
Vehicle	2.9 ± 0.3	2.8 ± 0.3	5.1 ± 1.0
MS301	27.4 ± 8.8	15.1 ± 8.1	7.4 ± 0.3
MS302	21.8 ± 0.4	14.7 ± 7.5	7.1 ± 0.7
MS303	69.4 ± 11.2*	76.9 ± 1.0*	69.4 ± 5.8*
MS304	2.6 ± 0.3	6.5 ± 1.2	9.1 ± 1.4
MS305	18.2 ± 1.2	29.1 ± 1.9	10.0 ± 1.0
MS306	14.3± 1.4	8.6 ± 1.4	7.1 ± 0.7
MS307	13.6 ± 3.6	26.1 ± 1.1	33.4 ± 2.8
MS308	13.3 ± 2.6	20.7 ± 1.7	7.1 ± 0.7
MS309	59.7 ± 1.8*	64.3 ± 1.7*	61.0 ± 1.0 *
MS310	15.0 ± 5.0	10.0 ± 1.0	15.0 ± 5.0
MS311	19.3± 9.3	12.2 ± 2.1	7.1 ± 0.7
MS312	32.1 ± 3.2	23.8 ± 3.0	28.6 ± 2.8
MS313	63.7 ± 2.0*	11.8 ± 1.0	6.8 ± 0.9
MS314	8.8 ± 1.2	19.2 ± 1.9	10.0 ± 1.0
MS315	59.3 ± 5.2*	80.6 ± 2.8*	9.1 ± 0.9
MS316	21.2 ± 1.2	15.7 ± 6.6	13.6 ± 1.1
MS317	29.2 ± 1.2	16.7 ± 8.3	20.8 ± 4.2
MS318	2.8 ± 1.3	31.3 ± 9.7	19.4 ± 2.8
MS319	74.5 ± 0.5*	56.6 ± 0.6*	53.3 ± 8.2*
MS320	18.2 ± 2.2	15.6 ± 0.3	3.8 ± 0.4
MS321	51.5 ± 6.5*	64.3 ± 2.4*	10.8 ± 3.8
MS322	14.8 ± 0.5	18.7 ± 4.4	3.6 ± 0.4
MS323	6.2 ± 1.5	23.4 ± 5.2	17.9 ± 1.8
MS324	6.3 ± 0.6	15.6 ± 3.1	6.3 ± 1.6
GBP	86.0 ± 2.3 *	91.0 ± 3.7*	56.0 ± 3.3*

Each value represents the % reversal of allodynia (mean ± S.E.M.) of four rats; * denotes the values (≥ 50%), significantly different from their respective vehicle control at $p < 0.05$ (One-way ANOVA, followed by post-hoc Dunnett's test)

Table 7.13 Median effective dose (ED_{50}) of selected MS3XX compounds in CCI model

Treatment	ED_{50} values (mg/kg) in CCI model (TPE in min)			
	Spontaneous pain	Dynamic allodynia	Cold allodynia	Mechanical hyperalgesia
MS303	25.6 (120)	87.2 (30)	34.5 (120)	29.7 (30)
MS315	13.2 (120)	39.9 (30)	55.9 (60)	40.7 (60)
MS319	50.2 (60)	41.1 (60)	14.9 (30)	32.2 (30)

Table shows the ED_{50} values (mg/kg) in CCI model at different time points calculated at time of peak effect (TPE in min)

Table 7.14 Median effective dose (ED_{50}) of selected MS3XX compounds in PSNL model

Treatment	ED_{50} values (mg/kg) in PSNL model (TPE in min)			
	Spontaneous pain	Dynamic allodynia	Cold allodynia	Mechanical hyperalgesia
MS303	28.4 (30)	40.2 (60)	38.9 (60)	27.9 (60)
MS315	24.2 (60)	41.2 (30)	33.4 (60)	16.6 (60)
MS319	34.8 (30)	18.4 (60)	31.9 (30)	17.1 (30)

Table shows the ED_{50} values (mg/kg) in PSNL model at different time points calculated at time of peak effect (TPE in min)

7.2.5 Efficacy in Carrageenan Induced Paw Edema and TNF-α Quantification

Table 7.15 Effect of MS3XX compounds on carrageenan induced paw edema

Treatment	Change in paw volume (mL) Mean ± S.E.M.			(%) Protection		
	60 min	120 min	180 min	60 min	120 min	180 min
Vehicle	0.23 ± 0.12	0.43 ± 0.12	0.67 ± 0.12	-	-	-
MS303	0.21 ± 0.05	0.39 ± 0.21	0.645 ± 0.09	10.9	8.2	3.8
MS315	0.08 ± 0.04	0.07 ± 0.03	0.11 ± 0.01	67.4*	83.5*	84.2*
MS319	0.11 ± 0.01	0.17 ± 0.02	0.10 ± 0.01	52.2*	60.0*	85.0*
Indomethacin	0.12 ± 0.05	0.17 ± 0.12	0.22 ± 0.11	50.0*	61.2*	66.9*

A single dose of test compounds (100 mg/kg, *i.p.*) was administered to each of the animal. Table shows the change in paw volume (mL) after 1% carrageenan. * represents significance at $p<0.05$ compared to vehicle (One way ANOVA followed by Dunnett's Test, n=6). Indomethacin was tested at the dose of 10 mg/kg *i.p.*

Table 7.16 Effect of compounds on TNF-α level

Treatment	TNF-α (pg/ml)	% inhibition of TNF-α production
Vehicle	3175.5 ± 161.6	-
MS303	2633.0 ± 44.5	21.1 ± 1.4
MS315	1115.4 ± 95.2	66.6 ± 2.7*
MS319	1003.7 ± 52.5	69.9 ± 1.7*

Table shows the concentration of TNF-α in the paw of carrageenan treated animals. * represents the significance at $p<0.05$, compared to vehicle control (One way ANOVA followed by Dunnett's test, n=4). All the compounds were tested at the dose of 100 mg/kg *i.p.*

7.2.6 Nitric Oxide Estimation in Brain and Sciatic Nerve

Table 7.17 Effect of MS3XX compounds on nitric oxide in brain and sciatic nerve

Total Nitrate/Nitrite (% of SHAM control)				
Treatment	**Brain**	**Sciatic Nerve**	**% Inhibition of Nitrosative stress (nitrite)**	
			Brain	**Sciatic Nerve**
SHAM	100 ± 7.8	100 ± 3.9	-	-
Vehicle	194.3 ± 15.3	193.7 ± 8.4	-	-
MS303	182.7 ± 2.3	170.6 ± 1.5	12.3	24.6
MS315	188.4 ± 1.1	136.0 ± 1.0	6.2	61.6*
MS319	187.0 ± 0.2	134.0 ± 1.9	7.1	62.9*

Table shows the concentration of nitric oxide in brain and sciatic nerve after CCI in rats. * represents the significance at $p<0.05$, compared to vehicle control (One way ANOVA followed by Dunnett's test, n=4). All the compounds were tested at the dose of 100 mg/kg *i.p.*

7.2.7 DPPH Scavenging Assay

Table 7.18 DPPH scavenging activity of MS3XX compounds

Treatment	IC_{50} (μM)
MS303	182
MS315	109
MS319	181
Curcumin	135

DPPH radical scavenging activity of test compounds. Values are represented as % scavenging comparedto vehicle, calculated from the average of triplicate experiments

7.2.8 Effect of Compounds on Cannabinoid Receptors

Table 7.19 Effect of MS3XX compounds on cannabinoid receptors

% Replacement of Specific Bound ^{3}H [CP 55,940] on CB_1 receptor by test compounds	
Treatment	**IC_{50}**
MS303	>1 μM
MS315	>1 μM
MS319	>1 μM
% Replacement of Specific Bound ^{3}H [CP 55,940] on CB_2 receptor by test compounds	
Treatment	**IC_{50}**
MS303	>1 μM
MS315	>1 μM
MS319	>1 μM

Equilibrium-competition binding of compounds vs. [^{3}H] CP55940 using either rat brain (CB_1) or rat spleen homogenates (CB_2). The data shown are average of triplicates

7.2.9 Effect of Compounds on Cathepsin S Enzyme

Table 7.20 Effect of compounds on cathepsin S enzyme

Treatment	% inhibition
Vehicle	-
MS315	21.3 ± 3.4
MS319	34.1 ± 1.7

Inhibition of recombinant human Cathepsin S by test compounds (50μM) in a fluorescence assay, employing Z-Leu-Leu-Arg-MCA as synthetic substrates. Data represent means of two experiments performed in triplicate

7.2.10 Effect on GABAergic Pathway

Table 7.21 Picrotoxin induced epilepsy (scPIC) model

Treatment	Antiepileptic activity (scPIC)	
	30 min	**240 min**
Vehicle	-	-
MS303	-	-
MS315	300	-
MS319	100	100
Diazepam	10	10

The figures in the table indicate the minimum dose whereby bioactivity was demonstrated in half or more of the mice (n=3). The animals were examined 30 min and 240 min. The line (-) indicates an absence of anticonvulsant activity at the maximum dose tested

Results and Discussion

7.3.1 Chemistry

A three step process was employed for the synthesis of 1,2,4-triazol-5-ones in yields ranging from 71 to 88%. The anilines employed for the synthesis of substituted semicarbazide were randomly selected that included 4-bromo, 2,6-dimethyl, 2,5-dimethyl, 2,4-dimethyl, 3-trifluoromethyl and 4-chloro aniline. The homogeneity of the compounds was monitored by performing TLC. The eluant system for all the compounds was DCM: CH_3OH (9.5:0.5). The ^{1}H-NMR spectra revealed that the NH protons resonated at δ~7.92-8.42 ppm which was D_2O exchangeable. The aryl ring protons resonated at δ~6.91-9.34 ppm. The percentage composition of C, H, N of all the compounds found from elemental analyses were within ± 0.4 % of the theoretical values (Table-7.2).

7.3.2 Efficacy in Acute Pain Models

In acetic acid-induced writhing test, all the tested compounds except **MS301**, **MS306**, **MS311** and **MS312** suppressed the writhing response significantly ($p<0.05$) in comparison to the control. Nine compounds namely **MS302**, **MS303**, **MS304**, **MS309**, **MS310**, **MS315**, **MS316**, **MS318** and **MS319** showed more than 70.0% inhibition. Of these compounds, **MS319** was observed to be the most active with 93.8% inhibition of writhing response. Indomethacin exhibited 96.1% inhibition at the dose of 10 mg/kg (Table-7.3).

In formalin test, among the 24 compounds tested, 17 compounds were effective in phase-I, whereas in phase-II, 23 compounds exhibited significant inhibition of pain. **MS312** was the most active compound with 73.2% inhibition of flinching and lickings in phase-I. Sixteen compounds showed more than 70.0% inhibition in phase-II, with a maximum inhibition (95.4%) exhibited by compound **MS303**. Standard drug indomethacin (10 mg/kg, *i.p.*) was effective only in phase-II (72.1% inhibition). (Table-7.4).

7.3.3 Efficacy in Neuropathic Pain Models (CCI and PSNL)

In the CCI model, intraperitoneal administration of compounds **MS303**, **MS315**, **MS316**, **MS321** and **MS322** reversed the spontaneous pain response throughout the time period of testing (30-120 min) similar to gabapentin. Compound **MS323** exhibited

activity up to 60 min. The onset of action of compounds **MS309** and **MS319** was at 60 min. Other compounds were ineffective in this test (Table-7.5).

Five compounds **MS313**, **MS315**, **MS319**, **MS320** and **MS322** were active in attenuating the dynamic allodynia throughout the 120 min of the experiment. Compound **MS303** was active only up to 60 min of the experiment. All other compounds were ineffective in this test (Table-7.6).

In the cold allodynia produced in CCI rats, significant reversal of paw withdrawal durations was observed at all time points by the administration of compounds **MS309**, **MS318**, **MS319** and **MS324**. Gabapentin was also found to be effective from 60 to 120 min. The onset of action for compounds **MS303** and **MS315** was at 60 min. Compounds **MS322** and **MS323** were effective only up to 60 min of the experiment (Table-7.7).

Mechanical hyperalgesia was significantly attenuated at all the time points by **MS315** similar to gabapentin. Compounds **MS313** and **MS321** were active up to 30 min, whereas compounds **MS303** and **MS319** were active up to 60 min (Table-7.8).

Overall, it appears that, in the CCI model of neuropathic pain, compounds that showed promising results include **MS303**, **MS315** and **MS319** effective in four tests, **MS322** in three tests and **MS309**, **MS313**, **MS321** and **MS323** active in two tests.

In the PSNL model, the paw withdrawal durations due to spontaneous ongoing pain were significantly reduced by compound **MS315** throughout the experiment similar to gabapentin. The compounds **MS309** and **MS323** exhibited activity only up to 30 min, whereas the compounds **MS303**, **MS319**, **MS321** and **MS322** were active up to 60 min of the experiment (Table-7.9).

The dynamic allodynia produced by PSNL was effectively reversed by compounds **MS303**, **MS313** and **MS315** at all the time points like gabapentin. Compounds **MS316**, **MS319** and **MS321** were active up to 60 min of the experiment. All other compounds were inactive in the test (Table-7.10).

Cold allodynia produced by the PSNL model was completely reversed by the compounds **MS315** and **MS319** like gabapentin. Compound **MS322** was active only up to 30 min of the experiment. The compounds **MS303** and **MS309** had onset of action at 60 min (Table-7.11).

Compound **M303**, **MS309** and **MS319** significantly reversed mechanical hyperalgesia at all the time points like gabapentin. Compound **MS313** was active only up to 30 min of the experiment, whereas compounds **MS315** and **MS321** were active in the first 60 min of the experiment (Table-7.12).

Overall, it appears, in the PSNL model, compounds that exhibited promising results were **MS303**, **MS315** and **MS319** effective in four tests, **MS309** and **MS321** effective in three tests and **MS313** and **MS322** effective in two tests.

7.3.4 Structure-Activity Relationships

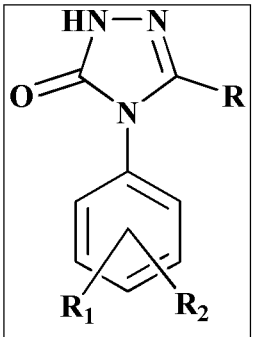

MS301-MS324

The results obtained in the nociceptive assays provide an insight into the structure-activity relationships of the 1,2,4-triazol-5-ones. Functionalisation of the aryl ring of the semicarbazide fragment forming 1,2,4-triazol-5-one with dimethyl substitutions proved to be advantageous for antinociceptive efficacy. Compounds having 2,4-dimethyl substitution in the aryl fragment (**MS313** and **MS319**) significantly reversed the nociceptive parameters. Introduction of 2,5-dimethyl substitution in the aryl ring proved to be detrimental for the antinociceptive efficacy (**MS302**, **MS308** and **MS314)** in both CCI and PSNL animals. Introduction of electron releasing 2,6-dimethyl substitution (**MS303**, **MS309**, **MS315** and **MS322**) resulted in significant attenuation of one or more nociceptive parameters in neuropathic animals. Introduction of electron withdrawing groups like halogen (bromo in **MS317** and **MS323**, chloro in **MS322**,) at the *para* position in the aryl ring resulted in significant activity against spontaneous pain and cold allodynia. Trifluoromethyl substitution *meta* to the aryl ring was detrimental for activity except in case of **MS318** and **MS324** which were effective in cold allodynia in CCI animals.

In general, among the 2-propylpentanyl substituted triazolones (**MS301-MS306**), **MS303** significantly alleviated one or more nociceptive responses in CCI and PSNL rats. 4-phenoxyphenyl substitution in aryl triazolones (**MS307-MS312**), proved to be detrimental for the activity except compound **MS309** which was found to be effective in one or more nociceptive assays in neuropathic animals. Heteroaryl triazolones having 2-pyrazinyl substitutions exhibited pronounced activities against one or more nociceptive parameters in the neuropathic animals. Among **MS313-MS318** compounds, 4 compounds exhibited significant reversal of nociceptive assays in neuropathic animals. All the compounds with 2-nitro-5-furyl substitution (**MS319-MS324**) were found to be effective in one or more nociceptive testings.

7.3.5 ED_{50} Studies

Compounds exhibiting more than 90% reversal in one or more of the nociceptive assays (**MS303**, **MS315** and **MS319**) were taken further for ED_{50} studies. In the CCI model, compound **MS315** reversed spontaneous pain and dynamic allodynia with an ED_{50} value of 13.2 mg/kg and 39.9 mg/kg with TPE at 120 min and 30 min respectively. Compound **MS319** reversed cold allodynia with an ED_{50} value of 14.9 mg/kg exhibiting TPE at 30 min. Compound **MS303** reversed mechanical hyperalgesia with an ED_{50} value of 29.7 mg/kg with a TPE at 30 min (Table-7.13). In the PSNL model, compound **MS315** reversed spontaneous pain and mechanical hyperalgesia with an ED_{50} value of 24.2 mg/kg and 16.6 mg/kg respectively, both exhibiting TPE at 60 min. In dynamic and cold allodynia, **MS319** emerged as the most active compound with an ED_{50} value of 18.4 mg/kg and 31.9 mg/kg with TPE at 60 min and 30 min respectively (Table-7.14).

7.3.6 Mechanistic studies

The significant suppression of flinching in both the phases of formalin assay suggested the mediation of anti-inflammatory pathways. The probable role of the some selected compounds (**MS303**, **MS315** and **MS319**) in the inhibition of inflammatory mediators was investigated using carrageenan-induced paw edema model where edema results from the local action of multiple inflammatory mediators, starting with the stimulation of TNF-α and keratinocyte chemokines (KC), subsequently causing the release of IL-1β, and in turn, stimulating the release of prostanoids and sympathomimetic amines. A significant reduction in edema was

observed with compounds **MS315** and **MS319** at all the time points (Table-7.15). The TNF-α levels quantified in the carrageenan injected paw were also found to be inhibited by compound **MS315** and **MS319** (Table-7.16). Following nerve injury, subsequent generation of free radicals leads to oxidative and nitrosative stress which exaggerates the pain states. Peripheral nerve injuries have been shown to induce an increase in nitric oxide synthase (NOS) expression in dorsal root ganglion [88] as well as in the sciatic nerve [161]. Nine days after the lesion, the nitrite/nitrate content in brain and injured paws has been found to be increased by about two to four times respectively, as compared to sham animals. The putative role of nitric oxide (NO) in the pathophysiology of chronic nerve ligation as evident by significant increase in nitrite and nitrate levels in both brain and sciatic nerve led us to estimate the levels of nitrite, a metabolite of NO in brain and sciatic nerve of CCI rats. There was no significant reduction of nitrite in the brain of CCI rats as compared to vehicle treated animals with compounds **MS303**, **MS315** and **MS319**. However, a significant reduction was observed in the sciatic nerve of the CCI animals as compared to vehicle treated group with **MS315** and **MS319**, indicating inhibition of local NO (Table-7.17). The free radical scavenging efficacies of the compounds (**MS303**, **MS315** and **MS319)** in the DPPH assay indicated reduction in oxidative stress (Table-7.18). The affinity observed with CB_1 and CB_2 receptors was more than 1 μM in radiolignad binding assay as evident in case of the compounds **MS303**, **MS315** and **MS319** (Table-7.19).

Compound **MS319** exhibited 34.1% inhibition of cathepsin S (Table-7.20). Moreover, the possible mediation of GABAergic pathway was explored by assessing the anticonvulsant potential of the test compounds in picrotoxin-induced seizure. The compounds **MS315** (300 mg/kg) and **MS319** (100 mg/kg) exhibited protection in the scPIC screen indicating enhancement of peripheral GABAergic neurotransmission (Table-7.21).

The present study reports the synthesis, acute antinociceptive, antihyperalgesic and antiallodynic activities of some novel 1,2,4-triazol-5-one derivatives. Efficacy of the compounds in both acute and chronic models of pain and the proposed contribution of inflammatory reactions in the generation and maintenance of neuropathic pain after nerve injury led us to explore the possible role of 1,2,4-triazol-5-one derivatives in the suppression of inflammatory component of neuropathic pain. Significant reduction in

carrageenan induced paw edema by **MS315** and **MS319** supported their anti-inflammatory profile. Both the compounds significantly inhibited TNF-α levels in carrageenan-injected paw homogenates. Inhibition of local nitric oxide and reduction in oxidative stress support their peripheral antinociceptive action. Also, protection exhibited by **MS315** and **MS319** in the picrotoxin induced epilepsy indicates up-regulation of GABA also.

CHAPTER 8

SERIES IV - TRIAZOLO-THIADIAZOLES

8.1 Chemistry

8.1.1 Rationale of Design

In recent years, the condensed bridgehead nitrogen heterocyclic system of triazolo-thiadiazole, which may be considered as the cyclic analog of thiosemicarbazide and biguanide has received considerable attention because of a wide spectrum of biological activities exhibited, specifically anti-convulsant [187], analgesic [246] anxiolytic [193] and anti-inflammatory [191] properties. Moreover, literature reveals that acylthiosemicarbazides and their corresponding cyclized 1,3,4-thiadiazole derivatives possess anti-inflammatory [247] and analgesic [248] activities. In view of the above reports, design and synthesis of pharmacophoric hybrids of aryl semicarbazides into triazolo-thiadiazole template was accomplished followed by assessment of their antinociceptive potential and underlying mechanism of action.

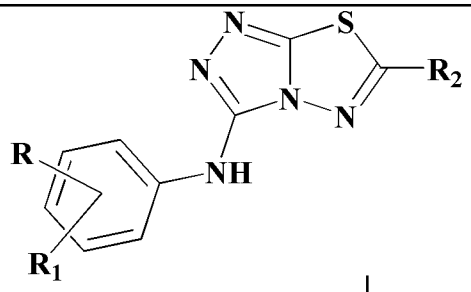

MS401-MS425

R_1	R_2
H	4-Br
H	4-Cl
2-CH_3	4-CH_3
2-CH_3	5-CH_3
2-CH_3	6-CH_3

R
4-aminobutanyl
2-propylpentanyl
4-nitro benzyl
isoniconityl
4-(2,4-dioxo-3-azaspiro[5.5]-undecan-3-yl)butanyl

8.2.2 Synthesis

Step-1: Synthesis of substituted potassium dithiocarbazinates

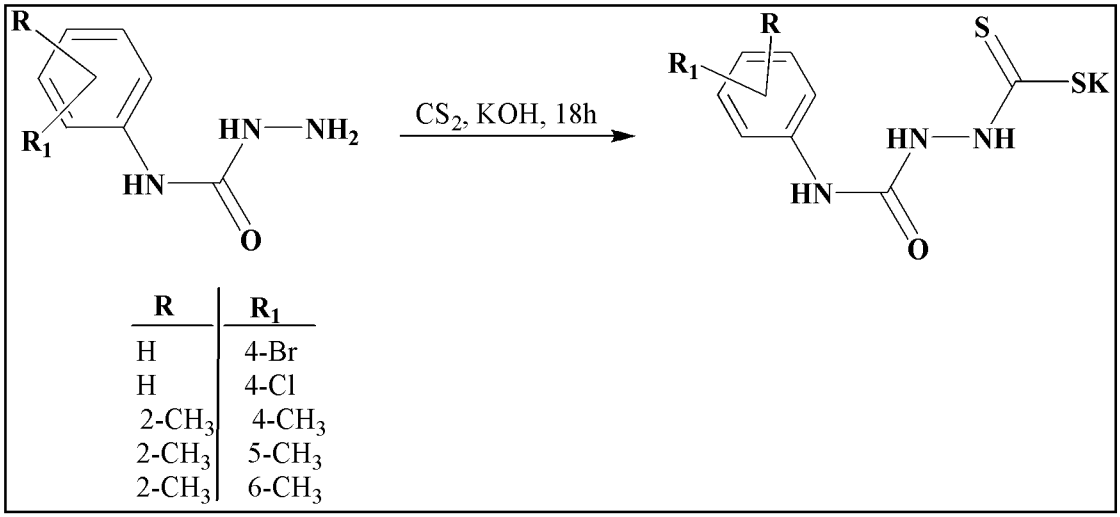

R	R_1
H	4-Br
H	4-Cl
2-CH_3	4-CH_3
2-CH_3	5-CH_3
2-CH_3	6-CH_3

Substituted phenyl semicarbazide (1.0 equiv.) was added to a solution of potassium hydroxide (1.5 equiv.) in methanol (50 mL) at 0-5°C under stirring. To this, carbon disulfide (0.5 equiv.) was added dropwise with constant stirring. The reaction mixture was stirred continuously for 12 h at room temperature. The precipitated potassium dithiocarbazinate salt was filtered, washed with anhydrous ether and dried in vacuum. The potassium salt thus obtained was used in the next step without further purification.

Step-2: Synthesis of 4-amino-5-substituted-3-mercapto-(4H)-1,2,4-triazoles

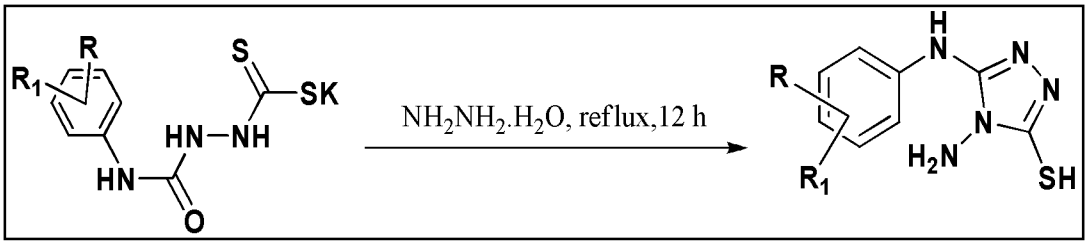

Potassium dithiocarbazinate derivatives, (1.0 equiv.) obtained from the first step and hydrazine hydrate (99%, 2.0 equiv.) in water (25 mL) were refluxed for 10-15 h with occasional shaking. The reaction mixture was cooled to room temperature and diluted with cold water (10 mL). On acidification with dilute hydrochloric acid, a white precipitate resulted which was filtered, washed with cold water, dried and recrystallized from ethanol.

Step-3: Synthesis of 3,6-disubstituted-[1,2,4]-triazolo-[3,4-b]-1,3,4-thiadiazoles

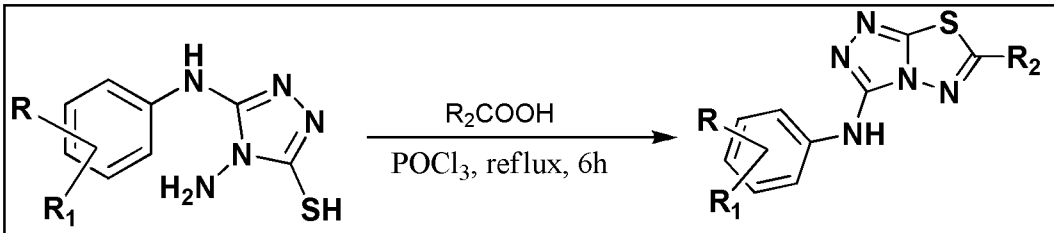

	R_2
4	4-aminobutanyl
5	2-propylpentanyl
6	4-nitro benzyl
7	isoniconityl
8	4-(2,4-dioxo-3-azaspiro[5.5]undecan-3-yl)butanyl

An equimolar mixture (0.01 mol) of 4-amino-5-substituted-3-mercapto-(4H)-1,2,4-triazoles and various carboxylic acids in phosphorous oxychloride (10 mL) were refluxed for 5 h. After the completion of the reaction, the reaction mixture was slowly poured into crushed ice with vigorous stirring and neutralized with sodium bicarbonate. The precipitated solid was filtered washed with cold water and recrystallized from ethanol.

Table 8.1 Physical data of 3,6-disubstituted-[1,2,4]-triazolo-[3,4-b]-1,3,4-thiadiazoles

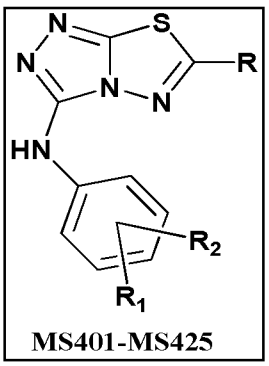

MS401-MS425

Compound	R	R_1	R_2	M.F.	M.W.	Yield (%)	M.P. (°C)
MS401	H	4-Br	4-aminobutanyl	$C_{12}H_{13}BrN_6S$	353.24	64	185
MS402	H	4-Cl	4-aminobutanyl	$C_{12}H_{13}ClN_6S$	308.79	72	192
MS403	2-CH_3	4-CH_3	4-aminobutanyl	$C_{14}H_{18}N_6S$	302.40	71	178
MS404	2-CH_3	5-CH_3	4-aminobutanyl	$C_{14}H_{18}N_6S$	302.40	68	152
MS405	2-CH_3	6-CH_3	4-aminobutanyl	$C_{14}H_{18}N_6S$ S	302.40	61	144
MS406	H	4-Br	2-propylpentanyl	$C_{16}H_{20}BrN_5S$	394.33	69	157
MS407	H	4-Cl	2-propylpentanyl	$C_{16}H_{20}ClN_5S$	349.88	78	171
MS408	2-CH_3	4-CH_3	2-propylpentanyl	$C_{18}H_{25}N_5S$	343.49	73	153
MS409	2-CH_3	5-CH_3	2-propylpentanyl	$C_{18}H_{25}N_5S$	343.49	75	138
MS410	2-CH_3	6-CH_3	2-propylpentanyl	$C_{18}H_{25}N_5S$	343.49	80	128
MS411	H	4-Br	4-nitrobenzyl	$C_{15}H_9BrN_6O_2S$	373.23	81	203
MS412	H	4-Cl	4-nitrobenzyl	$C_{15}H_9ClN_6O_2S$	328.78	65	216
MS413	2-CH_3	4-CH_3	4-nitrobenzyl	$C_{17}H_{14}N_6O_2S$	366.40	62	192
MS414	2-CH_3	5-CH_3	4-nitrobenzyl	$C_{17}H_{14}N_6O_2S$	366.40	68	183
MS415	2-CH_3	6-CH_3	4-nitrobenzyl	$C_{17}H_{14}N_6O_2S$	366.40	70	161
MS416	H	4-Br	isonicotinyl	$C_{14}H_9BrN_6S$	373.23	68	199
MS417	H	4-Cl	isonicotinyl	$C_{14}H_9ClN_6S$	328.78	69	207
MS418	2-CH_3	4-CH_3	isonicotinyl	$C_{16}H_{14}N_6S$	322.39	77	176
MS419	2-CH_3	5-CH_3	isonicotinyl	$C_{16}H_{14}N_6S$	322.39	73	162
MS420	2-CH_3	6-CH_3	isonicotinyl	$C_{16}H_{14}N_6S$	322.39	71	151
MS421	H	4-Br	4-(2,4-dioxo-azaspiro [5.5]undecan-3-yl) butanyl	$C_{22}H_{25}BrN_6O_2S$	517.44	80	174
MS422	H	4-Cl	4-(2,4-dioxo-3 aza spiro[5.5] undecan-3-yl)butanyl	$C_{22}H_{25}ClN_6O_2S$	472.99	75	183

MS423	2-CH_3	4-CH_3	4-(2,4-dioxo-3-aza spiro[5.5] undecan-3-yl)butanyl	$C_{24}H_{30}N_6O_2S$	466.60	74	159
MS424	2-CH_3	5-CH_3	4-(2,4-dioxo-3-aza spiro[5.5] undecan-3-yl)butanyl	$C_{24}H_{30}N_6O_2S$	466.60	75	141
MS425	2-CH_3	6-CH_3	4-(2,4-dioxo-3-aza spiro[5.5] undecan-3-yl)butanyl	$C_{24}H_{30}N_6O_2S$	466.60	72	124

Table 8.2 Spectral and elemental analyses data of 3,6-disubstituted-[1,2,4]-triazolo-[3,4-b]-1,3,4-thiadiazoles

Compound	^{1}H-NMR (δ ppm, DMSO-d_6)	Elemental Analyses (Calculated/Found)[a]			Mass Spectroscopy (m/z)
		C (%)	H (%)	N (%)	
MS401	δ 2.01 (p, 2H), 2.63 (t, 2H), 2.84 (t, 2H), 4.78 (br s, 2H, D_2O exchangeable), 6.91 (d, 2H), 7.13 (d, 2H), 8.24 (br s, 1H, D_2O exchangeable)	40.80 40.78	3.71 3.74	23.79 23.80	352.01
MS402	δ 2.03 (p, 2H), 2.66 (t, 2H), 2.83 (t, 2H), 4.72 (br s, 2H, D_2O exchangeable), 7.01 (d, 2H), 7.22 (d, 2H), 8.63 (br s, 1H, D_2O exchangeable)	46.68 46.70	4.24 4.25	27.22 27.24	310.06
MS403	δ 2.02 (p, 2H), 2.14 (s, 3H), 2.37 (s, 3H), 2.68 (t, 2H), 2.84 (t, 2H), 4.84 (br s, 2H, D_2O exchangeable), 6.57 (d, 1H), 6.87-6.91 (m, 2H), 9.10 (br s, 1H, D_2O exchangeable)	55.61 55.60	6.00 6.01	27.79 27.78	303.13
MS404	δ 2.04 (p, 2H), 2.13 (s, 6H), 2.38 (s, 3H), 2.66 (t, 2H), 2.86 (t, 2H), 4.59 (br s, 2H, D2O exchangeable), 6.67-6.69 (m, 2H), 6.94 (d, 1H), 9.12 (br s, 1H, D_2O exchangeable)	55.61 55.63	6.00 6.03	27.79 27.80	303.13
MS405	δ 2.01 (p, 2H), 2.14 (s, 6H), 2.66 (t, 2H), 2.88 (t, 2H), 4.71 (br s, 2H, D2O exchangeable), 6.69 (t, 1H), 6.96 (d, 2H), 9.41 (br s, 1H, D_2O exchangeable)	55.61 55.62	6.00 6.03	27.79 27.81	303.13
MS406	δ 0.93-1.10 (t, 6H), 1.35-1.40 (m, 4H), 1.56-1.62 (q, 4H), 2.66-2.68 (t, 1H), 6.94 (d, 2H), 7.16 (d, 2H), 8.43 (br s, 1H, D_2O exchangeable)	48.73 48.74	5.11 5.13	17.76 17.78	393.06
MS407	δ 0.96-1.11 (t, 6H), 1.37-1.41 (m, 4H), 1.54-1.59 (q, 4H), 2.65-2.67 (t, 1H), 7.04 (d, 2H), 7.25 (d, 2H), 8.81 (br s, 1H, D_2O exchangeable)	54.92 54.94	5.76 5.78	20.02 20.04	351.11

MS408	δ 0.97-1.11 (t, 6H), 1.36-1.42 (m, 4H), 1.55-1.60 (q, 4H), 2.14 (s, 3H), 2.37 (s, 3H), 2.66-2.69 (t, 1H), 6.59 (d, 1H), 6.87-6.92 (m, 2H), 9.40 (br s, 1H, D_2O exchangeable)	62.94 62.96	7.34 7.33	20.39 20.39	344.18
MS409	δ 0.96-1.12 (t, 6H), 1.36-1.41 (m, 4H), 1.54-1.60 (q, 4H), 2.13 (s, 3H), 2.36 (s, 3H), 2.67-2.69 (t, 1H), 6.57-6.61 (m, 2H), 6.91 (d, 1H), 8.89 (br s, 1H, D_2O exchangeable)	62.94 62.99	7.34 7.35	20.39 20.42	344.18
MS410	δ 0.95-1.12 (t, 6H), 1.36-1.42 (m, 4H), 1.56-1.61 (q, 4H), 2.15 (s, 6H), 2.64-2.67 (t, 1H), 6.67 (t, 1H), 6.98 (d, 2H), 9.41 (br s, 1H, D_2O exchangeable)	62.94 62.96	7.34 7.36	20.39 20.41	344.18
MS411	δ 6.94 (d, 2H), 7.13 (d, 2H), 7.89 (d, 2H), 8.45 (d, 2H), 8.91 (br s, 1H, D_2O exchangeable	43.18 43.20	2.17 2.19	20.14 20.16	371.98
MS412	δ 7.02 (d, 2H), 7.23 (d, 2H), 7.90(d, 2H), 8.46 (d, 2H), 8.95 (br s, 1H, D_2O exchangeable)	48.33 48.34	2.43 2.45	22.54 22.56	330.03
MS413	δ 2.14 (s, 3H), 2.36 (s, 3H), 6.58 (d, 1H), 6.88-6.94 (m, 2H), 7.91 (d, 2H), 8.54 (d, 2H), 9.12 (br s, 1H, D_2O exchangeable)	55.73 55.75	3.85 3.87	22.94 22.96	323.10
MS414	δ 2.13 (s, 3H), 2.37 (s, 3H), 6.66-6.71 (m, 2H), 6.90 (d, 2H), 7.92 (d, 2H), 8.45 (d, 2H), 8.64 (br s, D_2O exchangeable, 1H)	55.73 55.75	3.85 3.86	22.94 22.95	323.10
MS415	δ 2.15 (s, 6H), 6.65 (t, 1H), 6.96 (d, 2H), 7.91 (d, 2H), 8.47 (d, 2H), 9.21 (br s, 1H, D_2O exchangeable)	55.73 55.75	3.85 3.87	22.94 22.96	323.10
MS416	δ 6.93 (d, 2H), 7.14 (d, 2H), 7.81 (d, 2H), 8.08 (d, 2H), 9.71 (br s, 1H, D_2O exchangeable)	45.05 45.07	2.43 2.45	22.52 22.53	373.98
MS417	δ 7.01 (d, 2H), 7.25 (d, 2H), 7.83 (d, 2H), 8.10 (d, 2H), 9.12 (br s, 1H, D_2O exchangeable)	51.14 51.15	2.76 2.78	25.56 25.57	328.03
MS418	δ 2.13 (s, 3H), 2.34 (s, 3H), 6.56 (d, 1H), 6.87-6.92 (m, 2H) 7.81 (d, 2H), 8.10 (d, 2H), 8.76 (br s, 1H, D_2O exchangeable)	59.61 59.63	4.38 4.40	26.07 26.09	322.10
MS419	δ 2.14 (s, 3H), 2.35 (s, 3H), 6.66-6.70 (m, 2H), 6.90 (d, 2H), 7.81 (d, 2H), 8.09 (d, 2H), 9.66 (br s, 1H, D_2O exchangeable)	59.61 59.61	4.38 4.39	26.07 26.08	322.10

MS420	δ 2.16 (s, 6H), 6.65 (t, 1H), 6.96 (d, 2H), 7.82 (d, 2H), 8.03 (d, 2H), 9.65 (br s, 1H , D_2O exchangeable)	59.61 59.62	4.38 4.39	26.07 26.08	322.10
MS421	δ 1.42-1.53 (m, 10H), 2.08-2.17 (m, 6H), 2.91 (t, 2H), 3.01 (t, 2H), 6.92 (d, 2H), 7.13 (d, 2H), 9.32 (br s, 1H, D_2O exchangeable)	51.07 51.09	4.87 4.90	16.24 16.28	516.09
MS422	δ 1.42-1.53 (m, 10H), 2.08-2.15 (m, 6H), 2.94 (t, 2H), 3.02 (t, 2H), 7.02 (d, 2H), 7.22 (d, 2H), 9.08 (br s, 1H, D_2O exchangeable)	55.86 55.86	5.33 5.35	17.77 17.79	474.14
MS423	δ 1.43-1.54 (m, 10H), 2.09-2.17 (m, 9H), 2.35 (t, 3H), 2.92 (t, 2H), 3.02 (t, 2H), 6.59 (d, 1H), 6.88-6.93 (m, 2H), 9.63 (br s, 1H, D_2O exchangeable)	61.78 61.79	6.48 6.48	18.01 18.02	467.22
MS424	δ 1.43-1.53 (m, 10H), 2.08-2.15 (m, 9H), 2.35 (s, 3H), 2.91 (t, 2H), 3.03 (t, 2H), 6.65-6.69 (m, 2H), 6.89 (d, 2H), 9.64 (br s, 1H, D_2O exchangeable)	61.78 61.79	6.48 6.51	18.01 18.03	467.22
MS425	δ: 1.42-1.54 (m, 10H), 2.07-2.17 (m, 6H), 2.25 (s, 6H), 2.93 (t, 2H), 3.02 (t, 2H), 6.66 (t, 1H), 6.97 (d, 2H), 9.62 (br s, 1H, D_2O exchangeable)	61.78 61.80	6.48 6.49	18.01 18.03	467.22

8.2 Pharmacology

8.2.1 Acetic acid Induced Writhing Model

Table 8.3 Neurotoxicity and effect of [MS(401-425)] on writhing induced by acetic acid in mice

Treatment	Neurotoxicity[a]		Acetic Acid Induced Writhing[b]	
	0.5 h	4 h	Number of writhes (30 min)	% Inhibition
Vehicle	-	-	53.0 ± 3.5	-
MS401	-	-	3.5 ± 1.1	93.6*
MS402	-	-	4.5 ± 0.4	91.3*
MS403			17.0 ± 1.4	67.9*
MS404			27.5 ± 4.6	48.2*
MS405	-	-	11.0 ± 0.7	79.3*
MS406	-	-	19.0 ± 1.4	64.6*
MS407	-	-	17.0 ± 2.8	67.9*
MS408	-	-	26.0 ± 1.1	50.9*
MS409	-	-	20.0 ± 1.4	62.2*
MS410	-	-	5.0 ± 2.1	90.2*
MS411	-	-	3.0 ± 0.7	94.0*
MS412	-	-	23.0 ± 1.0	56.6*
MS413			28.5 ± 1.8	46.2*
MS414	-	-	27.5 ± 0.4	48.2*
MS415	-	-	39.5 ± 2.5	25.5
MS416	-	-	24.5 ± 1.8	53.8*
MS417	-	-	22.5 ± 1.1	57.5*
MS418	-	-	16.0 ± 3.5	69.8*
MS419	-	-	22.0 ± 0.7	58.5*
MS420	-	-	4.0 ± 0.6	92.6*
MS421	-	-	25.5 ± 1.1	51.9*
MS422	-	-	20.0 ± 1.4	62.2*
MS423	-	-	17.0 ± 3.2	68.0*
MS424			29.5 ± 3.9	44.3*
MS425	-	-	12.5 ± 1.1	76.4*
Indomethacin[c]			2.0 ± 4.6	96.1*

[a]Doses of 30, 100 and 300 mg/kg were administered. The figures in the table indicate the minimum dose whereby bioactivity was demonstrated in half or more of the mice (three in each group). The animals were examined at 0.5 and 4 h. The line (-) indicates an absence of neurotoxicity at the maximum dose tested. [b]A single dose of test compounds (100 mg/kg, *i.p.*) was administered to each of the mice. *denotes significantly different from the vehicle control at $p<0.05$. [c] Indomethacin was tested at the dose of 10 mg/kg *i.p.*

8.2.2 Formalin Test

Table 8.4 Effect of [MS(401-425)] on formalin induced pain in mice

Treatment	Formalin Induced Flinchings			
	Phase-I (0-5 min)	% Inhibition	Phase-II (10-30 min)	% Inhibition
Vehicle	57.5 ± 4.8	-	73.5 ± 0.8	-
MS401	50.0 ± 1.4	13.4	23.0 ± 0.7	68.5*
MS402	20.0 ± 7.8	65.5*	7.0 ± 1.4	90.9*
MS403	31.5 ± 2.5	45.2*	22.5 ± 1.1	69.8*
MS404	50.1 ± 0.1	13.4	32.0 ± 7.1	56.3*
MS405	32.5 ± 1.1	43.4*	27.5 ± 6.7	62.4*
MS406	33.5 ± 4.3	41.5*	17.5 ± 1.8	76.8*
MS407	30.0 ± 4.9	47.9*	9.5 ± 1.4	87.9*
MS408	31.5 ± 3.4	47.7*	10.5 ± 1.0	86.4*
MS409	32.2 ± 4.5	43.8*	27.0 ± 2.8	63.4*
MS410	28.5 ± 1.8	50.5*	10.5 ± 1.1	85.7*
MS411	21.1 ± 1.4	63.4*	11.5 ± 3.2	84.1*
MS412	15.5 ± 1.7	73.2*	27.5 ± 1.8	62.1*
MS413	20.5 ± 1.4	65.3*	24.0 ± 5.63	67.9*
MS414	44.0 ± 2.5	23.4	27.5 ± 1.8	62.3*
MS415	51.5 ± 1.8	10.9	24.5 ± 4.6	66.6*
MS416	34.1 ± 2.6	40.4*	8.0 ± 2.1	89.9*
MS417	25.3 ± 4.9	56.0*	21.0 ± 10.6	71.7*
MS418	44.5 ± 2.8	22.6	34.1 ± 7.4	53.6*
MS419	30.0 ± 2.1	47.9*	6.5 ± 1.1	91.5*
MS420	27.0 ± 2.5	52.3*	4.5 ± 0.4	93.5*
MS421	21.1 ± 5.6	63.5*	30.5 ± 1.9	58.3*
MS422	21.1 ± 3.5	63.1*	23.5 ± 1.8	68.1*
MS423	22.1 ± 3.6	61.3*	21.0 ± 0.8	71.0*
MS424	48.5 ± 1.7	15.2	29.0 ± 4.9	60.6*
MS425	29.0 ± 2.8	49.1*	18.5 ± 4.9	74.7*
Indomethacin	54.9 ± 7.4	4.7	20.5 ± 3.1	72.1*

Each value represents the mean ± S.E.M. of six mice.* denotes t significant at $p<0.05$ (One-way ANOVA, followed by post-hoc Dunnett's test). [b] Indomethacin was tested at the dose of 10 mg/kg

8.2.3 Peripheral Nerve Injury CCI

Table 8.5 Effect of [MS(401-425)] on spontaneous pain in CCI model

Treatment	Spontaneous Pain		
	% Reversal in CCI (Mean ± S.E.M.)		
	30 min	60 min	120 min
Vehicle	8.9 ± 1.2	4.6 ± 1.6	4.5 ± 0.2
MS401	68.2 ± 5.5*	52.5 ± 3.8*	15.4 ± 4.6
MS402	89.2 ± 4.2*	79.8 ± 8.4*	81.1 ± 1.3*
MS403	11.2 ± 5.5	19.5 ± 3.8	15.4 ± 4.6
MS404	26.0 ± 6.0	26.8 ± 3.8	3.4 ± 0.3
MS405	62.2 ± 2.2*	54.0 ± 0.7*	14.3 ± 0.5
MS406	14.2 ± 4.2	19.8 ± 8.4	21.1 ± 1.3
MS407	18.5 ± 9.5	12.2 ± 1.2	14.5 ± 1.9
MS408	26.3 ± 1.1	13.4 ± 7.6	19.1 ± 7.2
MS409	20.9 ± 3.2	14.7 ± 6.7	15.7 ± 3.3
MS410	21.3 ± 1.2	12.1 ± 1.1	21.1 ± 1.1
MS411	94.6 ± 1.0*	87.0 ± 4.3*	67.3 ± 0.3*
MS412	18.5 ± 2.8	21.0 ± 3.9	5.2 ± 0.5
MS413	4.4 ± 1.2	7.4 ± 4.3	30.2 ± 3.3
MS414	12.2 ± 9.5	33.5 ± 9.8	26.8 ± 4.6
MS415	12.3 ± 2.3	7.9 ± 1.1	21.3 ± 2.3
MS416	66.3 ± 1.1*	13.4 ± 7.6	19.1 ± 7.2
MS417	60.9 ± 3.2*	54.7 ± 6.7*	15.7 ± 3.3
MS418	4.4 ± 1.2	67.4 ± 4.3*	50.2 ± 3.3*
MS419	12.1± 3.2	18.8 ± 2.2	2.1 ± 0.2
MS420	77.3 ± 1.2*	87.6 ± 4.4*	62.1 ± 1.5 *
MS421	19.2 ± 2.2	30.0 ± 0.7	14.3 ± 0.5
MS422	61.5 ± 2.8*	12.1 ± 3.9	5.2 ± 0.5
MS423	34.2 ± 2.1	27.7 ± 3.7	15.7 ± 1.9
MS424	18.3 ± 3.8	14.6 ± 3.9	5.2 ± 1.4
MS425	54.2 ± 2.1*	53.7 ± 3.7*	11.7 ± 1.9
GBP	71.2 ± 2.8*	91.2 ± 6.2*	88.8 ± 3.7*

Each value represents the % reversal of allodynia (mean ± S.E.M.) of four rats; * denotes the values (≥ 50%), significantly different from their respective vehicle control at $p < 0.05$ (One-way ANOVA, followed by post-hoc Dunnett's test)

Table 8.6 Antiallodynic effect of [MS(401-425)] against dynamic allodynia in CCI model

Treatment	Dynamic Allodynia		
	% Reversal in CCI (Mean ± S.E.M.)		
	30 min	60 min	120 min
Vehicle	3.4 ± 0.8	2.3 ± 0.3	0.0 ± 0.0
MS401	64.4 ± 3.6*	7.4 ± 3.6	14.0 ± 0.0
MS402	94.9 ± 7.1*	82.9 ± 3.2*	85.9 ± 2.1*
MS403	21.4 ± 1.2	14.3 ± 1.2	12.1 ± 9.3
MS404	17.3 ± 1.2	24.9 ± 3.8	17.3 ± 1.9
MS405	60.2 ± 3.2*	61.2 ± 2.3*	13.0 ± 2.1
MS406	25.2 ± 3.2	32.2 ± 3.2	32.2 ± 2.3
MS407	21.4 ± 1.5	14.3 ± 3.4	7.1 ± 2.1
MS408	11.3 ± 2.1	9.1 ± 6.3	3.6 ± 0.4
MS409	14.8 ± 0.9	22.1 ± 6.4	27.6 ± 6.2
MS410	15.2 ± 9.8	20.6 ± 4.4	15.7 ± 2.3
MS411	96.4 ± 3.6*	58.5 ± 4.3*	58.3 ± 1.2*
MS412	16.4 ± 3.6	18.5 ± 4.3	18.3 ± 1.2
MS413	7.7 ± 0.2	24.5 ± 6.3	7.7 ± 0.1
MS414	20.9 ± 5.2	10.4 ± 9.6	33.2 ± 2.6
MS415	7.1 ± 0.0	3.6 ± 0.4	1.4 ± 0.1
MS416	3.6 ± 0.4	17.7 ± 0.8	3.6 ± 0.1
MS417	17.3 ± 1.9	9.9 ± 5.5	2.2 ± 0.2
MS418	14.3 ± 12.2	17.3 ± 1.2	24.3 ± 9.2
MS419	15.4 ± 2.2	7.7 ± 0.8	19.7 ± 5.3
MS420	98.2 ± 3.2*	51.2 ± 3.0*	53.2 ± 3.0*
MS421	10.2 ± 3.2	1.2 ± 2.3	33.0 ± 2.1
MS422	64.8 ± 0.9*	52.1 ± 6.4*	17.6 ± 6.2
MS423	18.2 ± 3.2	31.2 ± 3.0	21.2 ± 3.0
MS424	5.8 ± 1.4	2.1 ± 0.2	3.6 ± 0.8
MS425	57.8 ± 2.1*	51.1 ± 3.1*	18.3 ± 4.2
GBP	45.4 ± 2.9	59.0 ± 7.4*	53.7 ± 8.3*

Each value represents the % reversal of allodynia (mean ± S.E.M.) of four rats; * denotes the values (≥ 50%), significantly different from their respective vehicle control at $p < 0.05$ (One-way ANOVA, followed by post-hoc Dunnett's test)

Table 8.7 Antiallodynic effect of [MS(401-425)] against cold allodynia in CCI model

Treatment	Cold Allodynia		
	% Reversal in CCI (Mean ± S.E.M.)		
	30 min	60 min	120 min
Vehicle	3.6 ± 0.7	4.3 ± 1.9	5.4 ± 2.1
MS401	70.5 ± 3.1*	59.0 ± 3.1*	10.8 ± 4.0
MS402	85.4 ± 1.4*	75.7 ± 2.4*	70.6 ± 2.2*
MS403	24.8 ± 11.0	19.9 ± 6.1	8.4 ± 1.9
MS404	20.0 ± 2.0	28.0 ± 4.1	3.1 ± 1.1
MS405	15.5 ± 3.1	19.0 ± 3.1	10.8 ± 4.0
MS406	20.4 ± 1.4	35.7 ± 2.4	30.6 ± 2.2
MS407	25.0 ± 9.0	20.5 ± 7.5	6.2 ± 1.8
MS408	26.8 ± 5.4	29.0 ± 3.2	20.4 ± 1.0
MS409	1.2 ± 0.9	3.0 ± 0.8	4.3 ± 2.1
MS410	18.0 ± 4.8	12.6 ± 2.1	9.1 ± 5.7
MS411	66.5 ± 8.5*	61.9 ± 2.6*	13.8 ± 2.0
MS412	65.0 ± 9.0*	10.5 ± 7.5	6.2 ± 1.8
MS413	9.8 ± 2.2	17.3 ± 5.3	15.3 ± 3.4
MS414	25.2 ± 1.2	32.1 ± 4.3	15.3 ± 2.1
MS415	5.6 ± 2.1	1.7 ± 0.8	9.0 ± 1.4
MS416	17.0 ± 1.7	3.8 ± 0.1	1.9 ± 0.2
MS417	16.5 ± 3.8	7.2 ± 0.8	5.2 ± 0.9
MS418	60.2 ± 1.9*	55.1 ± 2.1*	19.1 ± 1.9
MS419	10.1 ± 1.2	7.9 ± 2.3	15.1 ± 0.2
MS420	61.2 ± 2.1*	75.1 ± 1.2*	54.1 ± 3.3*
MS421	16.2 ± 2.4	19.0 ± 1.2	25.1 ± 1.7
MS422	15.3 ± 1.2	28.6 ± 2.1	5.6 ± 0.5
MS423	54.2 ± 1.2*	62.1 ± 4.3*	15.3 ± 2.1
MS424	13.3 ± 1.8	13.6 ± 2.1	18.2 ± 2.1
MS425	56.2 ± 2.4*	59.0 ± 1.2*	15.1 ± 1.7
GBP	43.0 ± 5.2	58.2 ± 7.5*	54.3 ± 4.3*

Each value represents the % reversal of allodynia (mean ± S.E.M.) of four rats; * denotes the values (≥ 50%), significantly different from their respective vehicle control at $p < 0.05$ (One-way ANOVA, followed by post-hoc Dunnett's test)

Table 8.8 Antihyperalgesic effect of [MS(401-425)] in CCI model

Treatment	Mechanical Hyperalgesia		
	% Reversal in CCI (Mean ± S.E.M.)		
	30 min	60 min	120 min
Vehicle	4.7 ± 2.1	4.9 ± 1.0	5.3 ± 0.5
MS401	13.1 ± 1.2	14.1 ± 2.1	17.2 ± 2.1
MS402	83.4 ± 8.9*	82.7 ± 0.2*	78.2 ± 8.9*
MS403	6.2 ± 1.2	3.2 ± 1.2	7.1 ± 1.3
MS404	27.1 ± 1.9	7.3 ± 0.6	2.2 ± 0.2
MS405	61.6 ± 5.8*	58.0 ± 1.3*	11.9 ± 5.9
MS406	72.1 ± 9.0*	69.2 ± 3.2*	18.2 ± 8.9
MS407	9.4 ± 1.2	8.9 ± 1.3	14.3 ± 2.3
MS408	19.0 ± 7.3	20.5 ± 3.9	29.1 ± 6.4
MS409	4.1 ± 0.7	17.8 ± 3.0	12.3 ± 1.2
MS410	10.0 ± 3.0	17.9 ± 3.2	7.0 ± 4.0
MS411	78.2 ± 3.2*	93.5 ± 1.5*	61.2 ± 3.2*
MS412	13.1 ± 2.4	12.9 ± 9.5	21.1 ± 4.1
MS413	23.2 ± 3.4	63.9 ± 9.5*	9.2 ± 1.2
MS414	15.8 ± 2.0	11.2 ± 2.0	11.3 ± 2.3
MS415	23.6 ± 11.1	17.1 ± 4.6	2.2 ± 0.2
MS416	7.5 ± 0.1	13.2 ± 2.1	13.2 ± 1.6
MS417	69.0 ± 7.3*	10.5 ± 3.9	19.1 ± 6.4
MS418	8.8 ± 0.9	8.6 ± 5.0	12.5 ± 1.9
MS419	13.6 ± 5.8	18.0 ± 1.3	15.9 ± 5.9
MS420	88.9 ± 7.8*	58.9 ± 1.2*	13.1 ± 3.2
MS421	4.3 ± 0.34	12.6 ± 5.6	5.8 ± 1.2
MS422	4.2 ± 2.1	18.2 ± 3.9	19.0 ± 2.0
MS423	75.8 ± 2.0*	61.2 ± 2.0*	11.3 ± 2.3
MS424	21.3 ± 9.8	9.4 ± 1.2	4.3 ± 1.3
MS425	65.4 ± 4.2*	8.0 ± 4.3	4.0 ± 1.2
GBP	51.2 ± 2.1*	58.0 ± 3.2*	61.0 ± 2.1*

Each value represents the % reversal of allodynia (mean ± S.E.M.) of four rats; * denotes the values (≥ 50%), significantly different from their respective vehicle control at $p < 0.05$ (One-way ANOVA, followed by post-hoc Dunnett's test)

8.2.4 Peripheral Nerve Injury - PSNL

Table 8.9 Effect of [MS(401-425)] on spontaneous pain in PSNL model

Treatment	Spontaneous Pain		
	% Reversal in PSNL (Mean ± S.E.M.)		
	30 min	60 min	120 min
Vehicle	3.2 ± 0.3	2.9 ± 0.3	1.2 ± 0.1
MS401	73.7 ± 5.5*	58.5 ± 4.0*	9.9 ± 1.7
MS402	91.9 ± 11.5*	67.3 ± 12.3*	61.0 ± 7.2*
MS403	18.7 ± 1.3	22.0 ± 5.3	15.0 ± 9.6
MS404	16.7 ± 2.3	23.9 ± 3.1	12.3 ± 3.5
MS405	52.1 ± 1.3*	60.2 ± 2.9*	2.0 ± 7.3
MS406	29.9 ± 1.5	27.3 ± 2.3	21.0 ± 7.2
MS407	22.6 ± 4.8	8.3 ± 2.1	4.2 ± 2.2
MS408	31.5 ± 1.2	12.4 ± 2.1	21.6 ± 4.2
MS409	23.1 ± 4.4	32.9 ± 5.6	9.8 ± 3.9
MS410	32.2 ± 6.3	32.3 ± 6.4	11.1 ± 5.3
MS411	79.9 ± 8.5*	94.9 ± 5.3*	65.2 ± 3.2*
MS412	15.6 ± 1.8	15.6 ± 3.1	16.3 ± 4.3
MS413	7.9 ± 3.2	6.4 ± 2.1	4.3 ± 2.1
MS414	34.5 ± 2.5	31.6 ± 4.2	29.3 ± 3.8
MS415	16.5 ± 3.2	12.1 ± 9.0	9.8 ± 2.9
MS416	31.2 ± 3.1	28.0 ± 4.0	11.0 ± 7.3
MS417	22.0 ± 5.2	7.0 ± 2.1	7.0 ± 2.2
MS418	71.5 ± 1.2*	12.4 ± 2.1	11.6 ± 4.2
MS419	11.9 ± 4.7	4.3 ± 1.6	1.2 ± 1.7
MS420	91.8 ± 3.2*	79.1 ± 4.2*	74.3 ± 4.3*
MS421	26.7 ± 11.2	21.9 ± 4.3	19.6 ± 5.9
MS422	72.2 ± 6.3*	52.3 ± 6.4*	11.1 ± 5.3
MS423	32.0 ± 4.8*	19.4 ± 8.3	21.5 ± 5.3
MS424	21.3 ± 4.5	11.3 ± 3.4	7.3 ± 3.1
MS425	66.7 ± 11.2*	11.9 ± 4.3	9.6 ± 5.9
GBP	92.2 ± 2.6*	92.3 ± 4.1*	81.4 ± 3.2*

Each value represents the % reversal of allodynia (mean ± S.E.M.) of four rats; * denotes the values (≥ 50%), significantly different from their respective vehicle control at $p < 0.05$ (One-way ANOVA, followed by post-hoc Dunnett's test)

Table 8.10 Antiallodynic effect of [MS(401-425)] against dynamic allodynia in PSNL model

Treatment	Dynamic Allodynia		
	% Reversal in PSNL (Mean ± S.E.M.)		
	30 min	60 min	120 min
Vehicle	4.1 ± 1.0	2.5 ± 0.3	1.9 ± 0.5
MS401	75.2 ± 14.1*	14.8 ± 7.3	22.0 ± 9.3
MS402	82.0 ± 4.1*	89.9 ± 15.1*	90.9 ± 3.2*
MS403	14.5 ± 3.1	14.4 ± 1.9	9.0 ± 2.1
MS404	34.2 ± 3.1	21.1 ± 3.2	21.1 ± 7.3
MS405	63.0 ± 3.2*	53.9 ± 9.0*	12.0 ± 3.0
MS406	22.0 ± 4.1	29.9 ± 15.1	30.9 ± 3.2
MS407	12.9 ± 15.6	23.9 ± 11.2	9.4 ± 1.1
MS408	11.0 ± 2.0	21.0 ± 2.0	8.9 ± 1.4
MS409	38.0 ± 4.1	25.3 ± 11.0	23.2 ± 9.0
MS410	13.2 ± 3.2	11.9 ± 4.9	3.2 ± 1.2
MS411	81.2 ± 7.3*	77.9 ± 6.3*	67.0 ± 4.3*
MS412	11.1 ± 3.1	64.1 ± 3.2*	63.2 ± 5.3*
MS413	21.7 ± 4.2	12.0 ± 3.9	19.6 ± 3.2
MS414	34.0 ± 4.9	29.4 ± 4.0	23.0 ± 1.3
MS415	21.3 ± 4.0	9.8 ± 2.1	5.9 ± 2.0
MS416	17.8 ± 2.0	9.0 ± 1.8	8.9 ± 2.9
MS417	19.8 ± 5.6	14.9 ± 2.8	13.0 ± 3.9
MS418	25.0 ± 8.9	32.0 ± 6.5	11.0 ± 2.0
MS419	32.0 ± 1.2	11.0 ± 3.9	4.1 ± 2.2
MS420	67.0 ± 4.2*	81.1 ± 4.2*	3.4 ± 1.1
MS421	33.0 ± 3.2	23.9 ± 9.0	12.0 ± 3.0
MS422	68.0 ± 4.1*	65.3 ± 11.0*	13.2 ± 9.0
MS423	64.0± 4.9*	59.2 ± 4.0*	13.0 ± 1.3
MS424	14.1 ± 4.5	7.8 ± 2.9	3.9 ± 2.0
MS425	74.0 ± 3.2*	53.5 ± 4.2*	12.7 ± 5.3
GBP	51.2 ± 2.8*	56.0 ± 4.7*	58.0 ± 4.3*

Each value represents the % reversal of allodynia (mean ± S.E.M.) of four rats; * denotes the values (≥ 50%), significantly different from their respective vehicle control at $p < 0.05$ (One-way ANOVA, followed by post-hoc Dunnett's test)

Table 8.11 Antiallodynic effect of [MS(401-425)] against cold allodynia in PSNL model

Treatment	Cold Allodynia		
	% Reversal in PSNL (Mean ± S.E.M.)		
	30 min	60 min	120 min
Vehicle	3.1 ± 0.8	2.5 ± 1.3	2.3 ± 1.2
MS401	60.0 ± 5.6*	59.0 ± 6.5*	17.6 ± 5.2
MS402	97.3 ± 15.2*	68.3 ± 1.2*	55.5 ± 3.0*
MS403	22.2 ± 2.2	24.2 ± 1.2	1.2 ± 0.1
MS404	21.1 ± 1.2	21.9 ± 2.9	1.8 ± 1.0
MS405	64.1 ± 1.1*	61.2 ± 5.6*	20.1 ± 2.2
MS406	7.3 ± 15.2	38.3 ± 1.2	25.5 ± 3.0
MS407	27.4 ± 4.7	21.8 ± 3.8	11.1 ± 4.3
MS408	21.7 ± 3.9	15.6 ± 1.2	6.9 ± 2.8
MS409	9.0 ± 2.1	9.0 ± 3.2	3.2 ± 2.1
MS410	16.2 ± 6.1	15.0 ± 5.2	8.0 ± 1.2
MS411	77.2 ± 5.2*	68.1 ± 12.1*	55.6 ± 1.6*
MS412	67.4 ± 4.7*	19.8 ± 3.2	11.1 ± 4.3
MS413	65.2 ± 3.5*	65.8 ± 1.9*	13.0 ± 4.1
MS414	51.4 ± 3.1*	17.1 ± 2.1	15.3 ± 1.1
MS415	19.1± 1.4	16.7 ± 3.8	17.3 ± 4.1
MS416	15.2 ± 5.2	13.1± 7.5	11.2 ± 11.2
MS417	22.1 ± 3.5	25.8 ± 1.9	23.0 ± 4.1
MS418	16.2 ± 12	16.0 ± 2.9	33.3 ± 1.3
MS419	31.0 ± 1.2	5.6 ± 2.3	4.1 ± 1.2
MS420	78.9 ± 12.8*	60.0 ± 5.8*	55.9 ± 1.3*
MS421	34.1 ± 11.1	21.7 ± 3.0	31.2 ± 5.6
MS422	11.0 ± 1.0	13.9 ± 2.0	18.3 ± 2.9
MS423	67.9 ± 4.5*	54.1 ± 2.3*	4.0 ± 1.1
MS424	19.0 ± 3.4	21.9 ± 2.0	9.3 ± 1.9
MS425	51.7 ± 4.2*	70.7 ± 5.3*	4.3 ± 0.5
GBP	54.0 ± 2.8*	58.0 ± 3.9*	68.0 ± 3.2*

Each value represents the % reversal of allodynia (mean ± S.E.M.) of four rats; * denotes the values (≥ 50%), significantly different from their respective vehicle control at $p < 0.05$ (One-way ANOVA, followed by post-hoc Dunnett's test)

Table 8.12 Antihyperalgesic effect of [MS(401-425)] in PSNL model

Treatment	Mechanical Hyperalgesia		
	% Reversal in PSNL (Mean ± S.E.M.)		
	30 min	60 min	120 min
Vehicle	2.9 ± 0.3	2.8 ± 0.3	5.1 ± 1.0
MS401	24.0 ± 3.2	23.0 ± 4.0	15.0 ± 3.0
MS402	72.2 ± 4.5*	56.2 ± 1.6*	66.1 ± 3.2*
MS403	21.0 ± 3.0	18.9 ± 3.0	3.2 ± 1.0
MS404	21.1 ± 4.5	26.7 ± 5.6	4.5 ± 2.1
MS405	16.3 ± 11.3	5.9 ± 12.0	14.0 ± 5.0
MS406	32.2 ± 4.5	36.2 ± 1.6	22.1 ± 3.2
MS407	18.9 ± 3.0	8.3 ± 3.0	12.0 ± 3.2
MS408	31.0 ± 2.0	34.0 ± 4.0	29.0 ± 3.0
MS409	11.9 ± 11.0	21.3 ± 3.0	3.0 ± 2.0
MS410	21.0 ± 4.0	11.9 ± 4.0	12.0 ± 8.9
MS411	76.4 ± 11.2*	85.4 ± 11.9*	12.4 ± 4.2
MS412	12.9 ± 3.9	12.0 ± 3.4	11.0 ± 3.0
MS413	23.9 ± 3.0	34.0 ± 9.3	3.0 ± 0.9
MS414	23.9 ± 3.8	21.0 ± 1.0	4.8 ± 1.0
MS415	11.0 ± 3.0	4.0 ± 1.0	3.0 ± 1.0
MS416	54.1 ± 4.5*	56.7 ± 5.6*	4.5 ± 2.1
MS417	54.0 ± 2.0*	64.0 ± 4.0*	71.0 ± 3.0*
MS418	23.9 ± 3.0	61.0 ± 9.3*	3.0 ± 0.9
MS419	32.0 ± 4.0	30.9 ± 4.0	12.0 ± 2.0
MS420	72.0 ± 1.2*	77.1 ± 3.0*	61.0 ± 8.0*
MS421	18.0 ± 7.8	3.0 ± 1.2	9.0 ± 1.0
MS422	9.0 ± 4.0	9.0 ± 3.6	29.0 ± 9.0
MS423	53.9 ± 3.8*	61.0 ± 1.0*	14.8 ± 1.0
MS424	12.0 ± 2.0	11.0 ± 2.8	4.0 ± 1.0
MS425	19.0 ± 4.3	28.5 ± 2.9	2.8 ± 2.0
GBP	86.0 ± 2.3 *	91.0 ± 3.7*	56.0 ± 3.3*

Each value represents the % reversal of allodynia (mean ± S.E.M.) of four rats; * denotes the values (≥ 50%), significantly different from their respective vehicle control at $p < 0.05$ (One-way ANOVA, followed by post-hoc Dunnett's test)

Table 8.13 Median effective dose (ED_{50}) of selected MS4XX compounds in PSNL model

Treatment	ED_{50} values (mg/kg) in CCI model (TPE in min)			
	Spontaneous pain	Dynamic allodynia	Cold allodynia	Mechanical hyperalgesia
MS402	17.0 (60)	7.6 (30)	16.9 (60)	14.6 (60)
MS411	13.9 (30)	8.9 (30)	28.7 (30)	13.5 (60)
MS420	22.9 (60)	14.3 (30)	21.4 (60)	12.9 (30)

Table shows the ED_{50} values (mg/kg) in CCI model at different time points calculated at time of peak effect (TPE in min)

Table 8.14 Median effective dose (ED_{50}) of selected MS4XX compounds in PSNL model

Treatment	ED_{50} values (mg/kg) in PSNL model (TPE in min)			
	Spontaneous pain	Dynamic allodynia	Cold allodynia	Mechanical hyperalgesia
MS402	14.9 (30)	13.9 (60)	28.1 (30)	>100
MS411	18.5 (60)	19.5 (30)	21.9 (30)	28.1 (60)
MS420	21.4 (60)	22.7 (60)	>100	>100

Table shows the ED_{50} values (mg/kg) in PSNL model at different time points calculated at time of peak effect (TPE in min)

8.2.5 Efficacy in Carrageenan Induced Paw Edema and TNF-α Quantification

Table 8.15 Effect of MS4XX compounds on carrageenan induced paw edema

Treatment	Change in paw volume (ml), Mean ± S.E.M.			(%) Protection		
	60 min	120 min	180 min	60 min	120 min	180 min
Vehicle	0.23 ± 0.12	0.43 ± 0.12	0.67 ± 0.12	-	-	-
MS402	0.11 ± 0.01	0.21 ± 0.02	0.19 ± 0.01	54.5*	50.4*	71.4*
MS411	0.13 ± 0.04	0.16 ± 0.03	0.15 ± 0.01	43.3*	62.6*	77.2*
MS420	0.11 ± 0.01	0.21 ± 0.02	0.13 ± 0.01	54.7*	50.1*	81.7*
Indomethacin	0.12 ± 0.05	0.17 ± 0.12	0.22 ± 0.11	50.2*	61.2*	66.9*

A single dose of test compounds (100 mg/kg, *i.p.*) was administered to each of the animal. Table shows the change in paw volume (ml) after 1% carrageenan. * represents significance at $p<0.05$ compared to vehicle (One way ANOVA followed by Dunnet Test, n=6). Indomethacin was tested at the dose of 10 mg/kg *i.p.*

Table 8.16 Effect of compounds on TNF-α level

Treatment	TNF-α (pg/ml)	% inhibition of TNF-α production
Vehicle	3175.5 ± 161.6	-
MS402	580.0 ± 94.5	82.6 ± 2.8*
MS411	375.0 ± 49.9	88.8 ± 1.5*
MS420	601.0 ± 104.2	82.0 ± 3.1*

Table shows the concentration of TNF-α in the paw of carrageenan treated animals. * represents the significance at $p<0.05$, compared to vehicle control (One way ANOVA followed by Dunnett's test, n=4). All the compounds were tested at the dose of 100 mg/kg *i.p.*

8.2.6 Nitric Oxide Estimation in Brain and Sciatic Nerve

Table 8.17 Effect of MS4XX compounds on nitric oxide in brain and sciatic nerve

Total Nitrate / Nitrite (% of SHAM control)				
Treatment	**Brain**	**Sciatic Nerve**	**% Inhibition of Nitrosative stress (nitrite)[a]**	
			Brain	**Sciatic nerve**
SHAM	100 ± 7.8	100 ± 3.9	-	-
Vehicle	194.3 ± 15.3	193.7 ± 8.4	-	-
MS402	175.7 ± 0.9	148.0 ± 0.5	19.4	48.7*
MS411	171.6 ± 0.3	138.5 ± 6.9	24.4	58.3*
MS420	173.0 ± 0.8	136.6 ± 4.3	22.3	61.2*

Table shows the concentration of nitric oxide in brain and sciatic nerve after CCI in rats. * represents the significance at $p<0.05$, compared to vehicle control (One way ANOVA followed by Dunnett's test, n=4). All the compounds were tested at the dose of 100 mg/kg *i.p.*

8.2.7 DPPH Scavenging Assay

Table 8.18 DPPH scavenging activity of MS4XX compounds

Treatment	IC_{50} (μM)
MS402	190
MS411	201
MS420	209
Curcumin	135

DPPH radical scavenging activity of test compounds. Values are represented as % scavenging comparedto vehicle, calculated from the average of triplicate experiments

8.2.8 Effect of Compounds on Cannabinoid Receptors

Table 8.19 Effect of MS4XX compounds on cannabinoid receptors

% Replacement of Specific Bound ^{3}H [CP 55,940] on CB_1 receptor by test compounds	
Treatment	**IC_{50}**
MS402	>1 μM
MS411	>1 μM
MS420	>1 μM
% Replacement of Specific Bound ^{3}H [CP 55,940] on CB_2 receptor by test compounds	
Treatment	**IC_{50}**
MS402	>1 μM
MS411	>1 μM
MS420	>1 μM

Equilibrium-competition binding of compounds vs. [^{3}H] CP55940 using either rat brain (CB_1) or rat spleen homogenates (CB_2). The data shown are average of triplicates

8.2.9 Effect of Compounds on Cathepsin S Enzyme

Table 8.20 Effect of compounds on cathepsin S enzyme

Treatment	% inhibition
Vehicle	-
MS402	35.9 ± 2.8
MS411	52.6 ± 1.5*

Inhibition of recombinant human Cathepsin S by test compounds (50 μM) in a fluorescence assay, employing Z-Leu-Leu-Arg-MCA as synthetic substrates. Data represent means of two experiments performed in triplicate

8.2.10 Effect on GABAergic Pathways

Table 8.21 Effect on GABAergic mechanism

Treatment	Antiepileptic Activity (scPIC)[c]	
	30 min	**240 min**
Vehicle	-	-
MS402	100	100
MS411	-	-
MS420	-	-
Diazepam	10	10

The Figures in the table indicate the minimum dose whereby bioactivity was demonstrated in half or more of the mice (n=3). The animals were examined 30 min and 240 min. The line (-) indicates an absence of anticonvulsant activity at the maximum dose tested

8.3 Results and Discussion

8.3.1 Chemistry

The synthesis of substituted triazolo-thiadiazoles was achieved by a three-step process to give the titled compounds in yields ranging between 61% and 81%. The anilines employed for synthesis of phenyl semicarbazides were randomly selected that included 4-bromo, 4-chloro, 2,4-dimethyl, 2,5-dimethyl, and 2,6-dimethyl anilines (Table-8.1). The synthesis of N-spiro GABA was accomplished as reported in our earlier work [249]. The homogeneity of the compounds was monitored by performing TLC. The eluant system for all the compounds was DCM:CH_3OH (9.5:0.5). The NH proton resonated at δ~8.43-9.71 ppm and was found to be D_2O exchangeable. The percentage composition of C,H, N of all the compounds found from elemental analyses were within ± 0.4 % of the theoretical values (Table-8.2).

8.3.2 Efficacy in Acute Pain Models

In the writhing model, all of the compounds tested, except **MS415**, suppressed the acetic acid-induced writhing response significantly ($p<0.05$) in comparison to the control. Compounds **MS401**, **MS402**, **MS405**, **MS410**, **MS411**, **MS420** and **MS425** showed more than 70% inhibition. Of these, **MS411** emerged as the most active with 94.0% inhibition. Standard drug Indomethacin exhibited 96.1% inhibition in this assay at 10 mg/kg (Table-8.3).

In phase-I of formalin test, 19 compounds showed significant inhibition, **MS412** being the most active compound (73.2%), whereas in phase-II of the formalin test, all of the tested compounds exhibited significant inhibition of pain. Twelve compounds showed more than 70% efficacy in phase-II of this model, with **MS420** being most active showing 93.5% inhibition. Indomethacin (10 mg/kg) showed 4.7% inhibition in phase-I, whereas 72.1% inhibition in phase-II. Ten compounds showed efficacy more than Indomethacin in phase-II of formalin test (Table-8.4).

8.3.3 Efficacy in Neuropathic Pain Models (CCI and PSNL)

In the CCI model, compounds **MS402**, **MS411** and **MS420** reversed the spontaneous pain response throughout the time period of testing (30 min – 120 min) similar to gabapentin. Compounds **MS416** and **MS422** were effective only up to 30 min whereas compounds **MS401**, **MS405**, **MS417** and **MS425** were effective up to 60 min. The

onset of action of compound **MS418** was at 60 min. Other compounds were ineffective in this test (Table-8.5).

Three compounds, **MS402**, **MS411** and **MS420** were effective in attenuating the dynamic allodynia throughout the 120 min experiment. Compound **MS401** was effective only up to 30 min of the experiment whereas compounds **MS405**, **MS422** and **MS425** were effective up to 60 min. All other compounds were ineffective in this test (Table-8.6).

In the cold allodynia produced in CCI rats, significant reversal of paw withdrawal durations was observed at all time points by the administration of compounds **MS402** and **MS420**. Gabapentin was found to be effective from 60 to 120 min. Compound **MS412** was effective only up to 30 min whereas compounds **MS401**, **MS411**, **MS418**, **MS423** and **MS425** were effective up to 60 min of the experiment (Table-8.7).

Mechanical hyperalgesia was significantly attenuated at all the time points by **MS402** and **MS411** similar to gabapentin. Compounds **MS417** and **MS425** were effective only up to 30 min whereas compounds **MS405**, **MS406**, **MS420** and **MS423** were effective till 60 min. Compound **MS413** exhibited irregular activity pattern, being effective only at one time point (60 min) (Table-8.8).

Overall, it appears that, in the CCI model of neuropathic pain, compounds that showed promising results include **MS402**, **MS411**, **MS420** and **MS425** effective in four tests, **MS401** and **MS405** effective in three tests and **MS417**, **MS418**, **MS422** and **MS423** effective in two tests.

In the PSNL model, the paw withdrawal durations due to spontaneous ongoing pain were significantly reduced by compounds **MS402**, **MS411** and **MS420** throughout the experiment similar to gabapentin. The compounds **MS418** and **MS425** were effective up to 30 min of the experiment, whereas compounds **MS401**, **MS405** and **MS422** exhibited activity up to 60 min (Table-8.9).

The dynamic allodynia produced in the PSNL model was effectively reversed by compounds **MS402** and **MS411** at all the time points like gabapentin. Compound **MS401** was effective only up to 30 min of the experiment whereas compounds **MS405**, **MS420**, **MS422**, **MS423** and **MS425** were effective up to 60 min of the experiment. The onset of action for compound **MS412** was at 60 min (Table-8.10).

Cold allodynia produced in the PSNL model was completely reversed by the compounds **MS402**, **MS411** and **MS420**. Compounds **MS412** and **MS414** were effective only up to 30 min of the experiment, whereas compounds **MS401**, **MS405**, **MS413**, **MS423** and **MS425** were effective up to 60 min of the experiment (Table-8.11).

Compounds **MS402**, **MS417** and **MS420** significantly reversed mechanical hyperalgesia at all the time points similar to gabapentin. Compounds **MS411**, **MS416** and **MS423** were effective in the first 60 min of the experiment. Compound **MS418** exhibited irregular activity, being effective at only one time point (60 min) (Table-8.12).

Overall, it appears, in the PSNL model, compounds that exhibited promising results included **MS402**, **MS411** and **MS420** effective in four tests, **MS401**, **MS405**, **MS423** and **MS425** effective in three tests and **MS412**, **MS418**, **MS422** effective in two tests.

8.3.4 Structure – Activity Relationships

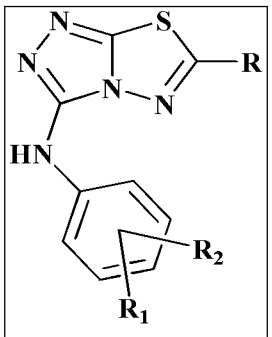

MS401-MS425

The results obtained in the nociceptive assays provide an insight into the structure-activity relationships of the triazolo-thiadiazoles. Functionalisation of the aryl ring of the semicarbazide fragment forming triazolo-thiadiazoles with dimethyl substitutions proved to be advantageous for antinociceptive efficacy. Compounds having 2,4-dimethyl substituted aryl semicarbazide fragment (**MS413**, **MS418** and **MS423**) significantly reversed one or more nociceptive parameters in both CCI and PSNL animals. Introduction of 2,5-dimethyl substituted aryl ring proved to be detrimental for the antinociceptive efficacy in both CCI and PSNL animals. Only one compound **MS414** with 2,5-dimethylphenyl substitution was found to be effective against cold allodynia in PSNL animals. Introduction of electron releasing 2,6-dimethyl

substitution (**MS405**, **MS420** and **MS425**) resulted in significant attenuation of one or more nociceptive parameters in neuropathic animals. Introduction of electron withdrawing halogen (bromo) *para* to the aryl ring resulted in significant activity against one or more nociceptive assays. Compounds with *para* bromo substituted aryl ring like **MS401**, **MS406**, **MS411** and **MS416** were effective in CCI animals whereas compounds **MS401**, **MS411**, **MS416** and **MS421** were found to be effective in one or more nociceptive parameters in PSNL animals. Compounds with *para* chloro substituted aryl ring (**MS402**, **MS412**, **MS417** and **MS422**) resulted in significant attenuation of one or more nociceptive parameters in neuropathic animals.

Accounting for the nociceptive efficacies observed with triazolo-thiadiazoles in the neuropathic pain models, it can be generalized that unlike 2-propylpentanyl substitution at the R_2 position (**MS406-MS410**), 2-aminobutanyl substitution (**MS401**, **MS402** and **MS405**) at R_2 position was beneficial for the activity. Aryl substitution with 4-nitobenzyl group (**MS411-MS415**) and heteroaryl substitution with isonicotinyl group (**MS416**, **MS417**, **MS418** and **MS420**) resulted in significant attenuation of nociceptive parameters. N-spiro GABA substitution (**MS421**, **MS422**, **MS423** and **MS425**) also proved to be additive for the antinociceptive efficacy.

8.3.5 ED_{50} Studies

Compounds exhibiting more than 90% reversal in one or more of the nociceptive assays (**MS402**, **MS411** and **MS420**) were taken further for ED_{50} studies. In the CCI model, compound **MS411** reversed spontaneous pain with an ED_{50} value of 13.9 mg/kg with TPE at 30 min. Compound **MS402** reversed dynamic and cold allodynia with an ED_{50} value of 7.6 and 16.9 mg/kg with TPE at 30 min and 60 min respectively. Compound **MS420** reversed mechanical hyperalgesia with an ED_{50} value of 12.9 mg/kg exhibiting at 30 min (Table-8.13). In the PSNL model, compound **MS402** reversed spontaneous pain and dynamic allodynia with an ED_{50} value of 14.9 mg/kg and 13.9 mg/kg showing TPE at 30 min and 60 min respectively. In cold allodynia and mechanical hyperalgesia, compound **MS411** came out to be the most effective compound with an ED_{50} value of 21.9 mg/kg and 28.1 mg/kg exhibiting TPE at 30 min and 60 min respectively (Table-8.14).

8.3.6 Mechanistic Studies

The selected compounds, **MS402**, **MS411** and **MS420** evaluated in carrageenan induced paw edema model showed a significant reduction in paw edema throughout the period of 180 min (Table-8.15) indicating that the respective compounds could possess some role in exerting their analgesic action through the blockade of peripheral mediators. The carrageenan injected paws were harvested and TNF-α levels were quantified. All the three compounds, **MS402**, **MS411** and **MS420** were found to significantly inhibit TNF-α level (Table-8.16).

As mentioned in the earlier chapters, some selected compounds, **MS402**, **MS411** and **MS420** were tested for their effect on nitric oxide after CCI nerve injury. All the tested compounds exhibited significant reduction ($p<0.05$) of nitric oxide in sciatic nerve (Table-8.17). However, none of the compounds significantly attenuated nitrosative stress in the brain indicating the role of the compounds in inhibition of local nitric oxide. Following nerve injury, oxidative stress exaggregates pain states. The compounds were studied for their free radical scavenging activity using DPPH method. **MS402** exhibited free radical scavenging efficacies activities with an IC_{50} value of 190 μM. Compounds **MS411** and **MS420** exhibited IC_{50} of 201 and 209 μM respectively (Table-8.18).

Compounds **MS402**, **MS411** and **MS420** were studied for their affinity for cannabinoid receptors. However, none of the compounds exhibited significant affinity for CB_1 and CB_2 receptors up to 1 μM (Table-8.19). The compounds **MS402** and **MS411** were also tested for inhibition of cathepsin S, a promising target in the treatment of neuropathic pain. Both the compounds, **MS402** and **MS411** inhibited cathepsin S to 35.9% and 52.6% respectively (Table-8.20). The possible mediation of GABAergic pathway was explored by assessing the anticonvulsant potential of the test compounds in picrotoxin-induced seizure. Among the three compounds tested, **MS402** exhibited protection in the scPIC screen (100 mg/kg) indicating enhancement of peripheral GABAergic neurotransmission (Table 8.21).

In conclusion, utilizing pharmacophoric hybrid approach, a series of structurally novel triazolo-thiadiazoles derivatives were synthesized and evaluated for acute antinociceptive, antiallodynic and antihyperalgesic potentials. In the carrageenan-induced paw edema model, where there is a pronounced local TNF-α response, the

compounds **MS402**, **MS411** and **MS420** significantly inhibited paw swelling as well as localized TNF-α levels, thereby suppressing the inflammatory component of neuropathic pain. The neuroprotection exhibited by the compounds **MS402**, **MS411** and **MS420** was also associated with their free radical scavenging abilities and subsequent attenuation of oxidative and nitrosative stress. Compounds **MS402** and **MS411** significantly inhibited cathepsin S. Also, **MS420** was found to act through GABAergic pathways.

CHAPTER 9

COMPREHENSIVE STRUCTURE-ACTIVITY RELATIONSHIP STUDIES

A comprehensive structure-activity relationship study undertaken on the synthesized compounds in all the series revealed the following findings,

In the acute pain test (acetic acid-induced writhing model), 71 compounds out of 81 suppressed the acetic acid-induced writhing response significantly in comparison to the control. **MS411** (94.0% inhibition of writhing response) emerged as the most active compound.

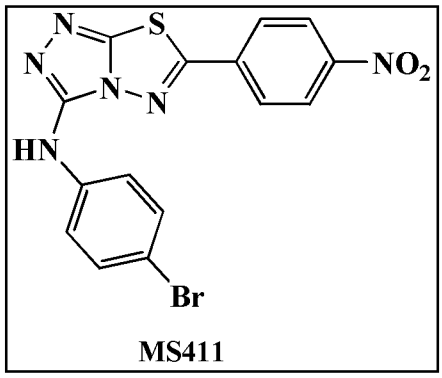

MS411

In the formalin-induced flinching model, series-1 (**MS101-MS116**) significantly suppressed phase-I of the flinching test. Compounds in series-2 (**MS201-MS216**), series-3 (**MS301-MS324**) and series-4 (**MS401-MS425**) were found to inhibit both the phases of the flinching test. The most active compounds in phase-I were **MS312** and **MS412** exhibiting 73.2% inhibition of flinching response. Compound **MS303** (95.5% inhibition of flinching response) emerged as the most active compound in phase-II.

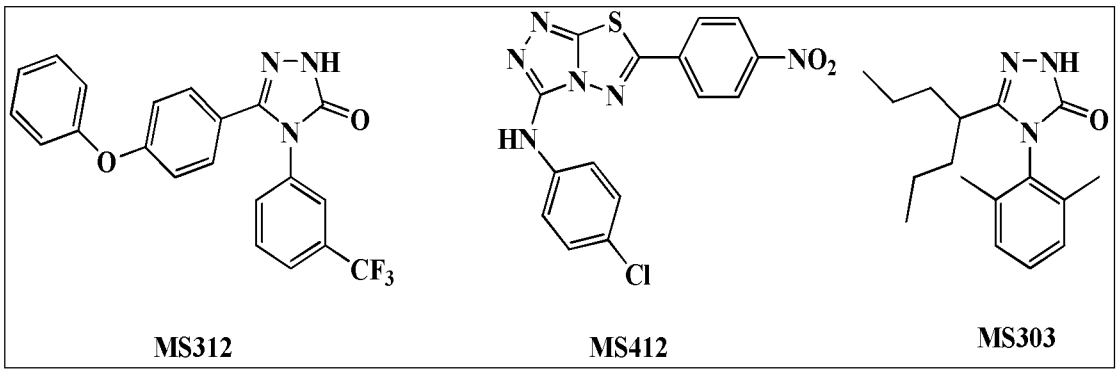

MS312 **MS412** **MS303**

With respect to various substituted phenyl semicarbazides utilized in synthetic schemes 1, 3 and 4, an overview of structure - activity relationships revealed that 2,6-dimethyl substituted semicarbazide fragment in the 1,2,4-triazol-5-ones (**MS303**, **MS315**) and triazolo-thiadiazoles (**MS420**) rendered significant activity against neuropathic pain. 2,4 dimethyl substitution in tetrahydropyrido-pyrazoles (**MS112)** and 1,2,4-triazol-5-ones (**MS319**) was also found to be additive to the activity. However, 2,5-dimethyl substitution was less contributory towards the biological activity in all the 3 series.

Halogen substituted aryl ring resulted in pronounced neuropathic pain activity, both in case of bromo substitution distal to aryl ring (**MS109** and **MS411**) and p-chloro substitution as in **MS110** and **MS402**. 3-Trifluoromethyl substituted phenyl ring in tetrahydropyrido-pyrazoles in synthetic scheme-1 (**MS107** and **MS115**) was unfavorable for biological activity rendering neurotoxicity in case of **MS103**. Also, introduction of 2,4-difluoro substitution (**MS107** and **MS115**) as well as fluoro coupled with methyl group (2-fluoro-5-methyl substitution) in the aryl ring (**MS108** and **MS116**) proved to be detrimental effect for the activity.

The order of activity with respect to various substitutions in the phenyl semicarbazides fragment of the synthesized compounds (tetrahydropyrido-pyrazoles (**MS1XX**), 1,2,4-triazol-5-ones (**MS3XX**) and triazolo-thiadiazoles (**MS4XX**) followed the order, 2,6-dimethyl > 2,4-dimethyl > 4-bromo > 4-chloro > 2,5-dimethyl > 3-trifluoromethyl > 2,4-difluoro > 2-fluoro-5-methyl

With respect to substitution with various aliphatic, aryl and hetero-aryl acids in tetrahydropyrido-pyrimidines (**MS2XX**), 1,2,4-triazol-5-ones (**MS3XX**) and triazolo-thiadiazoles (**MS4XX**), study of structure-activity relationships revealed that substitution with aliphatic acids, 2-propylpentanyl in triazol-5-ones (**MS303**) and 4-aminobutanyl in triazolo-thiadiazoles (**MS402**) resulted in pronounced activity.

Aryl substitution with 4-phenoxyphenyl group proved to be detrimental for the activity. However, 4-nitrobenzyl substitution in tetrahydropyrido-pyrimidines (**MS214**) and triazolo-thiadiazoles (**MS411**) resulted in significant activity against neuropathic pain.

Three hetero-aryl acids with isosnicotinyl, 2-pyrazinyl and 2-nitro-5-furyl substitution were utilized in synthetic schemes 2, 3 and 4. Isonicotinyl substitution proved to be

additive for activity in **MS216** and **MS420**. 2-Nitro-5-furyl (**MS315**) and 2-pyrazinyl (**MS319**) substitution were favorable for activity in triazol-5-ones.

A comparison of structure-activity relationship aspects of fused pyrazole based heterocycles revealed that tetahydropyrido-pyrazoles were more effective against neuropathic pain as compared to tetrahydropyrido-pyrimidines derivatives.

The most active compounds that have been found to be effective in both the neuropathic pain models were **MS109**, **MS110**, **MS112**, **MS214**, **MS216**, **MS303**, **MS315**, **MS319**, **MS402**, **MS411** and **MS420**. Of these, compound **MS420** exhibited antinociceptive activity (98.2%), 2 times more than that of the standard drug gabapentin in the dynamic allodynia assay (CCI).

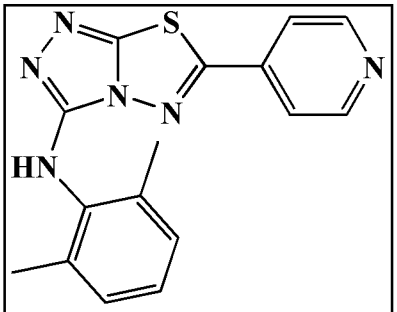

MS420

CHAPTER 10

SUMMARY & CONCLUSIONS

The present work was aimed at the design and synthesis of novel multifunctional leads for the treatment of neuropathic pain.

- A total of 81 compounds containing tetrahydropyrido-pyrazole (**16** compounds), tetrahydropyrido-pyrimidine (**16**), 1,2,4-triazol-5-one (**24**) and [1,2,4]-triazolo-[3,4-b]-1,3,4-thiadiazole (**25**) scaffolds were synthesized and evaluated for neurotoxicity and antinociceptive efficacies in acute and chronic models of pain.
- The structures of the synthesized compounds were confirmed by spectral analysis besides elemental analysis.
- Following assessment of neurotoxicity, acute antinociceptive efficacy of the synthesized compounds was assessed using two acute models of pain, acetic acid-induced writhing and formalin test. In the acetic acid-induced writhing model, 71 compounds out of 81 compounds, suppressed the acetic acid-induced writhing response significantly in comparison to the control. **MS411** (94.0% inhibition of writhing response) emerged as the most active compound. In the formalin-induced flinching model, series-1 (**MS101-MS116**) significantly suppressed phase-I of the flinching test. Compounds in series-2 (**MS201-MS216**), series-3 (**MS301-MS324**) and series-4 (**MS401-MS425**) were found to inhibit both the phases of the flinching test. The most active compounds in phase-I were **MS312** and **MS412** exhibiting 73.2% inhibition of flinching response. Compound **MS303** (95.5% inhibition of flinching response) emerged as the most active compound in phase-II.
- In another set of studies, two animal models of chronic pain (neuropathic pain), the chronic constriction injury (CCI) and partial sciatic nerve ligation (PSNL) models were used to evaluate the synthesized compounds for antineuralgic efficacy.
- In the CCI model, significant reversal of spontaneous pain was observed with 40 compounds, significant reversal of dynamic allodynia with 29 compounds, cold allodynia by 33 compounds, whereas mechanical hyperalgesia was significantly reversed by 30 compounds.

- In PSNL model, spontaneous pain was significantly reversed by 36 compounds, dynamic allodynia by 41 compounds, cold allodynia by 42 compounds, whereas 42 compounds significantly reversed mechanical hyperalgesia.
- Of the four series studied in animal models of peripheral neuropathic pain, series-1 (tetrahydropyrido-pyrazoles) was most active in all the behavioral assays.
- Based on number of compounds active in each series, the order of activity in the CCI model was found to follow the trend: series 1 > series 2 ~ series 4 > series 3. Similarly, the trend observed in case of PSNL model was series 1 ~ series 2 > series 4 > series 3.
- Eleven compounds, exhibiting more than 90% reversal in one or more nociceptive assays in the neuropathic animals, were taken further for median effective dose (ED_{50}) studies in CCI and PSNL model.
- In the CCI model, compound **MS110** was the most potent in spontaneous pain assay (ED_{50} = 10.4 mg/kg, peak effect at 60 min), **MS402** in dynamic allodynia (ED_{50} = 7.6 mg/kg, peak effect at 30 min), **MS319** in cold allodynia (ED_{50} = 14.9 mg/kg, peak effect at 30 min) and **MS420** in mechanical hyperalgesia (ED_{50} = 12.9 mg/kg, peak effect at 30 min).
- In PSNL model, compound **MS112** showed maximum reversal of spontaneous pain (ED_{50} = 7.4 mg/kg, peak effect at 30 min), similarly **MS402** in dynamic allodynia (ED_{50} = 13.9 mg/kg, peak effect at 60 min), **MS411** in cold allodynia (ED_{50} = 21.9 mg/kg, peak effect at 30 min) and **MS315** in mechanical hyperalgesia (ED_{50} = 16.6 mg/kg, peak effect at 60 min) exhibited highest reversal.
- Further studies were carried out on the selected compounds to evaluate their underlying mechanism of action in neuropathic pain. Among 11 compounds, 10 compounds (**MS110**, **MS112**, **MS214**, **MS216**, **MS303**, **MS315**, **MS319**, **MS402**, **MS411** and **MS420**) exhibited significant reduction in carrageenan induced paw edema, indicating their probable role in reducing peripheral inflammatory mediators. Quantification of TNF-α level in the carrageenan injected paw showed that 8 compounds (**MS109**, **MS110**, **MS112**, **MS315**, **MS319**, **MS402**, **MS411** and **MS420**) inhibited TNF-α. Compound **MS411** exhibited the highest inhibition of TNF-α (88.8%).

- The putative role of nitric oxide (NO) in the pathophysiology of chronic nerve ligation as evident by significant increase in nitrite and nitrate levels in both brain and sciatic nerve led us to estimate the levels of nitrite, metabolite of NO, in the brain and sciatic nerve of CCI rats. Eight compounds (**MS109**, **MS110**, **MS216**, **MS315**, **MS319**, **MS402**, **MS411** and **MS420**) inhibited nitric oxide in the sciatic nerve indicating inhibition of local nitric oxide by the compounds. **MS319** emerged as the most potent compound in the inhibition of nitric oxide (62.9%inhibition) in the sciatic nerve. None of the compounds were found to inhibit nitric oxide in the brain. The compounds also exhibited free radical scavenging activities in the DPPH (2-Diphenyl-1-picrylhydrazyl) assay thereby providing neuro-protection by the reduction of oxidative stress. The most potent compound in the DPPH assay was found to be **MS109** with an IC_{50} value of 81 μM.
- Further mechanistic studies were performed to assess the potential role of the selected compounds on some new targets of neuropathic pain like GABA, cannabinoid receptors (CB_1 and CB_2) and cathepsin S. In the subcutaeneous picrotoxin (scPIC)-induced seizure threshold test, 4 compounds (**MS109**, **MS112**, **MS319** and **MS402**) showed protection suggesting that these compounds act by GABA mediation. Radioligand binding assays were performed to assess the potential of the compounds to modulate cannabinoid (CB) receptors CB_1 in brain and CB_2 in spleen of rats. One compound (**MS109**) showed selective modulation in CB_1 assay with an IC_{50} of 49.6 nM with no effect on CB_2 receptor. The compounds were also screened for their inhibitory potential on the cysteine protease cathepsin S implicated in neuropathic pain. One compound (**MS411**) showed more than 50% inhibition of cathepsin S at 50 μM concentration.
- Neuropathic pain syndromes encompass wide range of symptoms likely to be mediated by multiple mechanisms. Therefore, blockade of just one of these mechanisms may not provide full pain relief in every patient. A better approach may be, as in this case, designing and developing novel compounds with more than just one mechanism of actions. Overall compounds showing multiple mechanisms for neuropathic pain could have a better candidature for future development.

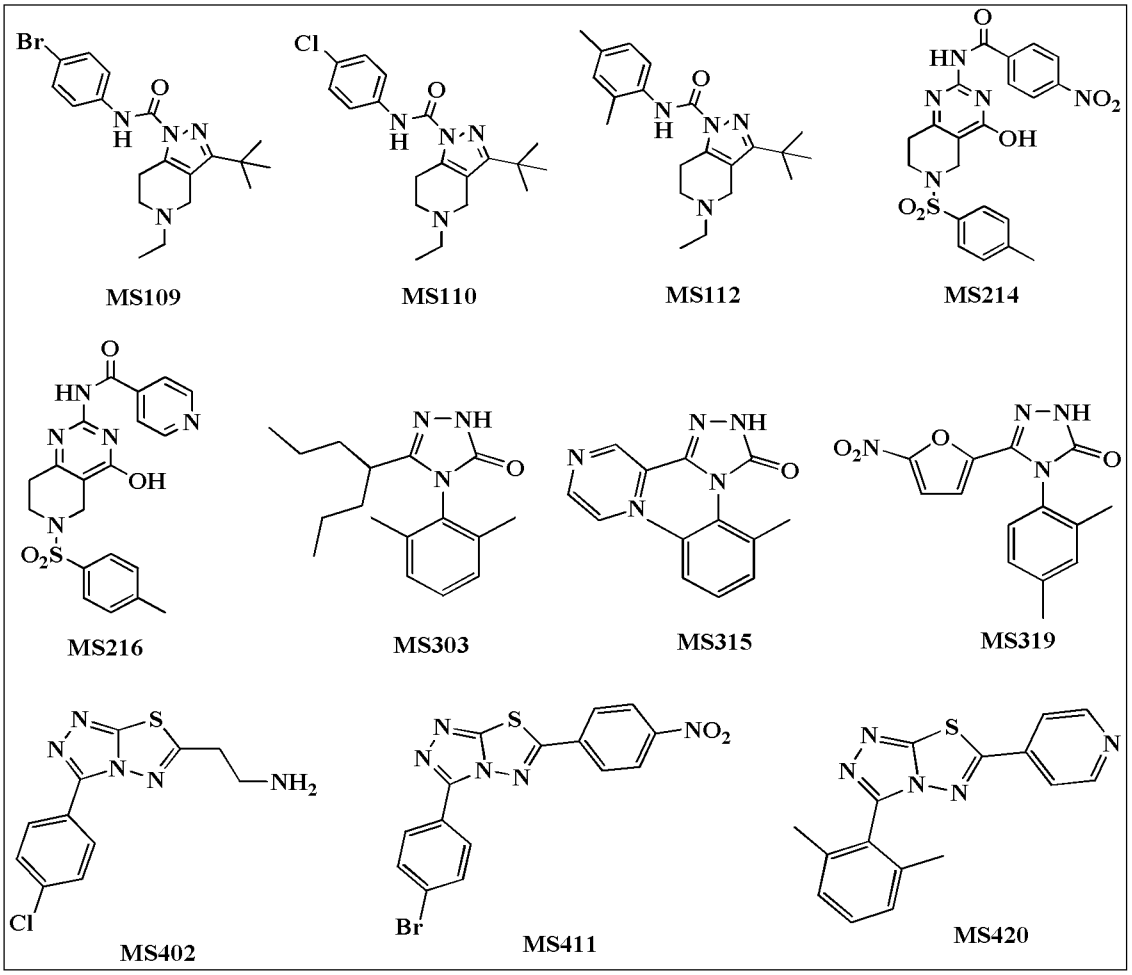

Figure10.1. Structures of most active compounds in neuropathic pain

FUTURE PERSPECTIVES

The present work elucidates the potential of some multifunctional leads to possess antinociceptive activities in various animal models of neuropathic pain.

As for antinociceptive activity, the studies could be extended further to various other nerve injury models involving the spared nerve injury (SNI) and spinal nerve ligation(SNL) models as well as disease induced neuropathy (diabetic neuropathy, cancer induced neuropathy, trigeminal neuralgia) and post-operative pain conditions.

Although all of the synthesized compounds have been found to possess a broad spectrum of activity, extensive studies are still required to confirm the hypothesized mechanisms of action of the compounds. In particular, the effect of compounds on other inflammatory cytokines (IL-1, IL-6) and other mediators, effect on electrophysiological parameters using whole-cell patch clamp experiments, radioligand binding assays for GABA receptors.

Oral efficacies of the compounds along with pharmacokinetic studies to determine bioavailability, half life, C_{max} etc. should be undertaken. Metabolism and elimination pattern of the compounds are yet to be explored.

REFERENCES

1. Merskey H and Bogduk N, IASP pain terminology, In: Classification of Chronic Pain. Bogduk H. (Eds), IASP, Seattle; 1994:209-14.
2. Baron R. Peripheral neuropathic pain: from mechanisms to symptoms. The Clinical Journal of Pain. 2000; 16:12-20.
3. Voscopoulos C, Lema M. When does acute pain become chronic? Br J Anaesth. 2010; 105:169-85.
4. Macefield VG. Physiological characteristics of low-threshold mechanoreceptors in joints, muscle and skin in human subjects. Clin Exp Pharmacol Physiol. 2005; 32:135-44.
5. Ueda H, Rashid MH, Molecular mechanisms of neuropathic pain. Drug News Perspect. 2003; 16:605-13.
6. Lee Y, Lee CH, Oh U. Painful channels in sensory neurons. Mol Cells. 2005; 20:315-24.
7. Kennedy JD. Neuropathic pain: molecular complexity underlies continuing unmet medical need. J Med Chem. 2007; 50:2547-56.
8. D'Mello R, Dickenson AH. Spinal cord mechanisms of pain. Br J Anaesth. 2008; 101:8-16.
9. Woolf CJ, Mannion RJ. Neuropathic pain: aetiology, symptom mechanisms and management. Lancet. 1999; 353:1959-64.
10. Jensen TS, Baron R. Translation of symptoms and signs into mechanisms in neuropathic pain. Pain. 2003; 102:1-8.
11. Zimmermann M. Pathobiology of neuropathic pain. Euro J Pharmacol. 2001; 429:23-37.
12. Claudia S. Painful neuropathies. Curr Opin Neurol. 2003; 16:623-28.
13. Backonja MM, Serra J. Pharmacologic management part 2: lesser-studied neuropathic pain diseases. Pain Med. 2004; 5:S48-S59.
14. Siddall PJ, Taylor DA, McClelland JM, Rutkowski SB, Cousins MJ. Pain report and the relationship of pain to physical factors in the first six months following spinal cord injury. Pain. 1999; 81:187-97.

15. Bernabei R, Gambassi G, Lapane K, Landi F, Gatsonis C, Dunlop, R, Lipsitz L, Steel K, Mor V. Management of pain in elderly patients with cancer. JAMA. 1998; 279:1877-82.

16. Scholz J, Broom DC, Youn DH. Blocking caspase activity prevents transsynaptic neuronal apoptosis and the loss of inhibition in lamina II of the dorsal horn after peripheral nerve injury. J Neurosci. 2005; 25:7317-23.

17. Julius D, Basbaum AI, Molecular mechanisms of nociception. Nature. 2001; 413:203-10.

18. Attal N, Bouhassira D. Mechanisms of pain in peripheral neuropathy. Acta Neurol Scand Suppl. 1999; 173:12-24.

19. Bridges D, Thompson SW, Rice AS. Mechanisms of neuropathic pain. Br J Anaesth. 2001; 87:12-26.

20. Waxman SG, Kocsis JD, Black JA. Type III sodium channel mRNA is expressed in embryonic but not adult spinal sensory neurons, and is reexpressed following axotomy. J Neurophysiol. 1994; 72:466-70.

21. Everill B, Kocsis JD. Reduction in potassium currents in identified cutaneous afferent dorsal root ganglion neurons after axotomy. J Neurophysiol. 1999; 82:700-08.

22. McGivern JG. Targeting N-type and T-type calcium channels for the treatment of pain. Drug Discov Today. 2006; 11:245-53.

23. Yaksh TL. Calcium channels as therapeutic targets in neuropathic pain. J Pain. 2006; 7:S13-S30.

24. Hudson LJ, Bevan S, Wotherspoon G, Gentry C, Fox A, Winter J. VR1 protein expression increases in undamaged DRG neurons after partial nerve injury. Eur J Neurosci. 2001; 13:2105-14.

25. Tohda C, Sasaki M, Konemura T, Sasamura T, Itoh M, Kuraishi Y. Axonal transport of VR1 capsaicin receptor mRNA in primary afferents and its participation in inflammation induced increase in capsaicin sensitivity. J Neurochem. 2001; 76:1628-35.

26. Mcgaraughty S, Jarvis MF. Purinergic control of neuropathic pain. Drug Dev Res. 2006; 67:376-88.

27. Ballini E, Virginio C, Medhurst SJ, Summerfield SG, Aldegheri L, Buson A, Carignani C, Chen YH, Giacometti A, Lago I, Powell AJ, Jarolimek W. Characterization of three diaminopyrimidines as potent and selective antagonists of $P2X_3$ and $P2X_{2/3}$ receptors with in vivo efficacy in a pain model. Br J Pharmacol. 2011; 163:1315-25.

28. Hökfelt T, Zhang X, Wiesenfeld-Hallin Z. Messenger plasticity in primary sensory neurons following axotomy and its functional implications. Trends Neurosci. 1994; 17:22-30.

29. Seltzer Z, Dubner R, Shir Y. A novel behavioral model of neuropathic pain disorders produced in rats by partial sciatic nerve injury. Pain. 1990; 43:205-18.

30. Jones MG, Munson JB, Thompson SW. A role for nerve growth factor in sympathetic sprouting in rat dorsal root ganglia. Pain. 1999; 79:21-29.

31. Michaelis M, Vogel C, Blenk KH, Jänig W.Algesics excite axotomised afferent nerve fibres within the first hours following nerve transection in rats. Pain. 1997; 72:347-54.

32. Michaelis M, Vogel C, Blenk KH, Arnarson A, Janig W. Inflammatory mediators sensitize acutely axotomized nerve fibers to mechanical stimulation in the rat. J Neurosci. 1998; 18:7581-87.

33. Lindenlaub T, Sommer C. Cytokines in sural nerve biopsies from inflammatory and non-inflammatory neuropathies. Acta Neuropathol. 2003; 105:593-602.

34. England S, Bevan S, Docherty RJ. PGE2 modulates the tetrodotoxin-resistant sodium current in neonatal rat dorsal root ganglion neurones via the cyclic AMP-protein kinase A cascade. J Physiol. 1996; 495:429-40.

35. Woolf CJ. The pathophysiology of peripheral neuropathic pain abnormal peripheral input and abnormal central processing. Acta Neurochir Suppl. 1993; 58:125-30.

36. Ikeda H, Heinke B, Ruscheweyh R, Sandkühler J. Synaptic plasticity in spinal lamina I projection neurons that mediate hyperalgesia. Science. 2003; 299:1237-40.

37. Woolf CJ, Salter MW. Neuronal plasticity: increasing the gain in pain. Science. 2000; 288:1765-69.

38. Latremoliere A, Woolf CJ. Central sensitization: a generator of pain hypersensitivity by central neural plasticity. J Pain. 2009; 10:895-26.

39. Bennett DL, French J, Priestley JV, McMahon SB. NGF but not NT-3 or BDNF prevents the A fiber sprouting into lamina II of the spinal cord that occurs following axotomy. Mol Cell Neurosci. 1996; 8:211-20.

40. Garry EM, Jones E, Fleetwood-Walker SM. Nociception in vertebrates: key receptors participating in spinal mechanisms of chronic pain in animals. Brain Res Rev. 2004; 46:216-24.

41. Scholz J, Woolf CJ. Can we conquer pain? Nat Neurosci. 2002; 5:1062-67.

42. Basbaum AI, Bautista DM, Scherrer G, Julius D. Cellular and Molecular Mechanisms of Pain. Cell; 139:267-84.

43. Coull JA, Beggs S, Boudreau D, Boivin D, Tsuda M, Inoue K, Gravel C, Salter MW, De Koninck Y. BDNF from microglia causes the shift in neuronal anion gradient underlying neuropathic pain. Nature. 2005; 438:1017-21.

44. Clark, AK, Yip PK, Malcangio M. The liberation of fractalkine in the dorsal horn requires microglial cathepsin S. J. Neurosci. 2009; 29:6945-54.

45. Pertovaara A, Kontinen VK, Kalso EA. Chronic spinal nerve ligation induces changes in response characteristics of nociceptive spinal dorsal horn neurons and in their descending regulation originating in the periaqueductal gray in the rat. Exp Neurol. 1997; 147:428-36.

46. Manzanares J, Julian MD, Carrascosa A. Role of the cannabinoid system in pain control and therapeutic implications for the management of acute and chronic pain episodes. Curr Neuropharmacol. 2006; 4:239-57.

47. Moore KA. Partial peripheral nerve injury promotes a selective loss of GABAergic inhibition in the superficial dorsal horn of the spinal cord. J Neurosci. 2002; 22: 6724-31.

48. Vanderah TW, Gardell LR, Burgess SE, Ibrahim M, Dogrul A, Zhong CM, Zhang ET, Malan TP Jr, Ossipov MH, Lai J, Porreca F. Dynorphin promotes abnormal pain and spinal opioid antinociceptive tolerance. J Neurosci. 2000; 20:7074-79.

49. Wieseler-Frank J. Central proinflammatory cytokines and pain enhancement. Neurosignals. 2005; 14:166–74.

50. Morris M. Antidepressants and antiepileptic drugs for chronic non-cancer pain. Am Fam Physician. 2005; 71:483-90.
51. Backonja MM. Use of anticonvulsants for treatment of neuropathic pain. Neurology. 2002; 59:S14–S17.
52. Bergouigan M. Cures heureuses de nevralgies facials essentielles parle diphenylhydantoinate de soude. Rev Laryngol Otol Rhinol. 1942; 63:34-41.
53. Chadda VS, Mathur M. Double-blind study of the Effect of diphenylhydantoin sodium on diabetic neuropathy. J Assoc Physicians India. 1978; 26:403-06.
54. Saudek CD, Werns S, Reidenberg MM. Phenytoin in the treatment of diabetic symmetrical neuropathy. Clin Pharmacol Ther. 1977; 22:196-99.
55. McCleane GJ. Intravenous infusion of phenytoin relieves neuropathic pain: a randomized, double-blind, placebo-controlled, crossover study. Anesth Analg. 1999; 89:985-88.
56. McNamara J. Drugs acting on the central nervous system. In: Harman G, Limbird LE, Morinoff PB, Ruddon RW, eds. Goodman and Gilman's the pharmacological basis of therapeutics. 9th ed. New York: McGraw-Hill, 1996:461-86.
57. Simpson DM, Onley R, McArthur JC, Khan A, Godbold J, Ebel-Frommer K. A placebo-controlled trial of lamotrigine for painful HIV-associated neuropathy. Neurology. 2000; 54:2115-19.
58. Rowbotham M, Harden N, Stacey B, Bernstein P, Magnus-Miller L. Gabapentin for the treatment of postherpetic neuralgia: A randomized controlled trial. JAMA. 1998; 280:1837-42.
59. Backonja M, Beydoun A, Edwards KR, Schwartz SL, Fonseca V, Hes M, LaMoreaux L, Garofalo E. Gabapentin for the treatment of painful neuropathy in patients with diabetes mellitus: A randomized controlled trial. JAMA. 1998; 280:1831-36.
60. Charles PT, Timothy A, Faumanc E. Pharmacology and mechanism of action of pregabalin: The calcium channel 2(alpha2-delta) subunit as a target for antiepileptic drug discovery. Epilepsy Res. 2007; 73:137-50.
61. Sullivan MD, Robinson JP Antidepressant and anticonvulsant medication for chronic pain. Phys Med Rehabil Clin N Am. 2006; 17:381-400.

62. Woodforde JM, Dwyer B, McEwen BW. Treatment of post-herpetic neuralgia. Med J Aust. 1965; 2:869-72.
63. Watson CP, Evans RJ, Reed K. Amitriptyline versus placebo in postherpetic neuralgia. Neurology. 1982; 32:671-73.
64. Kvinesdal B, Molin J, Froland A. Imipramine treatment of painful diabetic neuropathy. JAMA. 1984; 251:1727-30.
65. Sindrup SH, Gram LF, Brosen K. The selective serotonin reuptake inhibitor paroxetine is effective in the treatment of diabetic neuropathy symptoms. Pain. 1990; 42:135-44.
66. Sindrup SH, Bjerre U, Bejgaard A. The selective serotonin reuptake inhibitor citalopram relieves the symptoms of diabetic neuropathy. Clin Pharmacol Ther. 1992; 52:547-52.
67. Taylor K, Rowbotham MC. Venlafaxine hydrochloride and chronic pain. West J Med. 1996; 165:147-48.
68. Portenoy RK. Chronic opioid therapy in nonmalignant pain. J Pain Symptom Manage. 1990; 5:S46-S62.
69. Watson CP, Babul N. Efficacy of oxycodone in neuropathic pain: a randomized trial in postherpetic neuralgia. Neurology. 1998; 50:1837-41.
70. Harati Y, Gooch C, Swenson M. Double-blind randomized trial of tramadol for the treatment of the pain of diabetic neuropathy. Neurology. 1998; 50:1842-46.
71. Anderson VC, Burchiel KJ. A prospective study of long-term intrathecal morphine in the management of chronic nonmalignant pain. Neurosurg. 1999; 44:289-300.
72. Devers A, Galer BS. Topical lidocaine patch relieves a variety of neuropathic pain conditions: an open-label study. Clin J Pain. 2000; 16:205-8.
73. Teng James. Neuropathic Pain: Mechanisms and treatment options. Pain Practice. 2003; 3:8-21.
74. Porter RJ, Rogawski MA. New antiepileptic drugs: from serendipity to rational discovery. Epilepsia. 1992; 33:S1-6.
75. Serpell MG. Gabapentin in neuropathic pain syndromes: a randomised, double-blind, placebo-controlled trial. Pain. 2002; 99:557-66.

76. Max MB, Lynch SA, Muir J. Effect of despiramine, amitriptyline, and fluoxetine on pain in diabetic neuropathy. N Engl J Med. 1992; 326:1250-56.

77. Lai J, Hunter JC, Porreca F. The role of voltage-gated sodium channels in neuropathic pain. Curr Opin Neurobiol. 2003; 13:291-307.

78. Catterall WA. From ionic currents to molecular mechanisms: the structure and function of voltage-gated sodium channels. Neuron. 2000; 26:13-25.

79. Lai J, Porreca F, Hunter JC, Gold MS. Voltage-gated sodium channels and hyperalgesia. Annu Rev Pharmacol Toxicol. 2003; 44:371-97.

80. Winkler I, Blotnik S, Shimshoni J, Yagen B, Devor M, Biale M. Efficacy of antiepileptic isomers of valproic acid and valpromide in a rat model of neuropathic pain. Br J Pharmacol. 2005; 146:198-208.

81. Hargus NJ, Patel MK. Voltage-gated Na^+ channels in neuropathic pain. Expert Opin Investig Drugs. 2007; 16:635-46.

82. Veneroni O, Maj R, Calabresi M, Faravelli L, Fariello RG, Salvati P. Anti-allodynic effect of NW-1029, a novel Na^+ channel blocker, in experimental animal models of inflammatory and neuropathic pain. Pain. 2003; 102:17-25.

83. Brochu RM, Dick IE, Tarpley JW, McGowan E, Gunner D, Herrington J, Shao PP, Ok D, Li C, Parsons WH, Stump GL, Regan CP, Lynch JJ Jr, Lyons KA, McManus OB, Clark S, Ali Z, Kaczorowski GJ, Martin WJ, Priest BT. Block of peripheral nerve sodium channels selectively inhibits features of neuropathic pain in rats. Mol Pharmacol. 2006; 69:823-32.

84. Patel MK, Ko SH, Jochnowitz N. Reversal of neuropathic pain by α-hydroxyphenylamide: A novel sodium channel antagonist. Neuropharmacol. 2006; 50:865-73.

85. Akada Y, Ogawa S, Amano K. Potent analgesic Effect of a putative sodium channel blocker M58373 on formalin-induced and neuropathic pain in rats. Eur J Pharmacol. 2006; 536:248-55.

86. Kyle DJ, Victor I, Ilyin Sodium Channel Blockers. Med Chem. 2007; 50:2583-88.

87. Tsien RW, Wheeler DB. Voltage-gated calcium channels. In: Carafoli E, Klee CB, editors. Calcium as a cellular regulator. New York: Oxford University Press; 1999. 171-99.

88. Luo ZD, Chaplan SR, Higuera ES, Sorkin LS, Stauderman KA, Williams ME, Yaksh TL. Upregulation of dorsal root ganglion (alpha)2(delta) calcium channel subunit and its correlation with allodynia in spinal nerve-injured rats. J Neurosci. 2001; 21:1868-75.

89. Evans AR, Nicol GD, Vasko MR. Differential regulation of evoked peptide release by voltage-sensitive calcium channels in rat sensory neurons. Brain Res. 1996; 12:265-73.

90. Gruner W, Silva LR. Omega-conotoxin sensitivity and presynaptic inhibition of glutamatergic sensory neurotransmission in vitro. J Neurosci. 1994; 14:2800-808.

91. Diaz A, Dickenson AH. Blockade of spinal N- and P-type, but not L-type, calcium channels inhibits the excitability of rat dorsal horn neurones produced by subcutaneous formalin inflammation. Pain. 1997; 69:93-100.

92. Bowersox SS, Gadbois T, Singh T, Pettus M, Wang YX. Selective N-type neuronal voltage-sensitive calcium channel blocker, SNX-111, produces spinal antinociception in rat models of acute, persistent and neuropathic pain. J Pharmacol Exp Ther. 1996; 279:1243-49.

93. Klotz U. Ziconotide-a novel neuron-specific calcium channel blocker for the intrathecal treatment of severe chronic pain-a short review. Int J Clin Pharmacol Ther. 2006; 44:478-83.

94. Zamponi GW, Lewis RJ, Todorovic SM, Arneric SP, Snutch TP. Role of voltage-gated calcium channels in ascending pain pathways. Brain Res Rev. 2009; 60:84-9.

95. Raskin P, Donofrio PD, Rosenthal NR, Hewitt DJ, Jordan DM, Xiang J, Vinik AI; CAPSS-141 Study Group. Topiramate vs placebo in painful diabetic neuropathy: analgesic and metabolic effects. Neurol. 2004; 63:865-73.

96. Pomonis JD, Harrison JE, Mark L, Bristol DR, Valenzano KJ, Walker K. N-(4-tertiarybutylphenyl)-4-(3-cholorphyridin-2-yl)tetrahydropyrazine-1(2H)-carboxamide (BCTC), a novel, orally effective vanilloid receptor 1 antagonist with analgesic properties: II. In vivo characterization in rat models of inflammatory and neuropathic pain. J Pharmacol Exp Ther. 2003; 306:387-93.

97. Jensen PG, Larson JR. Management of painful diabetic neuropathy. Drugs Aging. 2001; 18:737-49.

98. Pappagallo M, Haldey EJ. Pharmacological management of postherpetic neuralgia. CNS Drugs. 2003; 17:771-80.

99. Honore P, Wismer CT, Mikusa J, Zhu CZ, Zhong C, Gauvin DM, Gomtsyan A, El Kouhen R, Lee CH, Marsh K, Sullivan JP, Faltynek CR, Jarvis MF.A-425619 [1-isoquinolin-5-yl-3-(4-trifluoromethyl-benzyl)-urea], a novel transient receptor potential type V1 receptor antagonist, relieves pathophysiological pain associated with inflammation and tissue injury in rats. J Pharmacol Exp Ther. 2005; 314:410-21.

100. Chizh BA, Illes P. P2X receptors and nociception. Pharm. Rev. 2000; 53:553-68.

101. Cockayne DA, Hamilton SG, Zhu QM, Dunn PM, Zhong Y, Novakovic S, Malmberg AB, Cain G, Berson A, Kassotakis L, Hedley L, Lachnit WG, Burnstock G, McMahon SB, Ford AP. Urinary bladder hyporeflexia and reduced pain-related behaviour in $P2X_3$-deficient mice. Nature. 2000; 407:1011-15.

102. Barclay J, Patel S, Dorn G, Wotherspoon G, Moffatt S, Eunson L, Abdel'al S, Natt F, Hall J, Winter J, Bevan S, Wishart W, Fox A, Ganju P. Functional downregulation of $P2X_3$ receptor subunit in rat sensory neurons reveals a significant role in chronic neuropathic and inflammatory pain. J Neurosci. 2002; 22:8139-47.

103. Burnstock G, Wood JN. Purinergic receptors: their role in nociception and primary afferent neurotransmission. Curr Opin Neurobiol. 1996; 6:526-32.

104. Jarvis MF, Burgard EC, McGaraughty S, Honore P, Lynch K, Brennan TJ, Subieta A, Van BT, Cartmell J, Bianchi B, Niforatos W, Kage K, Yu H, Mikusa J, Wismer CT, Zhu CZ, Chu K, Lee CH, Stewart AO, Polakowski J, Cox BF, Kowaluk E, Williams M, Sullivan J, Faltynek C. A-317491, a novel potent and selective non-nucleotide antagonist of $P2X_3$ and $P2X_{2/3}$ receptors, reduces chronic inflammatory and neuropathic pain in the rat. Proc Natl Acad Sci. USA. 2002; 99:17179-84.

105. Honore P, Donnelly-Roberts D, Namovic MT, Hsieh G, Zhu CZ, Mikusa JP, Hernandez G, Zhong C, Gauvin DM, Chandran P, Harris R, Medrano AP, Carroll

W, Marsh K, Sullivan JP, Faltynek CR, Jarvis MF. A-740003 [N-(1-{[(cyanoimino)(5-quinolinylamino) methyl]amino}-2,2-dimethylpropyl)-2-(3,4-dimethoxyphenyl)acetamide], a novel and selective $P2X_7$ receptor antagonist, dose-dependently reduces neuropathic pain in the rat. J Pharmacol Exp Ther. 2006; 319:1376-85.

106. Inoue K. The function of microglia through purinergic receptors: neuropathic pain and cytokine release. Pharmacol Ther. 2006; 109:210-26.

107. Obata K, Yamanaka H, Dai Y, Mizushima T, Fukuoka T, Tokunaga A, Noguchi K. Activation of extracellular signal-regulated protein kinase in the dorsal root ganglion following inflammation near the nerve cell body. Neuroscience. 2004; 126:1011-21.

108. Sorkin LS, Doom CM. Epineurial application of TNF elicits an acute mechanical hyperalgesia in the awake rat. J Peripher Nerv Syst. 2000; 5:96-100.

109. Homma Y, Brull SJ, Zhang JM. A comparison of chronic pain behavior following local application of tumor necrosis factor alpha to the normal and mechanically compressed lumbar ganglia in the rat. Pain. 2002; 95:239-46.

110. Schäfers M, Lee DH, Brors D, Yaksh TL, Sorkin LS. Increased sensitivity of injured and adjacent uninjured rat primary sensory neurons to exogenous tumor necrosis factor-alpha after spinal nerve ligation. J Neurosci. 2003; 23:3028-38.

111. Sommer C, Lindenlaub T, Teuteberg P, Schäfers M, Hartung T, Toyka KV. Anti-TNF-neutralizing antibodies reduce pain-related behavior in two different mouse models of painful mononeuropathy. Brain Res. 2001; 913:86-9.

112. Sommer C, Marziniak M, Myers RR. The effect of thalidomide treatment on vascular pathology and hyperalgesia caused by chronic constriction injury of rat nerve. Pain. 1998; 74:83-91.

113. Gilron I, Coderre TJ. Emerging drugs in neuropathic pain. Expert Opin Emerg Drugs. 2007; 12:113-26.

114. Levy D, Douglas WZ. NO Pain: Potential Roles of Nitric Oxide in Neuropathic Pain. Pain Practice. 2004; 4:11-8.

115. Ialenti A, Ianaro A, Moncada S, Di RM. Modulation of acute inflammation by endogenous nitric oxide. Eur J Pharmacol. 1992; 211:177-82.

116. Heneka MT, Feinstein DL. Expression and function of inducible nitric oxide synthase in neurons. J Neuroimmunol. 2001; 114:8-18.

117. Obrosova IG, Mabley JG, Zsengellér Z, Charniauskaya T, Abatan OI, Groves JT, Szabó C. Role for nitrosative stress in diabetic neuropathy: evidence from studies with a peroxynitrite decomposition catalyst. FASEB J. 2005; 19:401-3.

118. Luo ZD, Chaplan SR, Scott BP, Cizkova D, Calcutt NA, Yaksh TL. Neuronal nitric oxide synthase mRNA upregulation in rat sensory neurons after spinal nerve ligation: lack of a role in allodynia development. J Neurosci. 1999; 19: 9201-8.

119. Mabuchi T, Matsumura S, Okuda-Ashitaka E, Kitano T, Kojima H, Nagano T, Minami T, Ito S. Attenuation of neuropathic pain by the nociceptin/orphanin FQ antagonist JTC-801 is mediated by inhibition of nitric oxide production. The Eur J Neurosci. 2003; 17:1384-92.

120. De Alba J, Clayton NM, Collins SD, Colthup P, Chessell I, Knowles RG. GW274150, a novel and highly selective inhibitor of the inducible isoform of nitric oxide synthase (iNOS), shows analgesic effects in rat models of inflammatory and neuropathic pain. Pain. 2006; 120:170-81.

121. Payne JE, Bonnefous C, Symons KT, Nguyen PM, Sablad M, Rozenkrants N, Zhang Y, Wang L, Yazdani N, Shiau AK, Noble SA, Rix P, Rao TS, Hassig CA, Smith ND. Discovery of dual inducible/neuronal nitric oxide synthase (iNOS/nNOS) inhibitor development candidate 4-((2-cyclobutyl-1H-imidazo[4,5-b]pyrazin-1-yl)methyl)-7,8-difluoroquinolin-2(1H)-one (KD7332) part 2: identification of a novel, potent, and selective series of benzimidazole-quinolinone iNOS/nNOS dimerization inhibitors that are orally active in pain models. J Med Chem. 2010; 53:7739-55.

122. Annedi SC, Maddaford SP, Mladenova G, Ramnauth J, Rakhit S, Andrews JS, Lee DK, Zhang D, Porreca F, Bunton D, Christie L.Discovery of N-(3-(1-methyl-1,2,3,6-tetrahydropyridin-4-yl)-1H-indol-6-yl) thiophene-2-carboximidamide as a selective inhibitor of human neuronal nitric oxide synthase (nNOS) for the treatment of pain. J Med Chem. 2012; 54:7408-16.

123. Maddaford S, Renton P, Speed J, Annedi SC, Ramnauth J, Rakhit S, Andrews J, Mladenova G, Majuta L, Porreca F.1,6-Disubstituted indole derivatives as

selective human neuronal nitric oxide synthase inhibitors. Bioorg Med Chem Lett. 2011; 21:5234-38.

124. Yogeeswari P, Semwal A, Mishra R, Sriram D. Current approaches with the glutamatergic system as targets in the treatment of neuropathic pain. Expert Opin Ther Targets. 2009; 13:925-43.

125. Ji RR, Kohno T, Moore KA, Woolf CJ. Central sensitization and LTP: do pain and memory share similar mechanisms? Trends Neurosci. 2003; 26:696-705.

126. Zhou S, Bonasera L, Carlton SM. Peripheral administration of NMDA, AMPA or KA results in pain behaviors in rats. Neuroreport. 1996; 7:895-900.

127. Vissers KC, Geenen F, Biermans R, Meert TF. Pharmacological correlation between the formalin test and the neuropathic pain behavior in different species with chronic constriction injury. Pharmacol Biochem Behav. 2006; 84:479-86.

128. Parsons CG. NMDA receptors as targets for drug action in neuropathic pain. Eur J Pharmacol. 2001; 429:71-8.

129. Low SJ, Roland CL. Review of NMDA antagonist-induced neurotoxicity and implications for clinical development. Int J Clin Pharmacol Ther. 2004; 42:1-14.

130. Roytta M, Wei H, Pertovaara A. Spinal nerve ligation–induced neuropathy in the rat: Sensory disorders and correlation between histology of the peripheral nerves. Pain.1999; 80:161-170.

131. Wilcox GL, Fairbanks CA, Schreiber KL. Agmatine reverses pain induced by inflammation, neuropathy, and spinal cord injury. Proc Natl Acad Sci USA. 2000; 97:10584-89.

132. Villetti G, Bergamaschi M, Bassani F. Antinociceptive activity of the N-methyl-D-aspartate receptor antagonist N-(2-Indanyl)-glycinamide hydrochloride (CHF3381) in experimental models of inflammatory and neuropathic pain. J Pharmacol Exp Ther. 2003; 306:804-14.

133. Boyce S, Wyatt A, Webb JK. Selective NMDA NR_2B antagonists induce antinociception without motor dysfunction: correlation with restricted localisation of NR_2B subunit in dorsal horn. Neuropharmacol. 1999; 38:611-23.

134. Christoph T, Reibmüller E, Schiene K, Englberger W, Chizh BA. Antiallodynic Effect of NMDA glycineB antagonists in neuropathic pain: possible peripheral mechanisms. Brain Res. 2005; 1048:218-27.

135. Quartaroli M, Carignani C, Dal FG, Mugnaini M, Ugolini A, Arban R, Bettelini L, Maraia G, Belardetti F, Reggiani A, Trist DG, Ratti E, Di Fabio R, Corsi M. Potent antihyperalgesic activity without tolerance produced by glycine site antagonist of N-Methyl-D-Aspartate receptor GV196771A. J Pharmacol Exp Ther. 1999; 290:158-69.

136. Munger RL, Bennet GJ, Kajander KC. An experimental painful peripheral neuropathy due to nerve constriction. I. Axonal pathology in the sciatic nerve. Exp Neurol. 1992; 118:204-14.

137. Ta LE, Dionne RA, Fricton JR, Hodges JS, Kajander KC. SYM-2081-a kainate receptor antagonist reduces allodynia and hyperalgesia in a freeze injury model of neuropathic pain. Brain Res. 2000; 858:106-20.

138. Blackburn-Munro G, Bomholt SF, Erichsen HK. Behavioural Effect of the novel AMPA/GluR5 selective receptor antagonist NS1209 after systemic administration in animal models of experimental pain. Neuropharmacol. 2004; 47:351-62.

139. Schkeryantz JM, Kingston AE, Johnson MP. Prospects for metabotropic glutamate 1 receptor antagonists in the treatment of neuropathic pain. J Med Chem. 2007; 50:2563-68.

140. Kohara A, Nagakura Y, Kiso T, Toya T, Watabiki T, Tamura S, Shitaka Y, Itahana H, Okada M. Antinociceptive profile of a selective metabotropic glutamate receptor 1 antagonist YM-230888 in chronic pain rodent models. Eur J Pharmacol. 2007; 571:8-16.

141. Osikowicz M, Mika J, Makuch W, Przewlocka B. Glutamate receptor ligands attenuate allodynia and hyperalgesia and potentiate morphine effects in a mouse model of neuropathic pain. Pain. 2008; 139:117-26

142. Pauly TA, Sulea T, Ammirati M, Sivaraman J, Danley DE, Griffor MC, Kamath AV, Wang IK, Laird ER, Seddon AP, Menard R, Cygler M, Rath V. Specificity determinants of human cathepsin s revealed by crystal structures of complexes. Biochem. 2003; 42:3203-13.

143. Clark AK, Yip PK, Grist J, Gentry C, Staniland AA, Marchand F, Dehvari M, Wotherspoon G, Winter J, Ullah J, Bevan S, Malcangio M. Inhibition of spinal microglial cathepsin S for the reversal of neuropathic pain. Proc Natl Acad Sci. 2007; 104:10655-60.

144. Nakagawa TY, Rudensky AY. The role of lysosomal proteinases in MHC class II-mediated antigen processing and presentation. Immunol Rev. 1999; 172:121-29.

145. John JM, Wiener SS, Robin LT. Recent Advances in the Design of Cathepsin S Inhibitors. Current Top Med Chem. 2010; 10:717-32.

146. Ward YD, Thomson DS, Frye LL, Cywin CL, Morwick T, Emmanuel MJ, Zindell R, McNeil D, Bekkali Y, Girardot M, Hrapchak M, DeTuri M, Crane K, White D, Pav S, Wang Y, Hao MH, Grygon CA, Labadia ME, Freeman DM, Davidson W, Hopkins JL, Brown ML, Spero DM. Design and synthesis of dipeptide nitriles as reversible and potent cathepsin S inhibitors. J Med Chem. 2002; 45:5471-82.

147. Altmann E, Cowan-Jacob SW, Missbach M. Novel purine nitrile derived inhibitors of the cysteine protease cathepsin K. J Med Chem. 2004; 47:5833-36.

148. Irie O, Kosaka T, Ehara T, Yokokawa F, Kanazawa T, Hirao H, Iwasaki A, Sakaki J, Teno N, Hitomi Y, Iwasaki G, Fukaya H, Nonomura K, Tanabe K, Koizumi S, Uchiyama N, Bevan SJ, Malcangio M, Gentry C, Fox AJ, Yaqoob M, Culshaw AJ, Hallett A. Discovery of orally bioavailable cathepsin s inhibitors for the reversal of neuropathic pain. J Med Chem, 2008; 51:5502-05.

149. Song JH, Kim SG, No ZS, Hyun YL, Jeon DJ, Kim I. Discovery and synthesis of Novel N-cyanopyrazolidine and N-Cyanohexahydropyridazine Derivatives as Csthepsin Inhibitors. Bull Korean Chem Soc. 2008; 29:1467-71.

150. Ayesa S, Lindquist C, Agback T, Benkenstock K, Classon B, Henderson I, Hewitt E, Jansson K, Kallin A, Sheppard D, Samuelsson B. Solid-phase parallel synthesis and SAR of 4-amidofuran-3-one inhibitors of cathepsin S: effect of sulfonamide P3 substituents on potency and selectivity. Bioorg Med Chem. 2009; 17:1307-24.

151. Wood, WJL, Patterson AW, Tsuruoka H, Jain RK, Ellman JA. Substrate activity screenfing: a fagment-based method for the rapid identification of nonpeptidic protease inhibitors. J Am Chem Soc. 2005; 127:15521-27.

152. Patterson AW, Wood WJL, Ellman JA. Substrate activity screening (SAS): a general procedure for the preparation and screening of a fragment-based non-peptidic protease substrate library for inhibitor discovery. Nat Protocols. 2007; 2: 424-33.

153. Wei J, Pio BA, Cai H, Meduna SP, Sun S, Gu Y, Jiang W, Thurmond RL, Karlsson L, Edwards JP, Pyrazole-based cathepsin S inhibitors with improved cellular potency. Bioorg Med Chem Lett. 2007; 17:5525-28.

154. Lever IJ, Rice AS. Cannabinoids and pain. Handbook Exp. Pharmacol. 2007; 177:265-306

155. Felder CC, Glass M. Cannabinoid receptors and their endogenous agonists. Ann Rev Pharmacol Toxicol. 1998; 38:179-200.

156. Gaoni Y, Mechoulam R. Isolation, structure and partial synthesis of an active constituent of hashish. J Am Chem Soc. 1964; 86:1946-47.

157. Scott DA, Wright CE, Angus JA. Evidence that CB-1 and CB-2 cannabinoid receptors mediate antinociception in neuropathic pain in the rat. Pain. 2004; 109:124-31.

158. Morisset V, Ahluwalia J, Nagy I, Urban L. Possible mechanisms of cannabinoid-induced antinociception in the spinal cord. Eur J Pharmacol. 2001; 429:93-100.

159. Guindon J, Hohmann AG. Cannabinoid CB_2 receptors: a therapeutic target for the treatment of inflammatory and neuropathic pain. Br J Pharmacol. 2008; 153:319-334.

160. Bridges D, Ahmad K, Rice ASC. The synthetic cannabinoid WIN 55,212-2 attenuates hyperalgesia and allodynia in a rat model of neuropathic pain. Br J Pharmacol. 2001; 133:586-94.

161. Costa B, Colleoni M, Conti S, Trovato AE, Bianchi M, Sotgiu ML, Giagnoni G. Repeated treatment with the synthetic cannabinoid WIN 55,212-2 reduces both hyperalgesia and production of pronociceptive mediators in a rat model of neuropathic pain. Br J Pharmacol. 2004; 141:4-8.

162. Pullar S, Palmer AM. Pharmacotherapy for neuropathic pain: progress and prospects. Drug News Perspect. 2003; 16:622-30.

163. De VJ, Denzer D, Reissmueller E: 3-[2-Cyano-3-(trifluoromethyl) phenoxy]phenyl-4,4,4-trifluoro-1-butanesulfonate (BAY 59-3074): a novel cannabinoid CB_1/CB_2 receptor partial agonist with antihyperalgesic and antiallodynic effects. J Pharmacol Exp Ther. 2004; 310:620-32.

164. Ibrahim MM, Deng H, Zvonok A, Cockayne DA, Kwan J, Mata HP, Vanderah TW, Lai J, Porreca F, Makriyannis A, Malan TP Jr. Activation of CB_2 cannabinoid receptors by AM1241 inhibits experimental neuropathic pain: pain inhibition by receptors not present in the CNS. Proc Natl Acad Sci USA. 2003; 100:10529-33.

165. Hanus L, Breuer A, Tchilibon S, Shiloah S, Goldenberg D, Horowitz M, Pertwee RG, Ross RA, Mechoulam R, and Fride E. HU-308: a specific agonist for CB(2), a peripheral cannabinoid receptor. Proc Natl Acad Sci USA. 1999; 96:14228-33.

166. Whiteside GT, Gottshall SL, Boulet JM, Chaffer SM, Harrison JE, Pearson MS, Turchin PI, Mark L, Garrison AE, Valenzano KJ. A role for cannabinoid receptors, but not endogenous opioids, in the antinociceptive activity of the CB_2-selective agonist, GW405833. Eur J Pharmacol. 2005; 528:65-72.

167. Zeilhofer HU, Hanns M, Alessandra DL. GABAergic analgesia: new insights from mutant mice and subtype selective agonists. Trends Pharmacol Sci. 2009; 30:397-402.

168. Jasmin L, Rabkin SD, Granato A, Boudah A, Ohara PT. Analgesia and hyperalgesia from GABA-mediated modulation of the cerebral cortex. Nature. 2003; 424:316-20.

169. Jasmin L, Wu MV, Ohara PT. GABA puts a stop to pain. Curr Drug Target CNS Neurol. 2004; 3: 487–505.

170. Eaton MJ, Martinez MA, Karmally S. A single intrathecal injection of GABA permanently reverses neuropathic pain after nerve injury. Brain Res. 1999; 835:334-39.

171. Munro G, Lopez-Garcia JA, Rivera-Arconada I, Erichsen HK, Nielsen EØ, Larsen JS, Ahring PK, Mirza NR. Comparison of the novel subtype-selective GABAA receptor-positive allosteric modulator NS11394 [30 -[5-(1-hydroxy-1-methyl-ethyl)-benzoimidazol-1-yl]-biphenyl-2-carbonitrile] with diazepam,

zolpidem, bretazenil, and gaboxadol in rat models of inflammatory and neuropathic pain. J Pharmacol Exp Ther. 2008; 327:969-81.

172. Giardina WJ, Decker MW, Porsolt RD. An evaluation of the GABA uptake blocker tiagabine in animal models of neuropathic and nociceptive pain. Drug Dev Res. 1998; 44:106-13.

173. Hwang JH, Yaksh TL. The effect of spinal GABA receptor agonists on tactile allodynia in a surgically-induced neuropathic pain model in the rat. Pain. 1997; 70: 15-22.

174. Alves ND, De Castro-Costa CM, De-Carvalho AM, Santos FJC, Silveira DG. Possible analgesic effect of vigabatrin in animal experimental chronic neuropathic pain. Arq Neuropsiquiatr. 1999; 57:916-20.

175. Franek M, Vaculin S, Rokyta R. GABAB receptor agonist baclofen has non-specific antinociceptive effect in the model of peripheral neuropathy in the rat. Physiol Res. 2004; 53:351-55.

176. Smith GD, Harrison SM, Birch PJ, Elliott PJ, Malcangio M, Bowery NG. Increased sensitivity to the antinociceptive activity of (+/-)-baclofen in an animal model of chronic neuropathic, but not chronic inflammatory hyperalgesia. Neuropharmacol. 1994; 33:1103-08.

177. Knabl J, Witschi R, Hösl K, Reinold H, Zeilhofer UB, Ahmadi S, Brockhaus J, Sergejeva M, Hess A, Brune K, Fritschy JM, Rudolph U, Möhler H, Zeilhofer HU. Reversal of pathological pain through specific spinal $GABA_A$ receptor subtypes. Nature. 2008; 451:330-34.

178. Rice AS, Maton S. Gabapentin in postherpetic neuralgia: a randomized double-blind placebo-controlled study. Pain. 2001, 94:215-24.

179. Ameriks MK, Axe FU, Scott DB, Edwards JP, Gu Y, Karlsson L, Randal M, Sun S, Thurmond RL, Zhu J. Pyrazole-based cathepsin S inhibitors with arylalkynes as P1 binding elements. Bioorg Med Chem Lett. 2009; 19:6131-34.

180. Thurmond RL, Beavers MP, Cai H, Meduna SP, Gustin DJ, Sun S, Almond HJ, Karlsson L, Edwards J P. Nonpeptidic, noncovalent inhibitors of the cysteine protease cathepsin S. J Med Chem. 2004, 47:4799-801.

181. Cowart MD, Altenbach RJ, Liu H, Hsieh GC, Drizin I, Milicic I, Miller TR, Witte DG, Wishart N, Fix-Stenzel SR, McPherson MJ, Adair RM, Wetter JM, Bettencourt BM, Marsh KC, Sullivan JP, Honore P, Esbenshade TA, Brioni JD. Rotationally constrained 2,4-diamino-5,6-disubstituted pyrimidines: a new class of histamine H_4 receptor antagonists with improved druglikeness and in vivo efficacy in pain and inflammation models. J Med Chem. 2008; 51:6547-57.

182. Cheng Y, Tomaszewski M. 2010, US patent 20100113502 A1.

183. Oberborsch S, Bernd S, Corinna S, Michael H, Hagen-heinrich, Edward B. 2010, US patent 7,662,828, B2.

184. Zhou CH, Wang Y. Recent researches in triazole compounds as medicinal drugs. Current Med Chem. 2012; 19:239-80.

185. Alberto DZ, Nadine J, Maria PGJ, Maria RCA, Jose CM. European Patent 1,921,073.

186. Breslin MJ, Coleman PJ, Cox CD, Raheem JT, Schreier JD. WIPO Patent W02011/0222131.

187. Chapleo CB, Myers PL, Smith AC, Tulloch IF, Turner S, Walter DS. J Med Chem.1987; 30: 951-54.

188. Carroll WA, Kalvin DM, Perez MA, Floriancic AS, Wang Y, Donnelly-Roberts DL, Namovic MT, Grayson G, Honore P, Jarvis MF. Novel and potent 3-(2,3-dichlorophenyl)-4-(benzyl)-4H-1,2,4-triazole $P2X_7$ antagonists. Bioorg Med Chem Lett. 2007; 17:4044-48.

189. Carroll WA, Donnelly-Roberts D, Jarvis MF. Selective $P2X_7$ receptor antagonists for chronic inflammation and pain. Purinergic Signalling. 2009; 5:63-73.

190. Chakravarty PK, Zuegner LL, Parsons WH, Palucki B, Zhou B, Park MK, Fisher MH. US Patent 7,572,822.

191. Boschelli DH, Connor DT, Bornemeier DA, Dyer RD, Kennedy JA, Kuipers PJ, Okonkwo GC, Schrier DJ, Wright CD. 1,3,4-Oxadiazole, 1,3,4-thiadiazole, and 1,2,4-triazole analogs of the fenamates: in vitro inhibition of cyclooxygenase and 5-lipoxygenase activities. J Med Chem. 1993; 36:1802-10.

192. Palaska E, Sahin G, Kelicen P, Durlu NT, Altinok G. Synthesis and anti-inflammatory activity of 1-acylthiosemicarbazides, 1,3,4-oxadiazoles, 1,3,4-thiadiazoles and 1,2,4-triazole-3-thiones. Farmaco. 2002; 57:101-7.

193. Clerici F, Pocar D, Guido M, Loche A, Perlini V, Brufani M. Synthesis of 2-amino-5-sulfanyl-1,3,4-thiadiazole derivatives and evaluation of their antidepressant and anxiolytic activity. J Med Chem. 2001; 44:931-6.

194. Floriancic AS, Peddi S, Perez Medrano A, Li B, Namovic MT, Grayson G, Donnelly-Roberts DL, Jarvis MF, Carroll WA. Synthesis and in vitro activity of 1-(2,3-dichlorophenyl)-N-(pyridin-3-ylmethyl)-1H-1,2,4-triazol-5-amine and 4-(2,3-dichlorophenyl)-N-(pyridin-3-ylmethyl)-4H-1,2,4-triazol-3-amine P_2X_7 antagonists. Bioorg Med Chem Lett. 2008; 18:2089-92.

195. Jagerovic N, Hernandez-Folgado L, Alkorta I, Goya P, Navarro M, Serrano A, de Fonseca FR, Dannert MT, Alsasua A, Suardiaz M, Pascual D, Martin MI. Discovery of 5-(4-chlorophenyl)-1-(2,4-dichlorophenyl)-3-hexyl-1H-1,2,4-triazole, a novel in vivo cannabinoid antagonist containing a 1,2,4-triazole motif. J Med Chem. 2004**;** 47:2939-42.

196. Hopkins AL. Network pharmacology: the next paradigm in drug discovery. 2008; Nat Chem Biol. 2008; 4:682-90.

197. Pujol A, Mosca R, Farres J, Aloy P.Unveiling the role of network and systems biology in drug discovery. Trends Pharmacol Sci. 2010, 31:115-23.

198. Buccafusco JJ. Multifunctional receptor-directed drugs for disorders of the central nervous system. Neurotherapeutics. 2009; 6:4-13.

199. Iyengar S, Webster AA, Hemrick-Luecke SK, Xu JY, Simmons RMA. Efficacy of duloxetine, a potent and balanced serotonin-norepinephrine reuptake inhibitor in persistent pain models in rats. J Pharmacol ExpTher. 2004; 311:576-84.

200. Hochdorffer K, Marz-Berberich J, Nagel-Steger L, Epple M., Meyer-Zaika W, Horn AHC, Sticht H, Sinha S, Bitan G, Schrader T. Rational design of - sheet ligands against A42-induced toxicity. J Am Chem Soc. 2011; 133:4348-58.

201. Gogoi S, Antonio T, Rajagopalan S, Reith M, Andersen J, Dutta AK, Dopamine D_2/D_3 agonists with potent iron chelation, antioxidant and neuro protective

properties: potential implication in symptomatic and neuroprotective treatment of Parkinson's disease. Chem Med Chem. 2001; 6:991-95.

202. Hans RH, Wiid IJF, van Helden PD, Wan B, Franzblau SG, Gut J, Rosenthal PJ, Chibale K. Novel thiolactone-isatin hybrids as potential antimalarial and antitubercular agents. Bioorg Med Chem Lett. 2011; 21:2055-58.

203. Shalini M, Yogeeswari P, Sriram D, Stables JP. Cyclization of the semicarbazone template of aryl semicarbazones: synthesis and anticonvulsant activity of 4,5-diphenyl-2H-1,2,4-triazol-3(4H)-one. Biomed Pharmacother. 2009; 63:187-93.

204. Salgin-Gökşen U, Gökhan-Kelekçi N, Göktaş O, Köysal Y, Kiliç E, Işik S, Aktay G, Ozalp M. 1-Acylthiosemicarbazides, 1,2,4-triazole-5(4H)-thiones, 1,3,4-thiadiazoles and hydrazones containing 5-methyl-2-benzoxazolinones: synthesis, analgesic-anti-inflammatory and antimicrobial activities. Bioorg Med Chem. 2007; 15:5738-51.

205. Dunham NW, Miya TS. A note on a simple apparatus for detecting neurological deficit in rats and mice. J Am Pharm Assoc Sci Eds. 1957; 46:208-09.

206. Siegmund EA, Cadmus RA. A method for evaluating both non-narcotic and narcotic analgesics. Proc Soc Exp Biol.1957; 95:729-31.

207. Hunskaar S, Hole K. The formalin test in mice: dissociation between inflammatory and non-inflammatory pain. Pain.1987; 30:103-14.

208. Bennett GJ, Xie YK. A peripheral mononeuropathy in rat that produces disorders of pain sensation like those seen in man. Pain. 1988; 33:87-107.

209. Garth T, Whiteside JH, Jamie B, Lilly M, Michelle P, Susan G, Katharine W. Pharmacological characterisation of a rat model of incisional pain. Br J Pharmacol. 2004; 141:85-91.

210. Choi Y, Yoon YW, Na HS, Kim SH, Chung JM. Behavioral signs of ongoing pain and cold allodynia in a rat model of neuropathic pain. Pain. 1994, 59: 369-76.

211. Eliav E, Herzberg U, Ruda MA, Bennett GJ. Neuropathic pain from an experimental neuritis of the rat sciatic nerve. Pain. 1999; 83:169-182.

212. Caudle RM, Mannes AJ, Benoliel R, Eliav E, Iadarola MJ. Intrathecally administered cholera toxin blocks allodynia and hyperalgesia in persistent pain models. J Pain. 2001; 2:118-27.

213. Randall LO, Selitto JJ. A method for measurement of analgesic activity on inflamed tissue, Arch Int Pharmacodyn Ther. 1957; 111:409-19.

214. Fairbanks CA, Nguyen HO, Grocholski BM, Wilcox GL. Moxonidine, a selective imidazoline-a2-adrenergic receptor agonist, produces spinal synergistic antihyperalgesia with morphine in nerve-injured mice. Anesthesiology. 2000; 93:765-73.

215. Harris JM, Spencer PSJ. A modified plethysmographic apparatus for recording volume changes in the rat paw. Pharm Pharmacol. 1962; 14:464-66.

216. Sekut L, Yarnall D, Stimpson SA, Noel LS, Bateman-Fite R, Clark RL, Brackeen MF, Menius Jr JA, Connolly KA. Anti-inflammatory activity of phosphodiesterase (PDE)-IV inhibitors in acute and chronic models of inflammation. Clin. Exp Immunol. 1995; 100:126-132.

217. Padi SSV, Kulkarni SK. Minocycline prevents the development of neuropathic pain, but not acute pain: possible anti-inflammatory and antioxidant mechanisms. Eur J Pharmacol. 2008; 601:79-87.

218. Mellors A, Tappel AJ. The inhibition of mitochondrial peroxidation by ubiquinone and ubiquinol. Biol Chem. 1966; 241:4353-56.

219. Bradford MM. A rapid and sensitive method for the quantitation of microgram quantities of protein utilizing the principle of protein-dye binding. Anal Biochem. 1976; 72:248-54.

220. Leggett JD, Aspley S, Beckett SR, D'Antona AM, Kendall DA, Kendall DA. Oleamide is a selective endogenous agonist of rat and human CB_1 cannabinoid receptors. Br J Pharmacol. 2004; 141:253-62.

221. Hsieh CS, deRoos P, Honey K, Beers C, Rudensky AY. A role for cathepsin L and cathepsin S in peptide generation for MHC class II presentation. J Immunol. 2002; 168:2618-25.

222. Mathis C, Barry JD, Ungerer A. NMDA antagonist properties of gamma-L-glutamyl-L-aspartate demonstrated on chemically induced seizures in mice. Eur J Pharmacol.1990; 185:53-59.

223. Xia M, Pan M, Liotta F, Wachter MP. US Patent 2007, 0254911A1.

224. Albaugh P, Madison H. US Patent 1998, 5750702.

225. Bars LD, Gozariu M, Cadden SW. Animal models of nociception. Pharmacol Rev. 2001; 53:597-652.

226. Bass WB, Vanderbrook MJ. A note on an improved method of analgesic evaluation. J Am Pharm Assoc Sci Ed. 1952; 41:569-670.

227. Rosland JH, Tjolsen A, Maehle B, Hole K. The formalin test in mice-effect of formalin concentration. Pain 1990; 42:235-242.

228. Abbott FV, Franklin KB, Westbrook RF. The formalin test: scoring properties of the first and second phases of the pain response in rats. Pain. 1995; 60:910-102.

229. Abram SE, Dean C, O'Connor TC. Peroneal afferent nerve discharges underlying the behavioral response to the formalin test. Reg Anesth. 1996; 21:226-33.

230. Coderre TJ, Melzack R. The contribution of excitatory amino acids to central sensitization and persistent nociception after formalin-induced tissue injury. J Neurosci. 1992; 12:3665-70.

231. Abbadie C, Taylor BK, Peterson MA, Basbaum AI. Differential contribution of the two phases of the formalin test to pattern of c-fos expression in the rat spinal cord: studies with remifentanil and lidocaine. Pain. 1997; 69:101-10.

232. Chaplan SR, Malmberg AB, Yaksh TL. Efficacy of spinal NMDA receptor antagonism in formalin hyperalgesia and nerve injury evoked allodynia in the rat. J Pharmacol Exp Ther. 1997; 280:829-38.

233. Rocha AC, Fernandes ES, Quinta NL, Campos MM, Calixto JB. Relevance of tumour necrosis factor-alpha for the inflammatory and nociceptive responses evoked by carrageenan in the mouse paw. Br J Pharmacol. 2006; 148:688-95.

234. Okpo SO, Fatokun F, Adeyemi OO. Analgesic and antiinflammatory activity of *Crinum glaucum* aqueous extract. J Ethnopharmacol. 2001; 78:207-11.

235. Di Rosa M, Giroud JP, Willoughby DA. Studies of the mediators of the acute inflammatory response induced in rats in different sites by carrageenan and turpentine. J Pathol. 1971; 104:15-29.

236. Loram LC, Fuller A, Fick LG, Cartmell T, Poole S, Mitchell D. Cytokine profiles during carrageenan-induced inflammatory hyperalgesia in rat muscle and hind paw. J Pain. 2007; 8:127-36.

237. Naik AK. Tandan SK, Dudhgaonkar SP, Jadhav SH, Kataria M, Prakash VR, Kumar D. Role of oxidative stress in pathophysiology of peripheral neuropathy and modulation by N-acetyl-L-cysteine in rats. Eur J Pain. 2006; 10:573-79.

238. Mazzari S, Canella R, Petrelli L, Marcolongo G, Leon AN. (2-Hydroxyethyl)-hexadecanamide is orally active in reducing edema formation and inflammatory hyperalgesia by down-modulating mast cell activation. Eur J Pharmacol. 1996; 300: 227-36.

239. Quartilho A, Mata HP, Ibrahim MM, Vanderah TW, Porreca F, Makriyannis A, Malan TP Jr. Inhibition of inflammatory hyperalgesia by activation of peripheral CB_2 cannabinoid receptors. Anesthesiology. 2003; 99:955-56.

240. Pertwee, RG. Cannabinoid receptors and pain. Prog Neurobio. 2001; 63:569-611.

241. Breslin MJ, Coleman PJ, Cox CD, Raheem JT, Schreier JD. WIPO Patent W02011/0222131.

242. Salgin-Gökşen U, Gökhan-Kelekçi N, Göktaş O, Köysal Y, Kiliç E, Işik S, Aktay G, Ozalp M. 1-Acylthiosemicarbazides, 1,2,4-triazole-5(4H)-thiones, 1,3,4-thiadiazoles and hydrazones containing 5-methyl-2-benzoxazolinones: synthesis, analgesic-anti-inflammatory and antimicrobial activities. Bioorg Med Chem. 2007, 15:5738-51.

243. Tozkoparan B, Aktay G, Yesilada E. Synthesis of some 1,2,4-triazolo[3,2-b]-1,3-thiazine-7-ones with potential analgesic and antiinflammatory activities. Farmaco 2002; 57:145-52.

244. Navidpour L, Shafaroodi H, Abdi K, Amini M, Ghahremani MH, Dehpour AR, Shafiee A. Design, synthesis, and biological evaluation of substituted 3-alkylthio-4,5-diaryl-4H-1,2,4-triazoles as selective COX-2 inhibitors. Bioorg Med Chem. 2006; 14:2507-517.

245. Jagerovic N, Hernandez-Folgado L, Alkorta I, Goya P, Navarro M, Serrano A, de Fonseca FR, Dannert MT, Alsasua A, Suardiaz M, Pascual D, Martin MI. Discovery of 5-(4-chlorophenyl)-1-(2,4-dichlorophenyl)-3-hexyl-1h-1,2,4-triazole, a novel in vivo cannabinoid antagonist containing a 1,2,4-triazole motif. J Med Chem. 2004; 47:2939-42.

246. Schenone S, Brullo C, Bruno O, Bondavalli F, Ranise A, Filippelli W, Rinaldi B, Capuano A, Falcone G. Bioorg Med Chem. 2006; 14:1698-1705.

247. Song Y, Connor DT, Doubleday R, Sorenson RJ, Sercel AD, Unangst PC, Roth BD, Gilbertsen RB, Chan K, Schrier DJ, Guglietta A, Bornemeier DA, Dyer RD. Synthesis, structure-activity relationships, and in vivo evaluations of substituted di-tert-butylphenols as a novel class of potent, selective, and orally active cyclooxygenase-2 inhibitors. Thiazolone and oxazolone series. J Med Chem. 1999; 42:1151-60.

248. Amir M, Shikha K. Synthesis and anti-inflammatory, analgesic, ulcerogenic and lipid peroxidation activities of some new 2-[(2,6-dichloroanilino) phenyl]acetic acid derivatives. Eur J Med Chem. 2004; 39:535-45

249. P. Yogeeswari, D. Sriram, A.S.K. Kumar, A. Semwal, R.K. Mishra, Indian Patent Application No. 1138/CHE/2009 A (18/5/2009).

LIST OF PUBLICATIONS

1. Yogeeswari P, Arvind Semwal, Sriram D., Ragavendran J.V., Sreevatsan, N, **Monika Sharma**. Antiallodynic and antihyperalgesic activities of anticonvulsant GABA derivatives in both sciatic and spinal nerve ligation models of neuropathic pain, Pharmacol. Online 2010; 1:634-647.
2. **Monika S**, Reddy, A.S.K., Arvind S, Sriram D, Yogeeswari P. Effectiveness of newer lipophilic GABA analogues against epilepsy, Ind. J. Pharmacol. 2010; 42: 160-161.
3. Yogeeswari P, Sravan Kumar Patel, Ingala Vikram Reddy, Arvind Semwal, **Monika Sharma**, Gangadhar M, Siddarth Sai M, Sriram D. GABA derivatives for the treatment of epilepsy and neuropathic pain: A synthetic integeration of GABA into 1,2,4-Triazol-2H-one nucleus. Biomed. Ageing Pathol. 2012, In Press.
4. **Monika Sharma**, Gangadhar Matharasala, Vanamala Deekshith, Arvind Semwal, Dharmarajan Sriram and Perumal Yogeeswari. Discovery of Fused [1,2,4] triazolo [3,4-b][1,3,4]thiadiazoles as inhibitors of TNF-alpha: Pharmacophore hybrid approach for Treatment of Neuropathic Pain, Pain and Therapy, 2012, In Press.
5. **Monika Sharma**, Shraddha Suman Dash, Gangadhar Matharasala, Vanamala Deekshith, Dharmarajan Sriram and Perumal Yogeeswari. Novel Piperazinyl Derivatives with Anti-Hyperalgesic, Anti-Allodynic and Anti-Inflammatory activities Useful for the Treatment of Neuropathic Pain, Anti-Inflammatory & Anti-Allergy Agents in Medicinal Chemistry, 2012, In Press.
6. **Monika Sharma**, Soumya Gargipati, Binita Kundu, Deekshith Vanamala, Arvind Semwal, Dharmarajan Sriram, Perumal Yogeeswari. Novel 1,2,4-Triazol-5-ones as Tumor Necrosis Factor - alpha (TNF-α) Inhibitors for the Treatment of Neuropathic Pain, Chem. Biol. Drug. Des. (Under Revision).
7. Yogeeswari P, **Monika Sharma**, Matharasala Gangadhar, Srirama Karthick, Saketh Mallipeddi, Arvind Semwal, Sriram Dharamrajan, Novel Tetrahydro-Pyrazolo [4,3-c] Pyridines for the Treatment of Neuropathic Pain through their

multi-functional action on Cannabinoid (CB_1) receptor and Tumour Necrosis Factor-α: Synthesis and Neuropharmacology, Eur. J. Med. Chem. (Communicated).

8. **Monika Sharma**, Arvind Semwal, Vanamala Deekshith, Dharmarajan Sriram, Perumal Yogeeswari Discovery of Tetrahydropyrido[4,3-*d*]pyrimidine Derivatives for the Treatment of Neuropathic Pain. Bioorganic Chemistry (Communicated).

B) Papers Presented At National/International Conferences

1. **Monika Sharma**, M. Ganghadhar, Binita Kundu, Arvind Semwal, D. Sriram, P. Yogeeswari, Pharmacological profiling of triazolone derivatives as new leads for neuropathic pain treatment, XXXXIVth Annual Conference of Indian Pharmacological Society, 19-21 December 2011, Manipal, India.
2. **Monika S**, Gangadhar M, Sriram K, Sriram D and Yogeeswari P. Discovery of Novel Tetrahydropyridopyrazoles as new leads for the treatment of Neuropathic Pain. RSC MedChem-2011, 25-26th February 2011, Indian Institute of Chemical Technology, Hyderabad, India.
3. **Monika S**, Arvind S, Gangadhar M, Deekshith V, Sriram D, Yogeeswari P. Discovery of Novel in vivo TNF-alpha inhibitors for the treatment of Neuropathic Pain: Possible NO modulatory and antioxidant mechanisms. Current Trends in Pharmaceutical Sciences-2011, 12 November 2011, Birla Institute of Science and Technology, Pilani-Hyderabad Campus, Hyderabad, India.
4. Yukti Singh, **Monika Sharma**, D. Sriram, P. Yogeeswari, Neurotoxicological evaluation of BITS candidate drugs in four animals models, XXXXIVth Annual Conference of Indian Pharmacological Society, 19-21 December 2011, Manipal India.
5. V. Deekshith, **Monika Sharma**, D. Sriram, P. Yogeeswari, Evaluation of analgesic activity of new chemical entities in two rodent models of

pain, XXXXIVth Annual Conference of Indian Pharmacological Society, 19-21 December 2011, Manipal, India.

6. M. Gangadhar, **Monika Sharma**, D. Sriram, P. Yogeeswari, Preclinical evaluation of some novel heterocycles against postoperative pain, XXXXIVth Annual Conference of Indian Pharmacological Society, 19-21 December 2011, Manipal, India.
7. Gangadhar M, **Monika S**, Sriram D, Yogeeswari P. Pharmacological screening of some novel heterocycles for the treatment of Neuropathic Pain. Current Trends in Pharmaceutical Sciences-2011, 12 November 2011, Birla Institute of Science and Technology, Pilani-Hyderabad Campus, Hyderabad, India.
8. Yukti S, Deekshith V, **Monika S**, Sriram D, Yogeeswari P. Assessment of Anti-Inflammatory Properties of some Novel Heterocycles. Current Trends in Pharmaceutical Sciences-2011, 12 November 2011, Birla Institute of Science and Technology, Pilani-Hyderabad Campus, Hyderabad, India.
9. Deekshith V, **Monika S**, Sriram D and Yogeeswari P. Evaluation of Novel Chemical Entitites in Animal models for Analgesic Activity. Current Trends in Pharmaceutical Sciences-2011, 12 November 2011, Birla Institute of Science and Technology, Pilani-Hyderabad Campus, Hyderabad, India.

BIOGRAPHY OF Ms. MONIKA SHARMA

Ms. Monika Sharma completed her bachelor's degree in Pharmacy (B. Pharm) from H.N.B Garhwal University, Srinagar Uttarakhand in the year 2006 and Masters in Pharmacy (M.Pharm) form Northern India Engineering College (BBDGEI), Lucknow under Uttar Pradesh Technical University, Uttar Pradesh in 2008 with Pharmaceutical Chemistry specialization.

She has also worked as a Research Intern in Central Drug research Institute Lucknow, Uttar Pradeshfor 1 year and later worked as a Lecturer in Northern India Engineering College (BBDGEI), Lucknow for 6 months. She had been working as a research scholar at BITS, Pilani-Hyderabad Campus from 2009-2012 under the supervision of Prof. P. Yogeeswari. During her research tenure, she was awarded the senior research fellowship by Department of Biotechnology (DBT), New Delhi, India. She has to her credit five research publications. She is the member of various professional organizations like International Brain Research Organization (IBRO) and Inflammation Research Association (IRA).

BIOGRAPHY OF Prof. P. YOGEESWARI

Prof. P. Yogeeswari is presently working in the capacity of Associate Professor, Department of Pharmacy, Birla Institute of Technology & Science (BITS), Pilani-Hyderabd campus. She received her Ph.D. in the year 2001 from Banaras Hindu University (BHU), Varanasi. She has been involved in research for the past thirteen years and in teaching for eleven years. She is a collaborative research scientist of the Karolinska Institutet Sweden, National Institutes of Health (NIH), Bethesda, USA, National Cancer Institute (NCI), USA, National Institute of Mental Health and Neurosciences (NIMHANS), Bangalore, Indian Institute of Science (IISc), Bangalore and Department of Ophthalmology & Visual Sciences, University of Illinois, Chicago, USA, Department of Biochemistry & Biophysics,. She has to her credit more than 155 research publications, one patent and also is the expert reviewer of many international journals like Journal of Medicinal Chemistry (ACS), Bioorganic & Medicinal Chemistry (Elsevier), Recent Patents on CNS Drug Discovery (Bentham), Current Enzyme Inhibition (Bentham), Acta Pharmacologica Sinica (Blackwell Publishing), European

Journal of Medicinal Chemistry (Elsevier) and Natural Product Research (Taylor and Francis).

She is a lifetime member of Association of Pharmacy Teachers of India (APTI) and Indian Pharmacological Society (IPS). In addition, she has been working on various projects of UGC, CSIR, DBT (Indo Sweden), DST and ICMR.